

**ASSESSMENT OF PUBLIC EXPOSURE TO NATURALLY OCCURRING  
RADIOACTIVE MATERIALS FROM MINING AND MINERAL PROCESSING  
ACTIVITIES OF TARKWA GOLDMINE IN GHANA**

KNUST

**A thesis submitted to the Department of Chemistry, College of Science, Kwame Nkrumah  
University of Science and Technology, Kumasi**

**in partial fulfillment of the requirements for the degree of**

**DOCTOR OF PHILOSOPHY**

**in Chemistry**

**By:**

**Augustine Faanu, MSc. Environmental Science, BSc. (Hons) (Dip Ed.) Chemistry**

**FEBRUARY, 2011**

## *DECLARATION*

I hereby declare that this submission is my own work towards the PhD and to the best of my knowledge, it contains no materials previously published by another person nor material which has been accepted for the award of any other degree of the University, except where due acknowledgement has been given in the text.

Augustine Faanu, ID: 20065703  
(Student)

KNUST

.....  
Signature

.....  
Date

Certified by:

Prof. James H. Ephraim  
(Supervisor)

.....  
Signature

.....  
Date

Certified by:

Prof. Emmanuel O. Darko  
(Co-Supervisor)

.....  
Signature

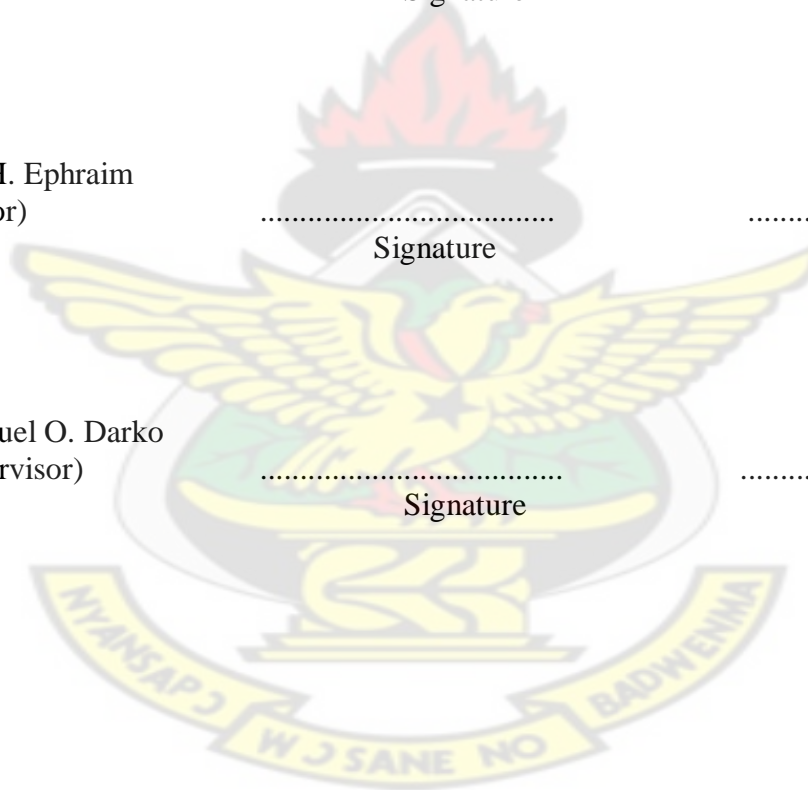
.....  
Date

Certified by:

.....  
Head of Chemistry Department

.....  
Signature

.....  
Date



## DEDICATION

This work is dedicated to entire membership of my family including those who have passed away and more especially to my two daughters Annie and Audrey Faanu.

# KNUST



## ABSTRACT

Mining has been identified as one of the potential sources of exposure to naturally occurring radioactive materials (NORM). However, mining companies are not being regulated for NORM in Ghana. Whilst the developed countries have identified NORM as potential problems and measures are being taken to address the issues, very little is being done in the developing countries. However, most of the NORM industries such as mining and mineral processing are located in developing countries such as Ghana. Currently, there are over two hundred (200) registered mining companies operating small, medium and large scale mining in Ghana. Tarkwa Goldmine is one of the largest gold mining companies in Ghana and has been in operation for the past 200 years with no data on radioactivity levels. The mine currently undertakes only surface mining and the process produces large volumes of tailings and waste that may contain NORM. Some of the NORM are soluble in water and have the tendency to leach into water bodies and farm lands. These studies have been carried out to determine the exposure of the public to NORM from processing of gold ore at the Tarkwa Goldmine in Ghana. Direct gamma spectrometry and neutron activation analysis (NAA) techniques were used to analyse for U/Th series and K-40 in soil, rock, water, food and particulate (dust) samples from the mining environment. The mean activity concentrations measured for  $^{238}\text{U}$ ,  $^{232}\text{Th}$  and  $^{40}\text{K}$  in the soil/rock samples were 15.2 Bq/kg, 26.9 Bq/kg and 157.1 Bq/kg respectively. For the water samples the mean activity concentrations were 0.54 Bq/L, 0.41 Bq/L and 7.76 Bq/L for  $^{226}\text{Ra}$ ,  $^{232}\text{Th}$  and  $^{40}\text{K}$  respectively. The mean activity concentrations of  $^{226}\text{Ra}$ ,  $^{232}\text{Th}$  and  $^{40}\text{K}$  in the food samples were 0.18, 0.14 and 45.00 Bq/kg respectively. The mean activity concentrations measured in the dust samples were 4.90 and 2.75  $\mu\text{Bq}/\text{m}^3$  for  $^{238}\text{U}$  and  $^{232}\text{Th}$  respectively. The total annual effective dose to the public was estimated to be 0.74 mSv. The results in this study compared well with

typical world average values. The results indicate an insignificant exposure of the public to technologically enhanced NORMS from the activities of the Goldmine. The radiological hazard due to  $^{226}\text{Ra}$ ,  $^{232}\text{Th}$  and  $^{40}\text{K}$  were carried out. The radium equivalent activity ( $\text{Ra}_{\text{eq}}$ ) and the calculated external and internal hazard indices, the absorbed dose rates and the corresponding annual effective dose were estimated in the soil and rock materials that might possibly be used as building materials. The results obtained in this study shows insignificant radiological hazards for the materials considered for use as construction materials for dwellings by the inhabitants in the study area. The results obtained in this study also shows that the background radiation levels are within the natural limits and compared well with similar studies for other countries. The study assessed the concentration of U, Th and K as well as other trace metals, anions and the physical parameters in water and soil samples in the goldmine and its surrounding areas. The mean concentrations of the U, Th and K were 0.020, 0.029 and 1.19 mg/L. The concentration of U, Th and K were variable in soil and rock samples taken from different locations in the study area with mean values varying in a range of 0.2 to 1.8  $\mu\text{g/g}$ , 0.9 to 2.6  $\mu\text{g/g}$  and 7037 to 71360  $\mu\text{g/g}$  respectively. The concentrations of U, Th and K are comparable to world average values of similar studies. The calculated Th/U ratios show that there has not been significant fractionation during weathering of the radioelements with a mean value of 2.5. The concentrations of the other trace metals, anions and the physical parameters are within the WHO guideline levels in drinking water. The mean values of the gross- $\alpha$  and gross- $\beta$  activity concentrations were 0.012 and 0.137 Bq/L which are also below the WHO recommended guideline values for drinking water.

## TABLE OF CONTENTS

	PAGE
DECLARATION	ii
DEDICATION	iii
ABSTRACT	iv
TABLE OF CONTENT	vi
LIST OF TABLES	ix
LIST OF FIGURES	xi
LIST OF ABBREVIATIONS	xiv
ACKNOWLEDGEMENT	xvii
CHAPTER ONE: 1.0 INTRODUCTION	1
1.1 General Introduction	1
1.2 Geochemistry of mine	5
1.3 Speciation of uranium and thorium	7
1.4 Statement of Problem	12
1.5 Objectives and scope	14
1.6 Importance of project	15
CHAPTER TWO: 2.0 LITERATURE REVIEW	17
2.1 Background	17
2.2 Sources of NORM	23
2.2.1 Cosmic radiation	24
2.2.2 Terrestrial radiation	26
2.2.3 Exposure from radon	34
2.2.3.1 Hazards associated with radon	40
2.2.4 Potential NORM producing industries	41
2.3 Hazards and risk associated with NORM	44
2.4 Biological Effect of Radiation	48
2.5 Instrumentation for radioactivity measurements	51
2.6 Physical and chemical parameters in the mine	57
2.7 Neutron Activation Analysis (NAA)	62
2.8 Gold processing methods	65
2.8.1 CIL Method	66
2.8.2 Heap Leach Method	69

CHAPTER THREE:	3.0	EXPERIMENTAL /METHODS	73
3.1		Description of the study area	73
3.2		Geology and Hydrogeology of the mining area	81
3.3		Meteorological data of the area	85
3.4		Samples collection	86
3.5		Sample preparations	89
	3.5.1	Analysis by gamma spectrometry	90
		3.5.1.1 Energy calibration	92
		3.5.1.2 Efficiency calibration	92
		3.5.1.3 Minimum detectable activity	93
		3.5.1.4 Determination of activity concentrations	94
		3.5.1.5 Calculation of dose from external gamma dose rates	95
		3.5.1.6 Calculation of doses due to soil/rock samples	96
		3.5.1.7 Activity concentrations due to ore dust and doses	97
		3.5.1.8 Determination of concentration of metals by NAA	100
		3.5.1.9 Airborne radon activity concentration and doses	102
		3.5.1.10 Calculation total annual effective dose	103
3.6		Radon measurements	104
	3.6.1	Determination of radon emanation fraction	107
3.7		Gross alpha and beta measurements in water samples	109
3.8		Statistical analysis of samples	110
3.9		Uncertainty estimation	110
3.10		Determination of physical parameters, trace metals and anions	113
	3.10.1	Determination of physical parameters	113
	4.8.2	Determination of anions	114
	4.8.3	Determination of trace metals	116
CHAPTER FOUR:	4.0	RESULTS	118
CHAPTER FIVE:	5.0	DISCUSSIONS	151
5.1		External Gamma Dose Rate at 1 meter above the ground	151
5.2		Activity concentrations, absorbed doses rates and annual effective doses	152
	5.2.1	Soil/rock	152
	5.2.2	Water	155
	5.2.3	Particulate/dust	159
	5.2.4	Food	161
5.3		Radon	162
5.4		Total annual effective dose	164
5.5		Radiological risk assessment	165
5.6		Gross alpha and gross beta measurements	168
5.7		Geochemical characteristics of the mine	169
	5.7.1	Physical Parameters	169

5.7.2	Anions	171
5.7.3	Trace and heavy Metals in water (cations)	172
5.7.4	Trace and major metals in soil and rock samples	177
CHAPTER SIX:	6.0 CONCLUSION AND RECOMMENDATIONS	182
6.1	Radiation exposure from NORM and impact on the public	182
6.2	Geochemical Characteristic of the study area	187
REFERENCES		191
APPENDICES		199



## LIST OF TABLES

- Table 2-1: Average radiation exposure from natural sources
- Table 2-2: Cosmogenic radionuclides
- Table 2-3: Population-weighted average cosmic ray dose rates
- Table 2-4: The Uranium decay series ( $4n + 2$ )
- Table 2-5: The Thorium decay series ( $4n$ )
- Table 2-6: The Actinium ( $^{235}\text{U}$ ) decay series ( $4n+3$ )
- Table 2-7: The Neptunium decay series ( $4n+1$ )
- Table 3-1: Communities and their population distribution around the mines
- Table 3-2: Characteristics of soils in the study area
- Table 4-1: Activity to dose rate conversion factors
- Table 4-2: Detriment-adjusted nominal risk coefficients for stochastic effects after exposure to radiation at low dose rate ( $10^{-2}$ )
- Table 5-1: The minimum detectable activities of  $^{238}\text{U}$ ,  $^{232}\text{Th}$  and  $^{40}\text{K}$ .
- Table 5-2: Average absorbed dose rate in air at 1 metre above soil and water sampling points in the various communities of the study areas and estimated annual effective dose.
- Table 5-3: Average activity concentrations, absorbed dose rates and annual effective doses due to  $^{238}\text{U}$ ,  $^{232}\text{Th}$  and  $^{40}\text{K}$  in soil in the study area.
- Table 5-4: Statistical summary of activity concentrations and estimated annual effective doses from water consumed from the study area.
- Table 5-5: Mean activity concentrations of  $^{238}\text{U}$  and  $^{232}\text{Th}$  in dust/air samples using direct gamma ray analysis, absorbed dose rate and annual effective doses for two periods.
- Table 5-6: Concentration of U and Th in dust samples using NAA and calculated activity concentrations.
- Table 5-7: The activity concentration of  $^{238}\text{U}$ ,  $^{232}\text{Th}$  and  $^{40}\text{K}$  in fresh food samples by direct gamma ray analysis.

- Table 5-8: The activity concentration of  $^{238}\text{U}$ ,  $^{232}\text{Th}$  and  $^{40}\text{K}$  in dried food samples by direct gamma ray analysis.
- Table 5-9: U-238 activity concentration ratios of soil to cassava samples
- Table 5-10: Th-232 activity concentration ratios of soil to cassava samples
- Table 5-11: K-40 activity concentration ratios of soil to cassava samples
- Table 5-12: Rn-222 concentration in air and soil and the corresponding estimated airborne annual effective doses.
- Table 5-13: Comparison of activity concentrations of  $^{238}\text{U}$ ,  $^{232}\text{Th}$  and  $^{40}\text{K}$  in soils in the study area and published data
- Table 5-14: Radon emanation coefficient of the soil, tailings and rock samples
- Table 5-15: Summary of annual equivalent doses and the estimated total effective dose from soil, water, dust, radon and external gamma dose rate to each individual member of the public.
- Table 5-16: Estimated risk components for the various exposure pathways studied
- Table 5-17: Results of the average activity concentration of  $^{226}\text{Ra}$ ,  $^{232}\text{Th}$  and  $^{40}\text{K}$  together with their total uncertainties, total absorbed dose, annual effective dose, radium equivalent activity and hazard indices of the samples in the study area
- Table 5-18: Comparison of the average activity concentrations, the radium equivalent activities ( $\text{Ra}_{\text{eq}}$ ) of soil, rocks, waste and tailings of the study area with published data.
- Table 5-19: Comparison of activity concentration of  $^{226}\text{Ra}$  and  $^{222}\text{Rn}$  emanation fraction (EF) of this study with different NORM waste from various industrial activities.
- Table 5-20: Comparison of activity concentrations  $^{238}\text{U}$ ,  $^{232}\text{Th}$  and  $^{40}\text{K}$  in soil, rock, waste and tailing samples for the first (I) and second (II) batch of samples.
- Table 5-21: Comparison of the absorbed dose rates and total annual effective doses due to soil, rock ore, waste rock, tailings for two different sampling periods.
- Table 5-22: The average activity concentrations of  $^{238}\text{U}$ ,  $^{232}\text{Th}$  and  $^{40}\text{k}$  in the first (I) and second (II) badge of water samples.
- Table 5-23: Gross- $\alpha$  and gross- $\beta$  activity concentrations (Bq/l) in water samples

Table 5-24: Statistical summary of water chemistry

Table 5-25: Summary of metals concentration and analytical uncertainties (mg/kg) of soil, tailings and rock samples of the mine.

## LIST OF FIGURES

Figure 1-1: Decay scheme of  $^{40}\text{K}$

Figure 2-1 Structure of the DNA molecule

Figure 2-2: Mechanisms of direct and indirect actions on DNA molecule

Figure 2-3: Semiconductor junction detector

Figure 2-4: Schematic diagram of the sequence of events in scintillation detector

Figure 3-1: Location of Tarkwa Goldmine in Ghana

Figure 3-2: Layout of Tarkwa Goldmine showing the sampling points.

Plate 3-1: Surface water body within the mine

Plate 3-2: Waste water from the gold processing plant to be discharged to the environment

Plate 3-3: Gold tailings dam

Plate 3-4: Heap leach treatment plant

Plate 3-5: Waste dump

Plate 3-6: Ore stockpile

Plate 3-7: Borehole in a community

Figure 3-3: Geological map of the study area

Figure 3-4: Rainfall data for 2008

Figure 3-5: Rainfall data from January to July 2009

Figure 3-6: Carbon in Leach (CIL) process plant flow diagram

- Figure 3-7: Heap Leach (HL) process flowchart
- Figure 4-1: Block diagram of the gamma spectrometry setup
- Figure 4-2: Schematic diagram of AAS
- Figure 5-1: Energy calibration curve using mixed standard radionuclides in a one litre Marinelli beaker
- Figure 5-2: Efficiency calibration curve as a function of energy for mixed radionuclides standard in a one litre Marinelli beaker
- Figure 5-3: Energy calibration curve using mixed radionuclides standard distributed in a plastic foil
- Figure 5-4: Efficiency calibration curve for mixed radionuclide standard in a plastic foil
- Figure 5-5: Energy Resolution of the HPGE detector at 1332 keV of  $^{60}\text{Co}$ .
- Figure 5-6: Comparison of absorbed dose rate from direct air measurement at one metre above the ground at soil, water and dust sampling points
- Figure 5-7: Relative contributions to total absorbed dose rate in air outdoor due to  $^{238}\text{U}$  and  $^{232}\text{Th}$  decay series elements and  $^{40}\text{K}$  for soil and rock samples
- Figure 5-8: Comparison of annual effective doses due to soil, water and dust samples as well as airborne radon
- Figure 5-9: Comparison of the activity concentration in different types of samples in the study area
- Figure 5-10: Comparison of activity concentrations of different water sources.
- Figure 5-11: A comparison of the total activity of the radionuclides in the soil sample with the activity concentration of K-40
- Figure 5-12: A comparison of the total activity of the radionuclides in the soil sample with the activity concentration of U-238
- Figure 5-13: A comparison of the total activity of the radionuclides in the soil sample with the concentration of  $^{232}\text{Th}$
- Figure 5-14: Percentage contribution of  $^{238}\text{U}$ ,  $^{232}\text{Th}$  and  $^{40}\text{K}$  in the soil samples to the total activity concentrations in the study area.

Figure 5-15: A comparison of percentage weighted values of pH, T, conductivity, TDS, U, Th and K in soil and rock samples in the study area.

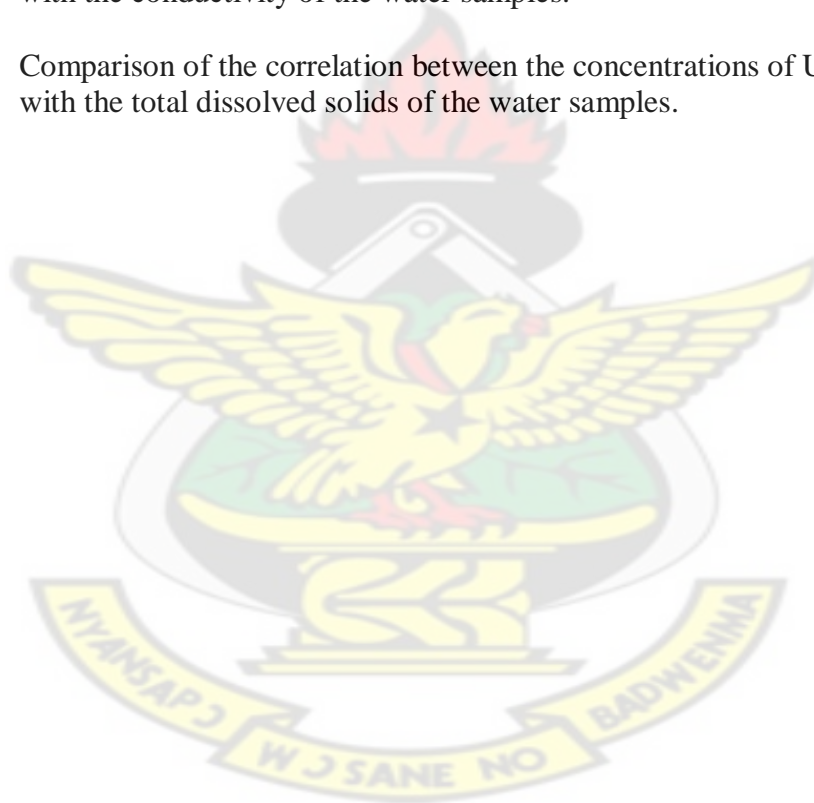
Figure 5-16: U versus Th (a), K versus Th (b) and K versus U (c) plots of the mean concentrations of soil and rock samples in the study area. The solid straight lines represent the best fitting lines and their corresponding correlation coefficients.

Figure 5-17: Comparison of concentration of U, Th, and K in the water samples with the pH of the samples to verify the relation of the concentration of the metals with pH.

Figure 5-18: Comparison of the correlation between the concentrations of U, Th, and K with the temperature conditions of the study area.

Figure 5-19: Comparison of the correlation between the concentrations of U, Th, and K with the conductivity of the water samples.

Figure 5-20: Comparison of the correlation between the concentrations of U, Th, and K with the total dissolved solids of the water samples.



## LIST OF ABBREVIATIONS

**UNSCEAR**- United Nations Scientific Committee on the effects of atomic radiation

**BSS**- Basic Safety Standards

**IAEA**- International Atomic Energy Agency

**ICRP** – International Commission for Radiological Protection

**NORM**- Naturally Occurring Radioactive Materials

**Te-NORM** – Technologically enhanced naturally occurring radioactive material

**EF** – Emanation fraction

**NAS** – National Academy of Sciences

**CIL** – Carbon in leach

**HL** – Heap leach

**NRC** – National Research Council

**EU** – European Union

**mSv** – millisievert ( $10^{-3}$  Sievert)

**DWAF** – Department of water affairs

**ILO** – International Labour Organisation

**Bq** – Becquerel

**Bq/g** – Becquerel per gram

**Bq/kg** – Becquerel per kilogram

**Bq/m<sup>3</sup>** – Becquerel per cubic meter

**Bq/L** – Becquerel per litre

**μSv** – microsievert

**GeV** – giga electrovolt

**nGy/h** – nano Gray per hour

**EC** – electron capture

**DNA** – deoxyribonucleic acid

**Kg/m<sup>3</sup>** – kilogram per cubic meter

**Bqhm<sup>-3</sup>** – Becquerel hour per cubic meter

**USEPA** – United States Environmental Protection Agency

**IFC** – International Finance Cooperation

**SCA** – single channel analyser

**MCA** – multi channel analyser

**ADC** – Analogue to digital converter

**MeV** – mega electrovolt

**NAI (TI)** – sodium iodide (Thallium)

**HPGE** – High purity germanium

**BEIR** – Biological effects of ionising radiation

**LET** – linear energy transfer

**SGMC** – State Gold Mining Corporation

**GFGL** – Goldfields Ghana Ltd.

**SAG** – semi autogenous

**HDPE** – High density polyethylene

**ADR** – Adsorption/Desorption/Recovery

**GPS** – Geographical Positioning System

**UMAT** – University of Mines and Technology

**NAA** – neutron activation analysis

**SSDL** – second standard dosimetry laboratory

**DCF** – dose conversion factor

**DDREF** – Dose and dose rate effective factor

**ALARA** – As low as reasonably achievable

**GHARR-1** – Ghana Research Reactor One

**MDA** – minimum detectable activity

**AAS** – Atomic Absorption Spectrophotometer

**PTFE** – Polytetrafluoroethylene

**SS** – soil sample

**WS** – water sample

**AS** – air sample

**FS** – food sample

**WHO** – World Health Organisation

**LNT** – Linear non-threshold

**TDS** – Total dissolved solid

**EC**- electrical conductivity

**U** – Uranium

**Th** – thorium

**K** – Potassium

**H<sub>in</sub>** – Internal hazard index

**H<sub>ex</sub>** – external hazard index

**Ra<sub>eq</sub>** – Radium equivalent activity

**SPSS** - Statistical Package for Social Sciences

## ACKNOWLEDGEMENT

First and foremost I would like to express my sincere gratitude to God Almighty for the protection, good health and spiritual guidance during the whole duration of this study.

This project was carried out with support of the Tarkwa Goldmine and the Radiation Protection Institute of the Ghana Atomic Energy Commission. The support is gratefully acknowledged. I am grateful to the staff of the Environmental, Mining and Safety Departments of Tarkwa Goldmine Ghana Ltd for their various forms of assistance during sampling at the mine site.

I wish to express my heartfelt gratitude to my supervisors, supervisors Professor James H. Ephraim and Professor Emmanuel O. Darko for the excellent support, directions, suggestions and above all patience in guiding me through the entire study. All the support from the Department of Chemistry and the School of Graduate Studies of the Kwame Nkrumah University of Science and Technology (KNUST) is gratefully appreciated and acknowledged.

I also wish to acknowledge the contribution of the following persons namely; Mr. David Kpegloh, Oscar Adukpo, Rita Kpordzro, Henry Lawluvi, Bernice Agyeman and Ali Ibrahim of the Radiation Protection for their help in the samples preparation. Mr. Nicholas Opata and Mr Nash of the National Nuclear Research Institute were also helpful in the NAA and AAS analysis and their assistance is gratefully acknowledged. Last but not the least my sincere gratitude also goes to Mr Rudolph Mba of the Radiological and Medical Sciences Research Institute for his assistance in the anions analysis.

# CHAPTER ONE

## 1.0 INTRODUCTION

### 1.1 General Introduction

Human beings are continually being exposed to ionising radiation from natural sources. There are two main contributors to natural radiation exposures: high-energy cosmic ray particles incident on the earth's atmosphere and radioactive nuclides that originated from the earth crust and are present everywhere in the environment, including the human body [UNSCEAR, 2000]. Humans are exposed to radionuclides through ingestion and inhalation (internal exposure) and/or irradiation from external gamma rays emitted from the radionuclide (external exposure).

The International Basic Safety Standards (BSS) for protection against ionizing radiation and the safety of radiation sources [IAEA, 1996] specify the basic requirements for the protection of health and the environment from ionizing radiation. These are based on the latest recommendations of the International Commission on Radiological Protection [ICRP, 2007] on the regulation of Practices and Interventions. The BSS is applied to both natural and artificial sources of radiation in the environment and the consequences on living and non-living species. The environment is defined within the framework of national laws and international legal instruments, and may be considered to include man, biota (living), abiota (non-living), physical surroundings and their interactions [Van der Steen and Van Weers, 1996]

NORM, an acronym for naturally occurring radioactive materials are present in several types of materials. Materials which may contain any of the primordial radionuclides or radioactive elements as they occur in nature, such as radium, uranium, thorium, potassium, and their radioactive decay products, that are disturbed as a result of human activities. However the

concentration of NORM in most natural substances is so low that the risk is generally regarded as negligible. Higher concentrations may arise as a result of human activities. In most NORM, several or all of the radioactive isotopes of the three primordial decay series ( $^{235}\text{U}$ ,  $^{238}\text{U}$  and  $^{232}\text{Th}$ ) are present in small concentrations in the natural matrix.

Irradiation of the human body from external sources is mainly by gamma radiation from radionuclides of the  $^{235}\text{U}$ ,  $^{238}\text{U}$  and  $^{232}\text{Th}$  decay series and from  $^{40}\text{K}$ . These radionuclides may be present in the body and irradiate various organs with alpha and beta particles as well as gamma rays [Cember, 1996; UNSCEAR, 2000; IAEA; 2005].

Mineral ores in the naturally undisturbed environments, the radionuclides in the decay series are more or less in radiological equilibrium. However, this equilibrium becomes disturbed through human activities such as mining and mineral processing, resulting in either an enrichment or depletion of some of the radionuclides concentrations compared to the original matrix. This disequilibrium is as a result of differences in the properties of the radionuclides in the series, due to geochemical migration processes and differences in their half-lives [Cember, 1996; UNSCEAR, 2000; Sato and Endo, 2001].

Naturally occurring uranium consists of three isotopes all of which are radioactive:  $^{238}\text{U}$ ,  $^{235}\text{U}$  and  $^{234}\text{U}$ . Uranium-238 and U-235 are the parent nuclides of two independent decay series whilst  $^{234}\text{U}$  is a decay product of the  $^{238}\text{U}$  series. Also, since  $^{234}\text{U}$  is an isotopic daughter of  $^{238}\text{U}$ , the deviation of the  $^{234}\text{U}/^{238}\text{U}$  activity ratio from unity due to chemical processes, including magmatic evolution, is far less probable than in the case of the non-isotopic combination of  $^{230}\text{Th}/^{238}\text{U}$  [Sato and Endo, 2001]. High concentrations of uranium (U) and thorium (Th) can be associated with igneous and sedimentary rock types [Bliss, 1978]. Under the equilibrium conditions, the radiation from these radionuclides is virtually trapped underground and exposures

are only possible through the drinking of contaminated ground water by humans. The alpha radiations from these radionuclides present a radiation hazard due to ingestion or inhalation of uranium ore dust and radon gas. The external radiation hazard on the other hand is mainly due to the gamma radiation from  $^{214}\text{Pb}$  and  $^{214}\text{Bi}$ , and also the beta radiation from  $^{234}\text{Th}$ ,  $^{234\text{m}}\text{Pa}$ ,  $^{214}\text{Pb}$ ,  $^{214}\text{Bi}$  and  $^{210}\text{Bi}$ .

Radon gas which is considered as one of the most hazardous radioactive gases in the environment is of health concern in radiological risk assessment. Radon-222 ( $^{222}\text{Rn}$ ) with a half-life of 3.82 days is a chemically inert gas and is produced through the radioactive decay of  $^{226}\text{Ra}$ , a member of the  $^{238}\text{U}$  decay series. The risk associated with the handling and disposal of materials contaminated with  $^{226}\text{Ra}$  are due primarily to  $^{222}\text{Rn}$  progeny (lead-210 and polonium-210), the inhalation of which has been known to be associated with increased risk of lung cancer [NAS, 1988]. The risks generally depend on the overall rate at which  $^{222}\text{Rn}$  is transported to the surrounding atmosphere through diffusion or advection and finally become released from the material matrix. The risk associated with radon in NORM materials is estimated by the term radon emanation fraction (EF). Radon emanation fraction is defined as the fraction of radon atoms formed in a solid that escapes from the solid and is free to migrate [White and Rood, 2001; Afifi et al., 2004]. The physical properties of  $^{226}\text{Ra}$  bearing material determine the  $^{222}\text{Rn}$  emanation fraction of the material [White and Rood, 2001]. These properties include: the distribution of  $^{226}\text{Ra}$  in the material; the structure of the material (whether massive or granular); type and magnitude of porosity of the material; the moisture content of the material. The amount of  $^{222}\text{Rn}$  emanating off the pore spaces is smaller when compared to the emanation fraction of a typical soil.

On the average, the annual global effective dose due to exposure to NORM has been estimated to be 2.4 mSv with a typical range between 1-10 mSv [UNSCEAR, 2000]. The main sources giving rise to this dose has been identified to be; cosmic rays, terrestrial gamma rays (referred to as external exposure), inhalation mainly of radon gas and ingestion of materials with NORM (referred to as internal exposures) [UNSCEAR, 2000]. Also 50 % of this global annual effective dose has been estimated to arise from radon exposure with a value of about 1.2 mSv [UNSCEAR, 2000].

Mining has been identified as one of the potential sources of exposure to NORM [UNSCEAR, 2000]. However, mining companies are not being regulated for NORM in most countries including Ghana since there are no guidelines for their regulation by the Radiation Protection Board. With the recent increase in awareness of the potential exposure situations of NORM, many countries are amending their Legislations and putting in place measures to address the problems of NORM. For instance, following the European Union (EU) Council Directive 96/29/EURATOM of 13<sup>th</sup> May 1996, where special provisions' concerning exposure to natural sources of radiation were put in place, a network was to be created to enable member states to share expertise and also to identify and promote good practices [IAEA, 2004]. Whilst the developed countries have identified NORM as potential problems and measures are being taken to address the issues, very little is being done in the developing countries. It is also worth noting that, most of the NORM industries such as mining and mineral processing, oil and gas exploration and extraction etc are located in developing countries such as Ghana. Some studies in some countries have also reported elevated activity concentrations levels during mining and mineral processing [IAEA, 2005].

In Ghana, the earliest European attempts to extract gold on a large scale concentrated in Tarkwa and Prestea in the late 19<sup>th</sup> century. The first official European gold mining company was the African Gold Coast Company and was registered on the 18<sup>th</sup> February 1878 [Hilson, 2002]. The activities in the mining sector have increased in recent times [Aryee and Aboagye, 2008]. As at 2008, a total of 212 mining companies were awarded mining leases and exploration rights [Aryee and Aboagye, 2008]. Tarkwa Goldmine which is located in the Wassa West District of the Western Region is the largest gold mining company in Ghana. Gold mining has long been an important economic activity in Ghana and has recently become the main industry in the country [Hilson, 2002]. From 1992, the mineral industry has become the single largest foreign exchange earner and gold accounts for about 95 % [Aryee, 2001]. The mines also contribute to the development of the areas they operate with the provision of schools, hospitals, roads, etc [Goldfields, 2007]. On the average about 324 metric tonnes of gold ore are processed annually yielding about 13,365, 000 oz of gold [Goldfields, 2007]. These mining operations consequently turn out large volumes of solid and liquid wastes in the form of waste dams; slime dams, tailings dams, which could contain elevated levels of NORM. These materials could also be washed onto surface water bodies and farm lands. Drinking of water from these water bodies, grazing by animals on these farm lands and farming of crops on these lands could be a potential source of exposure to NORM. Risk assessment and management of radionuclides entering or present in the environment as a result of industrial activities such as mining and mineral processing have not been carried out in almost all the mines in Ghana.

## **1.2 Geochemistry of U/Th decay series , K-40 and other chemical elements in the mining environment**

The geochemistry of the mines involves the study of the chemical composition, chemical processes and chemical reactions that govern the composition of rocks and soils, and the cycles

of matter and energy that transport the Earth's chemical components in time and space, and their interaction with the hydrosphere and the atmosphere. Geochemistry plays a major role in the occurrence and behaviour of metals including uranium and thorium in aqueous environment. The ultimate sink of chemicals including trace metals, anions, and uranium and thorium elements and their daughter elements are soils and sediments. In the case of ingestion and inhalation, the chemical toxicity of Uranium should be taken into account in addition to the radiological hazards. The leachate of trace metals from rocks and soil into water systems through natural processes can be accelerated by human activities such as mining and mineral processing. Trace metals are those elements that are not stoichiometric constituents of phases in a system of interest [White, 2007]. Studies of the trace metals contents provide geochemical and geological information. For instance, trace elements can provide useful clues as to the origin of sulphide ore deposits. The concentrations of trace elements such as cadmium (Cd) in the fossil shells of micro-organisms provide information about biological productivity and circulation patterns of ancient patterns. This has made trace element geochemistry a very powerful tool in the earth sciences [White, 2007].

The presence of significant quantities of uranium and thorium and their daughter elements as well as potassium (K) could result in radiological hazards. In addition significant levels of metals such as U, Th, K, As, Hg, Cd, Pb, Cu, Zn etc and anions such as  $\text{SO}_4^{2-}$ ,  $\text{NO}_3^-$ ,  $\text{PO}_4^{3-}$   $\text{Cl}^-$  could also result in chemical toxicity. Metals, unlike the toxic organic compounds are totally non degradable and able to accumulate in components of the environment where their toxicity is expressed. The toxicity of metals depends very much on the chemical form (speciation) of the element [Baird, 1999]. For some metals, the most toxic form is that having alkyl groups attached to the metal since most of such compounds are soluble in animal tissues

and can pass through biological membranes. The toxicity of a given metal present in a natural water-way depends on the pH, the amount of dissolved and suspended carbon due to interaction such as complexation [Baird, 1999]. In drinking water, the concentrations of trace metals are usually low and have no direct health problems except in situations when the water is polluted. However, the amount of trace metals ingested through food supply could be a significant source of exposure. For instance, when fish is consumed, the metals ingested originate from the water [Baird, 1999]. The extent to which a substance accumulates in humans and in any organisms depends upon the rate at which it is ingested from the source and the mechanism by which it is eliminated. Exposure to chemicals above recommended threshold limits could lead to health hazards such as damage to the liver, kidneys and the central nervous system of humans.

### **1.3 Speciation of uranium and thorium radionuclides in the environment.**

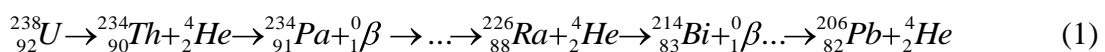
The chemical forms or speciation of an element can profoundly affect its toxicity. Chemical speciation may be defined as the various chemical and physical forms of the element which together make up the total concentration of that element of the sample. Chemical speciation is important because the chemical forms of an element determine its toxicity, its mobility in the environment and can also affect the bioavailability and the risk. In other words, it describes the chemical state of elements in solutions, solids (colloids) and gases (aerosols). Some factors which influence chemical speciation include; pH, redox potential, ionic strength, availability of inorganic and organic ligands, presence of microorganisms, kinds of interfaces during the interaction of solved and sorbed complexes. Knowledge of the chemical speciation will provide a realistic means of assessment of the risk to humans of environmental pollutants such NORM. Everyone is exposed to natural radiations mainly from uranium, thorium and potassium-40, all of which occur in the environment. For instance, environmental uranium

contains 99.28 % ( $^{238}\text{U}$ ), 0.72 % ( $^{235}\text{U}$ ) and 0.0058 % ( $^{234}\text{U}$ ). The concentration of depleted uranium is less than 0.711 % of  $^{235}\text{U}$  and contains approximately 99.80 % ( $^{238}\text{U}$ ), 0.2 % ( $^{235}\text{U}$ ) and 0.002 % ( $^{234}\text{U}$ ). Depleted uranium is 50 % less radioactive than environmental uranium.

Uranium like most heavy metals is chemically toxic and accumulates in kidneys (soluble) and also on bones. The dominant uranium valence states that are stable in geologic environments are uranous ( $\text{U}^{4+}$ ) and uranyl ( $\text{U}^{6+}$ ) states with uranyl being more soluble than the uranous [NRC, 1999]. The transport of uranium occurs generally in oxidising water and ground water as uranyl ion ( $\text{UO}_2^{2+}$ ) or as uranyl fluoride, phosphate, or carbonate complexes. In oxidising and acidic waters,  $\text{UO}_2^{2+}$  and uranyl fluoride complexes dominate whereas the carbonate and phosphate complexes dominate in near-neutral to alkaline oxidising conditions. Maximum sorption of uranyl ions on natural materials occurs at pH 5.0-8.5. For uranium to be fixed, and thereby accumulate, it requires reduction to  $\text{U}^{4+}$  by the substrate or by a mobile phase such as  $\text{H}_2\text{S}$  [NRC, 1999].

The relative mobility of the ions of the primordial nuclides in water is of the order of  $\text{U}^{6+} > \text{U}^{4+} \gg \text{Th}^{4+}$  [DWAF, 2002]. The +6 oxidation state forms soluble uranyl complex ions which play the most important role in uranium transport during weathering. Uranium occurs in numerous minerals such as pitchblende ( $\text{UO}_3 \cdot \text{UO}_2 \cdot \text{PbO}$ ) and carnotite ( $\text{K}_2\text{O} \cdot 2\text{U}_2\text{O}_3 \cdot \text{V}_2\text{O}_5 \cdot 3\text{H}_2\text{O}$ ).

Uranium-238 ( $^{238}\text{U}$ ) isotope decays by  $\alpha$ -emission to  $^{234}\text{Th}$  which also undergoes  $\beta$ -decay to form protactinium-234 ( $^{234}\text{Pa}$ ) as expression (1).

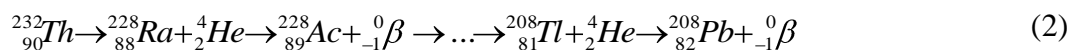


This reaction involves 14 nuclear decay steps resulting in the emission of eight (8)  $\alpha$ -particles and six (6)  $\beta$ -particles. In addition gamma photons are also emitted at energies of 1001 keV ( $^{234m}\text{Pa}$ ), 186 keV ( $^{226}\text{Ra}$ ), 352 keV ( $^{214}\text{Pb}$ ) and 609 keV ( $^{214}\text{Bi}$ ) and finally producing stable  $^{206}\text{Pb}$  to end the decay process.

In natural undisturbed soil,  $^{226}\text{Ra}$  is generally in equilibrium with uranium but in disturbed soils they might not necessarily be in equilibrium. The health implications of any metal (uranium, thorium and potassium) depend on the intake and the chemical form (speciation). The main pathway of uptake of uranium is via the food chain. For a better assessment of uranium transfer from geo-to bio-system and accumulation and distribution in the bio-system, knowledge about the chemical behaviour of uranium is important [Bernhard, 2005]. The exact knowledge of the quantity of uranium is a prerequisite for calculation and spectroscopic determination of chemical speciation. Uranium is present in the earth's crust in concentration of about 2.7 mg/kg [Enghag, 2004]. In the near-surface environment, U and Th may both be mobilised but in different ways. Even though in a naturally undisturbed environment, uranium is generally more soluble than thorium. At low pH, such as in acid-leach uranium mill, thorium becomes more soluble. For instance acid-leach milling might dissolve 30-90 % of the thorium in the ore [NRC, 1999]. Thorium has extremely low solubility in natural waters and is entirely transported in particulate matter. Thorium is adsorbed onto the surface of clay minerals. It is a naturally occurring radionuclide and is slightly metallic. When the metal is pure, it is silvery-white and air stable, but tarnishes in air becoming gray and finally black when contaminated with the oxide. Chemically, it is slowly attacked by water and also does not dissolve readily in most common acids, except hydrochloric acid. It also dissolves in concentrated nitric acid containing a small amount of catalytic fluoride ion. Thorium compounds

are more stable in the +4 oxidation state in aqueous systems. Thorium in the +4 state ( $\text{Th}^{4+}$ ) undergoes hydrolysis in aqueous solutions above pH 2-3 and is subject to extensive sorption by clay minerals and humic acid at near neutral pH. Thorium-232 ( $^{232}\text{Th}$ ) isotope decays very slowly. Its half-life is comparable to the age of the Universe. Other thorium isotopes occur in the thorium and uranium decay chains. Most of these are short-lived and hence much more radioactive than  $^{232}\text{Th}$  though on a mass basis they are negligible. The primary source of thorium is Monazite, a rare-earth and thorium phosphate mineral. It is also found in small amounts in most rocks and soils, where it is about four times more abundant than uranium. Thorium is adsorbed on the surface of clay minerals. It occurs in several minerals including thorite ( $\text{ThSiO}_4$ ), thorianite ( $\text{ThO}_2 \cdot \text{UO}_2$ ) and monazite a phosphate mineral ( $\{\text{Ce, La, Nd, Th}\} \text{PO}_4$ ) and the most common being monazite and may contain up to about 12 % thorium oxide. Thorium like uranium and plutonium can be used as a fuel in a nuclear reactor. Thorium-232 ( $^{232}\text{Th}$ ) absorbs slow neutrons to produce  $^{233}\text{U}$  which is fissile (this technique is employed in the determination of  $^{232}\text{Th}$  by neutron activation analysis). It undergoes radioactive decay emitting predominantly alpha radiation (8), beta radiation (5) and some gamma radiation.

The alpha radiation emitted through the decay of  $^{232}\text{Th}$  cannot penetrate human skin, however, if the exposure is internal through ingestion or inhalation there is an increased risk of cancers of the lung, pancreas, blood and liver diseases. In the decay series of  $^{232}\text{Th}$  gamma photons are also emitted at energies of 239 keV ( $^{212}\text{Pb}$ ), 583 keV ( $^{208}\text{Tl}$ ) and 911 keV ( $^{228}\text{Ac}$ ) which are used to determine the activity concentrations of  $^{232}\text{Th}$  by gamma spectrometry. Amplified decay reaction of  $^{232}\text{Th}$  is shown as expression (2).



Potassium has 24 known isotopes three of which occur naturally:  $^{39}\text{K}$  (93.3%),  $^{40}\text{K}$  which is the radioactive isotope of terrestrial importance (0.0117%) and  $^{41}\text{K}$  (6.7%). Naturally occurring  $^{40}\text{K}$  decays to stable  $^{40}\text{Ar}$  (11.2%) by electron capture and by positron emission, and decays to stable  $^{40}\text{Ca}$  (88.8%) by beta emission. During the decay process out of 100 disintegrations, 89 results in the release of beta particles with maximum energy of 1.33 MeV and 11 results in the release of gamma photons with maximum energy of 1.46 MeV. Potassium-40 ( $^{40}\text{K}$ ) decays by beta ( $\beta^-$ ) emission to  $^{40}\text{Ca}$  and by electron capture (E. C.) to  $^{40}\text{Ar}$  as shown in figure 1-1.

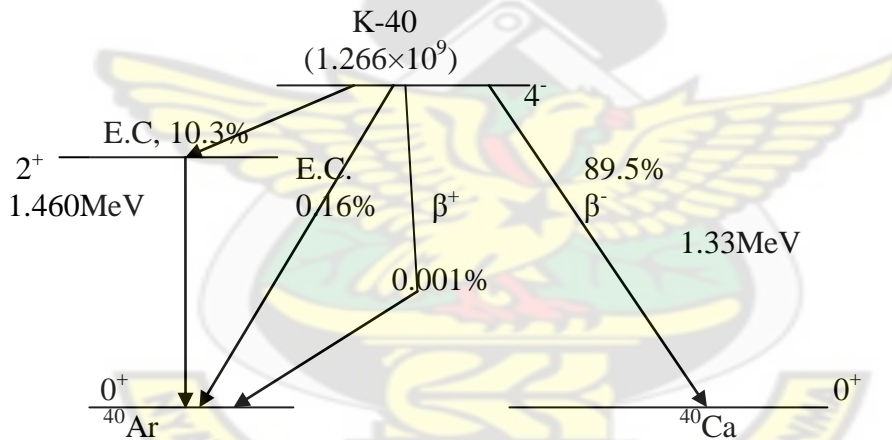


**Figure 1-1: Decay scheme of  $^{40}\text{K}$**

It has a half-life of  $1.250 \times 10^9$  years. The decay of  $^{40}\text{K}$  to  $^{40}\text{Ar}$  enables a commonly used method for dating rocks. Besides the dating, potassium isotopes have been used extensively as tracers in studies of weathering. They have also been used for nutrient cycling studies because potassium is a macronutrient required for life. The potassium content in the body is under homeostatic control and is little influenced by environmental variations and as a result the dose from  $^{40}\text{K}$  in the body is reasonably constant [NRC, 1999]. Potassium-40 occurs in natural

potassium (and thus in some commercial salt substitutes) in sufficient quantity that large amounts of those substitutes can be used as a radioactive source for classroom demonstrations. In healthy animals and people,  $^{40}\text{K}$  represents the largest source of radioactivity, greater even than  $^{14}\text{C}$ . In a human body of 70 kg mass, about 4,400 nuclei of  $^{40}\text{K}$  decay per second. The activity of natural potassium is 31 Bq/g [Knoll, 1989].

Natural waters contain several alpha and beta emitting isotopes in widely varying concentrations. When the water is ingested by humans they contribute to internal dose to the body. Alpha ( $\alpha$ ) emitters are particularly of concern because of their high linear energy transfer (LET). In Ghana, regulations on the levels of radioactivity in drinking water are based on the World Health Organisation (WHO) recommended values (WHO, 2004). The recommended levels in Ghana are set by the Ghana Standards Board (GSB, 2005). According to WHO guidelines, gross alpha radioactivity includes all the alpha emitters, excluding radon and gross beta radioactivity includes all beta emitters, except  $^3\text{H}$ . These guidelines ensure an exposure lower than 0.1mSv/yr assuming a water consumption rate of 2 litres/day. Measurement of high radioactivity concentration in the groundwater can be a good indicator for the high radioactivity levels in the rock aquifers. In Ghana even though the Ghana Standards Board has set limits of 0.1 Bq/L and 1.0 Bq/L for gross- $\alpha$  and gross- $\beta$  radioactivity in drinking water respectively, this is not being enforced. However it is important to determine the levels of radioactivity in drinking water in the study area and based on the results the necessary recommendation will be made to the appropriate authorities for action with ultimate aim of radiation protection of the public. Similar studies on radioactivity content of bottled water in Australia and Spain have reported values exceeding the recommended limits (Cooper et al., 1981 and Martin Sanchez et al., 1997).

#### **1.4 Statement of Problem**

In many cases, NORM producing industries such as mining companies have been in operation for long periods without any knowledge of the radiological aspects of the mining activity. The focus has always been on the regulation on the use of the artificial radionuclides in the mines by the Radiation Protection Board (RPB) of Ghana. In recent times, there is an increased awareness of the potential problems of NORM and this has resulted in most countries taking steps to implement regulations dedicated to natural sources of radiation in their national legislations.

The potential hazard occurs when the operator of the practice or the regulatory authority is not aware of the problems associated with the enhanced levels of NORM in raw materials, products, mine tailings and scales in pipes and no protective actions are put in place so that doses to workers and the public do not exceed the prescribed dose limits. The relevant route of exposure of the public is internal, via inhalation of dust and aerosols and ingestion of water and food. Mining results in large volumes of mine tailings that may contain enhanced levels of natural radionuclides. Leaching of radionuclides can result in contaminated ground and surface water bodies and thereby expose members of the public. Radionuclides, such as  $^{226}\text{Ra}$  and  $^{228}\text{Ra}$  are known to have high mobility in the environment due to their high comparative solubility in water. Most of these radionuclides are predominantly alpha emitters and alpha particles tend to cause more internal hazard.

Tarkwa Goldmine is one of the largest gold mining companies in Ghana and has been in operation for more than the past 200years. The mine currently undertakes only surface mining and the process produces large volumes of tailings and waste that may contain NORM. Some of the NORM are soluble in water and have the tendency for leaching into water bodies and farm lands. The mine operates within the Tarkwa Township and eight other smaller communities of

whose inhabitants depend on surface water and boreholes as their source of water. Farming is also an important activity within the mine's operational area. The soil, water bodies, dust and crops could be potential sinks for these radionuclides. The ultimate substrate of these radionuclides is the human body, which is the main concern of this study.

Also, the geological formation of the Tarkwa Goldmine is similar to the gold bearing conglomerates of the Witwatersrand Basin in South Africa where commercial quantities of uranium are processed from the gold tailings [Goldfields, 2007]. The above reasons are the bases for the choice of the Tarkwa Goldmine for this study. It is also important to note that NORM is identified as the major source of human exposure to ionising radiations and it is important to conduct studies in all NORM industries to establish reference data which will be useful for all stakeholders in the NORM industries in Ghana.

### **1.5 Objectives and Scope**

The general aim of the studies is to assess the risk to members of the public living in the vicinity of the Tarkwa Goldmine due to NORM as a result of the gold mining activities. The study focused on the determination of the levels and distribution of the naturally occurring radionuclides of the U/Th decay series and  $^{40}\text{K}$  as well as the geochemical characteristics within the Tarkwa Goldmine and the surrounding communities. As a result, soil, water and air samples were collected at selected points for analysis by gamma spectrometry using a high purity germanium detector (HPGE) and neutron activation analysis (NAA).

There is global concern about the health risk of NORM in mining and mineral processing and national regulatory authorities are establishing guidelines and criteria for radiation protection from NORM. The public, which is the focus of this study, has very little or no understanding of radiation and risks concepts. In general, perceptions about radiation derived from natural

sources, including radon, and from artificial sources may be different. There is also lack of understanding of the biological effects from both sources [IAEA, 2005]. At the end of the study, data on natural radioactivity levels in the study area will be disseminated to the public and as a result the knowledge and awareness on the issue of NORM in the study area will be increased.

The study has the following specific objectives;

- To determine the activity concentrations of the radionuclides U/Th series and  $^{40}\text{K}$ .
- To determine the radiation doses from these activity concentrations and compare with international recommended dose limits.
- To assess the hazard and risk to the public associated with these dose values.
- To conduct the geochemical studies by quantifying the levels of trace metals and anions as well as the physical parameters in water and soil samples within and around the mines.
- Recommend a suitable radiation protection programme for the mine if necessary.

## **1.6 Importance of Project**

In many developing countries including Ghana, the NORM industries have not been subjected to radiological regulatory control. Data on radionuclide concentrations in raw materials, residues and waste streams and data on public exposures are scanty [Darko et al, 2005; Darko and Faanu, 2007]. Consequently, there is general lack of awareness and knowledge of the radiological hazards and exposure levels by legislators, regulators and operators. Some studies conducted on two mines in Ghana have reported an average effective dose of  $0.3 \pm 0.01$  mSv [Darko et al., 2010]. Even though this value is below the recommended dose limit for members of the public for practices, there is the need for more work to be done to cover all the gold mines in Ghana so that a concrete decision can be taken to ascertain the NORM situation in Ghana. Ghana is also in the process of formulating guidelines on setting standards for the regulation of

NORM in the mining industry. The availability of data from such studies is very vital to all stakeholders involved since it will add to the data required for the development of guidelines for the regulation of NORM in Ghana.

# KNUST



## CHAPTER TWO

### 2.0 LITERATURE REVIEW

#### 2.1 Background

Industrial activities such as oil and gas extraction, coal and peat fired power generation, phosphate industries, zircon/zirconium industry, production of titanium dioxide pigments, mining and processing of metals such as copper, gold, aluminium, etc have been reported as potential sources of elevated naturally occurring radionuclides. The presence of NORM with elevated radionuclides concentrations could be an issue at any stage of an operation from the mineral feed stock, intermediate products, final products and the wastes generated during the process [IAEA, 2005]. In the past, the issue of NORM and the potential hazards associated with it has been relegated to the background. Consequently, until the 1970s radon and its progeny were regarded as radiation health hazards encountered only in the mining and processing of uranium ore. This notion has however changed markedly in recent times as a result of increased efforts made in many studies to measure radon in dwellings, mines other than uranium mines, workplaces suspected of high atmospheric radon levels [Van der Steen and Van Weers, 1996]. The above studies have raised awareness on the potential risk of NORM in the environment.

In the last decade, a number of international meetings have been dedicated to the radiological consequences of NORM and these have contributed to world-wide cognition of the issues involved [Van der Steen and Van Weers, 1996]. Despite these studies and meetings on NORM, there is still a back log of information on the awareness and their radiological hazards and levels of exposures in many countries by legislators, regulators and operators.

Much of the information on NORM has been based on studies carried out in developed countries. For instance, much of the data in the IAEA Technical Report Series number 419 has been based on studies in Europe and North America and this report also concluded that data from less developed countries is scarce [IAEA, 2003]. The report also highlighted some key issues which concern developing countries with respect to radiation exposure from NORM:

- That a large proportion of the world mining operations are located in less developed countries;
- Environmental radiation protection standards may be less stringent or their enforcement may be less strict;
- Artisanal mining and milling, and the artisanal industries with less stringent occupational health and safety were wide spread;
- Limited or no resources are available to deal with legacy wastes and for upgrading plants and the waste management infrastructure;
- Responsibilities for legacy wastes and contamination are unclear [IAEA, 2003].

Again, in the developed countries such as members of the European Union (EU), each member country is obliged to identify work activities that cannot be ignored from the radiological protection point of view. This action has increased the awareness of the potential problems enormously, and most of the EU member states have now implemented regulations dedicated to natural sources of exposure [EC, 1996]. Further to these, there are several IAEA reports on NORM with respect to occupational and public exposure situations that have been published recently [Van der Steen and Van Weers, 1996; IAEA, 2003 and ICRP, 2007] that have all contributed significantly to the recognition of the radiological consequences and risk associated with NORM. On the average, the annual global effective dose due to exposure to

NORM has been estimated to be 2.4 mSv with a typical range between 1-10 mSv [UNSCEAR, 2000]. The main sources giving rise to this dose has been identified to be; cosmic rays, terrestrial gamma rays (referred to as external exposure), inhalation mainly of radon gas and ingestion of materials with NORM (referred to as internal exposures) [UNSCEAR, 2000]. Also 50 % of this global annual effective dose has been estimated to arise from radon exposure with a value of about 1.2 mSv [UNSCEAR, 2000].

Studies have also established that, radiation exposure above certain threshold limits can damage living cells, causing death in some of them and modifying others [UNSCEAR, 2000]. However, in the case of low doses, studies are inconclusive as to the effect from the exposure to low background doses. It is also important to add that much of the studies on the effect of exposure to radiation have been based on the studies of the health records of survivors of the Atomic Bombing in Hiroshima and Nagasaki and also based on studies on animals [DWAF, 2002]. There are experimental evidences from animal studies that show that exposure to high levels of radiation could cause genetic effects. However, in the case of the low doses, it is assumed that exposure to background levels of natural radiation may lead to an additional risk of cancer, even though this has not yet been established [DWAF, 2002]. This is now a subject of debate and controversy. The United Nations through UNSCEAR is responding to these challenges by undertaking new initiatives which will be included in its future assessments of radiation sources, levels and effects. Some of the known effects resulting from radiation exposure are either damage to cells that are killed or modified. If the repair of the damage or modified cells is not perfect, the resulting modification will be transmitted to further cells and may eventually lead to cancer. The biological damage due to radiation exposure could lead to somatic stochastic effect or hereditary stochastic effects.

Stochastic effect is radiation effects, generally occurring without a threshold level of dose, whose probability is proportional to the dose and whose severity is independent of the dose [IAEA, 1996]. Radiation exposure has also been associated with most forms of leukaemia and other types of cancers affecting various organs such as lungs, breast and thyroid glands. It is also worth noting that radiation-induced cancer may manifest itself decades after exposure. The major long-term evaluation of populations exposed to radiation was based on studies of approximately 86,500 survivors of the atomic bombings of Hiroshima and Nagasaki, Japan [UNSCEAR, 2000]. This study revealed an excess of hundred cancer deaths in the population studied. Radiation exposure also has the potential to cause hereditary effects in the offspring of persons exposed to radiation. Studies on this effect have been based on animal species and it is yet to be detected in human populations [UNSCEAR, 2000].

However, some human activities such as mining and use of ores containing natural radioactive substances and the production of energy by burning coal that contain such substances are known to have enhanced the exposure from natural sources of radiation [UNSCEAR, 2000]. Such human activities generally give rise to radiation exposures that are only a small fraction of the global average level of natural exposure. However, specific individuals residing near installations releasing radioactive materials into the environment may be subject to higher exposures. It should be noted that, should some of the sites with high levels of radioactive residues be inhabited or re-inhabited, the settlers would incur radiation exposures that would be higher than the global average level of natural exposures [UNSCEAR, 2000].

There are several pathways by which the radioactive material can reach humans. The pathway largely depends on the processes involved and can be broadly categorised into; on-site, off-site, airborne, waterborne, food products, etc [O'Brien et al, 1998]. For on-site pathways, the

exposures tend to be direct from external gamma radiation or internal exposure resulting from inhalation of radioactive dust or radon progeny. Due to the presence of NORM in most soils and rocks, underground mining activities can lead to enhanced levels of radioactive dust, and radon isotopes and other radioactive isotopes [O'Brien and Cooper, 1998].

In open-pit mining, ventilation cannot be controlled and work practices have to be carefully controlled to minimise the radiological risk to the on-site workers [O'Brien et al., 1998]. There are also possibilities of the presence of NORM in buildings when the construction materials contain NORM. According to UNSCEAR report [UNSCEAR, 2000], the level of radionuclides in soil depends on the types of rock from which the soil originates. Various igneous, metamorphic and sedimentary rock types have widely different uranium and thorium concentrations. The levels studied in these types of rocks have shown that the levels are higher in granitic igneous and lower in sedimentary rocks [UNSCEAR, 2000 and DWAF, 2002].

Off-site exposure situation assessments also involve analysis of the potential exposures to humans living within or near the site where NORM is likely to be produced. Exposure to NORM under this situation will normally result from the transfer through environmental pathways or the use of industrial wastes containing NORM. Off-site exposure pathways are normally more indirect and complex and members of the public become the target of exposure. For instance transfer of radionuclides through the food chain [Dahlgard, 1996] by river and oceanic transport [McDonald et al., 1996], by atmospheric deposition, by re-suspension of radioactive dust, etc are some of the possible pathways through which members of the public may be exposed to radiation. Analysis of the pathways by which these materials can move through the environment is necessary to ensure that the impact of mining and mineral processing on the environment and the public is minimised [O'Brien et al., 1998].

On-site external exposures in industrial or mining situations could be due to the presence of NORM in stockpiles, waste piles, storage tanks, build-up of surface contamination on equipment, in pipes and storage tanks. External exposures to members of the public (off-site) can result from exposure to gamma radiation from passage of cloud shine or exposure to gamma radiation from material deposited on the ground (ground shine) [O'Brien et al., 1998]. The dominant exposure pathways in most situations are external gamma radiation, inhalation of radon gas and its decay products, ingestion of contaminated food and/or water [O'Brien et al., 1998]. The guiding principle in controlling the radiological impact of NORM in all these situations is the ALARA principle [ICRP, 1977] which states that all exposures should be kept as low as reasonably achievable (ALARA), social and economic factors taken into account.

The above scenarios are the basis for the choice of the method for this study.

The development of guidance by various countries is based on data on activity concentrations and radiation doses. At the International Atomic Energy Agency (IAEA) and International Labour Organisation (ILO) joint conference on Occupational Radiation Protection in Geneva in 2002, it was recognised that, exposures to NORM were generally stable and predictable with little or no likelihood of large accidental exposures. However, lack of knowledge and adequate controls could in some cases give rise to doses approaching or exceeding dose limits. It was also widely believed that, in order to optimise protection and resources, occupational doses below 1-2 mSv per year are unlikely to warrant significant regulatory attention since it will be a waste of resources. The main conclusion drawn from this conference was that, more explicit guidance was needed to determine which exposures arising from NORM activities should be subjected to regulatory control [IAEA, 2005]. The IAEA is yet to arrive at International consensus on the activity concentration levels that could be used to

apply to the concept of exclusion from regulatory control. The activity levels being considered for exclusion are 10 Bq/g for  $^{40}\text{K}$  and 1 Bq/g for uranium and thorium radionuclides. These are based on a consideration of worldwide distribution of activity concentrations in soil [IAEA, 2005]. The reported worldwide population-weighted average levels for the natural radionuclides for  $^{238}\text{U}$ ,  $^{226}\text{Ra}$ ,  $^{232}\text{Th}$  and  $^{40}\text{K}$  are 33, 32, 45 and 420 Bq/kg respectively [UNSCEAR, 2000].

## 2.2 Sources of NORM

All living organisms are continually exposed to ionizing radiation from natural sources. The levels of exposure vary depending on location and altitude. According to UNSCEAR 2000 report, the levels of exposure vary by a factor of about 3 [UNSCEAR, 2000]. The main sources of exposure are:

- I. Cosmic rays that come from outer space and from the surface of the sun;
- II. Terrestrial radionuclides that occur in the earth crust;
  - In building materials and in air,
  - Water and foods and,
  - In the human body.

It is thus important to carry out an assessment of the doses resulting from the above natural sources since it has been identified as the largest contributor to the collective dose of the world population. Cosmic radiation has been identified to be intense at higher altitudes whilst the concentration of uranium and thorium in soils are higher in localised areas. The exposure to radiation from concentration of  $^{40}\text{K}$  in foods has been found to be fairly constant and uniform for individuals everywhere in the world [UNSCEAR, 2000].

Table 2-1 shows the world wide average annual effective doses for the various sources.

**Table 2-1: Average radiation exposure from natural sources [UNSCEAR, 2000]**

Source	Worldwide average annual effective dose, mSv	Typical range
<u>External</u>		
Cosmic rays	0.4	0.3 – 1.0
Terrestrial rays	0.5	0.3 – 0.6
<u>Internal</u>		
Inhalation (radon)	1.2	0.2 – 10
Ingestion	0.3	0.2 – 0.8
<b>TOTAL</b>	<b>2.4</b>	<b>1 – 10</b>

### 2.2.1 Cosmic radiation

This type of radiation is produced as a result of the continuous interaction of cosmic-ray particles with nitrogen in the atmosphere. The types of radionuclides produced are known as cosmogenic radionuclides. Typically, they include:  $^3\text{H}$ ,  $^7\text{Be}$ ,  $^{14}\text{C}$  and  $^{22}\text{Na}$  as shown in Table 2-2 [UNSCEAR, 2000].

The production of these radionuclides is highest in the upper stratosphere but some energetic cosmic-rays neutrons and protons which survive in the lower stratosphere are able to produce the cosmogenic radionuclides as well. The annual average effective dose worldwide at sea level has been estimated to be  $320\mu\text{Sv}$  with the directly ionizing and indirectly ionising radiation component contributing  $270\mu\text{Sv}$  and  $48\mu\text{Sv}$  respectively. The dominant component of the cosmic ray field at the ground level is muons with energies between 1 and 20 GeV [UNSCEAR, 2000] and this contribute about 80 % of the absorbed dose rate in free air from the directly ionizing radiation. The population-weighted average absorbed dose rate from the directly ionizing and photon components of cosmic radiation at sea level is estimated to be  $31\text{ nGy/h}$  ( $280\mu\text{Sv/year}$ ) [UNSCEAR, 2000]. It is however more difficult to estimate the neutron radiation

component at the sea level because of the low response of instruments to high energy photons, which is the important component of the spectrum. The annual world average of the neutron components contribution to the cosmic radiation is estimated to be 120  $\mu\text{Sv}$ . The global value of the annual collective dose is about  $2 \times 10^6$  man-Sv and two thirds of the world's population that live at altitude of 0.5 km receive about one half of this dose [UNSCEAR, 2000].

Previous UNSCEAR reports on the assessment of the cosmogenic radionuclides have reported annual effective doses of 12  $\mu\text{Sv}$  for  $^{14}\text{C}$ , 0.15  $\mu\text{Sv}$  for  $^{22}\text{Na}$ , 0.01  $\mu\text{Sv}$  for  $^3\text{H}$  and 0.03  $\mu\text{Sv}$  for  $^7\text{Be}$ . These cosmogenic radionuclides are relatively homogeneously distributed on the surface of the earth [UNSCEAR, 1993, 2000].

**Table 2-2: Cosmogenic radionuclides [UNSCEAR, 2000]**

Element	Isotope	Half-life	Decay Mode
Hydrogen	$^3\text{H}$	12.33 a	Beta (100 %)
Beryllium	$^7\text{Be}$	53.29 d	EC <sup>a</sup> (100 %)
	$^{10}\text{Be}$	$1.51 \times 10^6$ a	Beta (100 %)
Carbon	$^{14}\text{C}$	5730 a	Beta (100 %)
Sodium	$^{22}\text{Na}$	2.602 a	EC (100 %)
Aluminium	$^{26}\text{Al}$	$7.41 \times 10^5$ a	EC (100 %)
Silicon	$^{32}\text{Si}$	172 a	Beta (100 %)
Phosphorus	$^{32}\text{P}$	14.26 d	Beta (100 %)
	$^{35}\text{P}$	25.34 d	Beta (100 %)
Sulphur	$^{35}\text{S}$	87.51 d	Beta (100 %)
Chlorine	$^{36}\text{Cl}$	$3.01 \times 10^5$ a	EC (1.9 %), Beta (100 %)
Argon	$^{37}\text{Ar}$	35.04 d	EC (100 %)
	$^{39}\text{Ar}$	269 a	Beta (100 %)
Krypton	$^{81}\text{Kr}$	$2.29 \times 10^5$ a	EC (100 %)

**Table 2-3: Population-weighted average cosmic ray dose rates [UNSCEAR, 2000].**

Conditions	Effective dose rates ( $\mu\text{Sv/a}$ )		
	Global directly ionising components.	Global Neutron component	Global total
Outdoors, at sea level	270	48	320
Outdoors, altitude adjusted <sup>a</sup>	340	120	460
Altitude, shielding and Occupancy adjusted <sup>b</sup>	280	100	380

- a altitude weighting factors applied at sea level for directly ionising (1.25) and neutrons (2.5).
- b building shielding factor of (0.8) and indoor occupancy factor of (0.8)

### 2.2.2 Terrestrial radiation

Radionuclides which have been in existence since the creation of the earth are known as primordial radionuclides. They include:  $^{40}\text{K}$  with a half life of  $1.28 \times 10^9$  years,  $^{232}\text{Th}$  with a half life of  $1.41 \times 10^{10}$  years, and  $^{238}\text{U}$  with a half life of  $4.47 \times 10^9$  years. Other primordial radionuclides of secondary importance include:  $^{235}\text{U}$  with a half life of  $7.04 \times 10^8$  years and  $^{87}\text{Rb}$  with a half life of  $4.70 \times 10^{10}$  years. Of these radionuclides, thorium and uranium lead a series of several radionuclides, many of which contribute to human radiation exposure.

A number of industrial operations outside the nuclear fuel cycle may cause the exposure of workers and members of the public to ionising radiation. These industries are called non-nuclear as they are not associated with the production of nuclear materials and do not make use of these materials as a result of their nuclear/radiological properties. The target radionuclides of interest are  $^{226}\text{Ra}$  ( $^{238}\text{U}$ ),  $^{232}\text{Th}$  and their daughter nuclides in the decay series and  $^{40}\text{K}$ .

The uranium atom, consists of three different isotopes: about 99.3% of naturally occurring  $^{238}\text{U}$ , about 0.7%  $^{235}\text{U}$  and trace quantities of (about 0.005%)  $^{234}\text{U}$ . The  $^{238}\text{U}$  and  $^{234}\text{U}$  belong to one family called the uranium series ( $4n+2$ ), while the  $^{235}\text{U}$  isotope belongs to another series called the actinium series ( $4n+3$ ). The most abundant (about 100%) of the naturally occurring radioisotopes  $^{232}\text{Th}$ , is the first member of another long series called the thorium series ( $4n$ ). The identification numbers are based on the divisibility of the mass numbers of each of the series by 4 [Cember, 1996]. Artificial radionuclides, on the other hand, are found in forms that are not easily accessed by members of the public, in an opposite way to what happens with the natural radionuclides with which man keeps a constant contact on a day to day basis. Some of the

potential NORM industries could be in operation for quite a long time before the potential exposure of members of the public and workers is realised.

The natural radionuclides exist in secular equilibrium in natural undisturbed environments [Cember, 1996]. Due to physicochemical processes in the earth crust, such as leaching and emanation, the radiological secular equilibrium in each series may be disturbed [UNSCEAR, 1993, 2000]. Under normal undisturbed secular equilibrium conditions, it has been established that, the mass ratio of  $^{235}\text{U}$  to  $^{238}\text{U}$  is about 0.0073 and activity ratio of 0.046 [UNSCEAR, 1993]. In the case of  $^{40}\text{K}$  they undergo beta decay to stable species ( $^{40}\text{Ca}$ ). These radionuclides are present in varying degrees in water, air, soil and in living organisms. As a result, human beings are exposed to external and internal irradiations by gamma rays, beta particles and alpha particles with varying ranges of energies [UNSCEAR, 1993].

The details of the decay series of these naturally occurring radionuclides are as shown in Tables 2-4, 2-5 and 2-6. A fourth member of the series is the artificially produced, radionuclide neptunium (4n+1) series, which is headed by  $^{241}\text{Pu}$  produced in the laboratory by neutron irradiation of reactor-produced  $^{239}\text{Pu}$  and ends with a stable  $^{209}\text{Bi}$ . It has a half-life of 13 years [Cember, 1996]. The decay series is shown in table 2-7.

**Table 2-4: The Uranium decay series (4n + 2) [Cember 1996 and Darko, 2004]**

Historic Name and Decay Scheme	Atomic Number	Specific Nuclide	Decay Mode	Half-Life
Uranium I ↓	92	<sup>238</sup> U	α	4.51x 10 <sup>9</sup> y
Uranium X <sub>1</sub> ↓	90	<sup>234</sup> Th	β	24.1 days
Uranium X <sub>2</sub> ↓	91	<sup>234</sup> Pa	β	1.18 min
Uranium II ↓	92	<sup>234</sup> U	α	2.45 x 10 <sup>5</sup> y
Ionium ↓	90	<sup>230</sup> Th	α	8.0 x 10 <sup>4</sup> y
Radium ↓	88	<sup>226</sup> Ra	α	1.62 x 10 <sup>3</sup> y
Ra Emanation ↓	86	<sup>222</sup> Rn	α	3.82 days
Radium A 99.98%    0.025 ↓	84	<sup>218</sup> Po	α and β	3.05 min
Radium B' ↓	82	<sup>214</sup> Pb	β	26.8 min
Astatine-218 ↓	85	<sup>218</sup> At	α	2 s
Radium C 99.96%    0.04% ↓	83	<sup>214</sup> Bi	β and α	19.7 min
Radium C' ↓	84	<sup>214</sup> Po	α	164 μ s
Radium C'' ↓	81	<sup>210</sup> Tl	β	1.32 min
Radium D ↓	82	<sup>210</sup> Po	β	22.3 y
Radium E ~100%    2 x 10 <sup>-4</sup> % ↓	83	<sup>210</sup> Bi	β and α	5.0 days
Radium F ↓	84	<sup>210</sup> Pb	α	138.4 days

	81	$^{206}\text{Tl}$	$\alpha$	4.20 min
Radium G (End Product)	82	$^{206}\text{Pb}$	Stable	-

**Table 2-5: The Thorium decay series (4n) [Cember, 1996 and Darko, 2004]**

Historic Name and Decay Scheme	Atomic Number	Specific Nuclide	Decay Mode	Half-Life
Thorium ↓	90	$^{232}\text{Th}$	$\alpha$	$1.41 \times 10^{10}$ y
Mesothorium I ↓	88	$^{228}\text{Ra}$	$\beta$	5.76 y
Mesothorium II ↓	89	$^{228}\text{Ac}$	$\beta$	6.13 h
Radiothorium ↓	90	$^{228}\text{Th}$	$\alpha$	1.91 y
Thorium X ↓	88	$^{224}\text{Ra}$	$\alpha$	3.66 days
Th Emanation ↓	86	$^{220}\text{Rn}$	$\alpha$	56 s
Thorium A ↓	84	$^{216}\text{Po}$	$\alpha$	150 ms
Thorium B ↓	82	$^{212}\text{Pb}$	$\beta$	10.6 hr
Thorium C 66.3%   33.7%	83	$^{212}\text{Bi}$	$\alpha$ and $\beta$	60.6 min
	84	$^{212}\text{Po}$	$\alpha$	$0.3 \mu\text{s}$
	81	$^{208}\text{Tl}$	$\beta$	3.1 min
	82	$^{208}\text{Pb}$	Stable	-

--	--	--	--	--

**Table 2-6: The Actinium ( $^{235}\text{U}$ ) decay series (4n+3) [Cember 1996 and Darko, 2004]**

Historic Name and Decay Scheme	Atomic Number	Specific Nuclide	Decay Mode	Half-Life
Actinouranium ↓	92	$^{235}\text{U}$	$\alpha$	$7.04 \times 10^8 \text{ y}$
Uranium Y ↓	90	$^{231}\text{Th}$	$\beta$	25.5 h
Protactinium ↓	91	$^{231}\text{Pa}$	$\alpha$	$3.28 \times 10^4 \text{ y}$
Actinium 98.8% 1.2%	89	$^{227}\text{Ac}$	$\alpha$ and $\beta$	21.8 y
Radioactinium ↓	90	$^{227}\text{Th}$	$\alpha$	18.7 days
Actinium K ↓	87	$^{223}\text{Fr}$	$\beta$	21.8 min
Actinium X ↓	88	$^{223}\text{Ra}$	$\alpha$	11.4 days
Ac Emanation ↓	86	$^{219}\text{Rn}$	$\alpha$	3.96
Actinium A ~100% ~5 x 10 <sup>-4</sup> %	84	$^{215}\text{Po}$	$\alpha$ and $\beta$	1.78 ms
Actinium B ↓	82	$^{211}\text{Pb}$	$\beta$	36.1 min
Astatine-215 ↓	85	$^{215}\text{At}$	$\alpha$	$\sim 10^4 \text{ s}$
Actinium C 99.7% 0.3%	83	$^{211}\text{Bi}$	$\alpha$ and $\beta$	2.15 min
Actinium C' ↓	84	$^{211}\text{Po}$	$\alpha$	0.52 s

Actinium C''	81	$^{207}_{81}\text{Tl}$	$\beta$	4077 min
↓ Actinium D (End Product)	82	$^{207}_{82}\text{Pb}$	Stable	-

**Table 2-7: The Neptunium decay series ( $4n+1$ )<sup>a</sup> [Cember, 1996 and Darko, 2004]**

Historic Name and Decay Scheme	Atomic Number	Specific Nuclide	Decay Mode	Half-Life
--------------------------------	---------------	------------------	------------	-----------



Plutonium ↓	94	$^{241}\text{Pu}$	$\beta$	14.4 y
Americium ↓	95	$^{241}\text{Am}$	$\alpha$	433 y
Neptunium ↓	93	$^{237}\text{Np}$	$\alpha$	$2.14 \times 10^6$ y
Protactinium ↓	91	$^{233}\text{Pa}$	$\beta$	27.0 days
Uranium ↓	92	$^{233}\text{U}$	$\alpha$	$1.59 \times 10^5$ y
Thorium ↓	90	$^{229}\text{Th}$	$\alpha$	$7.3 \times 10^3$ y
Radium ↓	88	$^{225}\text{Ra}$	$\beta$	14.8 days
Actinium ↓	89	$^{225}\text{Ac}$	$\alpha$	10.0 days
Francium ↓	87	$^{221}\text{Fr}$	$\alpha$	4.8 min
Astatine ↓	85	$^{217}\text{At}$	$\alpha$	32.3 ms
Bismuth 98% 2%	83	$^{213}\text{Bi}$	$\alpha$ and $\beta$	45.6 min
Polonium ↓	84	$^{213}\text{Po}$	$\alpha$	4 $\mu$ s
Thallium ↓	81	$^{209}\text{Tl}$	$\beta$	2.2 min
Lead ↓	82	$^{209}\text{Pb}$	$\beta$	3.25 h
Bismuth (End Product)	82	$^{209}\text{Bi}$	$\alpha$	$<2 \times 10^{18}$ y

The exposure to radiation could occur externally to the human body or internally within the human body. In the case of external exposures outdoors, it could be as a result of the presence of radionuclides in trace quantities in soils. The levels of radionuclides are related to the

type of rock from which the soil originates. According to the UNSCEAR 2000 report, higher radiation levels are associated with igneous rocks such as granite and the levels are lower in sedimentary rocks. Also phosphate rocks are known to contain relatively high content of radionuclides [UNSCEAR, 2000].

The activity concentrations of  $^{40}\text{K}$  in soil have been found to be higher than  $^{238}\text{U}$  and  $^{232}\text{Th}$ . According to the UNSCEAR report [UNSCEAR, 1982], activity concentrations of 370 Bq/kg, 25 Bq/kg, 25 Bq/kg have been reported for  $^{40}\text{K}$ ,  $^{238}\text{U}$  and  $^{232}\text{Th}$  respectively. Other sources have reported activity concentrations of 35 Bq/kg, 30 Bq/kg, and 400 Bq/kg for  $^{238}\text{U}$ ,  $^{232}\text{Th}$  and  $^{40}\text{K}$  respectively [Bozkurt et al., 2007; UNSCEAR, 2000].

The reported worldwide annual average absorbed dose rate in air from terrestrial gamma radiation is estimated to be 59 nGy/h in a typical range of 10 to 200 nGy $^{-1}$  [UNSCEAR, 2000]. The direct measurements of the indoor and outdoor absorbed dose rates in air in some countries have reported average values of 59 and 57 nGy/h respectively [UNSCEAR, 1993]. High dose rates have been measured in different parts of the world such as the Nile Delta where dose rates in air have been estimated to be in a range of 20-400 nGy/h and also in the Ganges Delta in a range of 260-400 nGy/h. Dose rates of the order of 12,000 nGy/h have also been measured in thorium-bearing carbonatite in an area near Mombasa on the coast of Kenya. In Brazil, where there is mixed thorium and uranium mineralization, dose rates measured are roughly in a range of 100-3500 nGy/h [UNSCEAR, 2000].

According to literature, thorium bearing and uranium bearing materials have resulted in higher absorbed dose rates around the world [UNSCEAR, 1993]. The estimation of the annual effective doses from these activity concentrations takes into account the following factors:

- The conversion coefficient from absorbed dose in air to effective dose of 0.7 Sv/Gy,

- Indoor and outdoor occupancy factors of 0.8 and 0.2 respectively and these are age and climate (location) dependent [UNSCEAR, 1993, 2000].

Internal exposure to radiation is mainly due to ingestion and inhalation of materials containing  $^{238}\text{U}$  and  $^{232}\text{Th}$  decay series and  $^{40}\text{K}$ . The committed effective doses are determined through analysis of the radionuclide contents in foods and water following an intake and in addition to bioassay data and knowledge on the metabolic behaviour of the radionuclides [UNSCEAR, 2000]. Concentrations of NORM in foods vary widely because of differences in background levels, climate and the agricultural conditions that prevail. The body content of  $^{40}\text{K}$  is about 0.18 % for adults and 0.2 % for children. The natural abundance is about  $1.17 \times 10^{-4}$  % and specific activity concentration of  $2.6 \times 10^8$  Bq/kg. The corresponding annual effective doses from  $^{40}\text{K}$  in the body are 165 and 185  $\mu\text{Sv a}^{-1}$  for adults and children respectively. The total annual effective dose from inhalation and ingestion of terrestrial radionuclides is 310  $\mu\text{Sv}$  of which 170  $\mu\text{Sv}$  is from  $^{40}\text{K}$  and 140  $\mu\text{Sv}$  from the long-lived radionuclides in the uranium and thorium series [UNSCEAR, 2000]. Uranium in the body is retained primarily in the skeleton and the concentrations have been found to be approximately similar in various types of bones. Similarly, thorium is mainly deposited on bone surfaces and retained for a long period following intake by ingestion and inhalation. The annual effective dose from reference values of U/Th series radionuclides has been evaluated to be 130  $\mu\text{Sv}$  [UNSCEAR, 1988, 1993] and re-evaluated in the year 2000 to be 120  $\mu\text{Sv}$  [UNSCEAR, 2000]. The main contributor to this dose is  $^{210}\text{P}$  (half-life, 138.9 days). This value compares well with the estimated value of 110  $\mu\text{Sv}$  derived from dietary consumption by adults and the reference concentrations in food and water.

### **2.2.3 Exposure from radon**

Radon is a gas with three natural isotopes of the radioactive element: Actinon, ( $^{219}\text{Rn}$ ) from the  $^{235}\text{U}$  decay series; Thoron ( $^{220}\text{Rn}$ ) from the  $^{232}\text{Th}$  decay series; and Radon ( $^{222}\text{Rn}$ ) from the  $^{238}\text{U}$  decay series [UNSCEAR, 1993].

Due to the low activity concentration of  $^{235}\text{U}$  and the short half-life of  $^{219}\text{Rn}$  of 3.96 s, the radiation exposure from  $^{219}\text{Rn}$  is not significant for human exposure. Radon-220 ( $^{220}\text{Rn}$ ), with a half-life of 55.6 s is of concern only when the concentration of  $^{232}\text{Th}$  is high.

The isotope of concern in terms of human radiation exposure is  $^{222}\text{Rn}$  which has a relatively longer half-life of 3.82 days. It is a noble gas with a slight ability to form compounds under laboratory conditions. It has a density of 9.73 g/L at 0 °C. The solubility of  $^{222}\text{Rn}$  in water at 0 °C is 510 cm<sup>3</sup>/L decreasing to 220 cm<sup>3</sup>/L at 25 °C and 130 cm<sup>3</sup>/L at 50 °C.

The production of  $^{220}\text{Rn}$  and  $^{222}\text{Rn}$  in terrestrial materials depends on the activity concentrations of  $^{228}\text{Ra}$  and  $^{226}\text{Ra}$  present, respectively which are predominantly alpha emitters. Radon is the most significant element of human irradiation by natural sources. The most significant mode of exposure is the inhalation of the short-lived products,  $^{210}\text{Pb}$  and  $^{210}\text{Po}$  of the parent isotope  $^{222}\text{Rn}$  [UNSCEAR, 1993; 1996 and 2000].

The concentrations of  $^{222}\text{Rn}$  in surface air are quite variable with time-average concentrations in the range of 2-30 Bq/m<sup>3</sup> [UNSCEAR, 1993]. In the soil and also in the root zone, radon concentrations may be higher by a factor of about 1000 than in the open air [UNSCEAR, 1996]. The average concentration varies widely depending on the composition of the soil and the bedrock. For soil with an average  $^{226}\text{Ra}$  concentration of 40 Bq/kg, the average  $^{222}\text{Rn}$  concentration in the soil water would be about 60 Bq/m<sup>3</sup>. Much higher values of 8000 Bq/m<sup>3</sup> and 50,000 Bq/m<sup>3</sup> have been measured in deep ground waters in areas such as Maine in the United States of America and in Finland respectively [UNSCEAR, 1996]. The action level of

radon recommended by the ICRP for which intervention is necessary is  $1000 \text{ Bq/m}^3$ . This value is based on an assumed occupancy of 2000 hours per year and this is equivalent to an effective dose of 6 mSv per year. This value is also the midpoint of a range of  $500\text{-}1500 \text{ Bq/m}^3$  [ICRP, 1993]. Radon can present hazards in a wide range of work places including the mining industry and other work places other than the mines. Specific measures need to be put in place to reduce radon concentrations in air and water to prevent concentrations reaching very high levels even in places where the concentrations of uranium and radium in raw materials may be very low [UNSCEAR, 2000]. The mechanisms by which radon enters buildings is pressure driven flow of gas from soil through cracks in the floor. In addition, most building materials produce some radon due to the presence of elevated levels of  $^{226}\text{Ra}$  and high porosity of the materials allow for the escape of the gas [Van der Steen and Van Weers, 1996].

It is also known that, inhalation of short-lived decay products  $^{210}\text{Pb}$  and  $^{210}\text{Po}$  of  $^{222}\text{Rn}$  and to a lesser extent  $^{220}\text{Rn}$  and their subsequent deposition along the walls of the various airways of the bronchial tree provide the main pathway for radiation exposure of the lungs [UNSCEAR, 2000]. The exposure is mostly due to the alpha particles emitted by these radionuclides as well as the beta particles and the gamma radiation emitted during the decay process. According to UNSCEAR 2000 report [UNSCEAR, 2000], there is a general agreement among scientists that it is the alpha particle irradiation of the secretary and basal cells of the upper airways that is responsible for the lung cancer risk in miners [UNSCEAR, 2000]. There are some uncertainties as to which cells are the most important for the induction of lung cancer

Radon generation and transport in porous materials involve solid, liquid and gaseous phases through the process of emanation, diffusion, advection, absorption in the liquid phase and

adsorption in the solid phase [Nielson et al., 1994 and Rogers et al., 1991]. The main mechanism for the entry of radon into the atmosphere is molecular diffusion.

Some factors that may influence the levels of  $^{222}\text{Rn}$  concentration in soil, water and air include the following:

1. Grain or particle and shape determine the emanation of radon from the soil. The emanation factor is inversely proportional to the grain size;
2. Soil moistures control the emanation of radon and diffusion in soil by capturing the radon recoils from the solid matrix;
3. Advection caused by wind and changes in barometric pressure between the building shield and the ground around the foundation;
4. Temperature, the solubility of radon in water decreases with temperature;
5. The geology, which determines the  $^{226}\text{Ra}$  concentration and climatic conditions;
6. The distribution and concentrations of the parent radium radionuclides in the bedrock and overburden and permeability of the soil;
7. Seasonal variation because  $^{222}\text{Rn}$  in soil gas vary over many orders of magnitude from place to place and also show a significant time variations at any given site.

Both theoretical estimates and laboratory tests have shown that radon adsorption on soil grains decreases rapidly with increasing water content, becoming more significant in the water content greater than about 0.3-0.4 of saturation [Rogers et al., 1991]. At high water content, the pores become blocked by water and diffusion decreases. If there is less adsorption of the radon gas, there is an increase in emanation factor at low water contents [UNSCEAR, 2000]. Also, the solubility of radon in water decreases with increasing temperature. The partition coefficient of radon between water and gas, the Ostwald Coefficient  $K$ , which is a measure of the ratio of

concentrations of radon in water to air [Andersen, 1992; Clever, 1979; Washington and Rose, 1992] varies from 0.53 at 0 °C to 0.23 at 25 °C in water and typically 0.30 at 15 °C. The partitioning as well as an increased emanation may cause the concentration of radon in air-filled pores to be higher under moist conditions than under dry conditions [Andersen, 1992; Washington and Rose, 1992].

The concentration of radon in soil gas  $C_{Rn}$  in the absence of radon transport is determined from the expression below [Nazaroff et al, 1988; Washington and Rose, 1992]:

$$C_{Rn} = C_{Ra} f \rho_s \varepsilon^{-1} (1 - \varepsilon) (m[k_T - 1] + 1)^{-1} \quad (4)$$

Where;

- $C_{Ra}$  - is the concentration of radium in soil, Bq/kg
- $f$  - is the emanation factor, 0.2
- $\rho_s$  - the density of the soil grains, 2700 kg/m<sup>3</sup>
- $\varepsilon$  - the total porosity, including both water and air phases, 0.25
- $m$  - the fraction of porosity that is water filled 0.95 and for dry soil  $m$  is zero.
- $k_T$  - is the partition coefficient for radon between the water and the air phases of 0.23 at 25 °C for warm moist soil.

Radon dissolved in water may enter indoor air through de-emanation when the water is used. The water supply contribution depends on the concentration of radon in the water used for showering and laundering and sometimes can be important. The concentration of radon in water may range over several orders of magnitude, generally being highest in well water, intermediate in ground water and lowest in surface water [UNSCEAR, 2000].

Improvements in ventilation systems may change radon concentrations by less than 50 %.

The outdoor radon concentrations can vary diurnally by a factor of as much as ten. The concentration of radon during the day time tends to be transported upwards away from the ground due to solar heating. At night and early morning, as a result of atmospheric (temperature) inversion conditions, the radon tends to be trapped closer to the ground [UNSCEAR, 2000].

For indoor Rn concentration, the distribution of worldwide values of 40 and 30 Bq/m<sup>3</sup> respectively of arithmetic and geometric mean have been reported [UNSCEAR, 2000]. Time-averaged concentrations in surface air in normal areas may be in a range of 2-30 Bq/m<sup>3</sup> [UNSCEAR, 1996]. The average concentrations of Rn in ground water vary widely depending on the composition of the soil and bedrock. In the case of plants (vegetables), <sup>222</sup>Rn decay products of <sup>210</sup>Pb and <sup>210</sup>Po are the major contributors to the dose to the plants. For instance, <sup>210</sup>Pb may be taken up by plants through roots and leaves. The average concentration of <sup>210</sup>Pb in leaves and needles are 10 and 5 Bq/kg respectively [UNSCEAR, 1996].

The dosimetric evaluation of the absorbed dose to the basal cells of the bronchial epithelium per unit exposure gives values in the range of 5–25 nGy per Bqh/m<sup>3</sup> for average indoor conditions. The central value is estimated to be 9 nGy per Bqh/m<sup>3</sup> for average indoor conditions with a breathing rate of 0.6 m<sup>3</sup>/h, aerosol median diameter of 100-150 nm and an attached fraction of 0.05 [ICRP, 1994; UNSCEAR, 1996 and 2000]. The average absorbed doses per unit exposure for different indoor and outdoor environments vary from 10 to 50 nSv per Bqh/m<sup>3</sup>.

An alternative to the dosimetric approach to the dose assessment is the use of the conversion convention of radon exposures developed by the ICRP from equality of detriments from epidemiological studies. The nominal mortality probability coefficient for radon for males and females is taken to be  $8 \times 10^{-5}$  per mJhm<sup>-3</sup> determined from the occupational studies of

miners. This coefficient is related to the detriment per unit effective dose of  $5.6 \times 10^{-5}$  per mSv for workers and  $7.3 \times 10^{-5}$  per mSv for the public [UNSCEAR, 1996]. The corresponding values of the conversion convention are  $1.43 \text{ mSv per mJhm}^{-3}$  and  $1.10 \text{ mSv per mJhm}^{-3}$  and these are calculated as  $(8 \times 10^{-5}/5.6 \times 10^{-5})$  and  $(8 \times 10^{-5}/7.3 \times 10^{-5})$  respectively [UNSCEAR, 2000]. From the range of dose conversion factors, from 6 to 15 nSv per Bqhm<sup>-3</sup> derived from the epidemiological studies and physical dosimetry [UNSCEAR, 1996] a value of 9 nSv per Bqhm<sup>-3</sup> used in the earlier UNSCEAR calculations is still appropriate for effective dose calculations [UNSCEAR, 1998, 1993]. Thus, from a measured radon concentration, and applying an indoor equilibrium factor of 0.4 or outdoor equilibrium factor of 0.6, an occupancy factor (indoor or outdoor) and the radon dose coefficient, the annual effective dose can be calculated [UNSCEAR, 2000].

In assessing the dose from the exposure to radon gas several exposure pathways need to be taken into account to determine the total annual effective dose. Some of the potential pathways include; inhalation of <sup>222</sup>Rn and its decay products present in air from all sources, radon gas dissolved in blood and radon gas in ingested tap water [UNSCEAR, 2000]. The annual effective dose can be calculated from the measured radon concentration in air as follows:

$$D_{Rn} = k(Rn)_A FC_{Rn} t_{exp} \quad (5)$$

Where;  $k(Rn)_A$  is the dose coefficient pertaining to the dose convention following ICRP publication 65 in mSv per Bq.h/m<sup>3</sup>.

F is the equilibrium factor of 0.4 or 0.6 for indoor and outdoor occupancy respectively.

$t_{exp}$  is the annual exposure time (h)

$C_{Rn}$  is the Rn concentration (Bq/m<sup>3</sup>).

### 2.2.3.1 Hazards associated with radon

The hazards and risk due to exposure to radon gas from NORM contaminated material is estimated from the radon emanation fraction. Radon emanation fraction (EF) is defined as the fraction of radon atoms formed in a solid that escapes from the solid and is free to migrate [White and Rood, 2001; Afifi et al., 2004]. The physical properties of  $^{226}\text{Ra}$  bearing material determine the  $^{222}\text{Rn}$  emanation fraction of the material [White and Rood, 2001]. These properties include: the distribution of  $^{226}\text{Ra}$  in the material; the structure of the material (whether massive or granular); type and magnitude of porosity of the material; the moisture content of the material. The amount of  $^{222}\text{Rn}$  emanating off the pore spaces is smaller when compared to the emanation fraction of a typical soil. It has been established that typical emanation coefficients for rocks and soils range from 0.05 to 0.7 [Nazaroff et al., 1988].

Studies conducted in various industries producing NORM have reported various EF values. In a study in which EF of  $^{222}\text{Rn}$  in TE-NORM scale wastes associated with oil and gas production was carried out, values between 0.02 to 0.087 were reported [Tanner, 1980]. Similarly, a study on the EF of  $^{222}\text{Rn}$  associated with metal processing (rare earth's and uranium milling) have reported a value of 0.3 [USEPA, 1993; Egidi and Hull, 1999]. Studies have also established that  $^{222}\text{Rn}$  EF of different NORM materials differs with the order as follows: mining > gypsum > oil and gas > coal power plant [Afifi et al., 2004]. It has also been established that, the variation of EF is independent of the  $^{226}\text{Ra}$  content and is strongly correlated to the grain surface density [Tanner, 1980; Colle et al., 1981; White and Rood, 2001]. The smaller the grain size, the higher the EF as reported in a study by Afifi et al (2004). As a result, the samples prepared for EF of  $^{222}\text{Rn}$  determination were not crushed or otherwise further reduced in size beyond that which occurred during the field sampling.

#### **2.2.4 Potential industrial activities from which NORM is produced.**

A number of industrial and other human activities have been identified as potential areas in which substantial amount of natural radionuclides could be turned out during processing and these are broadly categorised into the following:

1. Mineral processing industries
2. Fossil fuel combustion

During the process of mining, transportation and processing of these materials, the consequent emissions of radionuclides to air and water bodies could lead to potential exposure of humans [UNSCEAR, 2000]. Some of the industries in the above categories include:

- Phosphate processing e.g. fertilizer production;
- Metal ore processing including tinstone (tin), tantalite, columbite, fergusonite, koppite, arsenopyrites, etc;
- Uranium mining;
- Zircon sands;
- Titanium pigment products;
- Fossil fuels;
- Oil and gas extraction in which large volumes of production water could contain significant quantities of NORM predominantly  $^{226}\text{Ra}$  from scaling through precipitation in pipes;
- Building materials e.g. clay, Portland clinker, fly ash etc;
- Scrap metal industries.

Several studies have been carried out in some countries over the past decade on various NORM industries. From these studies, the levels of  $^{238}\text{U}$ ,  $^{232}\text{Th}$  and  $^{40}\text{K}$  in different media have been reported for different countries [IAEA, 2005]. All these studies have been carried out with

the primary aim of assessing the public and occupational exposure situations [UNSCEAR, 1982, 1988, 1996, 2000 and Darko et al., 2008]. A number of studies have been carried out in developed countries and very little work done in the less developed countries including Ghana. As a result there is very little data available with regards to the public and the occupational exposure levels [Darko et al., 2008].

A study in Ghana by Darko et al., (2010) in two of the mining companies to assess the levels of public exposure has reported an average annual effective dose of  $0.3 \pm 0.06$  mSv. Similar studies needed to be carried out in all the potential NORM industries in Ghana based on which effective guidelines could be formulated for the purpose of radiation protection of the public and the workers.

The methodology of this work was based on identifying all the potential exposure pathways through which an individual could be exposed internally or externally.

Internal exposure occurs from the inhalation of contaminated dust, ingestion of contaminated water, food and the inhalation of radon gas and its progeny.

This is important because, the pathway by which NORM can reach humans is quite complex, thus a significant approach to establish the pathways that contribute significantly is essential [O'Brien and Copper, 1998]. The environmental cycles for naturally occurring radionuclides are similar in principle and differing due to differences in radioactive decay times (Half-life) and differences in the chemical behaviour [O'Brien and Copper, 1998]. Generally there are two broad pathways of exposure:

#### **A. On-site Pathways.**

This pathway of exposure tends to be direct due to external exposure to gamma radiation and also internal exposure due to inhalation of radioactive dust or radon progeny. The build up of radioactive dust on floors, equipment surfaces, sludge in pipes and storage tanks during mining processes could be the sources of external exposure. In underground mines, the presence of NORM in rocks and soils could lead to enhanced levels of NORM unless careful attention is given to the design and use of suitable ventilation system in the mines [O'Brien and Copper, 1998]. In the case of the open-pit mines, as is the case of the Tarkwa Goldmine, work practices have to be carefully controlled to minimize the radiological risk to the on-site work-force [O'Brien and Copper, 1998]. The analysis of the on-site pathways involves detailed knowledge of the mining processes at the site.

#### **B. Off-site Pathways.**

This involves analysis of the scenarios through which people living in the vicinity of the mine could be exposed. The off-site exposures could occur from transfer of NORM through the environmental pathway or from the use of waste containing NORM [O'Brien and Copper, 1998]. The exposure tends to be indirect and more complex than the on-site exposure situations [O'Brien and Copper, 1998]. The transfer could be through the food chain [Dahlgaard, 1996] through water bodies (rivers and oceanic transport) [McDonald et al., 1996] and by atmospheric dispersion through re-suspension of radioactive dust. A conceptual analysis of the potential sources of exposure and pathways is necessary to ensure that unnecessary exposures are minimized [O'Brien and Copper, 1998]. Some of the exposure situations could include the use of mine waste as landfill or for building purposes.

Some of the source terms of NORM in both on-site and off-site could include; On-site the mine, NORM could be found in stockpiles, in storage tanks and also build-up on equipment

surfaces, pipes and storage tanks, etc [O'Brien and Copper, 1998]. In terms of public exposure (off-site) external exposures could result from exposure to gamma radiation from the passage of cloud shine and ground shine [O'Brien and Copper, 1998].

The radiological impact of internal exposures is usually assessed by direct measurement of the body burden to determine the activity concentrations and the doses to particular organ or group of organs by means of mathematical models. An overview of methodologies and equations for estimating annual doses resulting from exposure to NORM waste are cited in literature [O'Brien and Cooper 1998; Darko et al 2010; DOE, 2003].

Some of the industrial activities enhancing exposure from natural sources involve large volumes of raw materials containing natural radionuclides. Discharges from the industrial plants to air, water and the use of by-products and waste materials may be the main contributors to enhanced exposures of the general public. Estimated maximum exposures are greatest for phosphoric acid production and the mineral sands-processing industries. Under normal conditions of operations, annual doses are in the range of 1-10  $\mu\text{Sv/a}$ , although doses in the order of 100  $\mu\text{Sv/a}$  could be expected to be received by residents [UNSCEAR, 2000].

### **2.3 Hazards and risk associated with exposure to NORM in the mines.**

Risk from exposure to environmental level radiation requires an assessment of the radiological hazard following the exposure. According to the National Research Council (NRC) of USA, Risk is defined as the characterization of the potential adverse health effect of human exposures to environmental hazards [NRC, 1983]. Due to the stochastic nature of the adverse effects of the exposure, together with their extremely low probability of occurrence, risk assessments/estimates has always been based on studies on large population groups using mathematical models. The most current of such studies is that by the U.S. National Academy of

Sciences Committee on the Biological Effects of Ionizing Radiation (BEIR Committee) known as BEIR V Report [NAS, 1990] and the latest version of BEIR VII [NAS, 2006]: Health Effects of Exposure to low levels of Ionizing Radiation. This assessment was based on a review of new scientific information from several different studies including:

- Epidemiological studies of Japanese survivors of nuclear bombing during World War II;
- Radiation accidents;
- Patients who had been exposed to radiation during the course of their medical treatments;
- Laboratory studies on chemistry, physics and biology of ionizing radiation [Cember, 1996].

Studies by American Health Physics Society has recommended against quantitative estimation of radiation health risk below an individual dose of 50 mSv per year, additional to background radiation. The reason is that, there is no conclusive evidence of health risks for low dose rate up to 50 mSv/year [HPS, 1996].

The BEIR V Committee also found that, for all cancers except Leukaemia and also the genetic effects observed in laboratory studies, the data were compatible with the linear, zero threshold model. This model was therefore chosen as the basis for estimating the risk coefficients for solid tumours from low dose radiation and for leukaemia, the linear quadratic model was chosen for estimating the risk coefficients for leukaemia [Cember, 1996]. The committee also found that, for the incidence of radiogenic cancer, the data supported a dose related increase in the relative risk model in which the spontaneous incidence was multiplied by a factor that

depended on the specific cancer [Cember, 1996]. The relative risk model is generally expressed mathematically as follows [NRC, 1990].

$$\lambda(d) = \lambda_0[1 + f(d)g(\beta)] \quad (6)$$

Where;

$\lambda(d)$  is the total fatal cancer risk,

$\lambda_0$  is the individual's age and gender specific mortality rate for a given type of cancer in the absence of radiation exposure but that due to natural background,  $f(d)$  is a function of effective dose in Sievert and it depends on the type of cancer,  $g(\beta)$  is the excess risk function which is gender specific and also depends on the age at exposure of individual and the time since exposure.

From equation (6), the term  $1 + f(d)g(\beta)$  represents the radiation induced fatal cancer risk. In the BEIR V methodology, apart from the leukaemia which obeyed the linear-quadratic dose-response relationship, other cancers such as digestive tract cancer, respiratory tract cancer, female breast cancer and others all followed the linear dose-response relationship. The BEIR V methodology of cancer risk assessment could not be used for this work because it was important to determine the individual organ doses to the population in the study which was virtually not feasible. The excess absolute risk model is also used to compare the incidence of diseases or mortality in an exposed population minus that from an unexposed population whilst in the case of the relative risk model the risk component from an exposed population is divided by that from an unexposed population minus 1.0. It is almost impossible to determine unexposed population in reality.

The ICRP methodology of estimation of fatality cancer risk and hereditary effect was used instead of the risk estimation for this work [ICRP, 1991; 2007]. The ICRP methodology of

risk estimation for the purpose of radiological protection is normally based on the understanding of the biological effects due to radiation exposure. The ICRP in its 2007 recommendation, has noted that for absorbed doses ranging up to around 100mGy for both low and high linear energy transfer (LET), no tissues are judged to express clinically relevant functional impairment for deterministic effect [ICRP, 2007]. In their view, the emphasis now should be on stochastic effect and primarily on cancer and also hereditary disorders. In their review also, the Commission also recognises challenges with its linear non-threshold model and concludes that for the purposes of radiological protection, it is reasonable to assume that the incidence of cancer or hereditary disorders will rise in direct proportion to an increase in equivalent dose to organs and tissues below about 100 mSv [ICRP, 2007]. In addition, the new recommendations also recognises that, there are growing amount of evidence to suggest the incidence of radiation-associated health consequences such as heart diseases; stroke; digestive disorders and respiratory diseases, but data as at now is inconclusive

In addition to the assessment of the radiological hazard of NORM elements in a mine,  $^{226}\text{Ra}$  equivalent concentration ( $R_{\text{eq}}$ ), the external and internal hazard indices need to be calculated.  $R_{\text{eq}}$  is a widely used hazard index. It is based on the estimation that 370 Bq/kg of  $^{226}\text{Ra}$ , 259 Bq/kg of  $^{232}\text{Th}$  and 4810 Bq/kg of  $^{40}\text{K}$  produce the same gamma ray dose rate [Xinwei et al., 2006]. The values of the external and internal hazard indices must be less than 1.0 for the radiation hazard to be considered negligible i.e. the radiation exposure due to the radioactivity from the construction material is limited to 1.5 mSv/y [Beretka and Mathew, 1985]. Also, radon and its short-lived products are hazards to the respiratory organs and as a result, the internal exposure to radon and its daughter products is quantified using the internal hazard index.

#### **2.4 Biological Effect of Radiation**

The damage that may arise as a result of interaction of radiation with the human body may be death or modification of cells that will affect the function of organs or tissues resulting in deterministic or stochastic effect. The damage to the deoxyribonucleic acid (DNA) in the nucleus is the main initiating event by which radiation causes long-term harm to organs and tissues in the body [UNSCEAR, 2000]. It has been reported that double strand breaks in DNA are responsible for causing critical damage. Disrepair and radiation damage could also lead to potential for progression to cancer induction or hereditary disease [UNSCEAR, 2000]. The mechanism of the biological effect arising from exposure to ionizing radiation is a result of direct and indirect actions:

#### Direct Action

When the body is overexposed to ionizing radiation, a series of long and complex events are initiated through ionization or excitation of relatively few molecules in the body. The effects of radiation in which zero threshold doses are postulated could be thought to be as a result of direct ionisation and excitation of molecules with the consequent dissociation of the molecule [Cember, 1996]. The dissociation, due to ionization or excitation of an atom on the DNA molecule prevents the information originally contained in the gene from being transmitted to the next generation. Such point mutations may occur in germinal cells in which the point mutation is passed onto the next individual or it may occur in the somatic cells which results in a point mutation in the daughter cell. Since these point mutations are thereafter transmitted to succeeding generations of cells, it is clear that, for those biological effects of radiation that depend on point mutations, the radiation dose is cumulative, every little dose may result in a change in the gene burden, which is continuously transmitted [Cember, 1996].

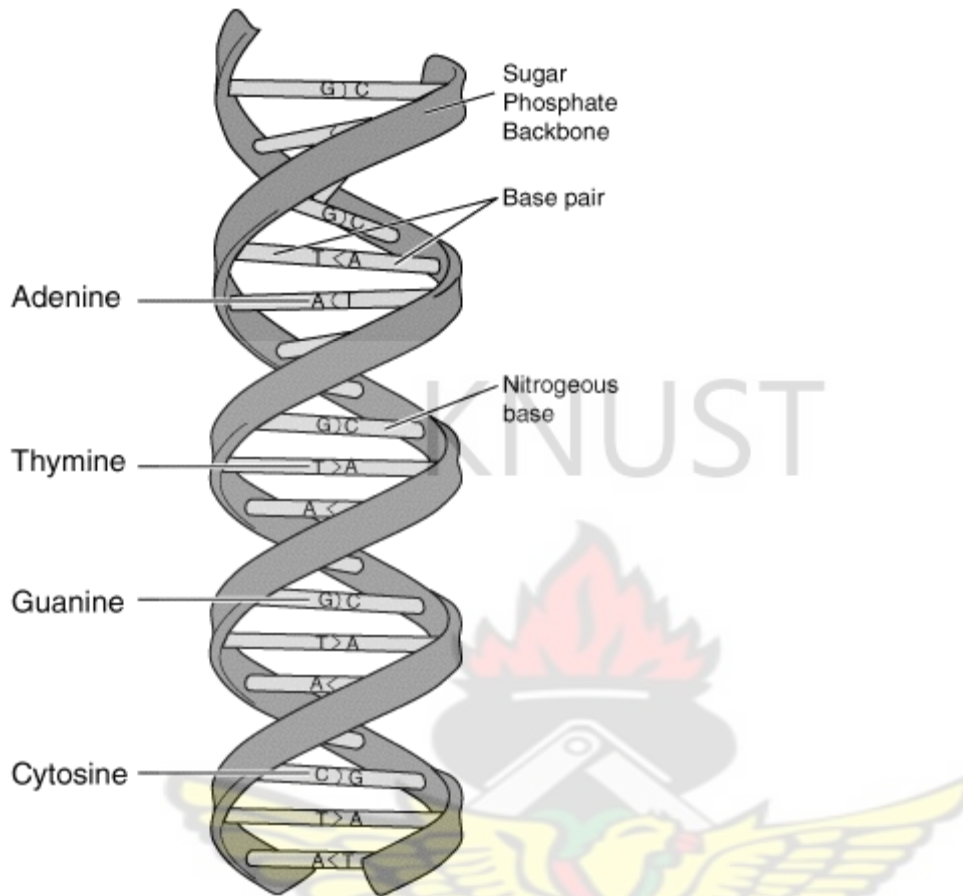
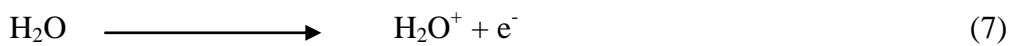


**Figure 2-1 Structure of the DNA molecule**

Indirect Action

About 70-75 % of the human body is made up of water and most of the direction action of radiation is therefore with water molecules. This leads to absorption of energy by water molecules which results in the production of highly reactive free radicals that are chemically toxic [Cember, 1996]

Thus, when the human body is irradiated with ionizing radiation, the following chemical reactions occur:





The free electron in equation (7) interacts with neutral water as follows:



The  $\text{H}^+$  and  $\text{OH}^-$  ions produced from these 4 equations above do not pose any hazard since the body fluids already contain significant concentrations of these ions. However, the free radicals  $\text{H}$  and  $\text{OH}$  may combine with like radicals or react with other molecules in solution [Cember, 1996]. The  $\text{OH}$  free radicals formed may combine with each other leading to the production of hydrogen peroxide as follows:



Similarly, the free  $\text{H}$  radicals combine to form gaseous hydrogen as follows:



Furthermore, if the irradiated water contains dissolved oxygen, the free  $\text{H}$  radical may combine with oxygen to form the Hydroperoxyl radical as follows:



The hydroperoxyl formed is not very reactive and has longer lifetime than the free  $\text{OH}$  radical and is able to combine with free  $\text{H}$  radical leading to the formation of  $\text{H}_2\text{O}_2$  as follows:



The  $\text{H}_2\text{O}_2$  formed in equations (11) and (14) are relatively stable compounds, very powerful oxidising agent and can affect molecules or cells that did not suffer radiation damage directly. The  $\text{H}_2\text{O}_2$  produced from equation (14) further enhances the toxicity of the radiation. The reaction mechanisms of both the direct and indirect actions are shown in figure 2-2.

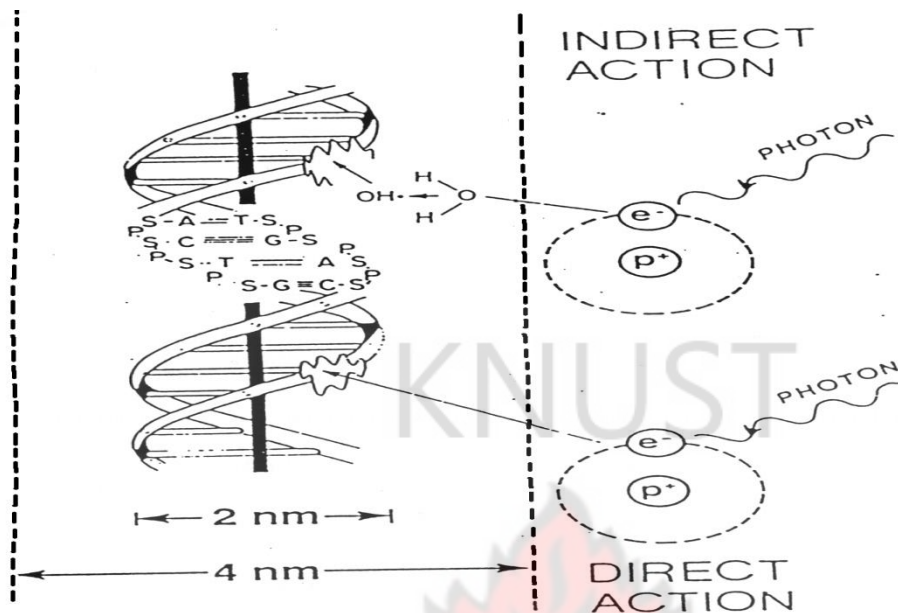


**Figure 2-2: Mechanisms of direct and indirect actions on DNA molecule.**

## 2.5 Instrumentation for measurement of natural radioactivity in environmental samples

There are many different types of instruments available for measuring ionising radiation in samples. Some of the instruments include: gas filled detectors (ionisation chamber counters, proportional counters, and Geiger-Muller counters); scintillation counters; and solid state detectors (semi conductor detectors). The basic requirement of the instruments is that, the radiation interacts with the detector in such a manner that the magnitude of the instrument's response is proportional to the radiation effect or the radiation property being measured [Cember, 1996 and IAEA, 1989]. For the detector to respond, the radiation must have undergone one of the following interactions:

- Photoelectric effect;
- Compton scattering;

- Pair production.

The result of the interaction in a detector is the appearance of a given amount of electric charge within the detector's active volume [Cember, 1996]. Ionising radiation (gamma rays) interacts with atoms in the sensitive volume of the detector to produce electrons by ionisation. The collection of the electrons leads to an output pulse (signal).

The energy required to produce ionisation event in semi conductor detectors is 3.5 eV in contrast to the gas filled detectors which requires a mean high energy of 30-35 eV [Cember, 1996]. A semi conductor is a substance that has electrical conducting properties midway between a conductor and an insulator. The most commonly used semiconductor materials are silicon and germanium. These elements belong to group IV of the periodic table implying each element has four (4) valence electron and will form crystal that consist of a lattice of atoms joined together by covalent bonds. Through the absorption of energy, the covalent bonds could be disrupted. Energy of 1.12 eV is required to knock out one of the valence electrons in silicon resulting in free electron and "hole" in the position formerly occupied by the valence electron. The free electron and hole can move about in the crystal lattice. Electrons adjacent the hole can jump into the hole and leave behind another hole. If the semi conductor is connected in a closed electrical circuit, current will flow through the semi conductor [Cember, 1996]. This implies that, the operation of the semi conductor radiation detector depends on having excess electrons or excess holes. A semi conductor with excess electrons is called n-type semi conductor, whilst the one with excess holes is called p-type semi conductor. These are achieved by adding an impurity to the crystal, either with excess number of electrons or an excess number of holes. If an atom of an element in group V such as phosphorus, arsenic, antimony etc is added to a pure silicon or germanium, four covalent bonds will be formed leaving behind an excess electron which is free to move about in

the crystal and to participate in the flow of electric current. Under this condition, the crystal is of the n-type. On the other hand, p-type semi conductor is produced by adding an impurity from a group III such as boron, aluminium, gadolinium or indium which have three valence electrons. As a result, only three covalent bonds are formed in the crystal lattice. The deficiency of one electron results in a hole leading to the formation of p-type semi conductor detector [Cember, 1996]. If a p region in silicon or germanium is adjacent to an n region, an n-p junction is created. If a forward bias is applied to the junction by connecting the p region to the positive terminal and the n region to the negative terminal, current will flow across the junction. However, if the polarity of the applied voltage is reversed, by connecting the n region to the positive terminal and the p region to the negative terminal, a condition known as reversed bias is achieved. Under this condition, no current will flow across the junction. The region around the junction is swept free by the potential differences created by the holes and electrons in the p and n regions. This region is known as the depletion layer and it is the sensitive volume of the solid-state detector.

Thus, when ionising radiation passes through the depletion layer, electron-hole pairs are produced as a result of ionising collisions between the ionising radiations and the crystal. The electric field then sweeps the holes and electrons apart, giving rise to a pulse in the load resistor as the electrons flow through the external circuit. Semi conductor detectors are especially useful for nuclear spectroscopy because of their inherently high energy resolution. Figure 2-3 is a block diagram of semiconductor junction detector.

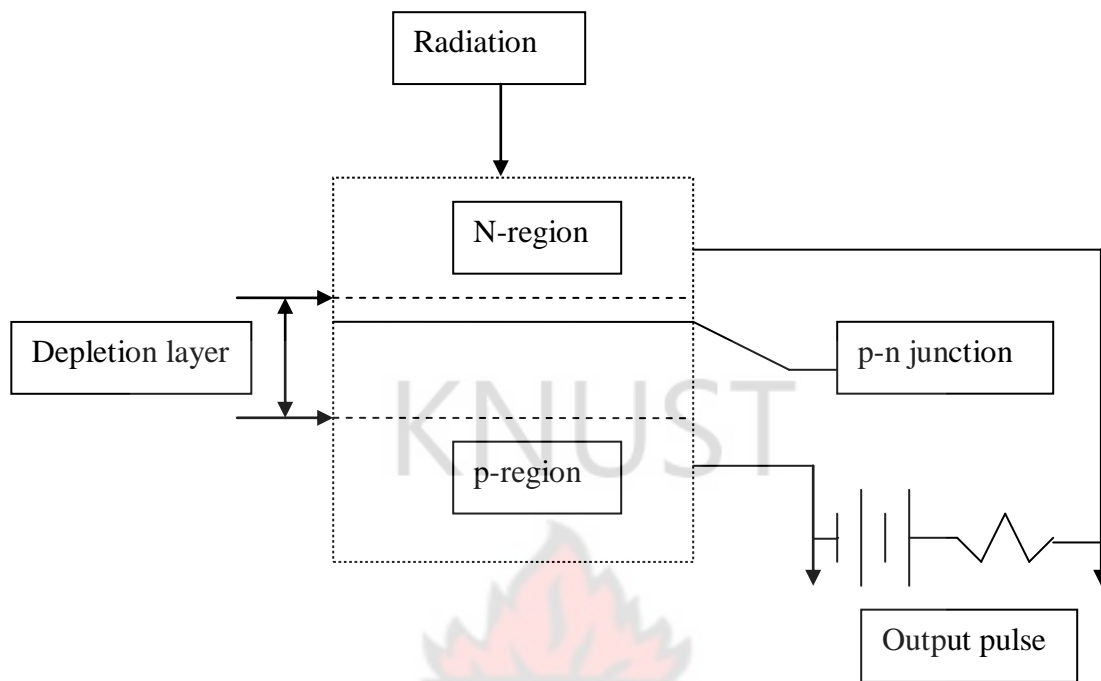


**Figure 2-3: Semiconductor junction detector.**

Nuclear spectroscopy is based on the analysis of radioactive isotopes by measuring the energy distribution of the source. The spectrometer separates the output pulses from the detector according to size. The output of the spectrometer provides detailed information that is useful in identifying unknown radioisotopes. Nuclear spectrometers are available in two types, either in single channel spectrometer (SCA) or multi channel analyser (MCA). The main use of the SCA is to discriminate between a desired radiation and other radiations that may be considered noise using a pulse height selector. On the other hand, MCA has an analogue-to-digital converter (ADC) to sort out all the output pulses according to their energies. The MCA also has a computer-type memory for storing the information from the ADC. Most MCA are built with a number of channels varying by a factor of 2 over a range of 128 to 4096 each with a storage capacity of  $10^5$  to  $10^6$  counts per channel [Cember, 1996].

The basis for nuclear spectroscopy is the location of spectral lines arising from the total absorption of charge particles or photons. For this reason, the resolution of the detector is important if spectral lines closed together are to be separated and observed. Energy resolution may be viewed as the extent to which a detector is able to distinguish between two closely lying energies (radioisotopes). The formal definition of energy resolution is given in terms of the full width at half maximum (FWHM) divided by the location of the peak centroid,  $E$ , as in equation (15).

$$\text{Resolution} = \frac{\text{Full width at half maximum}}{E} \quad (15)$$

Gamma radiation can also be measured using a scintillation detector consisting of Sodium Iodide crystal activated with thallium [NaI (Tl)] and optically coupled to a photomultiplier tube. The thallium activator present as an impurity in the crystal structure to the extent of 0.2 % converts the energy absorbed in the crystal to light. Sodium Iodide (NaI) (Tl) detectors have higher efficiency than high purity germanium (HPGe) detectors because of the high density of the crystal and high effective atomic number [Cember, 1996].

Gamma ray photons, in passing through the crystals of the detector, interact with the atoms of the crystal, by the mechanisms of photoelectric absorption, Compton scattering and pair production. This result in the production of primary ionising particles which includes; photoelectrons, Compton electrons, and positron–electron pairs which dissipate their kinetic energy by exciting and ionising the atoms in the crystal. The excited atoms return to the ground state by the emission of quanta of light. These light pulses upon striking the photosensitive cathode of the photomultiplier tube, cause electrons to be ejected from the cathode. These electrons are in turn accelerated to a second electrode called dynode which has a potential of 100 V positive with respect to the photocathode. Sometimes when an electron strikes the dynode,

several other electrons are ejected from the dynode, thereby multiplying the original photocurrent. This process is repeated about ten times and all electrons produced are collected by the plate of the photomultiplier tube. The current pulse which is produced is proportional to the energy of the ionising particle, is then amplified and counted by the detector. Figure 2-4 below shows schematically the sequence of events in the scintillation chamber.

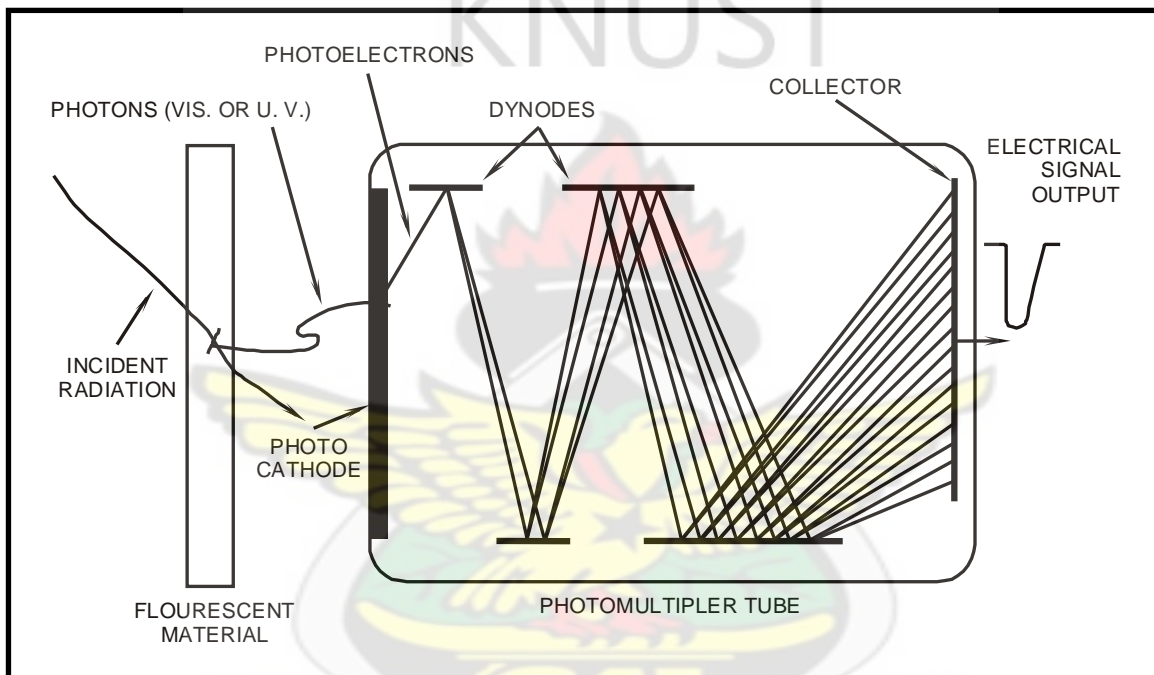


**Figure 2-4: Schematic diagram of the sequence of events in scintillation detector.**

The energy resolution of scintillation detectors [NaI (Tl)] is normally between 7- 9% for gamma radiation of energy of about 1 MeV whilst for semi conductor detectors (HPGe), the energy resolution is of the order of 0.1% [Sood, et al., 1981]. The smaller the value of the energy resolution, the better the detector's ability to resolve between two isotopes whose energies lie close to each other. Semi conductor detectors have better resolution than scintillation detectors.

## **2.6 Physical and chemical parameters in the mine**

The study area is known of its heavy mining activities for both small scale and large scale mining. All the mining companies are engaged in open pit (surface mining). Even though mining contributes significantly to Ghana's Economic Recovery Programme, it is at a great environmental cost as exploitation of the gold puts stress on water, soil, vegetation and poses human health hazards [Amonoo-Neizer and Amekor, 1993]. Previous studies in the study area have shown that for gold mining, mercury, arsenic and cyanide are common pollutants at high concentrations in urine of the inhabitants of Tarkwa [Asante et al., 2007]. Also many chemicals including those from less known e-wastes also enter the environment and remain environmental issues in Ghana [Asante and Ntow, 2009].

The source of water supply to inhabitants in the study area is ground water. The mining company in order to meet the demands for portable water has constructed boreholes and hand dug wells in the communities affected by their operations [Kortatsi, 2004]. In addition, surface water taken from river Bonsa at Bonsaso is treated by the Municipal Water Supply Company for use by the inhabitants in the study area. Runoff of environmental pollutants as a result of the mining and mineral processing of the Mining Company may also contaminate these water sources. A study on the multi-elemental contamination covering 22 trace elements in drinking water and urine from the mining town of Tarkwa, in Ghana has been published [Asante et al., 2007].

This study focused on quantifying the metals concentration with special interest in uranium (U) and thorium (Th), anions ( $\text{SO}_4^{2-}$ ,  $\text{NO}_3^-$ ,  $\text{PO}_4^{3-}$ ,  $\text{Cl}^-$ ) as well as physical parameters such as pH, temperature, conductivity, and total dissolved solids (TDS). Uranium and thorium which are rare earth elements, beside their chemical toxicity also have associated with them radiological hazard. Whilst there have been intensive geochemical studies in the study area on

metals, anions and physical parameters, limited data exist on the concentration of U and Th in water and soil of the area [Kortatsi, 2004]. Hence the need to determine the concentration of U, Th and K as well as other chemical and physical parameters of the study area to assess the quality of drinking water and their levels in soil. The study is important since it will give an indication of the relative reduction/oxidation potential of aqueous systems in the environment as well as in municipal water supply systems.

Uranium, thorium and potassium are amongst the most incompatible elements and are normally concentrated in granitic rocks that are the most abundant plutonic rocks in continental crust. They are generally similar in geochemical behaviour with U and Th belonging to the actinides series and both exist in the tetravalent state under reducing conditions. Whilst K is found mainly in feldspar, mica, leucite etc minerals, trace quantities of U and Th are found in major minerals such as quartz and feldspar [Galbraith and Saunders, 1983]. However, the concentrations of U and Th are higher in accessory minerals such as orthite or allanite, monazite, zircon etc which are concentrated in granitic rocks [Valkovic, 2000]. The content of U and Th generally increases with silicon dioxide ( $\text{SiO}_2$ ), during differentiation, fractional crystallisation, partial melting, etc in final stages of magmatic procedures [Rollinson, 1993].

The physical parameters such as pH, temperature and conductivity influence the concentration of many pollutants by altering their availability and toxicity. The temperatures at which environmental samples are collected and at which physicochemical measurements are made are important for data correlation and interpretation [Tay et al., 2009]. Also at high temperature, the toxicity of many substances may be increased. Also in addition to microbial activities, within an aquatic medium, temperatures and pH are two important parameters that govern the methylation of elements such as lead (Pb) and mercury (Hg) [Van Loon, 1982]. The

pH is a physical parameter that is used to characterise the acidity of the water since it has an influence on the solubility of pollutants in water. The pH and principal ion concentrations in most natural water systems are controlled by the dissolution of atmospheric carbon dioxide and soil-bound carbonate ions (Baird, 1999). The electrical conductivity (EC) is also a useful indicator of mineralisation in a water body which has a correlation with the total dissolved solids (TDS) in the water body. The levels of the physical and chemical parameters of the study area has been well established by various researchers [Kortatsi, 2004; Asklund and Eldvall, 2005; Asante et al., 2007]. One physical parameter that is of concern in water treatment is Total Dissolved Solids (TDS), which is a measure of salt and solids dissolved in water. The TDS and conductivity are directly related since both indicate the ionic strength of water. They are used to measure the purity of water.

For the anions,  $\text{SO}_4^{2-}$  is widely found in natural waters and its concentration could be at high levels in mine drainage. High concentrations of magnesium and sodium sulphate in drinking water can act as laxative to both humans and animals. The Sulphate ions in the sample react with  $\text{BaCl}_2$  to form  $\text{BaSO}_4$ . A colorimetric measurement of the absorption produced by the turbidity resulting from the precipitation of  $\text{BaSO}_4$  in acidic medium is proportional to the sulphate concentration.

High nitrate-nitrogen level in water contributes to excess plant growth (eutrophication). If the levels are too high it could lead to reduction in dissolved oxygen and can affect aquatic life. High levels can also lead to blue-baby syndrome (methemoglobinemia) in infants and in adults with particular enzyme deficiency [Baird, 1999].

Chloride is found in almost all natural waters and affects the tastes at levels above 250  $\text{mg l}^{-1}$ . High level of chloride also inhibits plant growth. Finally  $\text{PO}_4^{3-}$  exists in water bodies

through surface run off, cleaning operations, water treatment and sewerage.  $\text{PO}_4^{3-}$  is an essential anion for plant growth and too much of it in water can lead to excessive growth of aquatic plants due to over fertilisation leading to eutrophication. It can also affect fish life [Baird, 1999].

The trace metals in the water samples were determined using the Atomic Absorption Spectrometry (AAS). It is based on the principle that the atom in the ground state absorbs light of wavelengths that are characteristic to each element when light is passed through the atoms in the vapour state.

Atomic Absorption Spectrometry is an analytical technique which is used to determine the concentration of metals in solution using Atomic Absorption Spectrophotometer. The equipment consists of the following components:

- A lamp compartment which contains hollow cathode lamps of the analyte of interest.
- Atomising chamber which vaporises and atomises the sample in the flame transforming it into unexcited ground state atoms to absorb light at specific wavelength. The source of energy for the production of free atoms is usually heat commonly from an air/acetylene or nitrous oxide/acetylene flame. Usually, the sample is introduced as an aerosol into the flame and the burner aligned in the optical path so that the light beam passes through the flame, where the light is absorbed.
- An optical system which directs light from the source through the atom population into the monochromator. The monochromator isolates the specific analytical wavelength of the light emitted by the hollow cathode lamp from the other non-analytical lines including those of the fill gas.
- A photomultiplier tube to measure the light output accurately.
- The display of the results of the analysis.

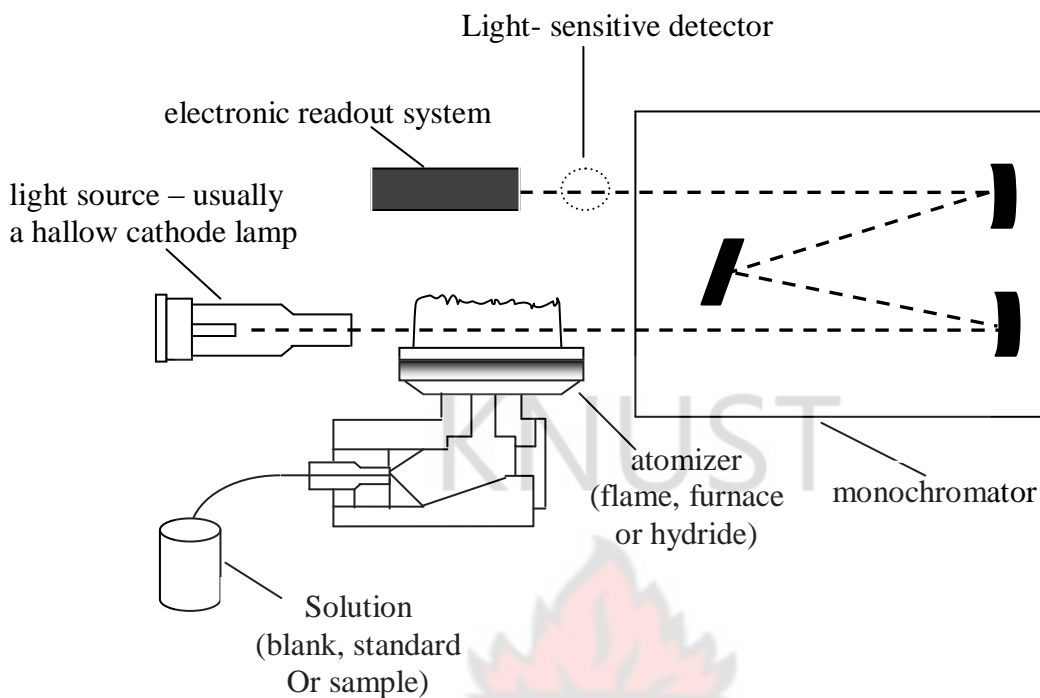


**Figure 2-5: Schematic diagram of AAS.**

The principle of operation of Atomic Absorption Spectrometer is based on the fact that, ground state metals absorb light at specific wavelength. The metal ions in solution are converted to atomic state by means of a flame. Light of appropriate wavelength is supplied and the amount of light absorbed is measured against a standard curve. The technique requires that a liquid sample is aspirated, aerosolised and mixed with combustible gases such as acetylene and nitrous oxide. The mixture is ignited in a flame with temperature in a range of 2100-2800 °C. During the combustion, atoms of the element of interest in the sample are reduced to free, unexcited ground state atoms which absorbs light at the characteristic wavelength. The characteristic wavelengths are element specific and this is determined when light beam from a lamp which consists of the element of interest is passed through the flame. A photomultiplier detects the amount of reduction of the light intensity due to absorption by the analyte which is directly related to the amount of element in the sample and the results displayed.

The previous studies in the study area had concluded that the metal concentrations were lower than expected. The studies had established that concentration values were higher than the WHO drinking water guidelines reported for Al, As, Cd, Cr, Fe, Mn, Ni, Pb and Zn [Kortatsi, 2004; Asklund and Eldvall, 2005].

## 2.7 Neutron Activation Analysis (NAA)

Neutron activation analysis is a two step analytical procedure in which some components in a material are activated (irradiated) with high flux of thermal neutrons. The activation process is nuclear reactions between the incident neutrons and target nuclei in the sample being irradiated. When thermal neutrons collide with the nucleus a number of reactions may occur but the most useful in NAA being radiative capture and the reaction is generally represented by equation (16) [Landsberger, 1994].



Where;

${}^A_Z$  is the target nucleus,

${}^{A+1}_Z^*$  is a compound nucleus in an excited state which de-excites with the emission of gamma ray called prompt gamma,

${}^{A+1}_Z$  is the product after irradiating the target nucleus which is radioactive.

The radioactivity produced after the irradiation is governed by the usual decay equation and generally represented by equation (17) [Landsberger, 1994]:

$$R = N \int_{\text{whole energy range}} \sigma(E)\phi(E)dE \quad (17)$$

Where  $R$  is the reaction rate,  $\Phi(E) dE$  is the neutron flux of neutrons with kinetic energy between  $E$  and  $E+dE$  in  $n.cm^{-2}s^{-1}$ ,  $\sigma(E)$  is the neutron capture cross-section in  $cm^2$  defined as the probability of a radiative capture reaction occurring in a collision between a neutron and a nucleus given in terms of area and dependent on the energy of the incident neutron,  $N$  is the number of atoms of the element in the sample.

During neutron irradiations, the dominant reaction rates are the thermal and epithermal components and because the neutron cross-section of the fast neutrons ( $R_{fast}$ ) is negligible the reaction rate of fast neutrons is small.

The activity of an element in a sample is given by the following general expression (18) [Landsberger, 1994]:

$$A = \sigma\phi(m/M)N_A SDC\theta P_\gamma \eta \quad (18)$$

Where:

$A$  is the measured activity in Bq from a product of an expected reaction;

$\sigma$  is the activation cross section of the reaction in  $cm^2$ ;

$\phi$  is the activating neutron flux in  $n.cm^{-2}s^{-1}$ ;

$m$  is the mass of element in g;

$M$  is the atomic weight of the element to be determined in g/mol;

$N_A$  is the Avogadro's constant, which is  $6.022 \times 10^{23}$  atoms/mol;

$S$  is the saturation factor which is given by  $S = [1 - \exp(-\lambda t_1)]$ ,  $\lambda$  is the constant of the reactive product and  $t_1$  is the duration of irradiation;

$D$  is the decay factor and it is given by  $D = \exp(-\lambda t_d)$  and  $t_d$  is the duration of decay;

$C$  is the correction factor for nuclide decay during the counting time given by  $C = [1 - \exp(-\lambda t_c)]$

and  $t_c$  is the duration of counting;

$\theta$  is the relative natural isotopic abundance of the activated isotope;

$P_\gamma$  is the probability of emission of photon with energy E; and

$\eta$  is the detector efficiency for the measured gamma radiation energy.

Equation (18) is simplified to equation (19) by the comparator method using the same geometry, equal weights of both sample and standard, with the same irradiation, decay and counting times.

$$C_{sam} = C_{std} \left( \frac{A_{sam}}{A_{std}} \right) \quad (19)$$

Where;

$C_{sam}$  is the unknown concentration of the element in the sample,

$C_{std}$  is the known concentration of the element in the standard,

$A_{sam}$  is the activity of the sample and  $A_{std}$  is the activity of the standard.

By using the terms D and C in equation (19) and also normalising the weights between standards and unknowns, the overall equation becomes equation (20) in ppm:

$$C_{sam} = C_{std} \left( \frac{A_{sam}}{A_{std}} \right) \left( \frac{D_{std}}{D_{sam}} \right) \left( \frac{C_{std}}{C_{sam}} \right) \left( \frac{W_{std}}{W_{sam}} \right) \quad (20)$$

Where  $W_{sam}$  and  $W_{std}$  are the weights of the sample and the standard respectively.

The product is required to be radioactive and capable of emitting at least one gamma-ray photon.

The gamma ray photon emitted is detected on a gamma ray detector using HPGE. If the activation product is stable, it cannot be detected. The duration of irradiation of the sample depends on the characteristics of the sample. The duration of the irradiation depends on the neutron flux density, mass of the sample and the efficiency of the gamma detector. The samples to be irradiated are specially sealed in capsules and transferred to the reactor core and irradiated with high flux neutrons. The activated components are then analysed to identify and determine quantitatively, the concentration of each radionuclide applying gamma spectrometry technique.

## 2.8 Gold Processing methods used by the Tarkwa Goldmine

Two main methods are used by the Tarkwa Goldmine to recover gold from the ore. The method used in the extraction of the gold from the ore depends on geological formation and the type of ore. Gold ore can occur in the form of pyrites, arsenopyrites and other sulphur matrix in the Birimian and Tarkwaian formations. The carbon in leach (CIL) and the heap leach (HL) methods are being employed by the Tarkwa Goldmine to recover the gold from the ore [Goldfields, 2007]. The cyanide solution strength is important in leaching the gold with a typical concentration range of 0.02-0.05% NaCN commonly used as the complexing agent and also the alkalinity of the solution with the optimum pH being 10.3 [Barsky et al., 1962]. To facilitate the leaching of gold by cyanide, there should be enough oxygen supply throughout the reaction period. The decomposition of cyanide by carbon dioxide and ground acids resulting in the production of hydrogen cyanide gas is minimised by using sufficient alkali such as lime (CaO) or caustic soda (NaOH) in the leach solution to maintaining the acidity in a range of 9 to 11. The gold in the pregnant cyanide solution is recovered by adsorption on activated carbon. Although activated carbon has been used in gold-silver recovery from cyanide solutions for several decades, the mechanism of gold adsorption on activated carbon is still not fully understood [Barsky et al., 1962]. The generally accepted chemical reaction for several decades known as Elsner's equation representing the dissolution of gold by cyanide is represented as follows.



The choice of any of the processing methods depends on the following:

- Porosity of the ore;
- Dissolution rate of the ore and;
- The ore grade.

For CIL the major controlling factors are grade and porosity.

### **2.8.1 The CIL process description**

The gold ore from the mine pits is transported to the crusher pad and tipped into the crusher. The crushed ore is then passed into a bin and fed into an apron feeder. The apron feeder feeds the ore via a 3 tier conveyor system onto a stockpile. Underneath the stockpile is a reclaim tunnel which houses 3 apron feeders. The apron feeders then feed a conveyor belt which in turn feeds a semi autogenous (SAG) mill. The slurry discharged from the mill is then passed over a screen so that the slurry is separated into particle sizes. Particles with sizes greater than 12 mm, known as scats are deposited onto the stockpile and intermittently returned to the milling circuit. The slurry passing through the screen is then pumped to the cyclone classification circuit where coarse particles are separated from the fine products. The coarse fraction is returned to the mill whilst the fine particles gravitate to a thickener via trash removal screens. In the thickener, the slurry is thickened from 22% solids to 50% solids and pumped out of the thickener to the carbon in leach tanks. The clear water from the thickener is reused in the plant. The CIL consist of 8 tanks in the series of which 7 contain activated carbon. Cyanide ( $\text{NaCN}$ ) is added to the circuit to ensure dissolution of the gold and get absorbed on the carbon. The slurry overflowing the last CIL tank forms the tailing which is pumped to the tailings storage facility. The carbon loaded with gold is recovered and cleaned of slurry. The carbon loaded with gold is then passed into an acid wash column where it is washed with hydrochloric acid ( $\text{HCl}$ ) solution to remove calcium. The carbon is then pumped into the elution column where acoustical solution at  $120\text{ }^{\circ}\text{C}$  is used to remove the gold from the carbon solution. The eluted carbon is passed through the regeneration Kiln which operates at a temperature of  $700\text{ }^{\circ}\text{C}$  to remove any organic fouling off the carbon. The gold bearing solution is pumped through the electro winning cells where the gold plates onto

stainless steel cathodes as gold particles. The gold is then removed from the cathodes with high pressure sprays and dried before being smelted into an induction furnace at 1400 °C. Fluxes are added before smelting to remove all impurities from the gold. The molten gold is then poured into moulds and allowed to cool down into bars.

# KNUST



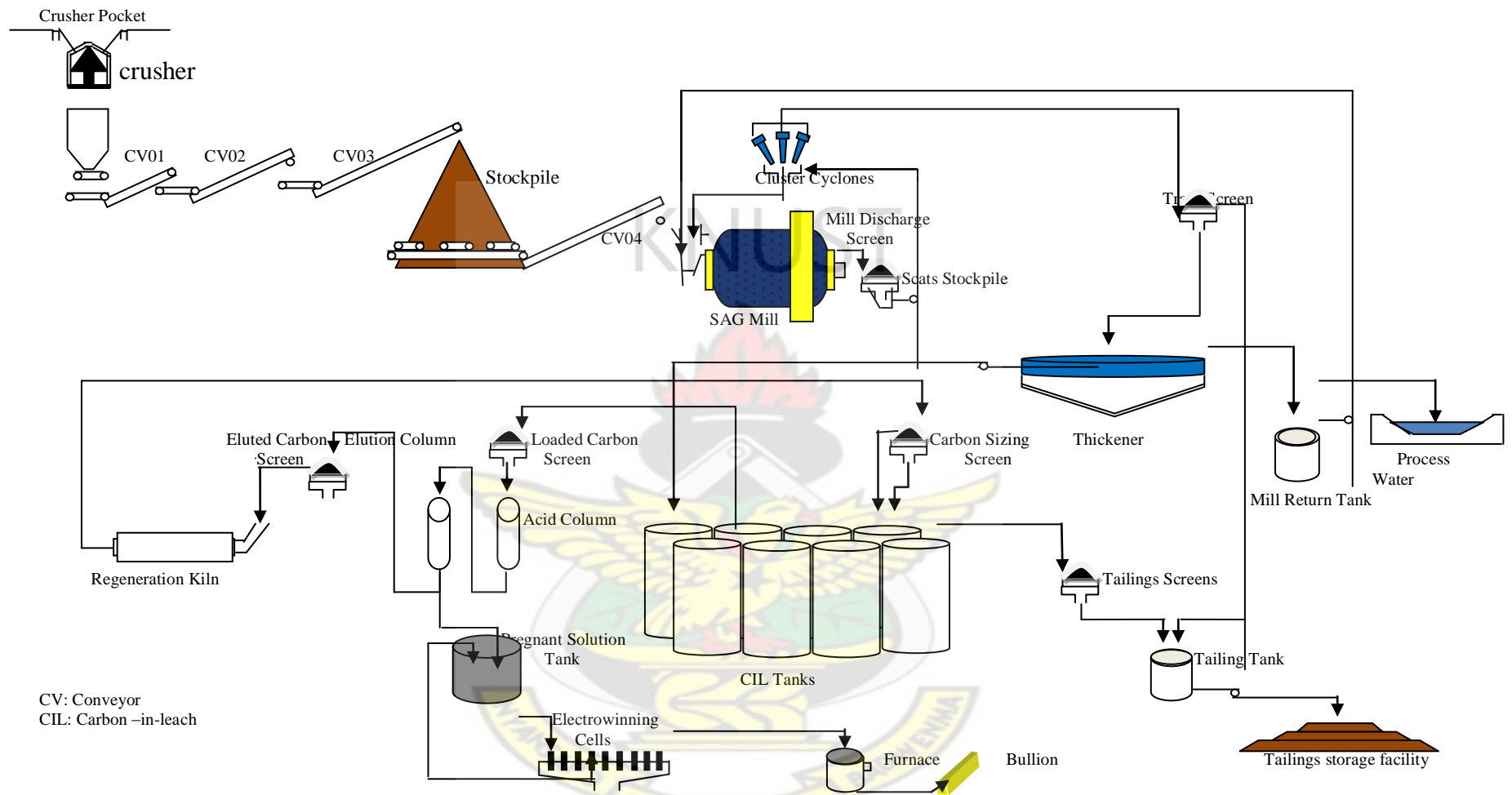


**Figure 2-5: Carbon in Leach (CIL) process plant flow diagram**

## **2.8.2 The Heap Leach (HL) process description**

### **I. Crushing and Screen**

The crushing plant is designed to crush the ore and reduced it to between 12.5 -19.0 mm product. The ore is directly tipped into a primary gyratory crusher to reduce the product to sizes of 150-250 mm. The crushed product is fed into an apron feeder onto a conveyor to be transported to a secondary crusher. The secondary crushers are fed via screens of aperture of sizes of 50 mm and 19 mm for the upper and lower deck respectively. The secondary crushers are also gyratory and they crush to product of sizes 37.5 mm and fed into crushers via scalping screens. The under size from the screens (19 mm) joins the final product stream via another conveyor belt. The over size is fed back into a tertiary cone crusher and the product fed into tertiary screens of sizes 19 mm. The final crushed product is transferred to agglomeration via conveyor belts which are fitted with belt scales. The crushed ore stream is then discharged to a covered stockpile at the agglomeration plant via conveyor belt.

### **II. Agglomeration Stacking and Leaching**

The ore that has been crushed to the designed product size of 12.5 mm (80%) is placed on heaps in a conical pile. The agglomeration stockpile is designed for a live capacity of 1,350 tons. The ore passes over belt scales and under cement silos that add cement at a rate of 4.0 kg/ton of ore to bind the agglomerates. After being discharged into rotary agglomeration drums, barren process solution made of cyanide concentration of 1000 ppm is sprayed onto the ore to provide a moisture content of 5-10% for agglomerate formation and leaching process initiation. The crushed and agglomerated ore is then conveyed to the leach pad and stacked using Ramps and Grasshoppers conveyors, a Loading and Horizontal feed conveyor and a Radial Stackers. Leach solution is then applied to the heap after the heap is left to cure for about 3-4 days at a solution

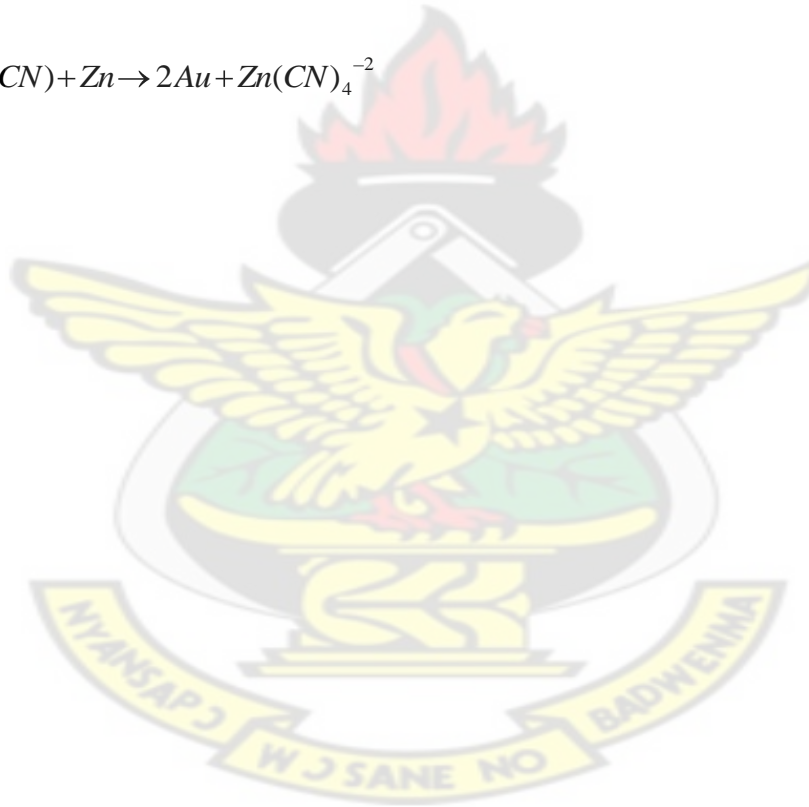
application rate of 10 litres /hour/m<sup>2</sup> at a solution pumping rate of 365-440 m<sup>3</sup>/hour and sodium cyanide (NaCN) consumption rate of 0.2 kg/ton on the average. The leach solution is collected after it has passed through the heap and directed into ponds based on a properly coordinated solution management practice.

The ponds are constructed with 2 mm High Density Polyethylene (HDPE) membranes liner over HDPE geogrid at the pond bottom over a 1.5 mm HDPE membrane liner over geotextile at the pond bottom and crest with a leak detection system at low point in the ponds. The ponds include; pregnant solution ponds, intermediate solution pond, barren solution pond, excess solution pond, treatment solution and containment ponds designed to contain solution based on accepted solution management practices and to contain excesses in case of heavy rainfall. Centrifugal pumps are used in pumping the solution. The pumps are fitted with floating intake lines so that the solution is withdrawn from the upper surface of the pond.

### **III. Metal Recovery**

Gold is recovered from the pregnant leach solutions through activated carbon Adsorption/Desorption/Recovery (ADR) plant. The pregnant solution flows in a sequence of 5 up flow closed-top carbon columns arranged in series. Each column contains on the average 2 tons of activated carbon. Desorption utilizes a pressurised elution process and its sized for 4 tons of carbon, after acid washing using 3% hydrochloric acid (HCl) for a period of 4-6 hours to remove any carbon foulants. Hot caustic pressure at a temperature of 135 °C and a pressure of 350 kPa with an elution flow rate of 1.5 bed volumes/hour and bed volume of 2.3 m for about 8 hours. Metal recovery is done using the Merrill Crowe Zinc Precipitation System at a maximum precipitation temperature of 90 °C and Zinc consumption rate of 2.5 gm Zn/gmAu+Ag. The precipitate filter is the Recessed Plate type and with a press feed rate of 25 m<sup>3</sup>/hour Gold

Recovery is greater than 95%. The filtered cake is washed of the press cloth and calcined at a temperature of about 500 °C for smelting. The calcined is fluxed using Silica, Borax, Sodium Nitrate, Soda Ash and fluorspar based on acceptable solution composition standards. The smelting of the calcine is done using a 660 kg red brass working capacity diesel fired tilting crucible with wet scrubber furnace. The bullion produced is sampled and weighed and the samples sent to the laboratory for assaying to recover the gold. The chemical reaction describing how the gold is recovered from the solution based on equation 22 where zinc reacts with cyanide yielding gold.



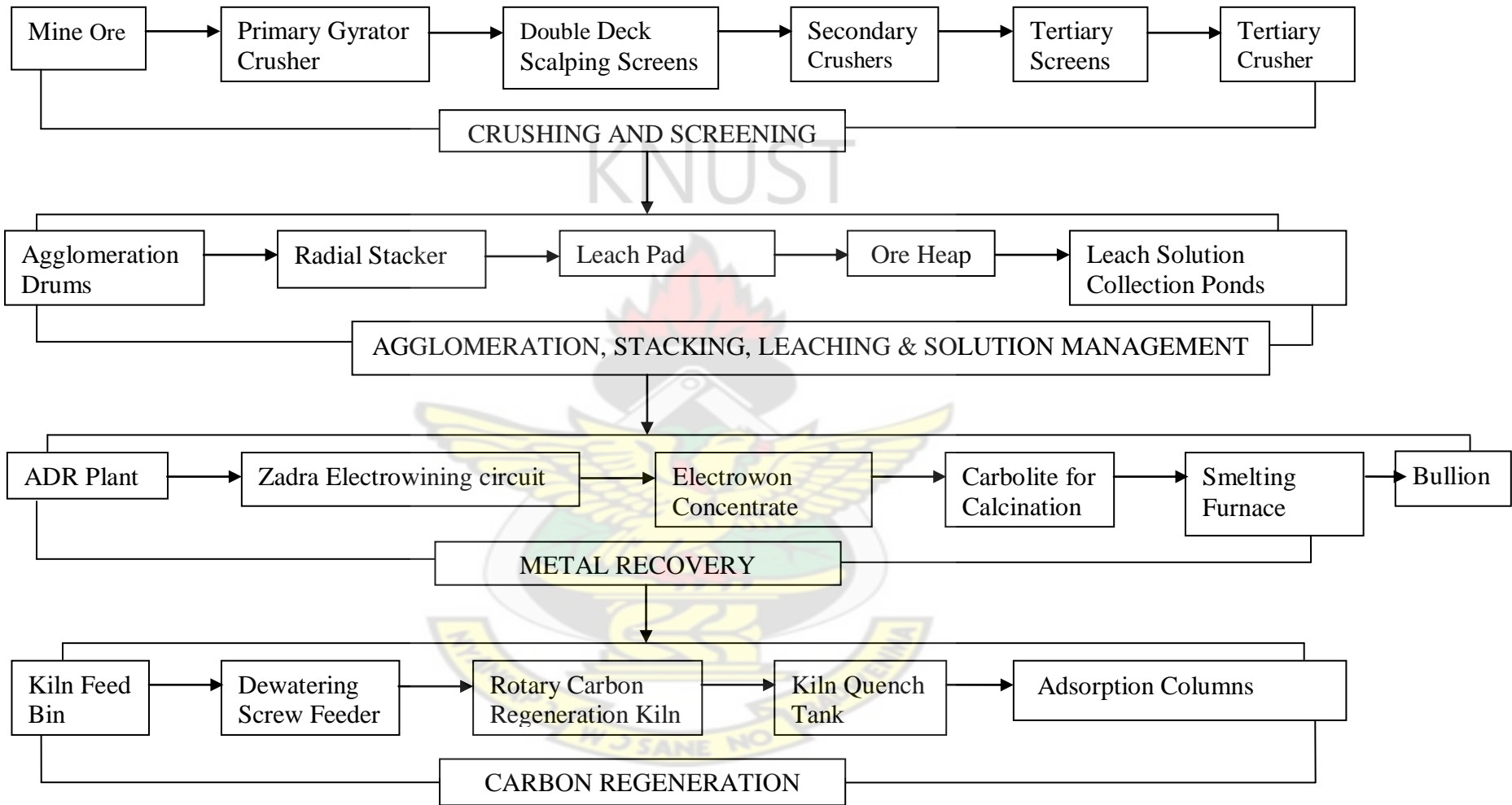


**Figure 2-6: Heap Leach (HL) process flowchart**

## CHAPTER THREE

### 3.0 EXPERIMENTAL

In this section, the location of the study area, the geology, sampling, sample preparation and analysis methods are described. Mathematical formalisms used for the calculation of activity concentrations of the natural radionuclides are described in detail. Determination of trace metals, anions and physical parameters in water are also discussed. Sampling was carried out at two different periods with the first sampling campaign carried out from 23/08/08 to 31/08/08 and the second sampling period from the 07/07/09 to 17/07/09. The following significant exposure pathways were considered as the basis for the types of samples to be collected for the study.

1. Workers:

- Direct gamma exposure
- Dust inhalation
- Radon inhalation

2. The public:

- Inhalation of suspended particulates
- Exposure to radon
- Ingestion of contaminated water sources (surface water {e.g. rivers, streams, etc}, ground water {e.g. boreholes, wells} and treated water)
- Ingestion of food crops grown on farm lands

### 3.1 Description of the study area

The study area is Tarkwa Goldmine and its surrounding communities including Tarkwa Township within the mines area of concession. The Tarkwa Goldmine was selected for the study for the following reasons:

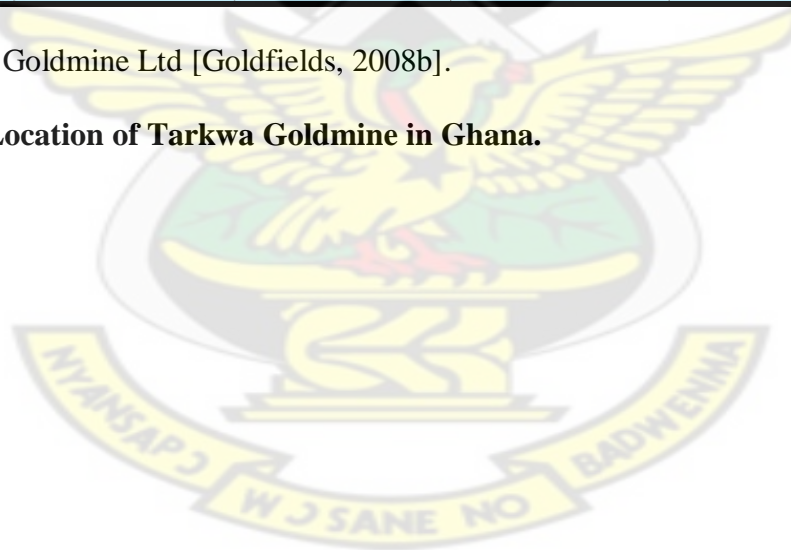
1. It is one of the largest gold mining Companies in Ghana with an annual production in excess of 900,000 ounces from its operations in Damang and Tarkwa [Goldfields, 2008a]. Mining in this area dates back to the 19<sup>th</sup> Century and it has gone through about five (5) development stages;
2. The geology of the area is similar to that of the Witwatersrand of South Africa where the gold bearing conglomerates contain some uranium in commercial quantities;
3. The bulk of the population is distributed in the area around the mines and the type of mining undertaken by the Tarkwa Goldmine.

The Goldmine is located in the Western Region of Ghana. The Tarkwa township is approximately 300 km west of Accra by road at latitude 5° 15' N and longitude 2° 00' W. The mine is about 4 km from Tarkwa Township with good access roads and well established infrastructure. Figure 3-1 shows the location of Tarkwa Goldmine in Ghana and figure 3-2 shows the concession of the mine and the surrounding communities where sampling was carried out. Table 3-1 shows the communities and their population distribution around the mines. Tarkwa is the administrative capital of the study area. Subsistence farming is the main occupation of the people and mining is the main industrial activity [Avotri et al., 2002]. Tarkwa lies within the main gold belt of Ghana that stretches from Axim in the southwest, to Konongo in the northeast [Kortatsi, 2004].



Source: Tarkwa Goldmine Ltd [Goldfields, 2008b].

**Figure 3-1: Location of Tarkwa Goldmine in Ghana.**



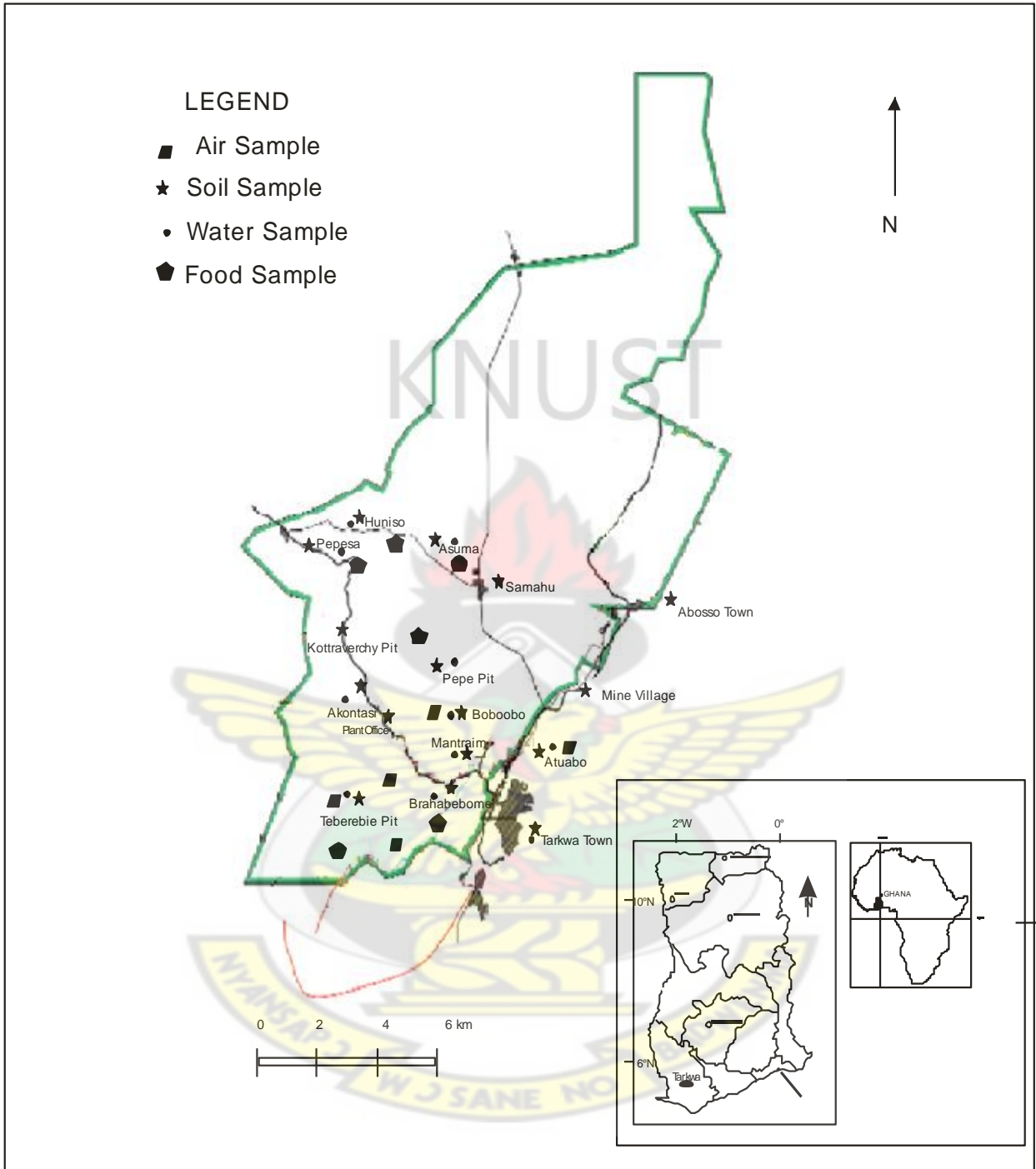


**Figure 3-2: Layout of Tarkwa Goldmine showing the sampling points.**

**Table 3-1: Communities and their population distribution around the mines [Goldfields Ghana Ltd, Community Affairs, 2008a]**

No	Community	Location coordinates	Population (2004 estimates)
1	Abekoase	N 5 <sup>0</sup> 22' 24.39" W 2 <sup>0</sup> 01' 07.49"	400
2	Brahabe bom	N 5 <sup>0</sup> 18' 47.44" W 1 <sup>0</sup> 59' 56.72"	1500-1800
3	Huniso	N 5 <sup>0</sup> 22' 59.51" W 2 <sup>0</sup> 03' 55.51"	1500-2000
4	New Atuabo	N 5 <sup>0</sup> 19' 22.34" W 1 <sup>0</sup> 58' 36.40"	5500-6000
5	Pepesa	N 5 <sup>0</sup> 19' 56.60" W 2 <sup>0</sup> 00' 11.36"	1500-1800
6	Samahu	N 5 <sup>0</sup> 21' 54.82" W 1 <sup>0</sup> 59' 58.46"	1500
7	Tebe	N 5 <sup>0</sup> 22' 55.97" W 2 <sup>0</sup> 01' 48.32"	300
8	Tarkwa Township	N 5 <sup>0</sup> 17' 13.58" W 1 <sup>0</sup> 59' 55.31"	80,000

The concession of the mines covers an area of 294.606 km<sup>2</sup> [Ofori, 2008].

Historically, the mine was previously owned by the State Gold Mining Corporation (SGMC) until 1993 when it was acquired by Goldfields [Ofori, 2008]. The mines operations covered underground mining until 1997 and later surface mining in 1999. Since 1999, all mining operations have been from open-pits following the closure of the underground mines. The total population of the Tarkwa Township is about 80,000 [Kuma, 2007] with an estimated population of the District being 236,000 [IFC, 2003; Darko et al., 2008]. In addition, there are eight communities dotted around the mines. Plates 3-1 to 3-7 show some of the locations within the mines and the communities where sampling was carried out.



**Plate 3-1: Surface water body within the mine.**



**Plate 3-2: Waste water from the gold processing plant to be discharged to the environment.**



**Plate 3-3: Gold tailings dam**



**Plate 3-4: Heap leach treatment plant**



**Plate 3-5: Waste dump**



**Plate 3-6: Ore stockpile**



**Plate 3-7: Borehole in a community**

### **3.2 Geology and Hydrogeology of the mining area**

Geologically, the gold ores are located within the Tarkwaian system, which forms a significant portion of the stratigraphy of the Ashanti Belt in south western Ghana. The basic minerals associated with the gold ore in Tarkwa Goldmine are copper, silver, sulphides, pyrites, iron oxides etc [Karpeta, 2000]. Intrusive igneous rocks contribute to about 20 % of the total thickness of the Tarkwaian system in the study area. The ore body consists of a series of sedimentary blanket quartz reef units similar to those mined in the Witwatersrand of South Africa. Three types of sedimentary rocks are present; namely conglomerates, quartzites (metamorphosed sandstones) and phyllites (metamorphosed shales). The operation is currently mining multiple reef horizons from six open-pits and there is a potential for underground mining in future. The geological formation of the mine is such that the gold bearing ore is situated

between waste belts with the major rock type being sedimentary. The Ashanti Belt is a north-easterly striking broadly synclinal structure made up of lower Proterozoic sediments and Volcanics underlain by the metavolcanics and metasediments of the Birimian system. The contact between the Birimian and the Tarkwaian systems is commonly marked by zones of intense shearing and is host to a number of significant shear hosted deposits including Prestea, Bogoso and Obuasi. The local geology is dominated by the Banket Series which consists of a well sorted conglomerates and pebbly quartzites with clasts generally considered to be Birimian in origin and containing significant gold mineralization, hosting the Tarkwa ore body. The rocks of the Tarkwaian system consist of the Kawere Group, the Banket series, the Tarkwa Phyllite and the Huni Sandstone. Most of the rocks that resemble sandstone at the surface are weathered equivalents of parent quartzites [Kuma and Younger, 2001]. The existing surface operation currently exploits narrow auriferous conglomerates from six pits namely: Pepe, Atuabo, Mantraim, Akontansi, Terberebie and Kottraverchy. In the Pepe area of the Banket series, the ore is approximately 32 metres thick and at the Kottraverchy up to about 270 metres thick [Goldfields, 2007]. The exploration is initially carried out by diamond drilling to produce a continuous core through the sequence of mineralised reefs. The geological map of the study is shown in figure 3-3.

Hydrogeologically, most of the major towns except Tarkwa and villages in the Wassa West District depend on groundwater as the main source of water supply through boreholes and hand dug wells [Kortatsi, 2004]. The groundwater occurrence is associated with the development of secondary porosity through fissuring and weathering since the area lack primary porosity due to the consolidated nature of the rocks. The weathering depths are greatest in the Birimian system with values between 90-120 m and for the Tarkwaian system especially in the Banket

series, quartzites, grits, conglomerates and Tarkwa phyllite weathering depths rarely exceed 20 m [Kortatsi, 2004]. Two types of soils exist in the Tarkwa-Prestea area and these are forest oxysol in the south and forest ochrosol-oxysol integrates in the north [Kortatsi, 2004]. The characteristics of the soils in the area are shown in table 3-2 [Kuma and Younger, 2001].

**Table 3-2: Characteristics of soils in the study area [Kuma and Younger, 2001].**

Soil type	Texture	Percentage, %			
		Gravel	Sand	Silt	Clay
Banket series	Silty-sand	2	59	29	10
	Laterite	69	14	10	7
Huni	Silty-sand	2	55	33	10
Kawere	Silt sand	0	47	40	13
Tarkwa phyllite	laterite	62	9	13	16
Weathered dyke	Silt	3	20	64	13



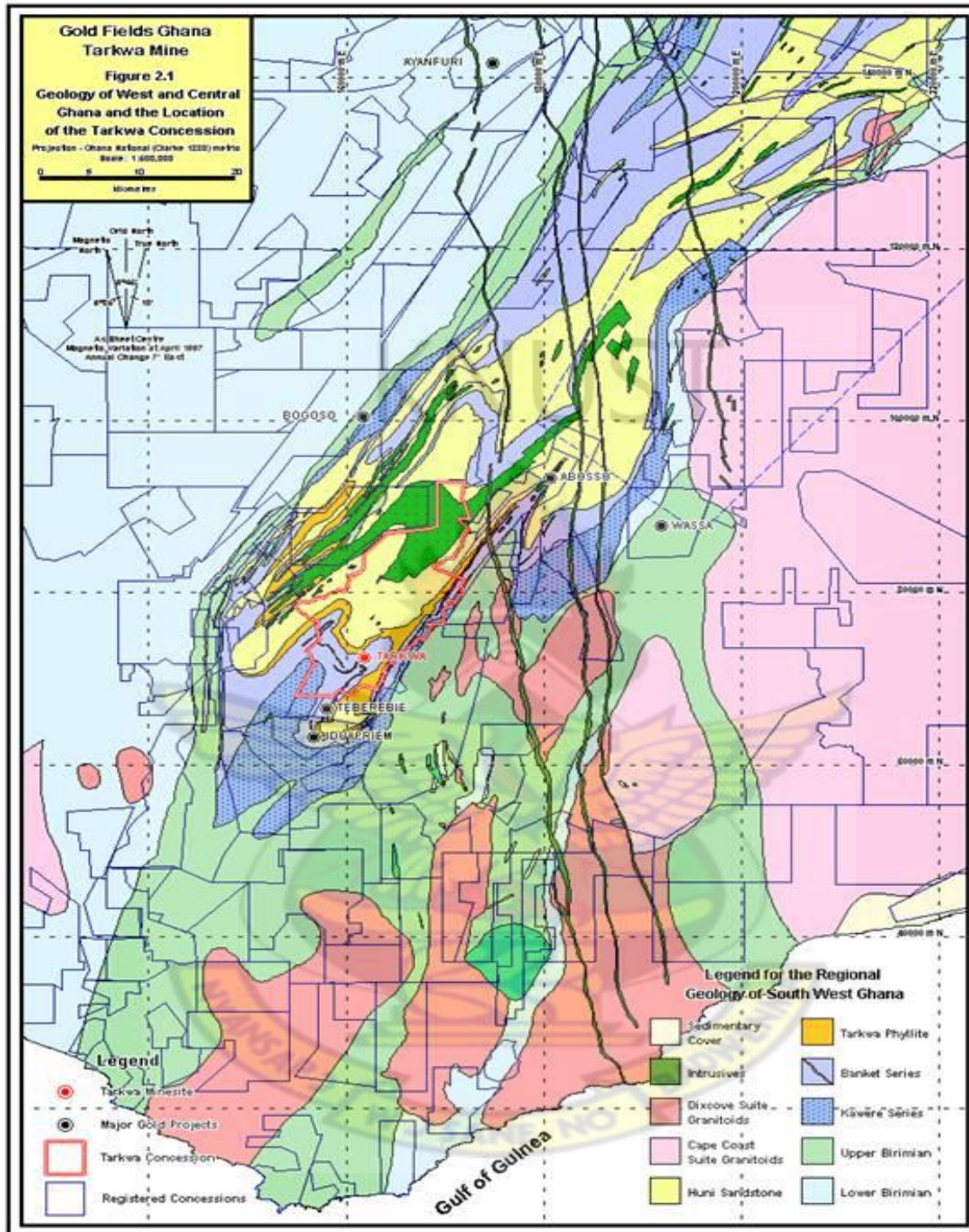
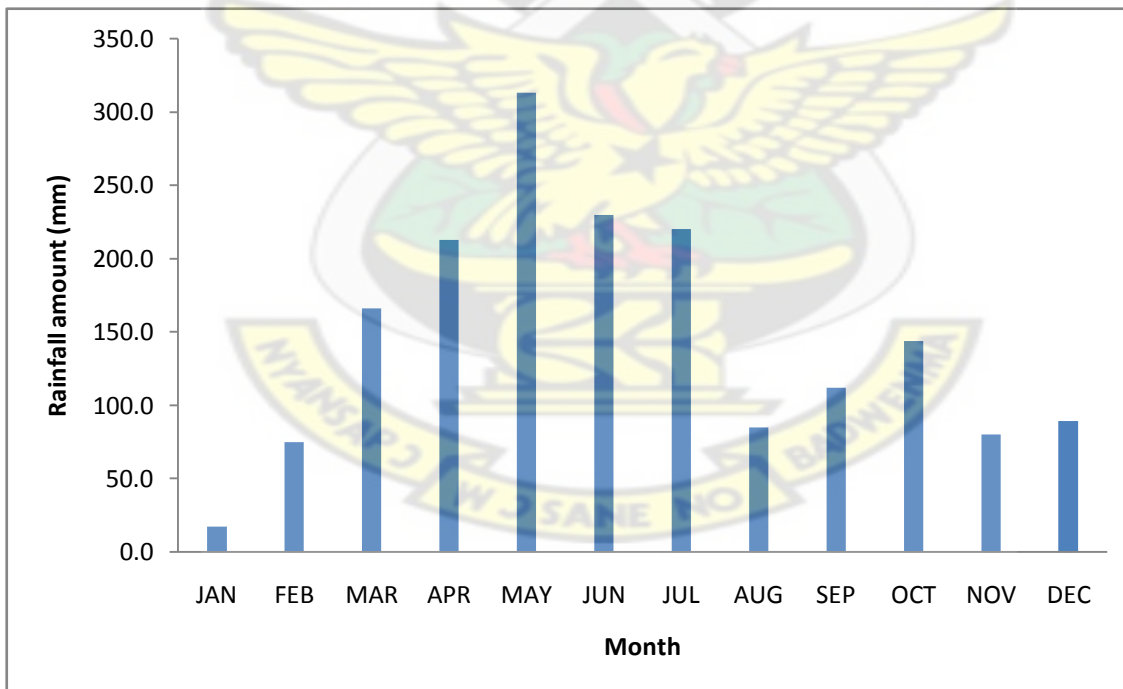


Figure 3-3: Geological map of the study area.

### 3.3 Meteorological data of the area.

The climate of Tarkwa is the tropical type characterised by two wet seasons; March –July and September-November. Data obtained from the mines Environmental Department shows the total annual rainfall figures measured for the year 2008 was 1744 mm with an average of 145 mm. The rainfall figures for August 2008 during which the first sampling was carried out was 85 mm when there was reduction in rainfall. The rainfall figures during the second sampling period in July 2009 was 256.6 mm and this period was very wet. The relative humidity of the area was in a range of 73-98 % with an average value of 86 %. The average atmospheric pressure was about 100.2 kPa in a range of 99.0-100.7 kPa and outdoor temperature in the range of 28-39 °C with average value of 34 °C.



**Figure 3-4: Rainfall data for 2008**

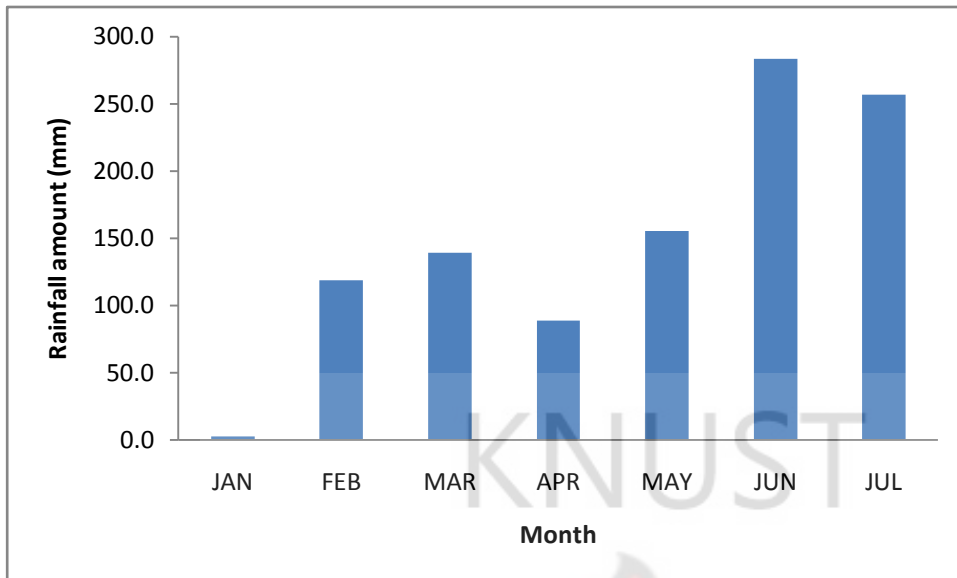


**Figure 3-5: Rainfall data from January to July 2009**

### 3.4 Samples collection

#### Soil/rock sampling

Soil samples were collected from the following locations within the mines and the surrounding communities including; Tarkwa Township, Abekoase, Brahabebom, Huniso, New Atuabo, Pepesa, Samahu and Tebe. In order to ensure representative samples were taken from the area for the analysis, initial survey was carried out in the area to determine the sampling points. The selection of the sampling locations was based on the accessibility to the public and proximity to the mine. In addition, the geological map of the area was used to identify the locations where samples will be taken. Based on these criteria, 38 locations were identified for the soil/rock samples and 29 water sample sources. For the dust/particulate matter samples, the number of samples was based on the locations where the Mine's Environment Department carries out dust monitoring. In the case of food (cassava) samples, only food products which were ready for harvesting was the criteria adopted. At the times of sampling only 6 farms had

cassava product ready for harvesting and only these were sampled for analysis. Within the mines, soil samples were collected at satellite nursery, rehabilitation plantation, ore stockpiles, tailings dams, heap leach pads, wastes dumps, open pits and the plant site. In the communities, samples were taken in areas (farms) where crops were grown. The sampling locations were marked using a Geographical Positioning System (GPS), Geo Explorer II.

The sampling strategy that was adopted for the soil/rock samples was random [ASTM, 1983, 1986; IAEA, 2004]. At each identified location samples were arbitrary collected within defined boundaries of the area of concern. Each location was divided into 50 m x 50 m grids and samples taken at different points and mixed together to give a sample. Each sampling point was selected independent of the location of all other sampling points. By this approach all locations within the area of concern had equal chance of being selected. The soil samples were taken using a coring tool to a depth of 5-10 cm. At each sampling location, samples of soil and rock were taken from at least five different sections of the area into labelled plastic bags. One kilogram (1 kg) of each sample was collected for analysis. The samples were transported to the laboratory for preparation and analysis.

### **Water sampling**

The water samples were taken from water sources within the Goldmine, Tarkwa Township and in the communities. These include Tarkwa Municipal water treatment plants (raw and treated water), Tarkwa Goldfields water treatment plant, tap water from houses, open pits, slime dams, rivers, streams, boreholes and underground water sources. The samples were collected into labelled two and half litres (2.5 L) plastic bottles. The bottles were acid washed with Concentrated  $\text{HNO}_3$  before the bottles were filled with water to ensure radionuclides remain in solution rather than adhering to the walls of the container. The bottles were also filled to the

brim without any head space to prevent CO<sub>2</sub> being trapped and dissolving in water which might affect the chemistry e.g. pH. The water samples were then transported to the Laboratory and stored in a fridge prior to preparation and analysis. The pH of the water samples were measured in the field and in the laboratory using pH meter model HANNA pH 211. The pH meter was calibrated with standard buffer solutions with pH 4.01, 7.0 and 9.21. The total dissolved solids (TDS) and conductivity were also measured in the laboratory using HACH multi-meter, model SanSion 5. The equipment was calibrated with standard solutions of 0.01M KCl and 0.1M KCl.

### **Dust sampling**

Dust samples were taken from locations where the mine's Environmental Department carries out its air/dust sampling. These are points that have been identified by the mine as potential sources where members of the public could be exposed to dust resulting from the mine's operations. The dust/air samples were taken from the following locations: New Atuabo community, Goldfields official club house, Boboobo community, Agricultural Hill near Ghana Telecom Mask in Tarkwa and the residential area of the lecturers of University of Mines and Technology (UMAT). The Agricultural Hill and the UMAT area are closed to Teberebie pit of the mines. Airborne particulate samples were collected onto 0.45 µm pore size filter paper using an air sampler, RADECO air sampler, model SAIC H-809C with a flow rate of 350 Litres/minute (0.35 m<sup>3</sup>/minute). The air sampler which was powered using a power generator, continuously suck dust onto the filter. In order to prevent dust being collected on the filter emanating from other sources such as vehicular movement, the equipment was set up at a location remote from the road side. The sampling was carried out for four (4) hours a day resulting in a throughput of 84 m<sup>3</sup>. At the end of the sampling period, the filters were labelled

and sealed in plastic bags to prevent the escape of gaseous radionuclide from the samples and transported to the laboratory for analysis.

### **Food sampling**

A number of farms are dotted around the mines concession and also in the communities. The main food crop grown in these farms is cassava. The roots of the cassava plant constitute the predominant foodstuff that is eaten by every household in the southern part of Ghana. About 2 kg of cassava samples were taken from different farms and transported in polyethylene bags to the laboratory for analysis.

### **3.5 Sample preparation for direct gamma spectrometry and neutron activation analysis.**

#### **Soil**

At the laboratory, the samples were air dried in trays for 7 days and then oven dried at a temperature of 105 °C for between 3-4 hours until the samples were well dried with a constant weight [IAEA, 1989]. The samples were then ground into a fine powder using a ball mill grinder and sieved through a 2 mm pore size mesh into a previously weighed one (1) litre Marinelli beaker. The Marinelli beakers with its content were then weighed again to determine the weight of the sample. The beakers were covered and sealed with a paper tape to prevent the escape of the gaseous radionuclides in the sample. The samples were stored for 30 days to allow for secular equilibrium between the long-lived parent radionuclide and their short-lived daughter radionuclides in the  $^{238}\text{U}$  and  $^{232}\text{Th}$  decay series and counted on a high purity germanium (HPGE) detector for 36000 s. The activity concentrations of the radionuclides of interest in the samples were reported on dry weight basis in Bq/kg.

## **Water**

The water samples were prepared into the one (1) Litre Marinelli beaker after filtration to remove all solid particles in the water. The samples were counted on a gamma detector (High Purity Germanium detector) for 36000 s. The activity concentrations of the radionuclides in the sample were reported in Bq/L.

## **Food**

In the laboratory, the cassava samples were thoroughly cleaned and the edible portion chopped into smaller pieces and air dried for about a week. The samples were freeze dried using a freeze drier model Christ LMC-1. After drying, the samples were grounded into powder and sieved through a 2 mm mesh into a 1 Litre Marinelli beaker and the dry weight of the sample determined. The samples were counted on a HPGE detector for 36000 s and the net counts of full energy events used to determine the activity concentrations of  $^{226}\text{Ra}$  ( $^{238}\text{U}$ ),  $^{232}\text{Th}$  and  $^{40}\text{K}$  in Bq/kg.

## **Air/Dust**

Two different analytical techniques were used to determine the activity concentration of the radionuclides. The airborne particulate samples on the air filters were each counted directly on the HPGE gamma detector and also neutron activation analysis (NAA) was used to determine the concentration of uranium-238 ( $^{238}\text{U}$ ) and thorium-232 ( $^{232}\text{Th}$ ) and their decay series radionuclides.

### **3.5.1 Analysis of samples using direct gamma spectrometry**

Direct instrumental analysis without pre-treatment (non-destructive) was used for the measurement of gamma rays for the soil, water, and air (dust) samples using a semi conductor detector. The activity concentrations of the radionuclides in samples were measured using

HPGE. The gamma spectrometry system consists of an n-type HPGE detector coupled to a computer based multi-channel analyser (MCA). The relative efficiency of the detector is 25 % with energy resolution of 1.8 keV at gamma ray energy of 1332 keV of  $^{60}\text{Co}$ . The identification of individual radionuclides was performed using their gamma ray energies and the quantitative analysis of the radionuclides was performed using gamma ray spectrum analysis software, ORTEC MAESTRO-32.

The detector was calibrated with respect to energy and efficiency before measurements. Standards of known concentrations of radionuclides homogeneously distributed on solid water in a 1 L Marinelli beaker and a circular plastic foil were used. Background measurements were taken and subtracted in order to obtain net counts for the samples. The spectrum obtained from the standard was used to carry out energy and efficiency calibrations which were used in the determination of the activity concentrations of the radionuclides in Bq/kg, Bq/l and Bq/m<sup>3</sup> for soil and food samples, water and dust samples respectively. Figure 4-1 shows a block diagram of the gamma spectrometry system.

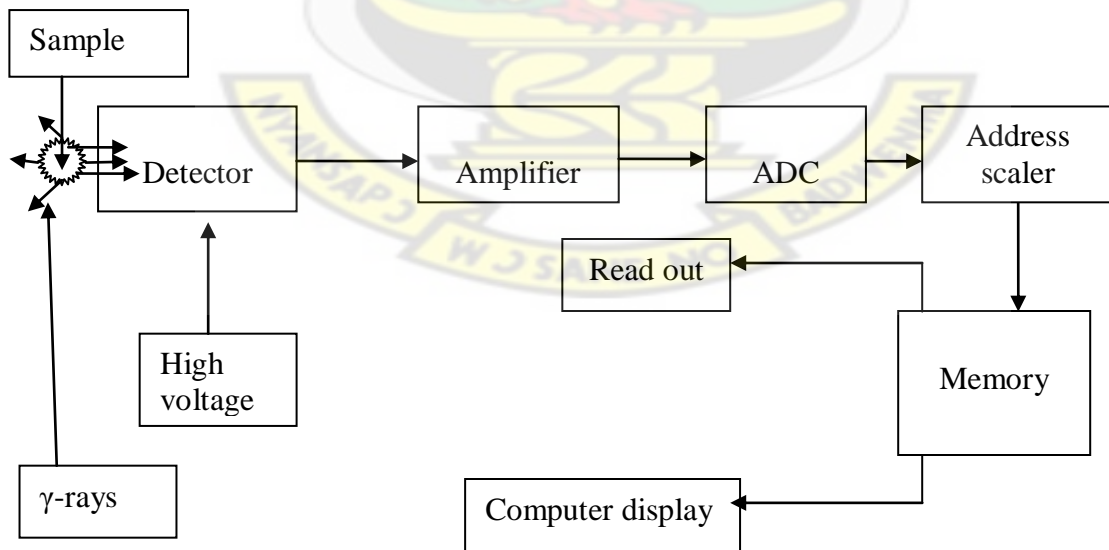


**Figure 3-6: Block diagram of the gamma spectrometry setup.**

### 3.5.1.1 Energy calibration of the gamma ray detector

One of the essential requirements in nuclear spectroscopy measurement is the ability to identify the photo peaks present in a spectrum produced by the detector system [IAEA, 1989]. This is achieved by carrying out energy calibration of the detection system.

The calibration was carried out by counting standard radionuclides of known activities with well defined energies within the energy range of interest from 60 keV to 2000 keV. The calibration standard was counted long enough to produce well defined photo peaks. The channel number that corresponds to the centroid of each full energy event on the MCA was recorded and plotted to obtain a linear curve with second order polynomial. The linear curve obtained from the data points is an indication that the system is operating properly [IAEA, 1989]. The system was checked each day of operation for the stability of the slope and intercept by measurement and plot of at least two different gamma energies. The standard was counted on the gamma detector for ten (10) hours (36000 s). The energy calibration was also carried out for the mixed radionuclides standard on the plastic foil for dust samples. The following radionuclides standards were used for the calibration:  $^{133}\text{Ba}$ ,  $^{57}\text{Co}$ ,  $^{139}\text{Ce}$ ,  $^{137}\text{Cs}$ ,  $^{54}\text{Mn}$ ,  $^{88}\text{Y}$  and  $^{65}\text{Zn}$ .

### 3.5.1.2 Efficiency calibration

The efficiency of the detector refers to the ratio of the actual events registered by the detector to the total number of events emitted by the source of radiation. An accurate efficiency calibration of the system is necessary to quantify radionuclides present in the sample. It is essential that all settings and adjustment of the detector system be carried out prior to determining the efficiencies and this should be maintained until a new calibration is undertaken [IAEA, 1989].

In general, the efficiency of detection decreases logarithmically as a function of energy and it is geometric dependent. Appropriate radionuclides must be selected for use as standards in efficiency calibration. It is recommended to have a number of calibration points approximately between 60 keV and 2000 keV [IAEA, 1989].

The mixed radionuclides standard used for the energy calibration was also used for the efficiency calibration. The standard was counted on the detector for 10 hours (36000 s). The net counts for each of the full energy events in the spectrum was determined and their corresponding energies used in the determination of the efficiencies. The expression used to determine the efficiencies is given as follows [Darko et al., 2007].

$$\eta(E) = \frac{N_T - N_B}{P_E A_{STD} T_{STD}} \quad (23)$$

Where;

$P_E$  is gamma emission probability for energy (E),

$\eta(E)$  is the efficiency of the detector,

$N_T$  is the total counts under a photopeak

$N_B$  is the background count

$A_{STD}$  is the activity (Bq) of the radionuclide in the calibration standard at the time of calibration,

$T_{STD}$  is the counting time of the standard.

### 3.5.1.3 Determination of minimum detectable activity

Minimum detectable activity (MDA) is defined as the smallest quantity of radioactivity that could be measured under specified conditions. The MDA is an important concept in low level counting particularly in environmental level systems where the count rate of a sample is almost the same as the count rate of the background. Under these conditions, the background is counted with a blank, such as sample holder, and everything else that may be counted with an

actual sample. In this work, 1liter Marinelli beaker filled with distilled water was counted for 36000s and the average background peaks used to determine MDA [Cember, 1996]. For  $^{226}\text{Ra}$  ( $^{238}\text{U}$  decay series), the minimum detectable activity was determined using average peak areas of the daughter gamma ray lines 295.2, 351.9 keV of  $^{214}\text{Pb}$  and 609.31, 1764.5 keV of  $^{214}\text{Bi}$ . The daughter gamma ray lines of 238.63 keV of  $^{212}\text{Pb}$ , 583.2 and 2614.53 keV of  $^{208}\text{Tl}$  and 911.21 keV of  $^{228}\text{Ac}$  keV were used to determine the MDA of  $^{232}\text{Th}$ . The MDA of  $^{40}\text{K}$  was determined using the gamma ray line at 1460.8 keV. The minimum detectable activities (MDA) were calculated according to equation (24).

$$MDA = \frac{\sigma\sqrt{B}}{\eta.P.T.W} (Bq/kg) \quad (24)$$

Where;

$\sigma$  is the statistical coverage factor equal to 1.645(confidence level 95%),  
 $B$  is the background for the region of interest of each radionuclide,  
 $T$  is the counting time in seconds,  
 $P$  is the gamma emission probability (gamma yield) of each radionuclide,  
 $W$  is the weight of the sample container, and  
 $\eta$  is the detector efficiency for the measured gamma ray energy.

#### 3.5.1.4 Determination of activity concentrations

The activity concentrations of  $^{238}\text{U}$ ,  $^{232}\text{Th}$  and  $^{40}\text{K}$  in the soil and water samples were calculated using the following analytical expression as shown in equation (25) [Darko et al., 2010].

$$A_{sp} = \frac{N_D e^{\lambda_p T_d}}{p.T_c.\eta.m} \quad (25)$$

Where;

N is the net counts of the radionuclide in the samples,

$T_d$  is the delay time between sampling and counting,

P is the gamma emission probability (gamma yield),

$\eta$  is the absolute counting efficiency of the detector system,

$T_c$  is the sample counting time,

m is the mass of the sample (kg) or volume (l),

$e^{\lambda_p T_d}$  is the decay correction factor for delay between time of sampling and counting, and

$\lambda_p$  is the decay constant of the parent radionuclide.

### **3.5.1.5 Calculation of annual effective dose from external gamma dose rate measurements**

At each sampling location, outdoor external gamma dose rates were measured using a digital environmental radiation survey meter (RADOS, RDS-200, Finland). The dose rate meter was calibrated at the Secondary Standard Dosimetry Laboratory (SSDL) of the Radiation Protection Institute of Ghana Atomic Energy Commission with a calibration factor provided. At each location, five measurements were made at 1 meter above the ground and the average value taken in  $\mu\text{Gy/h}$ . The annual effective dose ( $E_{\gamma, \text{ext}}$ ) was then estimated from the measured average outdoor external gamma dose rate from the equation (26) below:

$$E_{\gamma, \text{ext}} = D_{\gamma, \text{ext}} T_{\text{exp}} DCF_{\text{ext}} \quad (26)$$

Where;

$D_{\gamma, \text{ext}}$  is the average outdoor external gamma dose rate  $\mu\text{Gy/h}$ ,

$T_{\text{exp}}$  is the exposure duration per year, 8760 hours (365 days) and applying an outdoor occupancy factor of 0.2,

DCF<sub>ext</sub> is the effective dose to absorbed dose conversion factor of 0.7 Sv/Gy for environmental exposure to gamma rays [UNSCEAR, 2000].

### 3.5.1.6 Calculation of absorbed dose rate and annual effective dose due to radioactivity in soil/rock samples

The activity concentrations of <sup>238</sup>U in soil/rock samples was calculated from the average energies of 295.21 and 351.92 of <sup>214</sup>Pb and 609.31, 1764.49 keV of <sup>214</sup>Bi. The activity concentrations of <sup>214</sup>Pb and <sup>214</sup>Bi in secular equilibrium with their parents were assumed to represent <sup>238</sup>U activity concentration. Similarly, the activity concentrations of <sup>232</sup>Th was determined from the average energies of 238.63keV of <sup>212</sup>Pb, 583.19 and 2614.53 keV of <sup>208</sup>Tl and 911.21 keV for <sup>228</sup>Ac respectively. The activity concentrations of <sup>208</sup>Tl and <sup>228</sup>Ac in equilibrium with their parents were also assumed to represent the <sup>232</sup>Th activity concentration. The activity concentration of <sup>40</sup>K was determined from the energy of 1460.83 keV.

The external gamma dose rate from the samples was calculated from the activity concentrations of the relevant radionuclides from equation (27).

$$D \left( \text{Gy h}^{-1} \right) = 0.0417A_K + 0.462A_U + 0.604A_{Th} \quad (27)$$

Where;

A<sub>K</sub>, A<sub>U</sub> and A<sub>Th</sub> are the activity concentrations of <sup>40</sup>K, <sup>238</sup>U and <sup>232</sup>Th respectively, and Table 3-3 shows the dose conversion factors of <sup>40</sup>K, <sup>238</sup>U and <sup>232</sup>Th.

**Table 3-3: Activity to dose rate conversion factors [UNSCEAR, 2000]**

Radionuclide	Dose Coefficient (nGy/h per Bq/kg)
<sup>40</sup> K	0.0417
<sup>238</sup> U	0.462
<sup>232</sup> Th	0.604

The annual effective dose was calculated from the absorbed dose rate by applying the dose conversion factor of 0.7 Sv/Gy and an outdoor occupancy factor of 0.2 [UNSCEAR, 2000]. In the case of the water samples, the committed effective doses ( $E_{ing}$ ) were estimated from the activity concentrations of each individual radionuclide and applying the yearly water consumption rate for adults of 730 L/year (2 L/day multiplied by 365 days) and the dose conversion factors of  $^{238}\text{U}$ ,  $^{232}\text{Th}$  and  $^{40}\text{K}$  taken from the BSS and UNSCEAR report, [IAEA, 1996 and UNSCEAR, 2000] using equation (28). For the food samples, annual effective dose was calculated by applying the consumption rate of root crop of 170 kg/year, the activity concentrations of  $^{238}\text{U}$ ,  $^{232}\text{Th}$  and  $^{40}\text{K}$  and their dose conversion factors.

$$E_{Ing}(w) = A_{sp}(w) \cdot I_w \cdot \sum_{j=1}^3 DCF_{Ing}(U, Th, K) \quad (28)$$

Where,  $A_{sp}(w)$  is the activity concentration of the radionuclides in a sample in Bq/L,  $I_w$  is the intake of water in litres per year, and  $DCF_{Ing}$  is the ingestion dose coefficient in Sv/Bq taken from the BSS [IAEA, 1996].

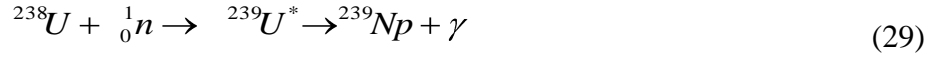
### 3.5.1.7 Determination of activity concentration of $^{238}\text{U}$ and $^{232}\text{Th}$ in ore dust by Neutron Activation Analysis (NAA) as well as the inhalation doses.

The dust samples collected on the filter paper were analysed by irradiating with neutrons from the Ghana Research Reactor-1 (GHARR-1). The process of mineral processing by the mine involves electromagnetic separation and other physical processes as well as chemical separation processes and all these result in the generation of dust. The dust particles collected on the air filters as described under section 3.4 (dust sample) were each folded into a rabbit capsule of diameter 1.6 cm and height 5.5 cm. The capsules were plugged with cotton wool and sealed with a soldering rod and labelled with the sample code.

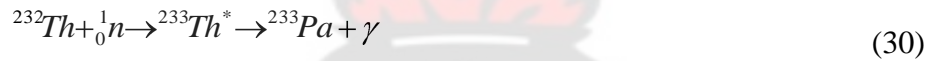
Similarly, a blank empty filter paper was also prepared in the same manner as the samples. A standard was also prepared using a standard reference material of known concentration of each analyte of interest. Rock reference materials for uranium and thorium, GBW07106-GSR-4 and GBW07107-GSR-5 respectively were used for the dust samples in the filter paper. The average weight of the dust samples on the filter papers was 0.005 g. As a result, in the preparation of the U and Th standards, 0.005g of each element was weighed onto the blank filter paper and prepared in the same manner as the samples.

The prepared samples, standards and blank were irradiated using GHARR-1 at the Ghana Atomic Energy Commission, operating at 15 KW with a thermal flux of  $5 \times 10^{11} \text{ n.cm}^{-2}.\text{s}^{-1}$ . The samples were transferred into the irradiation sites via pneumatic transfer system at a pressure of 0.6 Mpa. The samples were irradiated with a scheme for medium to long radionuclide for one hour (1 hour) and allowed to decay for 48 hours to two weeks until a suitable dead time was achieved. After irradiation, radioactivity measurement of the induced radionuclides was performed by a computer based gamma spectrometry set-up. The gamma spectrometry system consists of an n-type HPGE detector coupled to a computer based multi-channel analyser (MCA). The relative efficiency of the detector is 25 % with energy resolution of 1.8 keV at gamma ray energy of 1332 keV of  $^{60}\text{Co}$ . Through appropriate choice of cooling-time, the detector's dead time was controlled to be less than 10 %. The irradiated samples were each counted for two hours on the HPGE detector. The identification of individual radionuclides was performed using their gamma ray energies and the quantitative analysis of the radionuclides was performed using gamma ray spectrum analysis software, ORTEC MAESTRO-32.

The concentrations of uranium and thorium in  $\mu\text{g/g}$  (ppm) were determined from  $^{238}\text{U}$  and  $^{232}\text{Th}$  radionuclides by comparator method using the following nuclear reactions and gamma energy lines of 277.7 and 311.9 keV respectively [Landsberger, 1994].



The  $^{239}\text{U}$  formed after the neutron capture has very weak gamma energy and undergoes a beta-decay to form  $^{239}\text{Np}$  with the emission of gamma rays with energy of 277.7 keV and this was used to determine  $^{238}\text{U}$ . Similarly for  $^{232}\text{Th}$ , the  $^{233}\text{Th}$  formed after the neutron capture undergoes beta-decay to form  $^{233}\text{Pa}$  which emits gamma rays with energy of 311.9 keV and this was used to determine  $^{232}\text{Th}$ .



The elemental concentrations of U and Th determined in the dust samples in  $\mu\text{g}^{-1}$  using NAA were converted to activity concentrations of  $^{238}\text{U}$  and  $^{232}\text{Th}$  in  $\text{Bqm}^{-3}$  according to the following expression (31) (Tzortzis and Tsertos, 2004).

$$A_E = \frac{F_E \cdot \lambda_E \cdot N_A \cdot f_{A,E}}{M_E \cdot C} \quad (31)$$

Where;  $A_E$  is the activity concentration of radionuclide,  $F_E$  is the elemental concentration of uranium or thorium,  $M_E$  is the atomic mass ( $\text{kgmol}^{-1}$ ),  $\lambda_E$  is the decay constant ( $\text{s}^{-1}$ ),  $f_{A,E}$  is the fractional atomic abundance in nature,  $N_A$  is Avogadro's constant ( $6.023 \times 10^{23}$  atoms  $\text{mol}^{-1}$ ) and  $C$  is a constant value of 1,000,000 for U and Th.

The inhalation effective dose from  $^{238}\text{U}$  and  $^{232}\text{Th}$  in ore dust was calculated from equation (32) and the dose conversion factors taken from the BSS (IAEA, 1996).

$$E_{inh}(dust) = T * B_r * F_r * \sum_{j=1}^2 DCF_{j,inh}(U,Th) \cdot C_j \quad (32)$$

where; T is the exposure period in hours,  $B_r$  is the breathing rate for adult members of the public,  $F_r$  is the respirable fraction of dust,  $C_j$  is the activity concentration of U and Th in  $Bq\ m^{-3}$ .

$DCF_{j, inh}$  (U, Th) is the dose conversion factor for U and Th in  $Sv/Bq\ m^{-3}$ .

### 3.5.1.8 Determination of the concentration of metals in soil/rock and water samples by NAA

Similarly, soil samples were prepared by weighing 0.1 g of the finely ground powder into a polyethylene film, sealed using a soldering rod and labelled with the sample code. The sample was then placed in a rabbit capsule and sealed again before the samples were irradiated. For the water samples, 0.5 g of each sample was prepared into a polyethylene vial of 1.2 cm diameter and 2.3 cm height for irradiation. In order to ensure the sample is maintained intact during the irradiation, the sample was doubly encapsulated by placing the smaller polyethylene vial into a bigger capsule of diameter 1.6 cm and height of 5.5 cm. The IAEA-SOIL-7 reference material was used for the analysis. The concentration of the metals was quantified by comparator method using the same geometry, equal weights of both sample and standard, with the same irradiation, decay and counting times as follows [Landsberger, 1994].

$$C_{sam} = C_{std} \left( \frac{A_{sam}}{A_{std}} \right) \quad (33)$$

Where;

$C_{sam}$  is the unknown concentration of the element in the sample,

$C_{std}$  is the known concentration of the element in the standard,

$A_{sam}$  is the activity of the sample and  $A_{std}$  is the activity of the standard.

By normalising the weights between standards and unknowns, the overall equation becomes equation (34) in ppm:

$$C_{sam} = C_{std} (A_{sam}/A_{std})(D_{std}/D_{sam})(C_{std}/C_{sam})(W_{std}/W_{sam}) \quad (34)$$

Where  $W_{sam}$  and  $W_{std}$  are the weights of the sample and the standard respectively.

The product is required to be radioactive and capable of emitting at least one gamma-ray photon.

The gamma ray photon emitted is detected on a gamma ray detector using HPGE. If the activation product is stable, it cannot be detected. The duration of irradiation of the sample depends on the characteristics of the sample. Typically, two irradiation schemes were performed in the analysis. The duration of the irradiation depends on the neutron flux density, mass of the sample and the efficiency of the gamma detector. The longer the irradiation period the more radioactive the reaction product will be. In general, a short irradiation period is required for short-lived nuclides. Samples were irradiated for 10 s and counted for 10 minutes to determine the short-lived radionuclides. For the medium and long-lived radionuclides, samples were irradiated for 1 hour with a delay time between 2 to 3 weeks depending on the dead time (should be less than 10 %) and finally counted for 2 hours each on the gamma ray detector. The samples to be irradiated were specially sealed in capsules and transferred to the reactor core and irradiated with high flux neutrons. The activated components were then analysed to identify and determine quantitatively, the concentration of each radionuclide applying gamma spectrometry technique. If the activated component has a relatively short half-life, the analysis can be carried out whilst the sample is being irradiated and this is known as prompt method. On the other hand, if the activated component has a relatively long half-life, the analysis is postponed to a more convenient time to allow for cooling.

### 3.5.1.9 Measurement of airborne radon activity concentrations and calculation of inhalation dose as well as calculation of soil radon concentration.

Air borne radon activity concentrations were measured directly with a Genitron Alpha Guard, Model PQ 2000/mp50. The measurements were carried out outdoor in the field and indoor in residential areas. The temperature, atmospheric pressure and relative humidity were also recorded during the measurement. The Alpha Guard is provided with a large surface glass fibre filter, which allows only the gaseous  $^{222}\text{Rn}$  to pass through whilst the radon progeny are prevented from entering the ionisation chamber. The filter also protects the interior of the chamber from contamination by dusty particles. The data was evaluated using Alpha View/Expert Software, which automatically transforms radon daughter concentrations from working level (WL) to equilibrium equivalent concentration (ECC) in  $\text{Bqm}^{-3}$ .

The annual effective dose from radon gas in air was estimated from equation (35).

$$E_{inh}(Rn) = DCF_{Rn} F_{Rn} C_{Rn} T_{exp} \quad (35)$$

where;

$E_{inh}(Rn)$  is the annual effective dose from inhalation of radon,

$DCF_{Rn}$  is the dose per unit intake of radon via inhalation in  $\text{nSv/Bqhm}^{-3}$ , ( $9 \text{ nSv/Bqhm}^{-3}$ ) (UNSCEAR, 2000),

$F_{Rn}$  is equilibrium factor for outdoor and indoor occupancy, 0.6 and 0.4 respectively (UNSCEAR, 2000),

$C_{Rn}$  is the radon activity concentration in  $\text{Bqm}^{-3}$ , and

$T_{exp}$  is the exposure period of one year for outdoor occupancy, which is 1760 hours using outdoor occupancy factor of 0.2.

In addition, Radon concentrations in the soil ( $\text{kBqm}^{-3}$ ) were calculated using a proposal in UNSCEAR report from the activity concentrations of  $^{226}\text{Ra}$  (UNSCEAR, 2000).

$$C_{Rn} = C_{Ra} f \rho_s \varepsilon^{-1} (1 - \varepsilon) (m [k_T - 1] + 1)^{-1} \quad (36)$$

Where;

$C_{Ra}$  is the activity concentration of  $^{226}\text{Ra}$  in soil ( $\text{Bq/kg}$ ),

$f$  is the radon emanation factor, (0.2),

$\rho_s$  is the density of the soil grains, ( $2700 \text{ kgm}^{-3}$ ),

$\varepsilon$  is the total porosity, (0.25),

$m$  is the fraction of the porosity that is water filled, (0.95),  $m$  is zero if the soil is dry, and

$k_T$  is the partition coefficient of radon between the water and air phases, (0.23). Since the soil samples were dried before the activity concentrations were measured then,  $m$  is zero and the last term of equation (38) is omitted [UNSCEAR, 2000].

### 3.5.1.10 Calculation of effective doses and total annual effective dose

For the purpose of verifying compliance with dose limits, the total annual effective dose was determined. The total annual effective dose ( $E_T$ ) to members of the public was calculated using ICRP dose calculation method [ICRP, 1991]. The analytical expression for the total annual effective dose is determined by summing all the individual equivalent doses for the exposure pathways considered in this study. These include:

- External gamma irradiation from the gamma emitting radionuclides in the soil samples ( $E_\gamma(\text{U}, \text{Th}, \text{K})$ );
- Committed dose from ingestion of water containing  $^{238}\text{U}$ ,  $^{232}\text{Th}$  and  $^{40}\text{K}$  radionuclides  $E_{\text{ing}}(\text{W})$ ;
- Inhalation of radon gas from soil,  $E_{\text{inh}}(\text{Rn})$  and

- Inhalation of dust containing the Uranium and Thorium decay series of radionuclides,  $E_{inh}(U, Th)$ .

Thus:

$$E_T = E_\gamma(U, Th, K) + E_{ing}(W) + E_{inh}(Rn) + E_{inh}(U, Th) \quad (37)$$

Where;

$E_T$  is the total annual effective dose in Sievert,

$E_\gamma(U, Th, K)$  is the external gamma ray annual effective dose from the soil,

$E_{ing}(W)$  is the committed effective dose from consumption of water,

$E_{inh}(Rn)$  is the annual effective dose from the inhalation of radon gas in air,

$E_{inh}(U, Th)$  is the annual effective dose from the inhalation of dust with U/Th decay series radionuclides.

### 3.6 Determination of Hazard indices and risks

The radiological risk of NORM in soils in the study area which may be used as building materials was assessed by calculating the radium equivalent activity ( $Ra_{eq}$ ), the external hazard and internal hazard indices. The  $Ra_{eq}$  is a widely used hazard index and it was determined using equation (38) [Xinwei et al., 2006]:

$$Ra_{eq} = C_{Ra} + 1.43C_{Th} + 0.077C_K \quad (38)$$

Where;  $C_{Ra}$ ,  $C_{Th}$  and  $C_K$  are the activity concentrations of  $^{226}\text{Ra}$ ,  $^{232}\text{Th}$  and  $^{40}\text{K}$  respectively. In the definition of  $Ra_{eq}$ , it is assumed that 370 Bq/kg of  $^{226}\text{Ra}$ , 259 Bq/kg of  $^{232}\text{Th}$  and 4810 Bq/kg of  $^{40}\text{K}$  produce the same gamma ray dose rate. The above criterion only considers the external hazard due to gamma rays in building materials. The maximum recommended value of  $Ra_{eq}$  in raw building materials and products must be less than 370 Bq/kg for safe use. This means that the external gamma dose must be less than 1.5 mSv/year.

Another criterion used to estimate the level of gamma ray radiation associated with natural radionuclides in specific construction materials is defined by the term external hazard index ( $H_{ex}$ ) as shown equation (39) [OECD/NEA, 1979; Alam et al., 1999; Higgy et al., 2000].

$$H_{ex} = \frac{C_{Ra}}{370} + \frac{C_{Th}}{259} + \frac{C_K}{4810} \quad (39)$$

Where  $C_{Ra}$ ,  $C_{Th}$  and  $C_K$  are the activity concentrations of  $^{226}\text{Ra}$ ,  $^{232}\text{Th}$  and  $^{40}\text{K}$  respectively. The value of the external hazard index must be less than unity for the external gamma radiation hazard to be considered negligible. The radiation exposure due to the radioactivity from construction materials is limited to 1.5 mSv/y [OECD/NEA, 1979; Beretka and Mathew, 1985].

Another hazard index known as internal hazard index due to radon and its daughters was calculated from equation (40). This is based on the fact that, radon and its short-lived products are also hazardous to the respiratory organs.

$$H_{in} = \frac{C_{Ra}}{185} + \frac{C_{Th}}{259} + \frac{C_K}{4810} \quad (40)$$

Where  $C_{Ra}$ ,  $C_{Th}$  and  $C_K$  are the activity concentrations of  $^{226}\text{Ra}$ ,  $^{232}\text{Th}$  and  $^{40}\text{K}$  respectively. For construction materials to be considered safe for construction of dwellings, the internal hazard index should be less than unity.

In addition, the cancer and hereditary risks due to low doses without threshold dose known as stochastic effect were estimated using the ICRP cancer risk assessment methodology [ICRP, 1991; 2007]. In its 1990 recommendations, risks from radiation induced cancers were derived from observations of people exposed to high doses using a dose and dose rate effectiveness factor (DDREF). Risk estimates based on the observations of people exposed to

low doses has associated large uncertainties and therefore will contribute to quantitative risks estimates [ICRP, 1991]. The lifetime risks of fatal cancer recommended in the 1990 recommendations by the ICRP are  $5 \times 10^{-2} \text{ Sv}^{-1}$  for the members of the public and  $4 \times 10^{-2} \text{ Sv}^{-1}$  for occupationally exposed workers [ICRP, 1991].

In its latest recommendations of 2007, the Commission has retained its fundamental hypothesis for the induction of stochastic effects of linearity of dose and effect without threshold and a dose and dose-rate effectiveness factor (DDREF) of 2 to derive the nominal risk coefficients for low doses and low dose rates. In its latest recommendations, the system of regulations for radiological protection based on the 1990 recommendations has not changed [ICRP, 2007].

However, a new set of nominal risk coefficient has been derived to be used for the estimation of fatal cancer as well as hereditary effects. The recommended nominal risk coefficients in its 2007 recommendations are given in table 3-4. The new nominal risk coefficients were derived based upon data on cancer incidence weighted for lethality and life impairment whereas the 1990 values were based upon fatal cancer risk weighted for non-fatal cancer, relative life years lost for fatal cancers and life impairment for non-fatal cancer. However the combined detriment from stochastic effects in the new values has remained unchanged at around  $5 \text{ \% Sv}^{-1}$  [ICRP, 2007].

**Table 3-4. Detriment-adjusted nominal risk coefficients for stochastic effects after exposure to radiation at low dose rate ( $10^{-2}$ ) [ICRP, 2007].**

Exposed Population	<u>Cancer</u>		<u>Heritable effects</u>		<u>Total detriment</u>	
	2007	1990	2007	1990	2007	1990
Whole	5.5	6.0	0.2	1.3	5.7	7.3
Adult	4.1	4.8	0.1	0.8	4.2	5.6

The risk of exposure to low doses and dose rates of radiation to members of the public in the Tarkwa and surrounding from the mining and mineral processing activities of Tarkwa Goldmine were estimated as using the 2007 recommended risk coefficients [ICRP, 2007] and an assumed 70 years lifetime of continuous exposure of the population to low level radiation.

Fatality cancer risk = total annual effective dose (Sv) x cancer nominal risk factor.

Hereditary effect = total annual effective dose (Sv) x hereditary nominal effect factor.

The total annual effective dose estimated from the study area from the potential pathways of exposure of members of the public to ionising radiation was 0.74 mSv.

The basic approaches to radiation protection all over the world are consistent with the recommendations of ICRP publications [ICRP, 1991; 2007]. The recommendations are that, all exposures above the natural background radiation should be kept as low as reasonably achievable (ALARA) and below the individual dose limits of occupationally exposed workers of 20 mSv per year average over 5 years and for members of the public of 1 mSv per year. It is also important to note that, studies so far has not established the effect of radiation in the low dose rate range. A factor of 3-10 lower is required to satisfy most regulations [Xinwei et al., 2006]. As a result of this new limit, rock samples with a  $R_{eq}$  greater than 100 Bq/kg should not be used in the construction of dwellings [Xinwei et al., 2006].

### **3.6.1 Determination of radon emanation fraction**

The soil and rock samples were air-dried for one week and finally oven dried to remove any additional moisture from the samples. The dried samples were each transferred into a 1 litre Marinelli beaker without any treatment (i.e. coarse and bulky samples were not broken down before measurement) and sealed. The EF measurements were carried out on rock (massive) and

soil (granular) samples taken within the mines and the surrounding communities. The results from this study will be compared with results obtained from studies published in literature.

The samples were each counted on a High Purity Germanium Detector (HPGE) after sealing for 2 hours. The samples were then allowed to stay for 4 weeks for secular equilibrium to be established between  $^{226}\text{Ra}$  and its short-lived daughter nuclides of  $^{214}\text{Pb}$  and  $^{214}\text{Bi}$ . The activity concentration of  $^{226}\text{Ra}$  was determined from the average of the peak areas of  $^{214}\text{Pb}$  and  $^{214}\text{Bi}$ .

The radon emanation fraction was determined using the method described by White and Rood (2001). In this method, the emanation fraction is determined from the net count rates after sealing the sample container ( $C_1$ ) and the net count rate after secular equilibrium ( $C_2$ ). The EF determination is based on the increase of  $^{222}\text{Rn}$  concentration during the time interval between sealing ( $t_1$ ) and after 30 days ( $t_2$ ). The net count rates at  $t_1$  and  $t_2$  were expressed as follows;

$$C_1 = A_0 + N(1 - e^{-\lambda t_1}) \quad (41)$$

$$C_2 = A_0 + N(1 - e^{-\lambda t_2}) \quad (42)$$

Where:

$A_0$  is the count rate of  $^{222}\text{Rn}$  present in a sample at sealing time  $t_1$ ;

$N$  is the net count rate of  $^{222}\text{Rn}$  emanated after time  $t_2$ ;

$\lambda$  is  $^{222}\text{Rn}$  decay constant ( $\text{s}^{-1}$ ).

$A_0$  and  $N$  are determined by solving equations (41) and (42) as follows:

To solve the equations,  $x$  was put in place of  $1 - e^{-\lambda t_1}$  and  $y$  put in place of  $1 - e^{-\lambda t_2}$ . The results for  $N$ ,  $A_0$  and EF are given in equations (43), (44) and (45).

$$N = \frac{C_1 - C_2}{x - y} \quad (43)$$

$$A_0 = \frac{xC_2 - yC_1}{x - y} \quad (44)$$

$$EF = \frac{N}{A_0 + N} \quad (45)$$

The emanation fraction (EF) was calculated from equation (45).

### 3.7 Gross alpha and beta measurements in water samples

Twenty-nine water samples taken from bore-holes, tap water, water treatment plants, streams and waste water from the gold treatment plant were analysed for gross alpha ( $\alpha$ ) and gross beta ( $\beta$ ) radioactivity. Five hundred millilitres (500 ml) of each water sample was acidified with 1ml of concentrated HNO<sub>3</sub> and evaporated to near dryness on a hot plate in a fume hood. The residue in the beaker was rinsed with 1M HNO<sub>3</sub> and evaporated again to near dryness. The residue was dissolved in minimum amount 1M HNO<sub>3</sub> and transferred into a weighed 25mm stainless steel planchet. The planchet with its content was heated until all moisture has evaporated. It was then stored in a desiccator and allowed to cool and prevented from absorbing moisture.

The prepared samples were counted to determine alpha and beta activity concentration using the low background Gas-less Automatic Alpha/Beta counting system (Canberra iMatic™) calibrated with alpha (<sup>241</sup>Am) and beta (<sup>90</sup>Sr) standards. The system uses a solid state silicon (Passivated implanted Planar Silicon, PIPS) detector for alpha and beta detection. The alpha and beta efficiencies were determined to be 36.39±2.1% and 36.61±2.2 % respectively. The background readings of the detector for alpha and beta activity concentrations were 0.04±0.01 and 0.22±0.03 cpm respectively.

### 3.8 Statistical analysis of samples

Paired Sample t-test statistical technique of Statistical Package for Social Scientists (SPSS) statistical software was used to compare the Means of the radionuclides concentrations in the water and soil/rock samples. This technique was used because sampling was carried out at two different periods for the study; first batch October 2008 (relatively dry period) and second batch July 2009 (relatively wet period). If the probability value P is greater than the significance level at 5 % ( $P > 0.05$ ), then it implies that the paired sample Means are insignificant or the Mean of the two paired samples are equal. On the other hand if the P-value is less than the significance level at 5 % ( $P < 0.05$ ) then there is a significant difference between the means of the two sets of data. The paired sample t-test computes the difference between two variables for each case, and tests to find out if the average difference is significantly different from zero at 95 % Confidence level.

The paired sample t-test is calculated from the expression below:

$$t = \frac{\bar{d}}{\sqrt{s^2/n}} \quad (46)$$

Where  $\bar{d}$  is the Mean difference between two samples,  $s^2$  is the sample variance, n is the sample size and t is a paired sample t-test with n-1 being the degrees of freedom.

Analysis of variance (ANOVA) was used to compare the means of the elemental concentrations of uranium, Thorium and Potassium in the water samples in order to determine whether the differences in the elemental concentrations of the metals were significant or otherwise.

### 3.9 Uncertainty estimation

Every analytical measurement is always associated with a number of uncertainties which have to be identified and quantified. These uncertainties are also referred to as the quantification

of the doubts associated with the measurement namely random and systematic uncertainties. Random uncertainties vary from measurement to measurement and are equally likely to be positive or negative. Some of the factors which give rise to this type of uncertainty include fluctuation in environmental conditions, e.g. temperature, pressure, humidity, etc, due to differences in the chemical and physical composition of samples. Random uncertainties are always present in a series of measurement. Random uncertainties can be detected through repeated measurements but they cannot be eliminated.

The second type of uncertainty is referred to as systematic uncertainty. This type of uncertainty remains the same throughout a set of measurements. This may arise because the experimental set up is different from that assumed by theory or the instrument is being used outside of its calibration range. It may also arise due to an instrument being poorly calibrated or calibrated with poorly prepared standards. These types of uncertainties may be difficult to detect.

In any analytical measurement, results should be quoted accompanying a statement of the uncertainty in the measurement. Uncertainty estimation involves the following steps:

- Identifying all of the potential sources of uncertainty in the measurement,
- Estimation of the size of uncertainty from each source of uncertainty,
- Combine all of the estimated uncertainties to give an overall figure of merit for the quantity being measured.

In quoting the results of measurements, the quantity measured must be quoted with the uncertainty. In addition, a statement of the coverage factor and the confidence level should be stated.

In this study, the uncertainties associated with the determination of activity concentrations of each radionuclide were estimated from expression used in the calculation of the specific activity concentrations, viz equation (47).

$$A_{sp} = \frac{N \cdot e^{\lambda \cdot Td}}{\eta \cdot P \cdot M \cdot Tc} \quad (47)$$

Where;

$A_{sp}$  is the specific activity in Bq/kg,

N is the background corrected net peak area,

$\eta$  is the absolute detection efficiency,

P is the gamma ray yield,

Tc is the counting time of the sample,

$\lambda$  is the decay constant of individual radionuclides,

Td is the time between sampling and time of counting.

Some of the uncertainties identified for the quantification of the uncertainty in the determination of the specific activity concentrations include the following:

- Net peak area,
- Detection efficiency,
- Sample mass,
- Counting time.

The overall uncertainty in the determination of the activity concentrations was obtained using equation (48).

$$dA_{sp} = A_{sp} * \left[ \left( \frac{dN}{N} \right)^2 + \left( \frac{d\eta}{\eta} \right)^2 + \left( \frac{dM}{M} \right)^2 \right]^{\frac{1}{2}} \quad (48)$$

dN is determined from the uncertainty in the integration of the peak area of each full energy event.

dM is the standard uncertainty on the weighing balance used to weigh the samples and the standard uncertainty was quoted to be 0.1 mg, and

dη is the uncertainty in the efficiency calibration of the counting system.

### **3.10 Determination of physical parameters, trace metals and anions.**

The geochemical studies were carried out by determining the following parameters: pH; Total Dissolved Solids (TDS); Conductivity as well as the levels of anions such as phosphate ( $\text{PO}_4^{3-}$ ), sulphate ( $\text{SO}_4^{2-}$ ), nitrate ( $\text{NO}_3^-$ ) and Chloride ( $\text{Cl}^-$ ). The concentrations of trace metals such as cadmium (Cd), iron (Fe), zinc (Zn), copper (Cu), manganese (Mn), arsenic (As), chromium (Cr), lead (Pb) and mercury (Hg) were also investigated in water samples within the mine and its environs.

All life form on earth depends on water. Every human being consumes several litres of fresh water daily to sustain life. The water sources most often are not cleaned and need some purification before it can be used. The purification requires removing some physical parameters as well as chemical parameters. The purification requires understanding of the types of physical and chemical parameters that exist in the natural waters and the chemistry required to purify the water intended for drinking purposes.

#### **3.10.1 pH, Conductivity and total dissolved solids (TDS) determination**

The pH values of the water samples were measured using pH meter model HANNA pH 211 in conjunction with a glass electrode with a calomel reference electrode. The pH meter was calibrated with standard buffer solutions with pH 4.01, 7.0 and 9.21. The TDS and conductivity was measured using HACH multi-meter, model SanSion 5. The equipment was calibrated with

the following standard solutions, 0.01M KCl with absorbance of 1413  $\mu\text{s}/\text{cm}$  and 0.1M KCl with absorbance of 12880  $\mu\text{s}/\text{cm}$ .

### 3.10.2 Anions Determination

The following anions were determined in the water samples; phosphate ( $\text{PO}_4^{3-}$ ), sulphate ( $\text{SO}_4^{2-}$ ), nitrate ( $\text{NO}_3^-$ ), and chloride ( $\text{Cl}^-$ ). They were determined using a UV-VIS Spectrophotometer, Model UV-1201 manufactured by HIMADZU of Japan. For quality control purposes the equipment was calibrated with a set of five (5) standard solutions of each analyte of interest of different concentrations.

#### Nitrate

In the determination of nitrate ( $\text{NO}_3^-$ ), 5.0 mL of each of the filtered water sample was used in a labelled test tube. 1.0 ml of 30 % of NaCl was added to each sample, a blank of distilled water and the standard solutions. This was followed with the addition of 5.0 mL of concentrated  $\text{H}_2\text{SO}_4$ . Five (5) drops (0.25 mL) of brucine reagent was added to the samples and standards excluding the blank. The resultant solution of the samples was cling wrapped and placed on a water bath for about 25-30 minutes at a temperature of 90 ° C. The samples were then cooled and measured using the UV-spectrophotometer at a wavelength of 410 nm. Before the samples were measured, the prepared blank was used to zero the equipment by setting the absorbance to zero. The prepared nitrate standard solutions with concentrations 0.2, 0.4, 0.6, 0.8 and 1.0 ppm were measured on the instrument and their absorbance determined. A plot of the standard concentrations on the x-axis and the absorbance on the y-axis resulted in a linear calibration curve which was used to determine the concentration of  $\text{NO}_3^-$  in the water samples using the absorbance value.

## **Sulphate**

Determination of  $\text{SO}_4^{2-}$  was carried out using, a colorimetric measurement of the absorption produced by the turbidity resulting from the precipitation of  $\text{BaSO}_4$  in acidic medium which is proportional to the sulphate concentration. The Sulphate ions in the sample reacted with  $\text{BaCl}_2$  to form  $\text{BaSO}_4$ . The absorption occurs at a wavelength of 420 nm. In its determination, 10 mL each of filtered water samples, standard solutions and blank was measured into a labelled test tube and 1.0 mL of acid salt solution was added to the samples, standards and blank. This was followed with addition of 0.50 mL and 0.05 g of glycerol and  $\text{BaCl}_2$  respectively. This resulted in the precipitation of  $\text{BaSO}_4$ . This was then measured with the UV spectrophotometer at a wavelength of 420 nm and the absorbance determined. The concentration of the  $\text{SO}_4^{2-}$  was determined from the standard curve of the standard concentrations of sulphate and absorbances.

## **Phosphate**

The total phosphate ( $\text{PO}_4^{3-}$ ) in the water samples reacts with molybdate in an acid medium to produce a mixed phosphate/molybdate complex. Ascorbic acid reduces the complex, resulting in an intense molybdenum blue colour and which was measured at a wavelength of 880nm. In its determination, 10 mL of filtered water samples, standard solutions and blank were prepared into a labelled test tube and 2.0 mL of combined reagent of 1:4 combination of ascorbic acid to molybdate antimonyl reagent ratio was added. This resulted in the formation of an intense blue colour that was measured and the absorbance for each sample determined. The concentration of the  $\text{PO}_4^{3-}$  was determined from the standard curve of the phosphate standards.

## **Chloride**

Chloride (Cl) is found in almost all natural waters. Chloride in the water samples was determined by titration. The water samples were titrated against standard silver nitrate ( $\text{AgNO}_3$ )

solution with potassium chromate ( $K_2CrO_4$ ) as an indicator to form a yellowish pink end point of silver chloride ( $AgCl$ ) precipitate before a red silver chromate is formed. In its determination, 25.0 mL of the filtered water samples was transferred into a 250 mL conical flask and 3 drops of 0.27M  $K_2CrO_4$  indicator solution added and swirled to mix. A blank of 25.0 mL distilled water was also prepared in the same manner. The blank and resultant solutions of the samples were titrated against 0.0141M  $AgNO_3$  with  $K_2CrO_4$  as an indicator to form a yellowish pink colour at the end point. The blank determination was done first before the actual samples. The concentration of  $Cl^-$  in the water samples after titration was calculated using equation (49) in mg/L [WEF, 1995]:

$$mg(Cl^-) = \frac{(A - B) * M * 35.45 * 1000}{Volume\ of\ sample(mL)} \quad (49)$$

Where:

A is the titre value of sample;

B is the titre value of blank;

M is the molarity of  $AgNO_3$ ; and

The figure 35.45 is the atomic weight of  $Cl^-$ .

### 3.10.3 Trace Metals Determination

The trace metals in the water samples were determined using Atomic Absorption Spectrophotometer (AAS).

The water samples were first digested using microwave digester model ETHOS D Labstation. Five (5) g of each water sample was weighed into a labelled 100 mL polytetrafluoroethylene (PTFE) teflon bombs. The following reagents were added to the sample in the teflon bombs; 3.0 mL of concentrated  $HCl$  (35 %), 6.0 mL of concentrated  $HNO_3$  (65 %) and 0.25 mL industrial grade  $H_2O_2$  (30 %) in a fume hood. The samples were loaded on the

microwave carousel and secured tightly. The samples were digested for 21 minutes using the following operational parameters: 250 W for 05 minutes; 0 W for 01 minute; 250 W for 10 minutes, 450 W for 05 minutes and 5 minutes allowed for venting [Milestone Cook Book, 1996]. Reference standards for each element of interest, blanks and repeat of some samples were digested in the same way as the actual samples. After digestion, the Teflon bombs mounted on the microwave carousel were cooled in water to reduce the internal pressure and also allow volatilized substances to re-solubilise. The following metals determined after digestion of the samples; Hg, As, Cd, Pb, Zn, Cu, Fe, Mn, and Cr.

In the analysis for mercury and arsenic potassium permanganate and potassium iodide were added respectively before analysis. This was to ensure the reduction in the oxidation state of the Hg and As from +5 to +3 states required for their determination in the digested samples. For each metal, a set of standard solutions were prepared from stock solutions and used to calibrate the equipment to determine the useful range (linear) for the determination of each metal. The concentration of each element in a sample was determined from its standard calibration curve based on the absorbance obtained for the unknown sample in parts per million, ppm (mg/L).

## CHAPTER FOUR

### 4.0 RESULTS

In this work, seventy-two (72) composite samples each, for the two periods of sampling were sampled randomly within selected areas of the mine concession. This included 38 soil/rock samples, 29 water samples and 5 dust samples. Six (6) composite cassava samples were also taken from six farms within the mine and surrounding communities. The results obtained from the in-situ and laboratory measurements are summarized in Tables 4-1 to 4-29 and Figures 4-1 to 4-20.

In order to ascertain the quality and the reliability of measurements the HPGE detector was calibrated with respect to energy and efficiency using standard radionuclides in a one (1) litre Marinelli beaker with solid water as the matrix. For the soil, water and food samples, the mixed radionuclide standard source in solid water matrix was also used for the efficiency calibration. In the case of the dust samples collected on the filter paper, a mixed standard source of different radionuclides uniformly distributed in plastic foil was used for the efficiency calibration. The standard radionuclides that were used for the energy and efficiency calibrations are shown appendix I for the solid water matrix and the plastic foil matrix respectively. The corresponding energy and efficiency calibration curves obtained for two different geometries namely 1.0 Litre Marinelli beaker and Plastic foil are shown in Figures 4-1 to 4-4 respectively. The resolution of the high purity germanium detector was evaluated using  $^{60}\text{Co}$  at the energy of 1332 keV and the results is shown in figure 4-5 with an estimated value of 0.19 %. The Minimum Detectable Activities for  $^{238}\text{U}$  ( $^{226}\text{Ra}$ ),  $^{232}\text{Th}$  and  $^{40}\text{K}$  are shown in Table 4-1 with estimated values of 0.12, 0.11 and 0.15 Bq/kg respectively.

The terrestrial gamma dose rates measured at 1 meter above the ground at the sampling points in the study area are shown in Table 4-2. The mean absorbed dose rates measured in air at the soil and water sampling points were 38.1 and 42.5 nGy/h respectively.

The estimated average activity concentrations of  $^{238}\text{U}$ ,  $^{232}\text{Th}$  and  $^{40}\text{K}$  in the water, soil, air and food samples are shown in Tables 4-3, 4-4, 4-5, 4-6, 4-7 (fresh weight) and 4-8 (dry weight) respectively. They also include the results of the estimated absorbed dose rate and annual effective dose. Tables 4-9, 4-10 and 4-11 are the results of the ratio of soil to cassava activity concentrations. Table 4-12 also shows the results of the airborne and soil  $^{222}\text{Rn}$  activity concentrations as well as the estimated annual effective dose for the airborne radon concentration. The table also contains the environmental conditions under which the sampling was carried out including data on: temperature, atmospheric pressure and relative humidity. Table 4-13 is the results of activity concentrations of  $^{238}\text{U}$ ,  $^{232}\text{Th}$  and  $^{40}\text{K}$  in soils in the study area and published data.

Comparisons of the activity concentrations and estimated annual effective doses in soil and water samples are shown in Figures 4-6 to 4-12. Figure 4-13 shows the relative contributions to total absorbed dose rates in air outdoor due to  $^{238}\text{U}$ ,  $^{232}\text{Th}$  and  $^{40}\text{K}$  for soil and rock samples. Figure 4-14 illustrates the percentage contribution of  $^{40}\text{K}$ ,  $^{232}\text{Th}$  and  $^{238}\text{U}$  to the total activity, radium equivalent activity, external hazard index and internal hazard index.

Results of radon emanation fractions are shown in Table 4-14. A summary of the annual effective doses for the various exposure pathways considered in this study and estimated total annual effective dose are presented in Table 4-15. The estimated lifetime fatality cancer risk and hereditary disorders estimated from all the exposure pathways studied are reported in Table 4-16. The radiological hazards and risks associated with soil samples based on radium equivalent

activity, external and internal hazard indices in the study area were estimated and presented in Table 4-17. A comparison of  $^{226}\text{Ra}$  activity concentration and calculated radium equivalent activity concentrations with published data are shown in Table 4-18.

The results of the comparison of radon emanation fraction with published data for different types of samples are also given in Table 4-19. Comparison of the activity concentrations as well as the estimated annual effective doses in soil and water for the two sampling periods are shown in Tables 4-20 to 4-22. The results of the gross- $\alpha$  and gross- $\beta$  activity concentrations are shown in Table 4-23.

The results of the geochemical studies carried out on the water and soil samples in the study area are also shown in Tables 4-24 and 4-25. This includes the physical parameters and chemical parameters of the water samples such as pH, temperature, salinity, conductivity, total dissolved solid (TDS), metals and anions which are shown in Table 4-24. The concentrations of the trace metals and major metals in the soil samples determined by Neutron Activation Analysis (NAA) are presented in Table 4-25. Statistical analysis of the data using SPSS are shown in Tables 4-26 to 4-29. Figure 4-15 shows as comparison of percentage weighted values of pH, temperature, conductivity, total dissolved solids, uranium, thorium and potassium in soil and rock samples in the study area. Figure 4-16 also shows the plots of the comparison of the thorium versus uranium, potassium versus uranium and thorium versus potassium ratios in soil and rock samples. Finally Figures 4-17 to 4-20 show the comparison of relationship between the concentrations of physical parameters such as pH, temperature, conduction and total dissolved solids and the concentrations of uranium, thorium and potassium in the water samples.

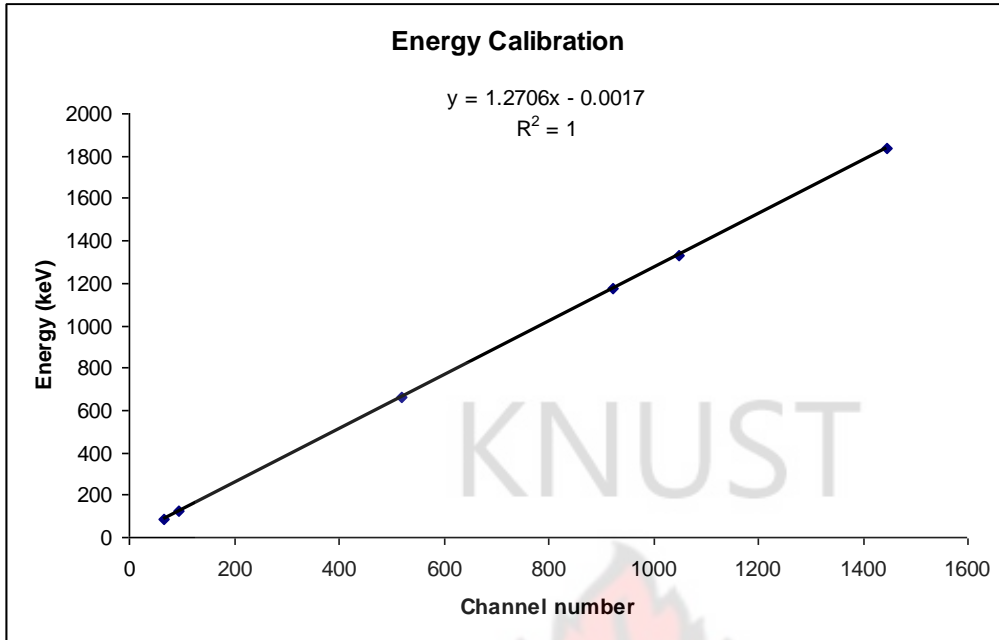


**Figure 4-1: Energy calibration curve using mixed standard radionuclides in a one litre Marinelli beaker.**

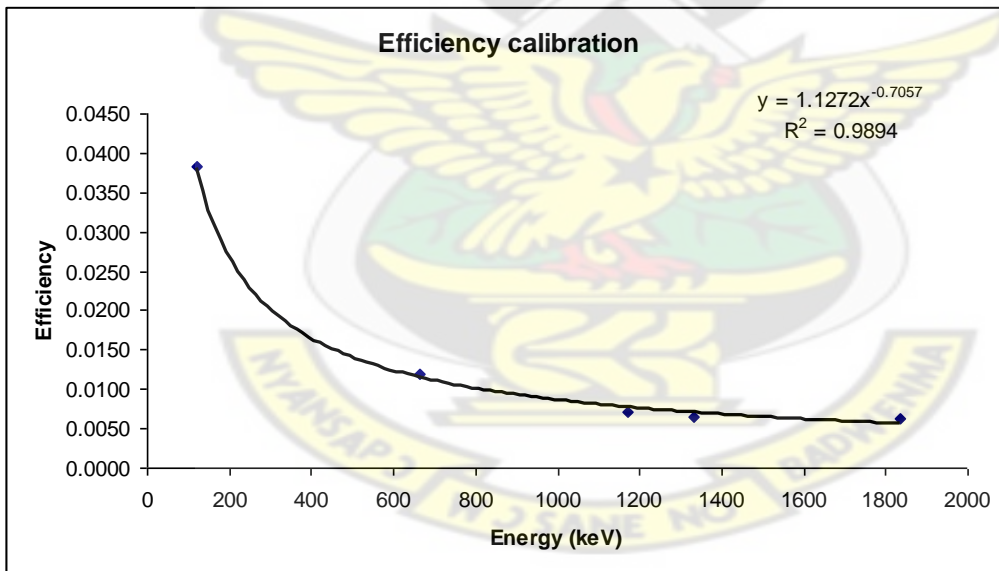


**Figure 4-2: Efficiency calibration curve as a function of energy for mixed radionuclides standard in a one litre Marinelli beaker.**

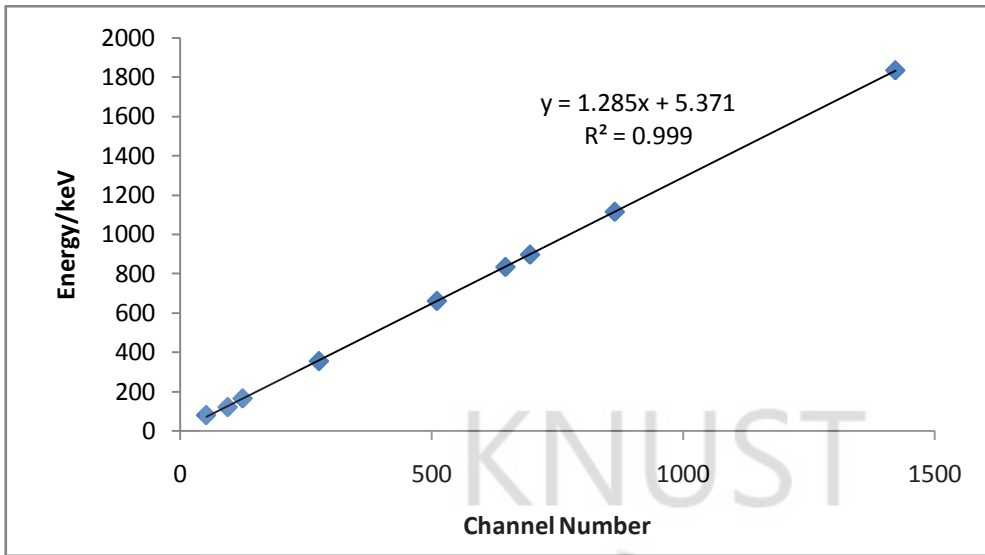


**Figure 4-3: Energy calibration curve using mixed radionuclides standard distributed in a plastic foil.**

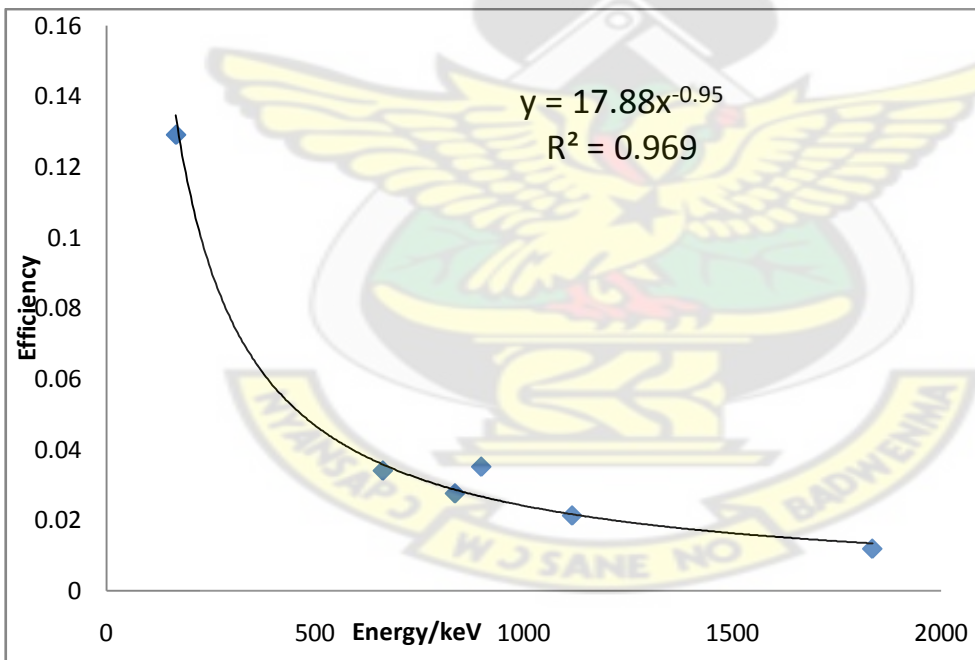


**Figure 4-4: Efficiency calibration curve for mixed radionuclide standard in a plastic foil**

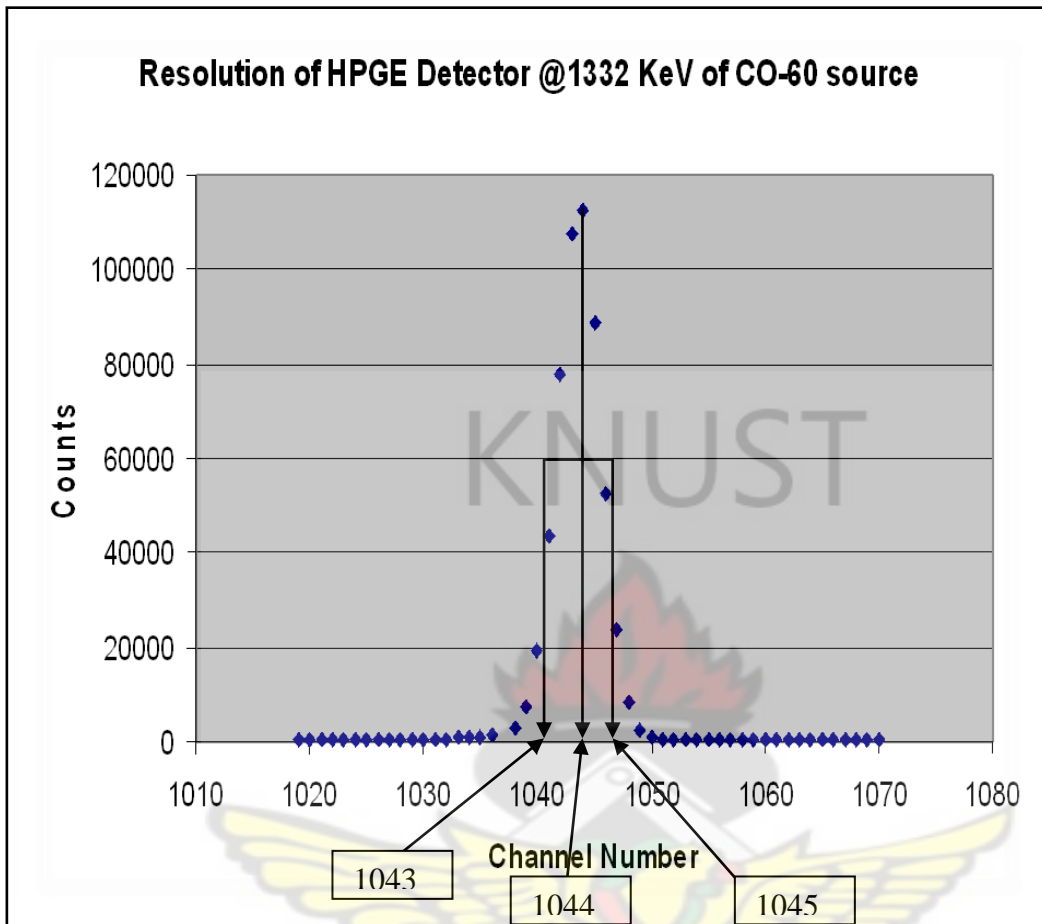


**Figure 4-5: Energy Resolution of the HPGE detector at 1332 keV of  $^{60}\text{Co}$ .**

$$\text{Resolution}(FWHM) = \frac{1045 - 1043}{1044} = 0.19 \% \quad (50)$$

The resolution of the detector measured at 1332 keV of  $^{60}\text{Co}$  source was 0.19 %.

**Table 4-1: The minimum detectable activities of  $^{238}\text{U}$ ,  $^{232}\text{Th}$  and  $^{40}\text{K}$ .**

Nuclide	MDA, Bq/kg
$^{238}\text{U}$	0.12
$^{232}\text{Th}$	0.11
$^{40}\text{K}$	0.15

**Table 4-2: Average absorbed dose rate measured in air at 1 metre above soil and water sampling points in the various communities of the study areas and calculated annual effective dose.**

Sampling location	Soil sampling		Water sampling	
	Absorbed dose rate, nGy/h	Annual effective dose, $\mu$ Sv	Absorbed dose rate, nGy/h	Annual effective dose, $\mu$ Sv
Abekoase	40.0	42.9	25.0	30.7
Brahabebom	30.0	36.8	40.0	49.1
Huniso	15.0	18.4	10.0	12.6
New Atuabo	55.0	67.5	50.0	61.3
Pepesa	30.0	36.8	65.0	79.7
Samahu	40.0	49.1	33.0	39.9
Tarkwa	57.0	69.5	68.0	83.4
Minesite	38.0	46.5	49.0	60.1
Range	15.0 – 57.0	18.4 – 69.5	10.0 – 68.0	12.6 – 83.4
Mean	38.1	45.9	42.5	52.1
Standard deviation	13.7	16.8	19.7	24.1



**Table 4-3: Average activity concentrations, absorbed dose rates and annual effective doses due to  $^{238}\text{U}$ ,  $^{232}\text{Th}$  and  $^{40}\text{K}$  in soil in the study area.**

Sample location	Activity concentrations, Bq/kg			Absorbed dose rate, nGy/h	Annual effective dose, mSv	Percentage contribution of radionuclides to absorbed dose rates (%)		
	$^{238}\text{U}$	$^{232}\text{Th}$	$^{40}\text{K}$			$^{238}\text{U}$	$^{232}\text{Th}$	$^{40}\text{K}$
Abekoase	16.5±1.5	13.7±1.2	125.8±10.7	21.2	0.14	37.1	39.5	23.5
Brahabebom	18.6±1.7	37.5±2.4	163.8±13.4	38.1	0.24	24.2	57.8	18.0
Huniso	7.7 ± 0.9	8.5 ± 0.9	76.2 ± 6.7	11.5	0.08	30.3	42.7	27.0
New Atuabo	13.3 ± 1.5	35.2 ± 2.5	194.6±15.5	35.5	0.23	17.3	59.0	23.7
Pepesa	12.2 ± 1.15	10.5±1.0	60.4±5.6	14.5	0.09	39.0	43.6	17.4
Samahu	17.9±1.6	23.3±1.8	153.3±12.7	28.7	0.18	29.0	44.2	22.1
Tarkwa township	25.5 ± 2.0	67.2±4.8	248.9±19.5	62.7	0.38	19.1	61.9	18.9
Minesite	9.6±1.2	19.1± 1.54	233.3 ± 18.4	26.6	0.16	17.9	44.6	37.5
Range	7.7 – 25.5	8.5 – 67.2	60.4 – 248.9	11.5 – 62.7	0.08 – 0.38	17.3 – 39.0	39.5 – 61.9	17.4 – 37.5
Mean	15.2	26.9	157.0	29.9	0.19	26.7	49.2	23.5
Standard deviation	5.7	19.5	68.2	16.2	0.1	8.5	8.8	6.5

**Table 4-4: Statistical summary of activity concentrations and estimated annual effective doses from water in the study area.**

Sample Location	Type of water sample	pH	Activity concentration, Bq/l			Annual effective dose, mSv
			<sup>238</sup> U	<sup>232</sup> Th	<sup>40</sup> K	
Abekoase	SW(stream)	5.84	0.55 ± 0.03	0.34 ± 0.03	7.46 ± 0.04	0.20
	UW(borehole)	5.32	0.76 ± 0.03	0.37 ± 0.02	11.14 ± 0.04	0.27
Brahabe bom	UW(borehole)	5.18	0.32 ± 0.03	0.52 ± 0.01	8.86 ± 0.04	0.19
Huniso	SW(river)	6.49	0.76 ± 0.03	0.41 ± 0.02	9.26 ± 0.04	0.27
	UW(borehole)	4.48	0.51 ± 0.06	0.21 ± 0.04	1.65 ± 0.08	0.15
New Atuabo	UW(borehole)	5.45	0.36 ± 0.04	0.40 ± 0.03	7.87 ± 0.05	0.18
Pepesa	SW(stream)	6.40	0.75 ± 0.02	0.39 ± 0.06	8.69 ± 0.05	0.16
	UW(borehole)	5.26	0.41 ± 0.03	0.31 ± 0.02	5.93 ± 0.05	0.26
Samahu	SW(stream)	6.92	0.37 ± 0.04	0.31 ± 0.03	9.93 ± 0.08	0.17
	UW(borehole)	6.10	0.39 ± 0.04	0.45 ± 0.02	8.61 ± 0.05	0.20
Tarkwa township	SW(rainwater)	5.91	0.29 ± 0.05	0.49 ± 0.02	11.99 ± 0.04	0.20
	TW(tap water)	6.33	0.58 ± 0.03	0.45 ± 0.02	8.69 ± 0.04	0.24
	UW(borehole)	5.48	0.46 ± 0.03	0.56 ± 0.01	5.13 ± 0.10	0.21
Minesite	SW (tailings)	6.75	1.03 ± 0.05	0.52 ± 0.04	8.91 ± 0.05	0.34
	PW (plant)	8.24	0.55 ± 0.04	0.28 ± 0.02	5.65 ± 0.05	0.19
	UW(mine pits)	6.00	0.76 ± 0.03	0.51 ± 0.05	9.07 ± 0.06	0.28
Bonsaso (control)	SW(River)	6.82	0.11 ± 0.09	0.51 ± 0.04	3.11 ± 0.06	0.10
Range		4.48 – 8.24	0.11 – 1.03	0.21 – 0.56	1.65 – 11.99	0.10 – 0.34
Mean		6.1	0.54	0.41	7.76	0.21
Standard deviation		0.9	0.23	0.10	2.70	0.06

SW-Surface water; UW-underground water; TW-tap water; PW-process water

**Table 4-5: Mean activity concentrations of  $^{238}\text{U}$  and  $^{232}\text{Th}$  in dust/air samples using direct gamma ray analysis, absorbed dose rate and annual effective doses for two periods.**

Sample location	Activity concentration, $\mu\text{Bq}/\text{m}^3$		Absorbed dose rate $\times 10^{-6}$ , nGy/h	Annual effective dose, nSv
	$^{238}\text{U}$	$^{232}\text{Th}$		
New Atuabo	3.62	4.29	4.40	4.05
Mine staff club house	<0.12	0.65	0.43	0.60
Boboobo (Tarkwa)	4.07	3.74	4.20	3.56
Agricultural Hill (Tarkwa)	0.82	2.08	1.70	1.93
UMAT lecturers residential area (Tarkwa)	11.10	3.00	6.80	3.12
Range	<0.12-11.10	0.65 - 4.29	0.43 – 6.80	0.60 – 4.05
Mean	4.90	2.75	3.51	2.65
Standard deviation	4.37	1.45	2.23	1.39

Legend: UMAT-University of Mines and Technology

**Table 4-6: Concentration of U and Th in dust samples using NAA and their calculated activity concentrations**

Sample Code	Dust concentration							
	I				II			
	Uranium ppm	$^{238}\text{U}$ $\mu\text{Bq}/\text{g}$	Thorium ppm	$^{232}\text{Th}$ $\mu\text{Bq}/\text{g}$	Uranium Ppm	$^{238}\text{U}$ $\mu\text{Bq}/\text{g}$	Thorium ppm	$^{232}\text{Th}$ $\mu\text{Bq}/\text{g}$
New Atuabo	<0.01	<0.12	0.71±0.12	2.89	<0.01	<0.12	0.65±0.10	2.65
Mine club House	3.53±0.53	43.60	1.38±0.21	5.62	4.10±0.21	50.60	1.42±0.21	5.78
Boboobo	2.28±0.31	28.10	1.19±0.18	4.84	2.15±0.32	26.50	1.12±0.17	4.56
Agricultural Hill	0.88±0.13	10.90	<0.01	<0.004	0.92±0.14	11.40	<0.01	<0.004
UMAT	0.69±0.10	8.52	2.03±0.31	8.26	0.69±0.10	8.52	1.94±0.29	7.90
Mean	1.80±0.27	23.00	1.30±0.21	5.40	2.00±0.19	24.00	1.30±0.19	5.20

I-First batch of dust samples

II- Second batch of dust samples

ppm-  $\mu\text{g}/\text{g}$

**Table 4-7: The activity concentration of  $^{238}\text{U}$ ,  $^{232}\text{Th}$  and  $^{40}\text{K}$  in fresh food samples by direct gamma ray analysis and committed annual effective doses.**

Sample ID	Activity Concentration, (Bq/kg)			Committed annual effective dose, ( $\mu\text{Sv}/\text{year}$ )
	$^{238}\text{U}$	$^{232}\text{Th}$	$^{40}\text{K}$	
Minesite	0.13±0.04	0.20±0.06	49.96±2.06	61.50
Tarkwa	0.24±0.110.	0.32±0.11	85.47±3.37	104.0
Samahu	0.30±0.16	0.01±0.001	29.34±1.32	33.60
Pepesa	0.07±0.02	0.10±0.06	32.60±1.44	38.80
Abekoase	0.10±0.05	0.08±0.03	38.96±1.66	45.00
Huniso	0.24±0.09	<0.11	36.62±1.58	40.40
Mean	0.18±0.08	0.14±0.05	45.00±1.90	54

**Table 4-8: The activity concentration of  $^{238}\text{U}$ ,  $^{232}\text{Th}$  and  $^{40}\text{K}$  in dried food samples by direct gamma ray analysis and calculated annual effective doses.**

Sample ID	Activity Concentration, (Bq/kg)			Committed annual effective dose, ( $\mu\text{Sv}/\text{year}$ )
	$^{238}\text{U}$	$^{232}\text{Th}$	$^{40}\text{K}$	
Minesite	0.52±0.17	0.88±0.25	229.80±9.46	281
Tarkwa	1.13±0.49	1.49±0.50	393.14±15.49	481
Samahu	1.36±0.72	0.03±0.003	134.96±6.05	154
Pepesa	0.30±0.10	0.47±0.26	149.95±6.63	179
Abekoase	0.47±0.21	0.39±0.16	179.19±7.63	208
Huniso	1.11±0.41	<0.11	168.43±7.25	188
Mean	0.82±0.35	0.65 ± 0.23	209.25±8.75	250

**Table 4-9: U-238 activity concentration ratios of soil to cassava samples**

Sample Location	Activity concentration of, Bq/kg			Ratio of soil to cassava concentrations	
	Soil	Cassava (fresh)	Cassava (dry)	Fresh	Dry
Minesite	20.36	0.13	0.52	156.61	39.15
Tarkwa	16.17	0.24	1.13	67.38	14.31
Samahu	32.83	0.30	1.36	109.43	24.14
Pepesa	12.24	0.07	0.30	174.86	40.80
Abekoase	9.15	0.10	0.47	91.50	19.47
Huniso	22.61	0.24	1.11	94.21	20.37

**Table 4-10: Th-232 activity concentration ratios of soil to cassava samples**

Sample Location	Activity concentration of, Bq/kg			Ratio of soil to cassava concentrations	
	Soil	Cassava (wet)	Cassava (dry)	Wet	Dry
Minesite	22.72	0.20	0.88	113.60	25.82
Tarkwa	19.29	0.32	1.49	60.28	12.95
Samahu	93.64	0.01	0.03	9364.00	3121.33
Pepesa	10.47	0.10	0.47	104.70	22.28
Abekoase	11.05	0.08	0.39	138.12	28.33
Huniso	19.41	<0.11	<0.11	<0.11	<0.11

**Table 4-11: K-40 activity concentration ratios of soil to cassava samples**

Sample Location	Activity concentration of, Bq/kg			Ratio of soil to cassava concentrations	
	Soil	Cassava (wet)	Cassava (dry)	Wet	Dry
Minesite	234.95	49.96	229.80	4.70	1.02
Tarkwa	121.03	85.47	393.14	1.42	0.31
Samahu	193.48	29.34	134.96	6.59	1.43
Pepesa	60.44	32.60	149.95	1.85	0.40
Abekoase	91.22	38.96	179.19	2.34	0.51
Huniso	191.76	36.62	168.43	5.24	1.14

**Table 4-12: Rn-222 concentration in air and soil and the corresponding estimated airborne annual effective doses.**

Sample location	Temperature (°C)	Atmospheric Pressure (kPa)	Relative Humidity (%)	Radon concentration		Airborne <sup>222</sup> Rn annual effective dose, mSv
				Airborne <sup>222</sup> Rn (Bqm <sup>-3</sup> )	Soil <sup>222</sup> Rn (kBqm <sup>-3</sup> )	
Abekoase	33.5	100.6	90.5	30.0	26.8	0.29
Brahabeom	30.0	100.3	98.0	31.5	30.2	0.30
Huniso	35.5	100.7	84.0	27.5	12.5	0.26
New Atuabo	29.5	100.5	95.0	29.5	21.5	0.28
Pepesa	38.0	100.8	84.0	30.0	19.8	0.29
Samahu	33.5	100.6	94.5	30.5	28.9	0.29
Tarkwa Township	34.0	99.9	89.7	32.7	41.3	0.31
Mine site	34.6	100.1	83.1	27.9	15.5	0.27
Range	29.5 -38.0	99.9 -100.8	83.1 - 98.0	27.5 - 32.7	12.5 – 41.3	0.26 - 0.31
Mean	33.6	100.4	89.9	30.0	24.6	0.29
Standard deviation	2.8	0.3	5.7	1.7	9.2	0.02

**Table 4-13: Comparison of activity concentrations of  $^{238}\text{U}$ ,  $^{232}\text{Th}$  and  $^{40}\text{K}$  in soils in the study area and published data (UNSCEAR, 2000; Darko et al., 2010)**

Country	Concentration in soil, Bq/kg					
	$^{238}\text{U}$		$^{232}\text{Th}$		$^{40}\text{K}$	
	Range	Mean	Range	Mean	Range	Mean
Ghana (This work)	8-26	15	9-67	27	60 -249	157
Ghana (Mine1) <sup>#</sup>		29		25		582
Ghana (Mine 2) <sup>#</sup>		35		21		682
Algeria <sup>+</sup>	2-110	30	2-140	25	66-1150	370
Egypt <sup>+</sup>	6-120	37	2-96	18	29-650	320
United States <sup>+</sup>	4-140	35	4-130	35	100-700	370
India <sup>+</sup>	7-81	29	14-160	64	38-760	400
Malaysia <sup>+</sup>	49-86	66	63-110	82	170-430	310
Lithuania <sup>+</sup>	3-30	50	9-46	25	350-850	600
United Kingdom <sup>+</sup>	2-330		1-180		0-3200	
Hungary <sup>+</sup>	12-66	29	12-45	28	79-570	370
Spain <sup>+</sup>			2-210	33	25-1650	470
World average <sup>+</sup>		33		45		420

Legend: + UNSCEAR 2000 Report; # Darko et al., 2010 for Ghana (Mine 1 and Mine 2 values)

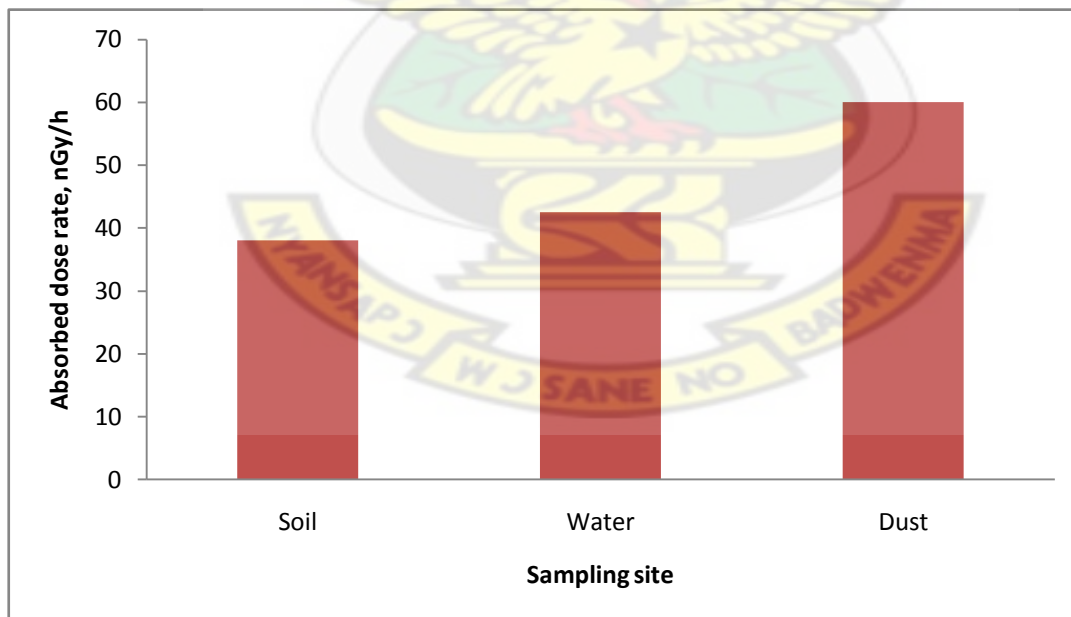


**Figure 4-6: Comparison of absorbed dose rate from direct air measurement at one metre above the ground at soil, water and dust sampling points.**

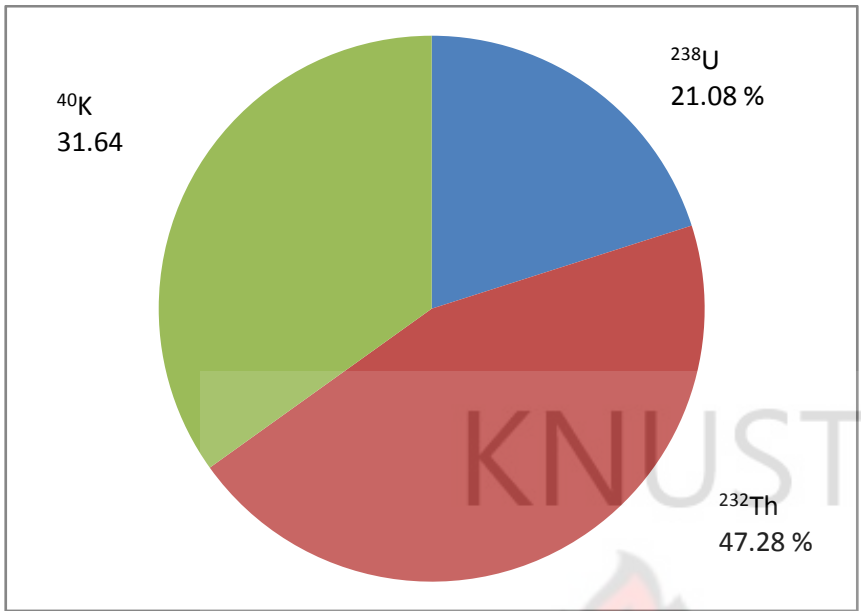


**Figure 4-7:** Relative contributions to total absorbed dose rate in air outdoor due to  $^{238}\text{U}$  and  $^{232}\text{Th}$  decay series elements and  $^{40}\text{K}$  for soil and rock samples.

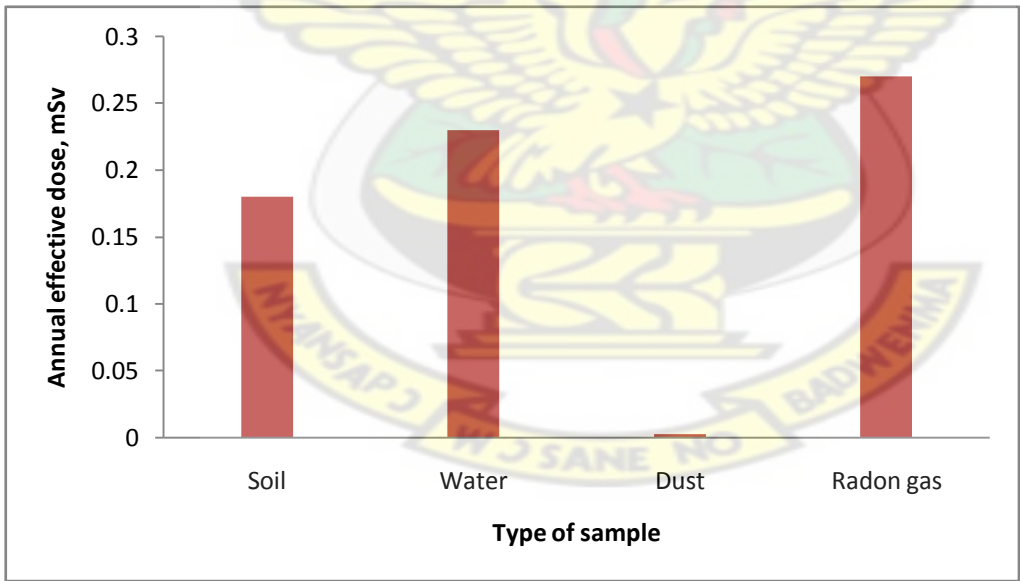


**Figure 4-8:** Comparison of annual effective doses due to soil, water and dust samples as well as airborne radon.

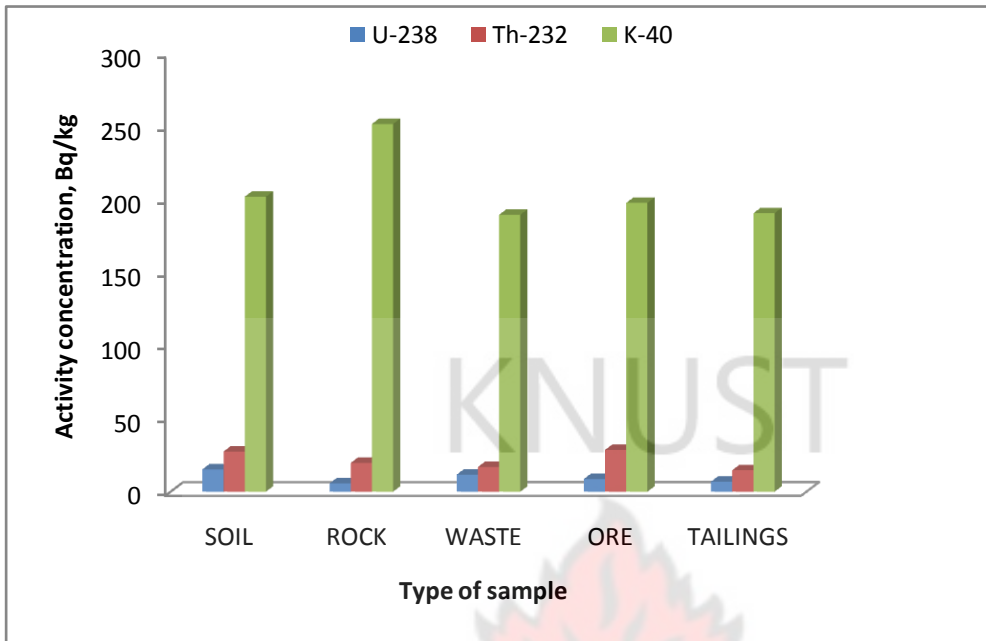
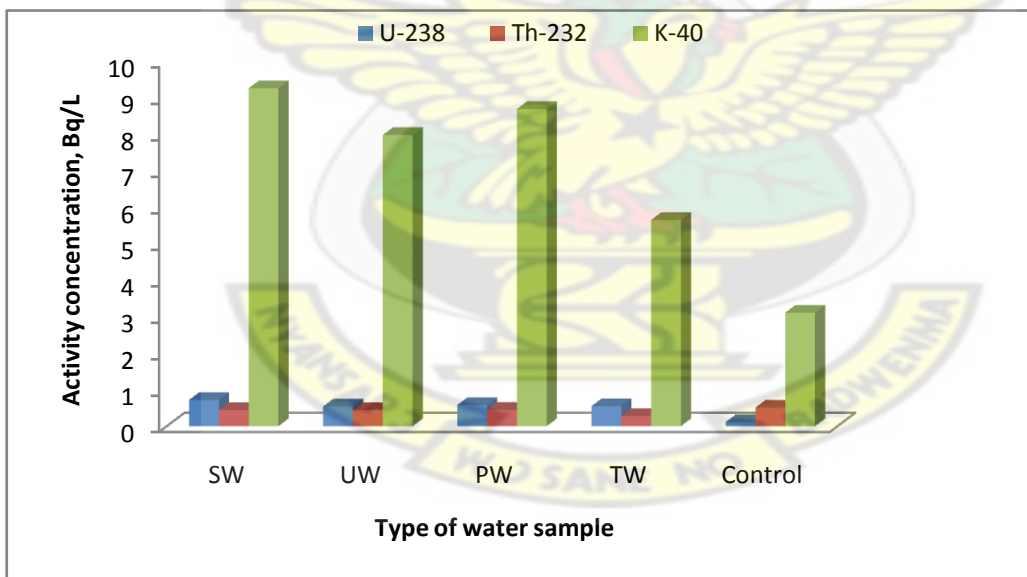
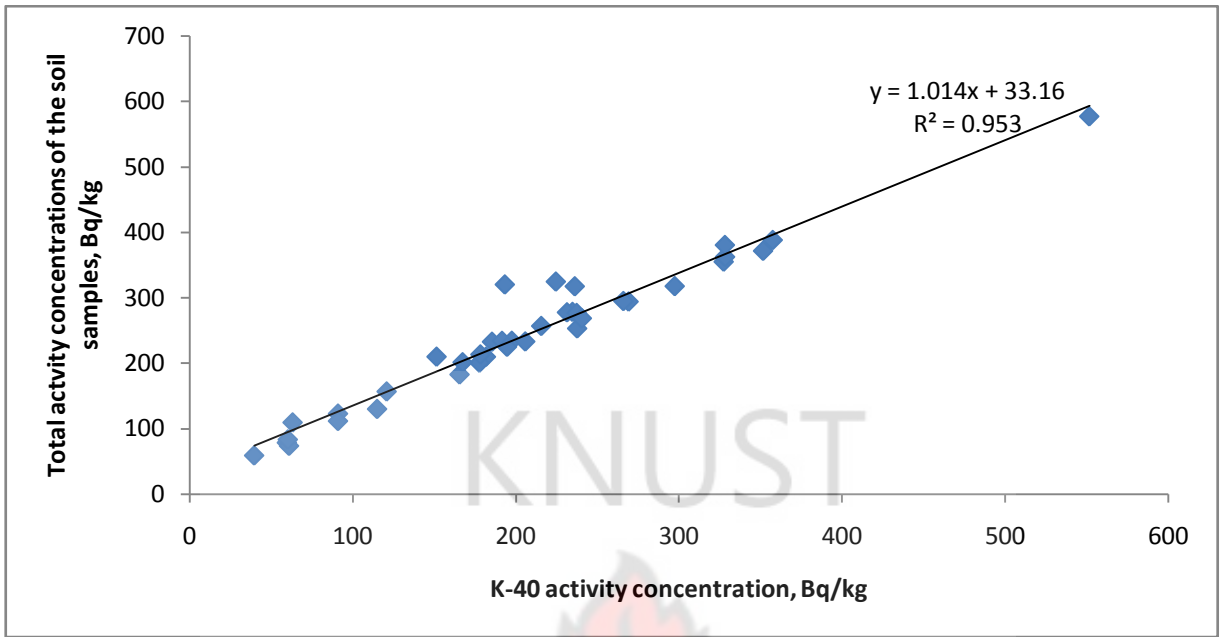


**Figure 4-9: Comparison of the activity concentration in different types of samples in the study area**

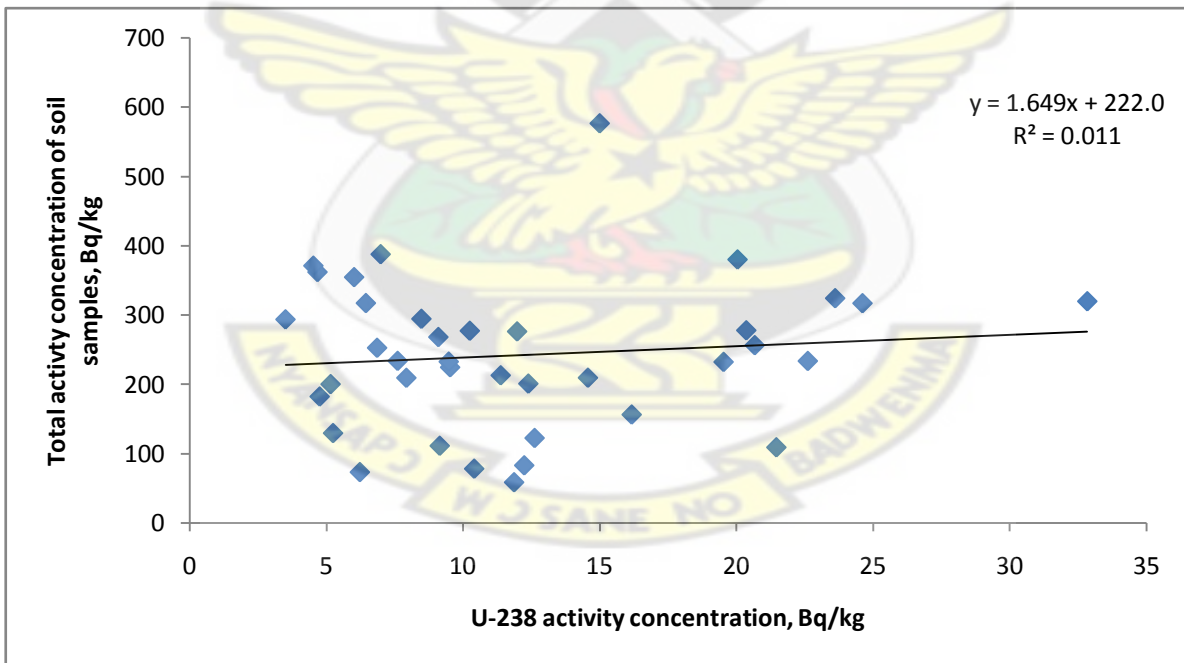


Legend: SW-surface water; UW-underground water; PW-mine process water; TW-treated (tap) water

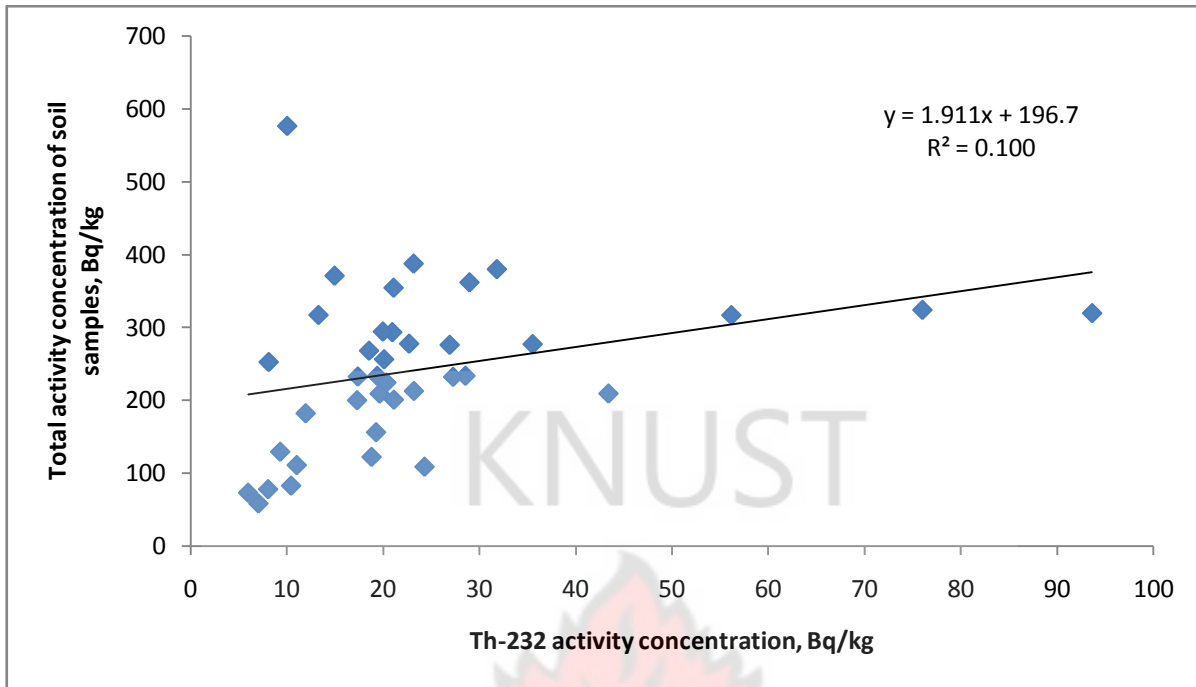
**Figure 4-10: Comparison of activity concentrations of different water sources.**



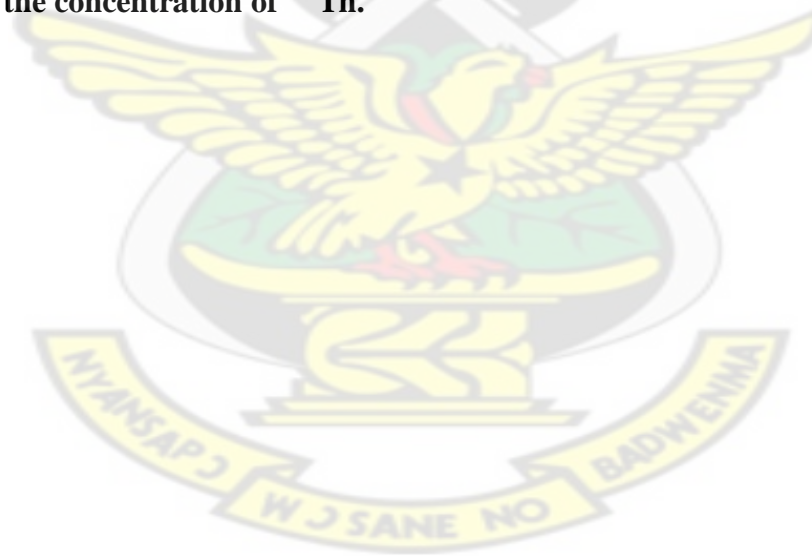
**Figure 4-11:** A comparison of the total activity of the radionuclides in the soil sample with the activity concentration of  $^{40}\text{K}$ .



**Figure 4-12:** A comparison of the total activity of the radionuclides in the soil sample with the activity concentration of  $^{238}\text{U}$ .



**Figure 4-13:** A comparison of the total activity of the radionuclides in the soil sample with the concentration of  $^{232}\text{Th}$ .



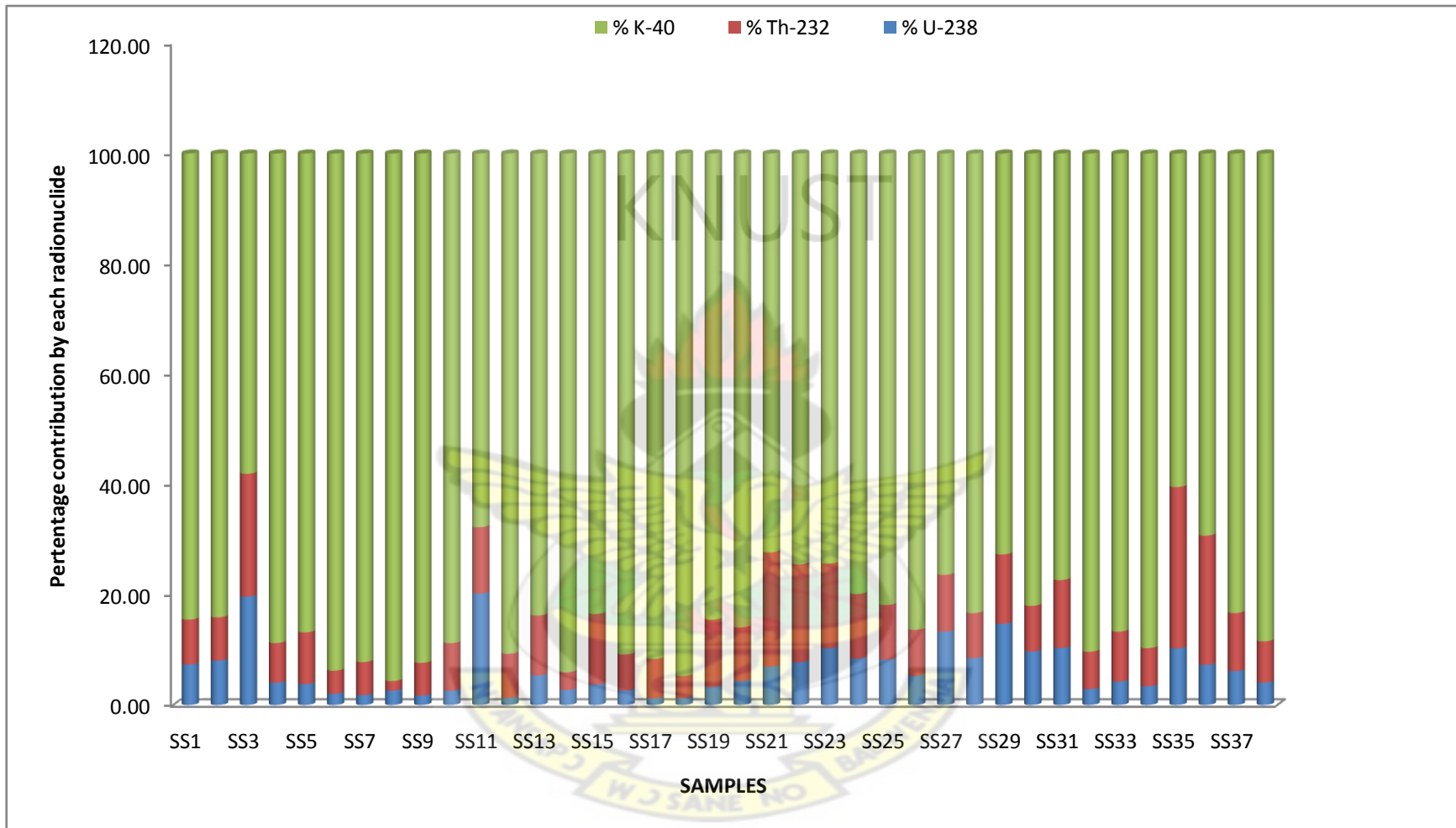


**Figure 4-14: Percentage contribution of <sup>238</sup>U, <sup>232</sup>Th and <sup>40</sup>K in the soil samples to the total activity concentrations in the study area.**

**Table 4-14: Radon emanation coefficient of the soil, tailings and rock samples**

Location	Number of Samples	<sup>226</sup> Ra, Bq/kg Average $\pm$ SD	EF $\pm$ SD
Mine Soil Tarkwa (GS)	6	19.65 $\pm$ 2.47	0.53 $\pm$ 0.03
Mine Rock Tarkwa (MS)	6	19.38 $\pm$ 10.06	0.55 $\pm$ 0.03
Mine North Heap Leach (M)	6	9.20 $\pm$ 0.35	0.53 $\pm$ 0.03
Mine South Heap Leach (M)	3	8.27 $\pm$ 1.07	0.55 $\pm$ 0.03
Mine Tailing (F)	6	10.31 $\pm$ 2.19	0.51 $\pm$ 0.03
Mine Waste (Rock) (MS)	12	8.52 $\pm$ 1.31	0.54 $\pm$ 0.03
Mine Pit (Teberebie) (M)	3	8.80 $\pm$ 0.63	0.80 $\pm$ 0.04
Mine Pit (Pepe) (M)	6	10.20 $\pm$ 0.93	0.53 $\pm$ 0.03
Mine Pit (Kontraverchy) (M)	6	9.74 $\pm$ 1.90	0.54 $\pm$ 0.03
Mine Pit (Akontansi) (M)	9	10.12 $\pm$ 1.82	0.53 $\pm$ 0.05
Ore Stockpile (MS)	3	6.50 $\pm$ 0.42	0.52 $\pm$ 0.03
Plant Site (M)	6	15.52 $\pm$ 5.72	0.52 $\pm$ 0.03
New Atuabo community (GS)	6	11.15 $\pm$ 1.75	0.52 $\pm$ 0.03
Goldfields Clubhouse (GS)	3	32.41 $\pm$ 7.13	0.56 $\pm$ 0.03
Brahabebom community (GS)	3	6.20 $\pm$ 0.54	0.52 $\pm$ 0.05
Samahu community (GS)	9	15.71 $\pm$ 6.51	0.63 $\pm$ 0.04
Boboobo community (GS)	3	29.80 $\pm$ 5.08	0.56 $\pm$ 0.03
Abekoase community (GS)	6	14.47 $\pm$ 5.13	0.54 $\pm$ 0.03
Huniso community (GS)	3	14.83 $\pm$ 4.01	0.57 $\pm$ 0.03
Pepesa community (GS)	3	19.54 $\pm$ 2.21	0.51 $\pm$ 0.03
UMAT/Agric Hill (GS)	6	28.91 $\pm$ 1.10	0.58 $\pm$ 0.03

Legend: GS- granular samples; M- mixed samples (granular and massive); MS- massive samples; F- fine particles samples, UMAT- University of Mines and Technology; EF-emanation fraction and SD-standard deviation.

**Table 4-15: Summary of annual equivalent doses and the estimated total effective dose from soil, water, dust, radon and external gamma dose rate to each individual member of the public.**

#	Exposure pathway	Average annual effective dose, mSv/year	Percentage contribution, %
1	External irradiation U, Th and K in Soil/rock sample by gamma spectrometry.	0.19	25.7
2	Ingestion U, Th and K in water samples by gamma spectrometry	0.21	28.4
3	Inhalation of U and Th in ore dust sample by gamma spectrometry	$3.0 \times 10^{-3}$	$4.0 \times 10^{-3}$
4	Radon measurement in air with Alpha Guard	0.29	39.2
5	Ingestion of U Th and K in food sample by gamma spectrometry (wet weight)	0.05	6.7
TOTAL ANNUAL EFFECTIVE DOSE		0.74	~100



**Table 4-16: Estimated risk components for the various exposure pathways studied**

#	Exposure pathway	Average equivalent dose, mSv/year	Fatality Cancer risk to population per year	Lifetime fatality cancer risk to population	Severe Hereditary effects per year	Estimated lifetime hereditary effects
1	External irradiation U, Th and K in Soil/rock sample by gamma spectrometry.	0.19	$1.5 \times 10^{-5}$	$7.3 \times 10^{-4}$	$3.8 \times 10^{-7}$	$2.7 \times 10^{-5}$
2	Ingestion U, Th and K in water samples by gamma spectrometry	0.21	$1.2 \times 10^{-5}$	$8.1 \times 10^{-4}$	$4.2 \times 10^{-7}$	$2.9 \times 10^{-5}$
3	Inhalation of U and Th in ore dust sample by gamma spectrometry	0.000003	$1.6 \times 10^{-10}$	$1.2 \times 10^{-8}$	$6.0 \times 10^{-12}$	$4.2 \times 10^{-10}$
4	Radon measurement in air with Alpha Guard	0.29	$1.6 \times 10^{-5}$	$1.1 \times 10^{-3}$	$5.8 \times 10^{-7}$	$4.1 \times 10^{-5}$
5	Ingestion of U Th and K in food sample by gamma spectrometry (wet weight)	0.05	$2.8 \times 10^{-6}$	$1.9 \times 10^{-4}$	$1.0 \times 10^{-7}$	$7.0 \times 10^{-6}$
	TOTAL	0.74	$4.1 \times 10^{-5}$	$2.8 \times 10^{-3}$	$1.5 \times 10^{-6}$	$1.0 \times 10^{-4}$

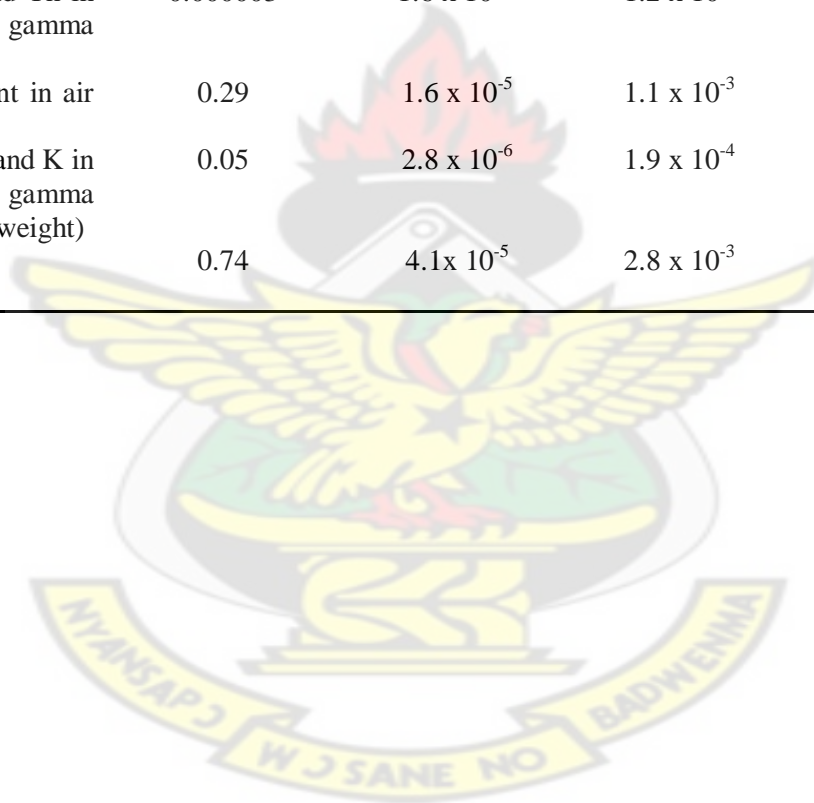


**Table 4-17: Results of the average activity concentration of  $^{226}\text{Ra}$ ,  $^{232}\text{Th}$  and  $^{40}\text{K}$  together with their total uncertainties, total absorbed dose, annual effective dose, radium equivalent activity and hazard indices of the samples from the study area**

Community	Activity concentration, Bq/kg			Absorbed dose rate, nGy/h	Annual effective dose, mSv	$\text{Ra}_{\text{eq}}$ , Bq/kg	Hazard Index	
	$^{226}\text{Ra}$	$^{232}\text{Th}$	$^{40}\text{K}$				External ( $H_{\text{ex}}$ )	Internal ( $H_{\text{in}}$ )
Abekoase	16.78±1.05	13.75±1.22	125.81±10.75	21.18	0.14	46.12	0.13	0.17
Brahabebom	18.11±1.14	37.50±1.20	163.79±13.40	38.08	0.24	84.36	0.23	0.28
Huniso	5.22±0.46	6.00±0.68	61.19±5.64	9.05	0.06	18.51	0.05	0.06
New Atuabo	13.45±0.97	35.18±2.40	194.58±15.47	35.49	0.22	78.73	0.21	0.25
Pepesa	14.63±0.88	10.47±0.99	60.44±5.56	14.50	0.09	34.26	0.09	0.13
Samahu	15.59±0.97	19.21±1.51	132.62±11.02	24.04	0.15	53.27	0.14	0.19
Tarkwa	23.05±1.33	67.16±1.33	248.88±19.48	62.72	0.39	138.26	0.37	0.44
Mine (rock)	8.56±0.78	20.39±1.65	194.87±18.31	23.32	0.13	55.51	0.13	0.15
Mine (tailings)	7.18±0.66	14.67±1.26	190.66±15.09	19.98	0.13	42.83	0.12	0.14
Mine (soil)	13.49±0.94	17.90±1.40	247.99±19.45	27.16	0.17	58.19	0.16	0.19
Range	2.26-30.57	6.00-93.64	39.81-551.72	9.09-79.79	0.06-0.49	18.51-179.37	0.05-0.48	0.06-0.57
Mean±Stdev	13.61±5.39	24.22±17.15	162.08±63.69	27.55±15.10	0.17±0.09	61.00±33.33	0.16±0.09	0.20±0.10

**Table 4-18: Comparison of the average activity concentrations, the radium equivalent Activities ( $Ra_{eq}$ ) of soil, rocks, waste and tailings of the study area with published data.**

Country	N	Specific activity concentration, Bq/kg			$Ra_{eq}$ , Bq/kg	Reference
		$^{226}\text{Ra}$	$^{232}\text{Th}$	$^{40}\text{K}$		
Australia	7	51.5	48.1	114.7	129.4	Beretka and Mathew (1985)
Austria	18	26.7	14.2	210	63.1	Sorantin and Steger (1984)
Algeria	12	41	27	422	112	Amrani and Tahtat (2001)
Brazil	1	61.7	58.5	564	188.8	Malanca et al. (1993)
China	46	56.5	36.5	173.2	122	Xinwei (2005)
Egypt	85	78	33	337	151	El Afifi et al. (2006)
India	1	37	24.1	432.2	104.7	Kumar et al. (1999)
Japan	16	35.8	20.7	139.4	-	Suzuki et al. (2000)
Netherlands	6	27	19	230	71.9	Ackers et al. (1985)
Tunisia	2	21.5	10.10	175.5	49.7	Hizem et al. (2005)
Turkey	145	40	28	248.3	99.1	Turhan and Gurbuz (2008)
Ghana	38	12.5	23.9	206.2	62.5	This work

Legend: N- number of samples

**Table 4-19: Comparison of activity concentration of  $^{226}\text{Ra}$  and  $^{222}\text{Rn}$  emanation fraction (EF) of this study with different NORM waste from various industrial activities.**

Industrial activity	$^{226}\text{Ra}$ activity concentration, kBq/kg	$^{222}\text{Rn}$ EF	Reference
Oil and gas production			
Oklahoma	76.1	0.087	White and Rood (2001)
Michigan	15.4	0.138	White and Rood (2001)
Phosphate industry			
Gypsum	1.2	0.200	USEPA (1993)
Slag	1.26	0.010	USEPA (1993)
Power plants generation			
Coal ash	0.14	0.020	USEPA (1993), Egidi and Hull (1997)
Metallurgical processing			
Uranium mining	0.92	0.300	USEPA (1993), Egidi and Hull (1997)
Rare earth's	666	0.300	USEPA (1993), Egidi and Hull (1997)
Gold mining	0.013	0.554	This work

**Table 4-20: Comparison of activity concentrations  $^{238}\text{U}$ ,  $^{232}\text{Th}$  and  $^{40}\text{K}$  in soil, rock, waste and tailing samples for the first (I) and second (II) batch of samples.**

Community	Specific activity/Bq/kg					
	$^{238}\text{U}$		$^{232}\text{Th}$		$^{40}\text{K}$	
	I	II	I	II	I	II
Abekoase	16.510	14.340	13.745	11.18	125.810	84.845
Brahabebome	12.620	3.990	18.820	16.47	91.220	230.810
Huniso	6.230	11.520	6.000	13.35	61.190	79.830
New Atuabo	13.275	8.925	35.175	15.72	194.575	128.770
Pepesa	12.240	15.860	10.470	10.34	60.440	53.381
Samahu	14.950	18.673	19.210	15.80	132.617	62.073
Tarkwa Township	25.273	27.615	64.418	66.77	245.745	289.760
Mine Site	9.572	8.363	19.086	17.63	233.133	205.720
Mean	13.834	13.661	23.365	20.91	143.091	141.899

**Table 4-21: Comparison of the absorbed dose rates and total annual effective doses due to soil, rock ore, waste rock, tailings for two different sampling periods.**

Community	Absorbed dose rate, nGy/h		Total annual effective dose, mSv/year	
	I	II	I	II
	Abekoase	13.35	14.08	0.09
Brahabebome	21.00	21.42	0.13	0.13
Huniso	9.05	16.71	0.06	0.1
New Atuabo	35.49	18.99	0.22	0.12
Pepesa	30.17	21.48	0.19	0.13
Samahu	24.04	20.76	0.15	0.13
Tarkwa Township	60.83	65.17	0.38	0.4
Mine Site	26.55	23.09	0.16	0.14
Mean	27.56	25.21	0.17	0.15

**Table 4-22: The mean activity concentrations of  $^{238}\text{U}$ ,  $^{232}\text{Th}$  and  $^{40}\text{K}$  in the first (I) and second (II) badge of water samples.**

Community	Specific activity, Bq/l								Annual effective dose mSv	
	pH		$^{238}\text{U}$		$^{232}\text{Th}$		$^{40}\text{K}$		I	II
	I	II	I	II	I	II	I	II		
Abekoase	6.12	7.81	0.57	0.53	0.34	0.38	10.54	8.73	0.22	0.21
Brahabebome	5.18	6.49	0.32	1.15	0.52	0.22	8.86	7.50	0.19	0.31
Huniso	5.49	6.87	0.64	1.22	0.31	0.97	5.47	25.57	0.21	0.53
New Atuabo	5.45	6.63	0.36	0.43	0.40	0.21	7.87	10.23	0.18	0.17
Pepesa	5.55	7.57	0.48	0.49	0.33	0.32	6.70	7.01	0.18	0.19
Samahu	6.17	7.84	0.48	0.50	0.43	0.48	8.63	13.23	0.21	0.25
Tarkwa	6.08	7.91	0.50	0.58	0.48	0.45	8.64	10.60	0.22	0.24
Mine Site	6.67	7.08	0.80	0.61	0.47	0.39	8.34	10.14	0.28	0.24
Control	6.82	7.10	0.11	0.82	0.51	0.63	3.11	9.45	0.10	0.32
Mean	5.95	7.26	0.47	0.70	0.42	0.45	7.57	11.38	0.21	0.27

**Table 4-23: Gross- $\alpha$  and gross- $\beta$  activity concentrations (Bq/l) in water samples**

Community	Activity concentration, Bq/l	
	gross alpha	gross beta
Abekoase	0.013	0.246
Brahabebome	0.011	0.096
Huniso	0.012	0.084
New Atuabo	0.013	0.063
Pepesa	0.012	0.374
Samahu	0.010	0.080
Tarkwa Township	0.008	0.071
Mine Site	0.017	0.101
Control	0.016	0.116
Mean	0.012	0.137

**Table 4-24: Statistical summary of water chemistry**

Community	pH	T/°C	Cond. /μScm	TDS	Cl <sup>-</sup>	NO <sub>3</sub> <sup>-</sup>	PO <sub>4</sub> <sup>3-</sup>	SO <sub>4</sub> <sup>2-</sup>	Fe	Cu	Zn	Pb	As	U	Th	K
Abekoase	6.12	26.6	539.0	238.2	31.0	2.30	0.060	51.9	0.09	0.010	0.008	<0.001	0.004	0.015	0.030	1.47
Brahabebome	5.18	25.6	277.0	130.1	62.0	1.30	0.010	35.1	0.16	0.005	0.012	<0.001	0.003	0.040	0.040	1.01
Huniso	5.49	27.1	289.2	152.3	5.0	2.40	0.025	34.0	0.42	<0.001	0.068	0.04	0.007	0.015	0.025	1.21
New Atuabo	5.45	26.2	385.5	181.9	83.0	0.75	0.020	6.50	<0.001	<0.001	0.080	<0.001	0.004	0.025	0.030	0.81
Pepesa	5.55	26.6	519.5	229.5	6.0	2.35	0.010	88.8	0.22	0.086	0.147	0.07	0.005	0.015	0.025	2.43
Samahu	6.17	26.3	162.8	71.4	18.2	1.75	0.025	15.6	0.21	<0.001	0.030	0.04	0.004	0.020	0.035	1.94
Tarkwa	6.08	26.7	562.0	245.2	59.2	1.46	0.014	32.0	0.03	<0.001	0.013	0.08	0.004	0.014	0.030	0.99
Mine Site	6.67	26.4	332.8	235.5	26.3	3.20	0.073	85.9	0.12	0.007	0.009	0.17	0.005	0.023	0.032	0.85
Control	6.82	26.5	57.2	24.4	2.0	1.90	<-0.514	10.1	0.41	<0.003	0.009	0.02	0.003	0.010	0.010	0.04
Min	3.55	25.5	2.4	17.3	0.2	0.2	<-0.514	4.30	<0.001	<0.001	<0.001	<0.001	0.002	0.010	0.010	0.02
Max	8.95	27.3	1208.0	893.0	150.0	9.9	0.28	285.9	0.43	0.086	0.283	0.168	0.008	0.040	0.060	3.84
Mean	5.94	26.4	347.2	167.6	32.5	1.93	0.030	40.0	0.21	0.027	0.042	0.07	0.004	0.020	0.029	1.19
Stdev	0.57	0.41	173.5	79.9	29.1	0.72	0.024	30.3	0.14	0.048	0.048	0.05	0.001	0.009	0.008	0.69

**Table 4-25: Summary of metals concentration and analytical uncertainties ( $\mu\text{g/g}$ ) of soil, tailings and rock samples of the mine.**

Element mg/kg	Type of sample with number samples (N) in parentheses						
	Rock (ore) (N=6)	Soil (pit) (N=6)	Rock (pit) (N=9)	Rock (CIL plant) (N=6)	Rock (HL plant) (N=9)	Soil (communities) (N=24)	Soil (Tarkwa) (N=18)
Mn	176±29	426±28	1309±21	3400±111	193±28	285±22	56±15
Si	5086±322	1347±425	2640±239	5329±143	4198±209	3335±399	2077±341
V	12±0.4	32±6	459±19	241±17	1.8±0.6	8.4±0.4	115±7
Al	1911±111	1843±299	2169±423	9532±370	7722±310	3.5±0.03	5179±260
La	57±9	21.3±3.6	113.5±13	35±4	17.6±2.2	5.4±0.7	23±3
As	3.5±0.3	<0.00001	<0.00001	<0.00001	3.9±0.04	9.0±0.8	14±0.6
Cr	150±55	124±39	<0.01	170±34	<0.01	<0.01	360±48
Sr	<0.10	2.4±0.3	116±36	<0.10	<0.10	<0.10	194±56
Sc	2.5±0.4	1.7±0.02	4.6±0.4	4.5±0.15	4.5±0.35	<0.001	9±0.44
Fe	2316±773	4692±886	7307±105	2330±863	2920±813	<0.10	2143±393
Co	5.8±1.0	<0.001	<0.001	<0.001	6.5±1.0	<0.001	2±0.1
Ti	<0.10	2159±135	3579±160	4274±140	370±31	828±535	3200±383
Mg	8300±600	<0.10	2354±565	5820±375	2272±158	2809±173	<0.10
Ca	<1.00	<1.00	7143±142	1429±571	<1.00	754±452	<1.00
Na	11900±74	2446±18	19904±74	5171±30	11560±52	3505±100	2465±21
K	52648±216	7037±363	71360±3256	14190±616	36904±2064	7051±368	7643±566
U	1.8±0.9	0.2±0.1	0.4±0.1	0.52±0.17	1.80±0.60	1.3±0.69	1.4±0.55
Th	2.6±0.4	0.9±0.3	2.1±1.1	1.28±0.43	2.60±0.70	1.5±0.74	1.6±0.67
Th/U	1.4	4.5	5.3	2.5	1.4	1.2	1.1

Legend: CIL – carbon-in-leach; HL – heap leach; N – number of samples.

**Table 4-26: Comparison between mean values of the activity concentrations of  $^{238}\text{U}$ ,  $^{232}\text{Th}$  and  $^{40}\text{K}$  as well as the absorbed dose rates and the annual effective doses due to soil/rock samples for the two sets of data.**

First and second batch results	$^{238}\text{U}$ activity concentration,	$^{232}\text{Th}$ activity concentration,	$^{40}\text{K}$ activity concentration,	Annual effective dose, mSv	Absorbed dose rate, nGy/h
	Bq/kg				
Probability value	0.483	0.186	0.164	0.151	0.089

\* Correlation is insignificant at  $p > 0.05$  and significant at  $P < 0.05$  level (2-tailed)

**Table 4-27: Correlation analysis using Pearson Correlation Matrix Method used to assess the correlation between  $^{238}\text{U}$ ,  $^{232}\text{Th}$  and  $^{40}\text{K}$  respectively due to soil/rock samples.**

Radioactive Isotope	$^{238}\text{U}$	$^{232}\text{Th}$	$^{40}\text{K}$
$^{238}\text{U}$	1	0.676*	-0.073
$^{232}\text{Th}$	0.676*	1	0.112
$^{40}\text{K}$	-0.073	0.112	1

\* Correlation is insignificant at  $p > 0.05$  and significant at  $P < 0.05$  level (2-tailed)

**Table 4-28: Comparison between means values of the activity concentrations of  $^{238}\text{U}$ ,  $^{232}\text{Th}$  and  $^{40}\text{K}$  water samples for the two sets of data.**

First and second batch results	$^{238}\text{U}$ activity concentration,	$^{232}\text{Th}$ activity concentration,	$^{40}\text{K}$ activity concentration,
	Bq/l		
Probability value	0.467	0.605	0.023

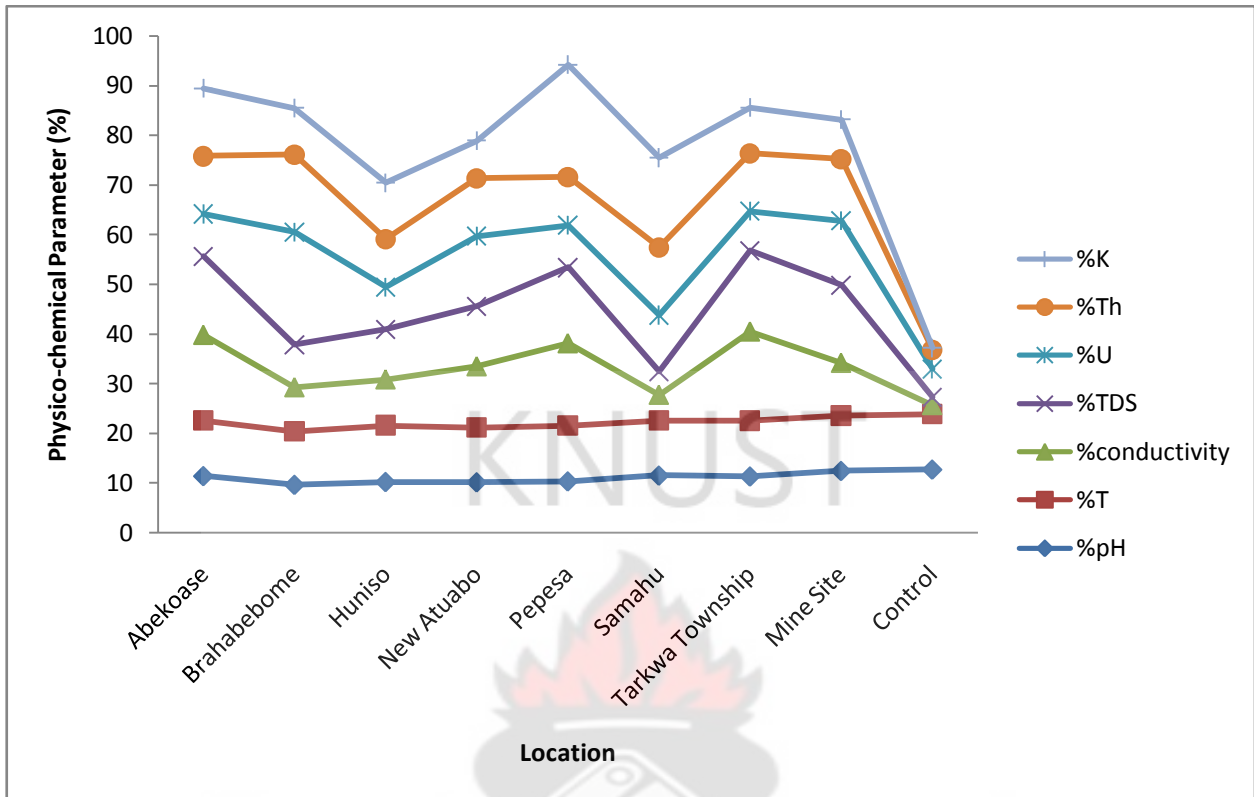
\* Correlation is insignificant at  $p > 0.05$  and significant at  $P < 0.05$  level (2-tailed)

**Table 4-29: Post-hoc test: Comparison of the means of the elemental concentrations of uranium, Thorium and Potassium in the water sample**

	Uranium	Thorium	Potassium
Uranium	-	0.997	0.00*
Thorium	0.997	-	0.00*
Potassium	0.00*	0.00*	-

\* Correlation is insignificant at  $p > 0.05$  and significant at  $P < 0.05$  level (2-tailed)

Note: The ANOVA test conducted concluded there was significant difference at 5 % (see Appendix 11).



Legend: K- potassium; Th-thorium, U-uranium, TDS-total dissolved solids, and T-temperature

**Figure 4-15: A comparison of percentage weighted values of pH, temperature, conductivity, TDS, U, Th and K in water samples in the study area.**

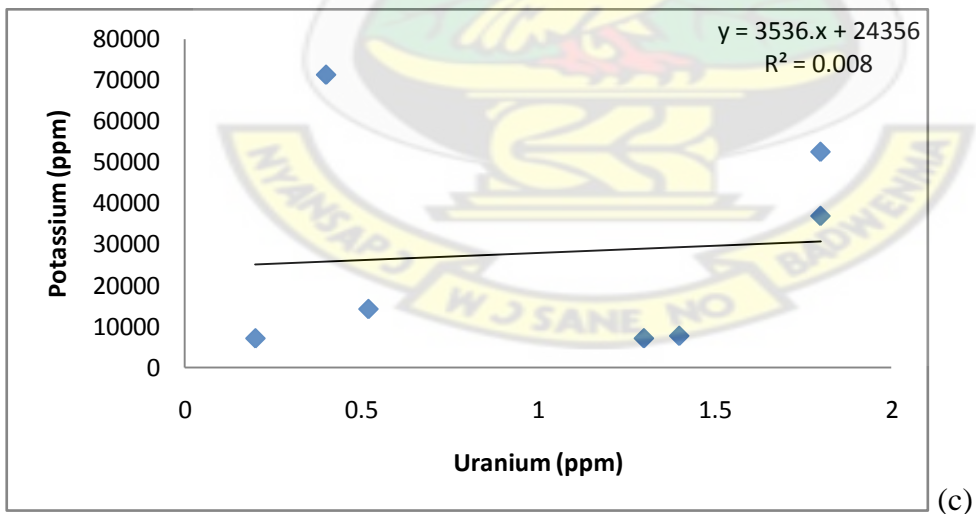
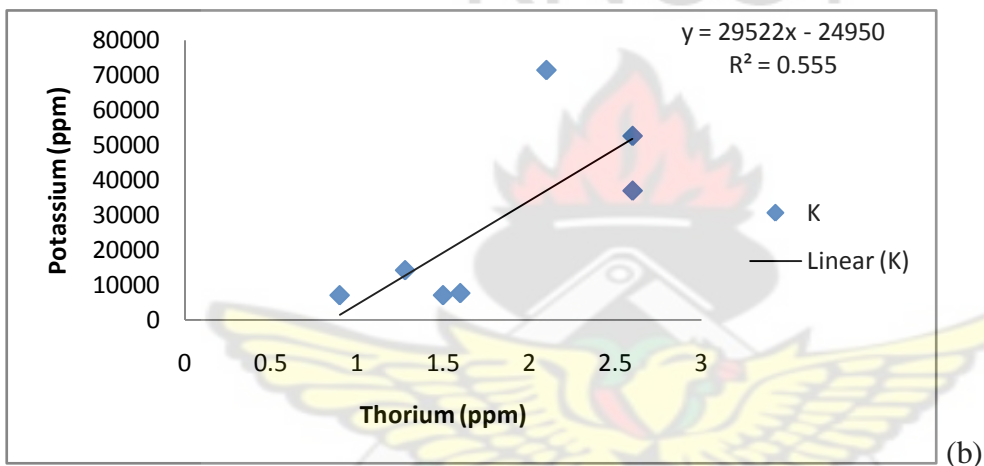
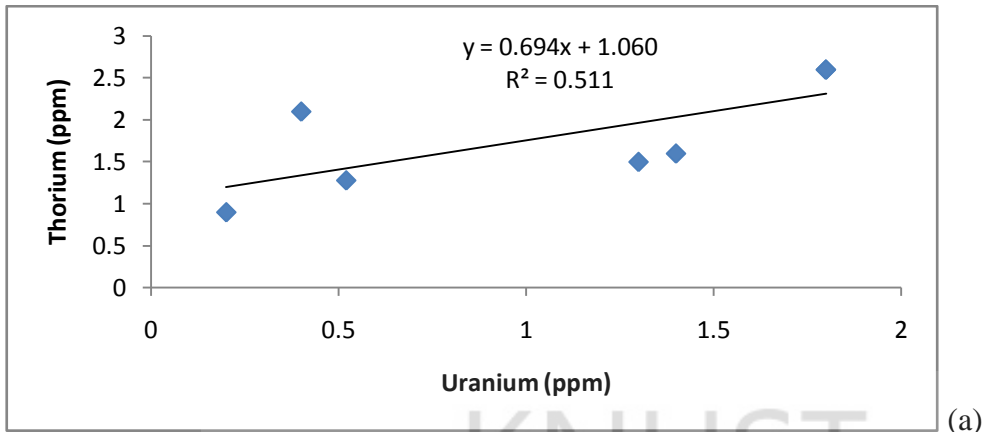


**Figure 4-16: Mean concentrations of U, Th and K in soil and rock samples in the study area. (a) U versus Th, (b) K versus Th and (c) K versus U. The solid straight lines represent the best fitting lines and their corresponding correlation coefficients.**

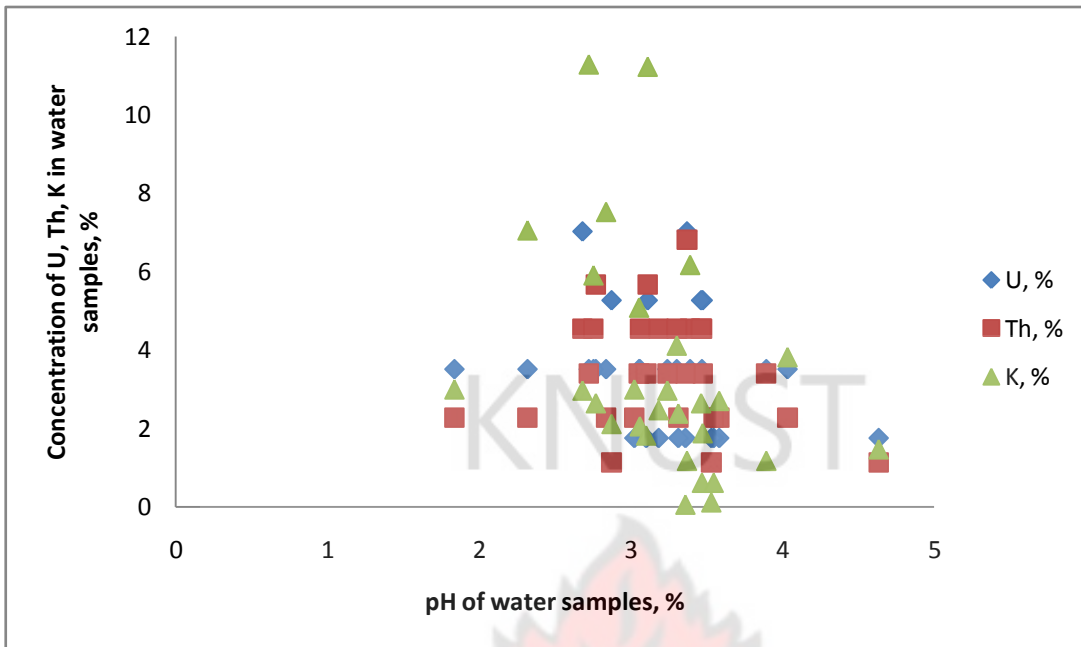


**Figure 4-17:** Comparison of concentration of U, Th, K in the water samples with the pH of the samples to verify the relation of the concentration of the metals with pH.

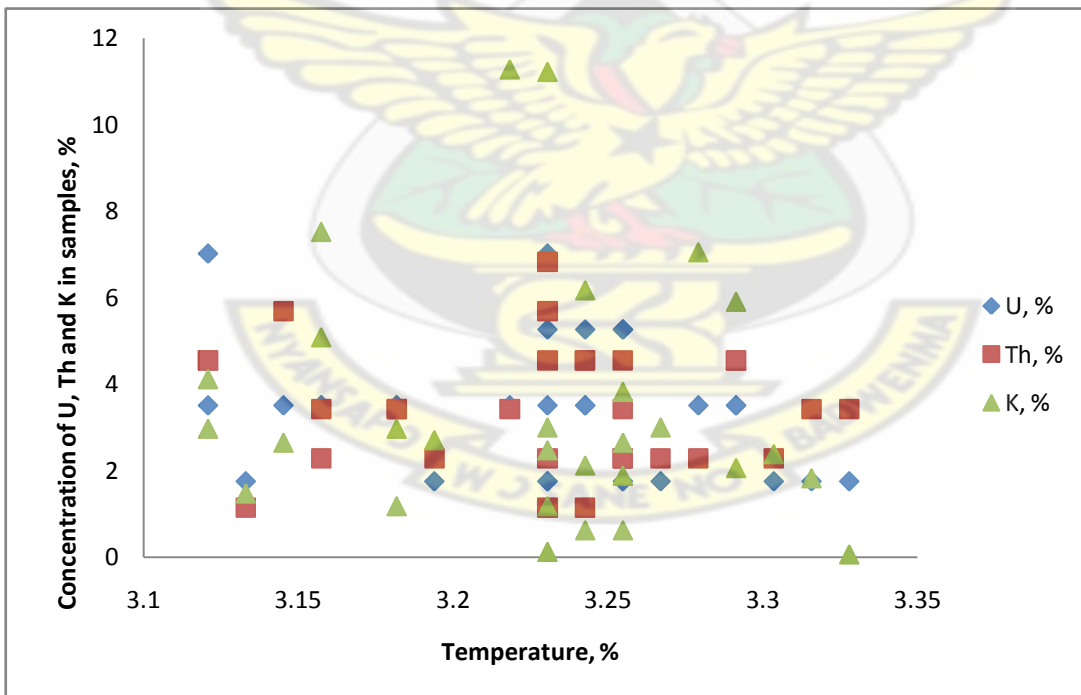


**Figure 5-18:** Comparison of the correlation between the concentrations of U, Th, and K with the temperature conditions of the study area.

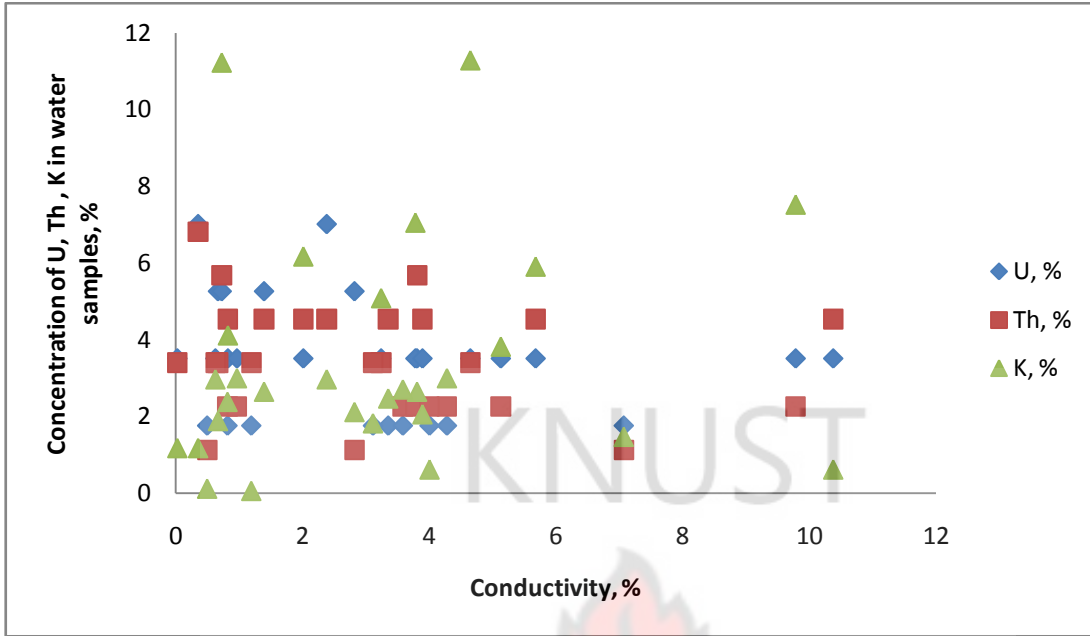


**Figure 4-19:** Comparison of the correlation between the concentrations of U, Th, and K with the conductivity of the water samples.

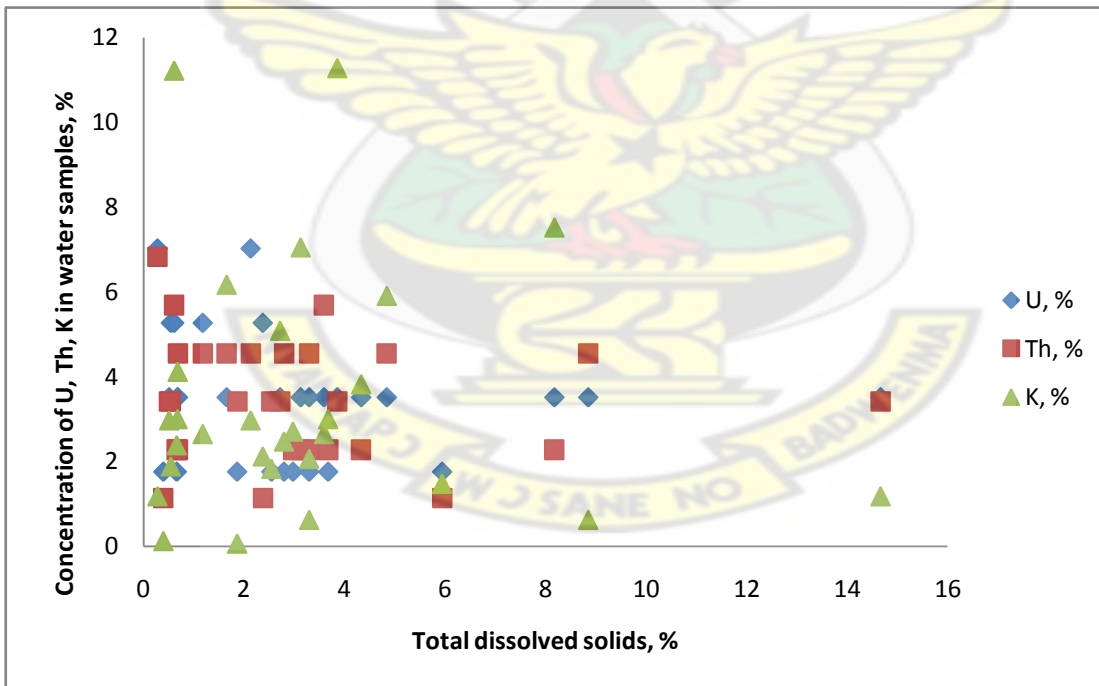


**Figure 4-20:** Comparison of the correlation between the concentrations of U, Th, and K with the total dissolved solids of the water samples.

## CHAPTER FIVE

### 5.0 DISCUSSIONS

#### 5.1 External Gamma Dose Rate at 1 meter above the ground.

The results of the absorbed dose rate measured in air at 1 metre above the ground at the soil and water sampling points at the mine site and at the various communities investigated are presented in Table 4-2. As can be observed, measured absorbed dose rates at the soil sampling points varied in a range of 15.0-57.0 nGy/h with a mean value of  $38.1 \pm 13.7$  nGy/h. The corresponding mean annual effective dose was estimated to be  $45.9 \pm 16.8$   $\mu$ Sv in a range of 18.4-69.5  $\mu$ Sv. At the water sampling points absorbed dose rates varied in a range of 10.0-68.0 nGy/h with a mean value of  $42.5 \pm 19.7$  nGy/h. The corresponding mean annual effective dose was estimated to be  $52.1 \pm 24.1$   $\mu$ Sv.

According to UNSCEAR report, the average absorbed dose rate in outdoor air from terrestrial gamma radiation is 59 nGy/h [UNSCEAR, 2000]. Comparing the results of the gamma absorbed dose rates in this study with the data in UNSCEAR report, the results of the absorbed dose rates in this study are by a factor of one lower than the range of dose rates reported by other countries [UNSCEAR, 2000; Darko et al., 2010]. The highest absorbed dose rate values of 57.0 and 68.0 nGy/h recorded in the soil and water sampling points in Tarkwa Township respectively also compare quite well with the worldwide average values. These values were measured at the Agricultural Hill and the University of Mines and Technology residential area which are relatively at higher altitude. It has been established that places at higher altitude are associated with higher external gamma dose rates. The results of the study in this mine are also lower than the results of similar studies carried out in other mines in Ghana [Darko, et al, 2010].

Figure 4-6 is the comparison of the results of the absorbed dose rate measured at the soil, water and dust sampling locations. The figure shows that absorbed dose rates at the sampling locations varied in a range of 38-60 nGy/h. These results compared well with published results [UNSCEAR, 2000]. The relative contribution of  $^{238}\text{U}$ ,  $^{232}\text{Th}$  and  $^{40}\text{K}$  to the absorbed dose rates is also illustrated with Figure 4-7. Thorium-232 ( $^{232}\text{Th}$ ) in the soil/rock samples contributed highest to the total absorbed dose rate, with an average value of 47.3% and a maximum of 70.9% followed by  $^{40}\text{K}$  with an average of 31.6% and a maximum of 63.%. Uranium-238 ( $^{238}\text{U}$ ) contributed the least with an average value of 21.1% and maximum of 48.0%. This implies that, in terms of their relative contributions to the absorbed dose rates,  $^{232}\text{Th}$  contributed most significantly followed by  $^{40}\text{K}$  and  $^{238}\text{U}$  in that order.

A comparison was made between the mean absorbed dose rates calculated from the soil activity concentrations with the absorbed dose rates measured directly in air at 1 m above the ground. The mean absorbed dose rate calculated from the soils is 30 nGy/h whilst that measured directly in air is 40 nGy/h. The mean absorbed dose rate measured in air was 1.3 times higher than that estimated from the soil activity concentrations. The difference could be attributed to the contribution of cosmic rays and statistical uncertainties in the measurements. The results in this study also compared quite well with those from other countries whilst in some cases they are lower [UNSCEAR, 2000].

## **5.2 Activity concentrations, absorbed dose rates and annual effective doses**

### **5.2.1 Soil/rock**

Table 4-3 shows the activity concentrations of  $^{238}\text{U}$ ,  $^{232}\text{Th}$  and  $^{40}\text{K}$  in the soil/rock samples as well as the calculated absorbed dose rate and the estimated annual effective doses. The percentage contributions of  $^{238}\text{U}$ ,  $^{232}\text{Th}$  and  $^{40}\text{K}$  to the absorbed dose rates are also provided.

The mean value of the activity concentrations of  $^{238}\text{U}$  is  $15.2 \pm 5.7$  Bq/kg in a range of 7.7-25.5 Bq/kg. For  $^{232}\text{Th}$  the mean activity concentration is  $26.9 \pm 19.5$  Bq/kg in range of 8.5-67.2 Bq/kg and that of  $^{40}\text{K}$  is  $157.0 \pm 68.2$  Bq/kg in a range of 60.4-248.9 Bq/kg. The uncertainties reported were based on counting statistics at two standard deviations ( $2\sigma$ ). The highest values for  $^{238}\text{U}$ ,  $^{232}\text{Th}$  and  $^{40}\text{K}$  were measured in soil samples taken from Agricultural Hill which is very close to Teberebie pit of the mine. The mean values of the activity concentrations of  $^{238}\text{U}$ ,  $^{232}\text{Th}$  and  $^{40}\text{K}$  are about two times lower than the world average values in normal areas [UNSCEAR, 2000].

The worldwide average activity concentrations of  $^{238}\text{U}$ ,  $^{232}\text{Th}$  and  $^{40}\text{K}$  in soil samples from various studies around the world have values of 35, 30 and 400 Bq/kg respectively [UNSCEAR, 2000]. Table 4-13 is a comparison of the mean activity concentration of  $^{238}\text{U}$ ,  $^{232}\text{Th}$  and  $^{40}\text{K}$  in soils in the study area with similar studies done in Ghana and with published reports from other countries (UNSCEAR, 2000 and Darko et al., 2010). The values compared well with published data from other countries and all values were below the world average values. The activity concentrations of the soil, rock, waste rock, ore and tailings in the study area are also compared and the results shown in Figure 4-9. The activity concentrations in the different types of samples are quite uniform and do not show any significant variations.

Figures 4-11 to 4-13 show the contribution of each individual radionuclide to the total activity concentration in the soil/rock samples. In Figure 4-11, a good correlation  $R^2 = 0.953$  exists between the  $^{40}\text{K}$  activity concentrations and the total activity concentration due to  $^{238}\text{U}$ ,  $^{232}\text{Th}$  and  $^{40}\text{K}$  in the soil/rock samples. In Figures 4-12 and 4-13 a poor correlation  $R^2 = 0.011$  and  $R^2 = 0.100$  respectively exists between  $^{238}\text{U}$  and  $^{232}\text{Th}$  concentrations and the total activity concentrations. It is seen from Figure 4-14 that, in terms of activity concentrations,  $^{40}\text{K}$

contributes significantly to the total activity among the three radionuclides in the soil/rock samples.

The mean gamma dose rate from terrestrial gamma rays calculated from soil activity concentration was 29.9 nGy/h in a range of 11.5-62.7 nGy/h which is by a factor of two lower than the dose rate measured in air at 1 metre above the ground. The difference between the measured ambient gamma dose rate in air and gamma dose rate calculated from the soil concentrations may be attributed to contributions from cosmic rays as well as measurement uncertainties. The absorbed dose rate due to the soil concentrations is also about two times lower than the worldwide average value of 60 nGy/h (UNSCEAR, 1993; 2000). This difference could be attributed to differences in geology and geochemical state of the sampling sites. The corresponding mean annual effective dose estimated from the soil concentrations is 0.19 mSv. In the determination of these values, a dose conversion factor of 0.7 Sv/Gy, and outdoor and indoor occupancy factors of 0.2 and 0.8 respectively were applied (UNSCEAR, 1993; 2000). In the UNSCEAR 2000 report, the world average values of outdoor and indoor components of effective doses estimated from soil concentrations gave values of 0.07 and 0.41 mSv/year respectively. The results in this study are about two times lower than the world average values. Also from Table 4-3, it can be seen that  $^{232}\text{Th}$  contributes more significantly to the total absorbed dose rate with a mean value of 49.2% followed by  $^{238}\text{U}$  with a mean value of 26.7% and  $^{40}\text{K}$  with mean value of 23.5%.

The results of the activity concentrations of  $^{238}\text{U}$ ,  $^{232}\text{Th}$  and  $^{40}\text{K}$  in soil/rock samples, the calculated absorbed dose rates and annual effective doses for the two batches of the samples taken at two different periods were compared and the results are shown in Tables 4-20 and 4-21. The samples were taken when it was relatively dry as compared to the other. The results of the

activity concentrations of  $^{238}\text{U}$ ,  $^{232}\text{Th}$  and  $^{40}\text{K}$  for the two periods did not vary significantly with p-values of 0.083, 0.186 and 0.164 respectively as shown in Table 4-26. This implies that, the soil/rock systems are more stable and secular equilibrium are easily achieved thus accounting for the insignificant difference for the two periods. Correlation analysis using Pearson Correlation Matrix Method was also used to assess the correlation between  $^{238}\text{U}$ ,  $^{232}\text{Th}$  and  $^{40}\text{K}$  respectively due to soil/rock samples and the results shown in Table 4-27. The results showed a strong positive correlation between  $^{238}\text{U}$  and  $^{232}\text{Th}$  with a correlation coefficient of 0.676. This implies that  $^{238}\text{U}$  and  $^{232}\text{Th}$  exist together in minerals and rocks. A weak positive correlation also existed between  $^{40}\text{K}$  and  $^{232}\text{Th}$  in the soil/rock samples with a correlation coefficient of 0.112. A negative correlation existed between  $^{40}\text{K}$  and  $^{238}\text{U}$  in soil/rock samples with a correlation coefficient of -0.073. This implies potassium and thorium seems to co-exist well as compared to potassium and uranium in rocks. The estimated mean absorbed dose rates were 27.56 and 25.21 nGy/h for the first and second batch samples respectively. The corresponding mean annual effective doses were 0.17 and 0.15 mSv respectively. The absorbed dose rates and the annual effective doses for the two periods were not also significantly different with p-values of 0.089 and 0.151 respectively. The results for the dry and wet seasons are therefore not significantly different.

### 5.2.2 Water

The mean activity concentrations of  $^{238}\text{U}$ ,  $^{232}\text{Th}$  and  $^{40}\text{K}$  in the water samples are shown in Table 4-4. The mean values for  $^{238}\text{U}$ ,  $^{232}\text{Th}$  and  $^{40}\text{K}$  are  $0.54 \pm 0.23$  Bq/l in a range of 0.11-1.03 Bq/l,  $0.41 \pm 0.10$  in a range of 0.21-0.56 Bq/l and  $7.76 \pm 2.70$  Bq/l in a range of 1.65-12.0 Bq/l respectively. The mean annual effective dose from the water concentrations is calculated to be 0.21 mSv in a range of 0.10-0.34 mSv. It is important to note that most of the water sources

investigated are underground water taken from boreholes and mine pits. The main source of water supply to the mines is underground water for both domestic uses as well as processed water for the plant. The highest activity concentration of 1.03 Bq/L and 0.52 Bq/L for  $^{238}\text{U}$  and  $^{232}\text{Th}$  respectively were measured in a water sample from the mine tailings dam which is a mixture of both underground and processed water discharged into the tailings dam. This is not for domestic use. The lowest values of 0.11 and 0.21 Bq/L were from River Bonsa at Bonsaso which is about 30 km at a remote location from the discharge points of the Mine. This sample was taken as control to compare with the results from the study area.

In this study the results of the  $^{232}\text{Th}$  activity concentrations in the water samples were quite high even though in most cases they are lower than the activity concentrations of  $^{238}\text{U}$ . This could be attributed to the generally acidic conditions of the area (with about 90% water samples being slightly acidic) with a mean pH value of 6.10 and also because thorium is known to be generally more soluble in underground water than in surface water. From Table 4-4 the only exception was the mine process water with a pH value of 8.24 and  $^{232}\text{Th}$  activity concentration of 0.28 Bq/L. The Ghana Standards Board (GSB) and World Health Organisation (WHO) require the pH range suitable for drinking water to be 6.5-8.5 [GSB, 2005 and WHO, 2004]. The concentration of radionuclides in groundwater depends on the kind of minerals derived from the rock aquifers, the chemical composition of the water and the soil ion retention time [Andreo and Carrasco, 1999]. As shown in Table 4-4, most of the water samples were slightly acidic whilst others were near neutral or slightly basic. The pH is a very important water quality parameter that has an important influence on the solubility and mobility of metals or radionuclides in water with solubility increasing with decreasing pH. At pH of approximately 7, the solubility of uranium and thorium is extremely low and at pH less than 5, its concentration increases

gradually. The results of the activity concentration of  $^{238}\text{U}$  and  $^{232}\text{Th}$  in this study were compared with the WHO Guideline Levels but all the results including their mean values were lower than the 1.00 Bq/L recommended values in drinking water. The WHO guideline value of annual effective dose in water has been set at 0.10 mSv/year [WHO, 2004]. The mean annual effective dose in this study is about twice the recommended annual effective dose in drinking water. Generally, the mean annual effective doses of all the water sources investigated in the various communities had values above the WHO recommended value of 0.10 mSv/year. Also, the activity concentrations  $^{238}\text{U}$  and  $^{232}\text{Th}$  of all the samples were lower than the recommended guideline values of 10.0 and 1.0 Bq/L respectively.

Figure 4-10 shows the comparison of the activity concentrations of the radionuclides in the different types of water sources investigated. It shows clearly that the activity concentrations of  $^{238}\text{U}$  in the different types of water samples are higher than that of  $^{232}\text{Th}$  which agrees with literature values. However, in the water taken as a control from a river the  $^{232}\text{Th}$  activity concentration was higher than  $^{238}\text{U}$ . This could be attributed to deposition of particulate matter into the water body or transportation by sediments containing  $^{232}\text{Th}$ .

The pH of the water samples was in a range of 4.48 to 8.24. The Ghana Standards Board (GSB) and World Health Organisation (WHO) required pH range suitable for drinking water to be 6.5-8.5 [GSB, 2005 and WHO, 2004]. As shown in Table 4-4, about 90 % of the water samples were slightly acidic whilst others were near neutral. The pH is a very important water quality parameter that has an important influence on the solubility and mobility of metals or radionuclides in water. The solubility increases with a decreasing pH. At pH approximately 7, the solubility of uranium and thorium is extremely low and at pH less than 5, the concentration gradually increases. Also the chemical properties of uranium and thorium in water are mostly

affected by their hydroxide. This implies that at neutral pH, uranium and thorium cannot be leached much from the fractures or pores of the rock as hydroxide. At pH<5 uranium and thorium are able to dissolve in the river water in the form of  $\text{UO}_2^{2+}$  and  $\text{Th}^{4+}$  which are then suitable for leaching [NRC, 1999]. The transport of uranium occurs generally in oxidising water and in ground water as uranyl ion ( $\text{UO}_2^{2+}$ ) or as uranyl fluoride ( $\text{UO}_2\text{F}_2$ ), phosphate, or carbonate complexes. In oxidising and acidic waters,  $\text{UO}_2^{2+}$  and uranyl fluoride complexes dominate whereas the carbonate and phosphate complexes dominate in near-neutral to alkaline oxidising conditions. Maximum sorption of uranyl ions on natural materials occurs at pH 5.0-8.5 [NRC, 1999]. The results in this work also showed that  $^{238}\text{U}$  is generally more soluble in water than  $^{232}\text{Th}$  in the water samples.

Thorium is more likely to be precipitated in the form of insoluble  $\text{Th}(\text{SO}_4)_2^0$  when pH<2.5 and mainly to form insoluble complexes with organic species when pH>2.5 [NRC, 1999]. The formation of the insoluble organic and inorganic complexes at the respective pH values accounts for the higher concentration of thorium than uranium in sediments.

Generally, water from underground sources has higher concentration of radionuclides from the natural origin than water from surface bodies. Almost all the samples used in the study were from underground sources. It should also be noted that some of the water sources studied were not meant for drinking.

For the water samples, the results of the activity concentrations and the estimated annual effective doses for the two periods were also compared and the results shown in Table 4-22. The pH of most of the second batch of water samples had values around 7.0 neutral conditions as compared to the first batch for which all the samples were acidic. The reason for this may be due to high rainfall during the second batch sampling period. The high rainfall during the second

sampling campaign could have resulted in surface runoff as well as facilitated the dissolution and leaching of radionuclides into water bodies and farmlands. This could result in humans being exposed to radiation through ingestion of water and food grown on these farmlands. The activity concentrations of radionuclides were slightly higher in the second batch of samples than the first even though the water samples were near neutral conditions. However the differences are not significant. The estimated mean annual effective doses for the first and second batch samples were 0.21 and 0.27 mSv respectively. The results of the activity concentrations of the two sets of water samples were not significantly different with p-values greater than 0.05 as shown in Table 4-28. To test if there were significant difference in the mean concentrations of U, Th and K, ANOVA was used. The analysis indicated that there were significant differences in the means at 5% significant level. Further test (multiple comparison tests) was conducted and the results are given in Table 4-29. From Table 4-29, it is clear that the mean concentrations of Th and K and U and K are significantly different whereas U and Th are not. This implies that U and Th may exist together in varying concentrations in different types of rocks and water samples.

### **5.2.3 Particulate/Dust**

Table 4-5 shows the results of the activity concentrations of the radionuclides from dust samples determined by direct gamma ray spectrometry. The activity concentrations of  $^{238}\text{U}$  ranged from  $<0.12$ - $11.10 \mu\text{Bq}/\text{m}^3$  with a mean value of  $4.90 \mu\text{Bq}/\text{m}^3$ . The activity concentration of  $^{232}\text{Th}$  in the dust samples also varied in the range of  $0.65$ - $4.29 \mu\text{Bq}/\text{m}^3$  with a mean value of  $2.75 \mu\text{Bq}/\text{m}^3$ . The corresponding estimated mean absorbed dose rate and mean annual effective dose were  $3.51 \times 10^{-6} \text{ nGy}/\text{h}$  and  $2.70 \text{ nSv}$  respectively, which are in the range of normal background doses. The contribution to the radiation exposure of the population in the study area can be considered to be insignificant.

The results of elemental uranium and thorium concentrations determined from the dust samples by NAA in  $\mu\text{g/g}$  are shown in Table 4-6. The Table also contains the activity concentrations calculated from the elemental uranium and thorium concentrations in  $\mu\text{g/g}$ . The mean concentration of uranium and thorium in the dust samples calculated were  $1.8\pm 0.3$  and  $1.3\pm 0.2$   $\mu\text{g/g}$  respectively and the corresponding activity concentrations are 23.52 and 5.31  $\mu\text{Bq/g}$  respectively. The results of the first batch of dust samples compared very well with the second batch of samples. These results do not contribute significantly to the exposure of members of the public in the study since the values are below the exemption criteria specified in the Basic Safety Standard (IAEA, 1996). The mean uranium and thorium concentrations were  $2.0\pm 0.2$  and  $1.3\pm 0.2$   $\mu\text{g/g}$  respectively for the second batch of samples. The corresponding activity concentrations of  $^{238}\text{U}$  and  $^{232}\text{Th}$  were 24.0 and 5.2  $\mu\text{Bq/g}$  respectively. The exemption levels of  $^{238}\text{U}$ ,  $^{232}\text{Th}$  and  $^{40}\text{K}$  recommended by the ICRP and adopted by the IAEA in any material are 10 Bq/g, 1 Bq/g and 100 Bq/g respectively [ICRP, 1991; IAEA, 1996]. The exemptions levels are normally specified by the National Regulatory Authority of a country and should meet the following criteria [IAEA, 1996]:

- The effective dose expected to be incurred by any member of the public due to the source is of the order of 10  $\mu\text{Sv}$  or less in a year, and
- The collective dose (population dose) committed by one year of performance of a practice is no more than about 1 man.Sv.

The activity concentrations of  $^{238}\text{U}$  and  $^{232}\text{Th}$  in the dust samples by direct gamma ray analysis and NAA are far below the exemptions levels of these radionuclides and doses are far below the exempt limit for members of the public.

#### 5.2.4 Food

Six packs of fresh cassava samples harvested from six (6) different farms within the study area were analyzed to quantify the activity concentrations of  $^{238}\text{U}$ ,  $^{232}\text{Th}$  and  $^{40}\text{K}$ . The analyses were based both on fresh weight as well as dry weight in Bq/kg. The results of the fresh weight analysis are given in Table 4-7. The mean activity concentrations of  $^{238}\text{U}$ ,  $^{232}\text{Th}$  and  $^{40}\text{K}$  were  $0.18\pm 0.08$ ,  $0.14\pm 0.05$  and  $45.00\pm 1.90$  Bq/kg respectively. The estimated average annual effective dose was  $54\ \mu\text{Sv/year}$  ( $0.054\ \text{mSv/year}$ ). Cassava is normally cooked before it is ingested and this was not considered at this time in this work however future work on different food products in the study area will consider the form in which they are ingested to investigate the effect boiling have on the cooked product.

The results of the analysis based on dry weight are also given in Table 4-8. The average activity concentrations of  $^{238}\text{U}$ ,  $^{232}\text{Th}$  and  $^{40}\text{K}$  were  $0.82\pm 0.35$ ,  $0.65\pm 0.23$  and  $209.25\pm 8.75$  Bq/kg respectively. The estimated average annual effective dose was  $250\ \mu\text{Sv/year}$  ( $0.25\ \text{mSv/year}$ ). The results of the wet weight are lower than the dry weight. The reason for this could be attributed to loss in weight of the samples. Comparing the two sets of results with the exemption levels of  $^{238}\text{U}$  (10 Bq/g),  $^{232}\text{Th}$  (1 Bq/g) and  $^{40}\text{K}$  (100 Bq/g), indicate lower values. It implies that the levels of radioactivity in the cassava samples are insignificant and will not pose any radiological hazard from ingestion.

The activity ratios of each radionuclide in the soil samples to the cassava samples were calculated from their activity concentrations. The results are shown in Tables 4-9 to 4-11. Comparing the activity concentrations of each radionuclide in the soil samples to the cassava samples, shows that the activity concentration of the radionuclides in the cassava samples are by a factor of 67 to 157 lower than in the corresponding soil samples. This indicates that the uptake

of the radionuclides by the cassava samples is insignificant. It can also be observed in Tables 4-9 to 4-11 that the activity ratios are higher in the fresh samples than the dried samples.

### 5.3 Radon

Radon gas which has been known to contribute about 50% to the average annual radiation exposure from natural sources was also determined. The activity concentration of  $^{222}\text{Rn}$  measured in air and the component estimated from the soil concentrations are given in Table 4-12. For the  $^{222}\text{Rn}$  concentration measured in air, the results varied in a range of 27.5-32.7  $\text{Bq/m}^3$  with a mean value of  $30.0 \pm 1.7 \text{ Bq/m}^3$ . The calculated annual effective dose from inhalation ranged from 0.26-0.31 mSv with a mean value of  $0.29 \pm 0.02 \text{ mSv}$ . The results in this study compared well with results published in UNSCEAR 1996 and 2000 reports for normal areas around the world with values in a range of 2-30  $\text{Bq/m}^3$  in air [UNSCEAR, 2000]. The results are also below the action level of radon concentration in air of  $1000 \text{ Bq/m}^3$  for which intervention is required. The corresponding annual effective dose is 6 mSv/year using an assumed outdoor occupancy of 1760 hrs per year [ICRP, 1991 and UNSCEAR, 2000]. This means that the area studied does not have significant levels of  $^{222}\text{Rn}$  gas. The environmental conditions under which the measurements were carried out are also shown in Table 4-12. These include temperature, atmospheric pressure, and relative humidity with mean values of  $33.6 \text{ }^\circ\text{C}$ ,  $0.0104 \text{ kPa}$  and  $89.9\%$  respectively.

The activity concentrations of  $^{222}\text{Rn}$  in the soil matrix calculated from the activity concentration of  $^{226}\text{Ra}$  in the soil samples are also given in Table 4-12. The mean activity concentration of  $^{222}\text{Rn}$  in the soil was  $24.6 \text{ kBq/m}^3$  in a range of 12.5-41.3  $\text{kBq/m}^3$ . The effective doses were calculated only for the airborne radon due to inhalation by humans since soil radon could be significant only when the soil is accidentally ingested.

The results of  $^{222}\text{Rn}$  emanation fraction (EF) in the samples as well as the mean activity concentration of  $^{226}\text{Ra}$  are shown in Table 4-14. The result of the EF varied in a range of 0.51 in mine tailings (fine particles) to 0.80 in a mine pit samples containing granular and massive particles. The result from this study has also confirmed previous studies which indicate that the variation of EF is independent of the  $^{226}\text{Ra}$  content in the sample and is strongly correlated with the grain surface density (White and Rood, 2001). The results in this study for both granular and massive samples also show that the EF of the different types of samples are almost the same contrary to what has been reported in earlier EF studies where the smaller the grain size the higher the EF as follows  $\text{EF}(\text{GS}) > \text{EF}(\text{M}) > \text{EF}(\text{MS})$ . The reason for this similarity in values could be attributed to the similar porosity of the soils in the study area since the soil is generally considered to be sandy in nature. Generally, the  $^{222}\text{Rn}$  EF of different Te-NORM wastes can be ordered as follows: mining > gypsum > oil and gas > coal power plant (Afifi et al., 2004). The EF values in this study are compared with similar studies as shown in Table 4-19. The mean EF values for this study are 0.554 which is about 1.8 times higher than EF values of similar rare metals [USEPA, 1993]. The typical reported emanation coefficients for rocks and soils range from 0.05 to 0.70 [Nazaroff et al., 1988]. The EF values of this study also compared well with the typical values in soil and rocks. It also confirms that the value of the EF is independent of the activity concentration of  $^{226}\text{Ra}$ . The mean activity concentrations of  $^{226}\text{Ra}$  varied in a range of 6.20 Bq/kg in a soil sample at Brahabebome community to 32.41 Bq/kg in a soil sample at the mine's club house area. The highest value of 32.41 Bq/kg of  $^{226}\text{Ra}$  compares well with the worldwide average value of 32 Bq/kg [UNSCEAR, 2000]. The mean  $^{226}\text{Ra}$  activity concentration of the sample with highest EF value is 8.80 Bq/kg, which also confirms that the

variation of EF is independent of the  $^{226}\text{Ra}$  activity concentration in the sample and is strongly correlated with the grain surface density [White and Rood, 2001].

#### 5.4 Total annual effective dose

The basic approach to radiation protection is consistent all over the world and is based on the recommendations of the ICRP in its publications 60 and 103 [ICRP, 1990; 2007]. The recommendations stipulate that, any exposure above the natural background radiation be kept as low as reasonably achievable but below the individual dose limits, which for occupationally exposed workers is 20 mSv average over 5 years but not exceeding 50 mSv in any single year and for members of the public is 1 mSv/year. The dose limits were set based on prudent approach by assuming that, there is no threshold dose below which there would be no effect.

In the light of these dose limits, the total annual effective dose was estimated from all the potential exposure scenarios and compared with the recommended dose limits. A summary of the estimated equivalent doses and the total annual effective dose are given in Table 4-15. The mean annual effective doses estimated from direct external gamma ray exposure from natural radioactivity concentrations in soil/rocks, exposure from drinking water containing natural radioactivity, inhalation of airborne radon, ingestion of food (cassava) and inhalation of dust containing  $^{238}\text{U}$  and  $^{232}\text{Th}$  were 0.19, 0.21, and 0.29, 0.05 mSv and 2.65 nSv respectively. The corresponding total annual effective dose for all the exposure pathways was 0.74 mSv. From Table 4-15, it can be observed that, the various components contributing to the total effective dose ranged from  $3.0 \times 10^{-6}$  mSv (0.004%) in dust samples to 0.29 mSv (39.2%) due to airborne radon. The highest contribution to the total effective was due to airborne radon with 39.2% followed by ingestion of water (28.4%) and 25.7%) due to external of U, Th and K in soil/rock samples respectively. The rest of the components had relative contributions less than 10% with

least coming from U and Th in ore dust with 0.004%. The total annual effective dose of 0.74 mSv/year is also below the ICRP recommended dose limit of 1 mSv/year for members of the public from practices.

A comparison of the annual effective doses calculated from the soil, water, dust and airborne radon gas is shown in Figure 4-8. It shows that the airborne radon and water contributes most significantly whilst the contribution from dust is the least to the exposure in the population of the study area. In general however, the annual effective doses calculated from the various samples are considered insignificant.

### **5.5 Radiological risk assessment**

The radiological fatality cancer risks for population as well as severe hereditary effects were evaluated by using the ICRP risk assessment methodology [ICRP, 1991; 2007]. The ICRP envisages that, with the availability of new data on dose-response due to low dose range, that below and around 100 mSv, it is scientifically reasonable to assume that the incidence of cancer or hereditary effects will rise in direct proportion to an increase in the equivalent dose in the relevant organs or tissues [ICRP, 2007]. As a result, the practical system of radiological protection recommended by the Commission should continue to be based on the assumption that at doses below and around 100 mSv, a given increment in dose will produce a directly proportionate increment in the probability of incurring cancer or hereditary effects attributable to radiation. A model generally known as Linear Non-Threshold (LNT) is adopted and used in combination with adjudged value of dose and dose rate effectiveness factor (DDREF) of 2 for the management of risks from low dose radiation exposure [ICRP, 2007].

The evaluation of risk covered the various exposure pathways considered for this study. The ICRP risk assessment methodology [ICRP, 1991; 2007] was adopted for this work and the

results shown in Table 4-16. The results of the cancer and non-cancer risk components were evaluated from the annual equivalent dose components of the pathways and the total annual effective dose of 0.74 mSv/year.

The results of the lifetime fatality cancer risk to members of the public are in the range of  $1.2 \times 10^{-8}$  due to radionuclide in the ore dusts to  $1.1 \times 10^{-3}$  due to inhalation of airborne radon. This means that approximately 1 person out of 100,000,000 people is likely to suffer from some form of cancer from inhalation of ore dusts and this risk is considered insignificant. Also in the case of  $1.1 \times 10^{-3}$  due to airborne radon, it also means that approximately 1 person out of 1,000 people are likely to suffer from cancer related diseases from irradiation due to low background radiation exposure. The estimated total lifetime fatality cancer risk and the lifetime hereditary effect were  $2.8 \times 10^{-3}$  and  $1.0 \times 10^{-4}$  respectively. This means that approximately 3 persons out of 1,000 people are likely to suffer from cancer related diseases from irradiation due to low background radiation exposure. In the case of lifetime hereditary effect, approximately 1 person out of 10,000 is likely to suffer from some form of hereditary diseases. This means that the lifetime fatality cancer risk is slightly above the USEPA acceptable range of risks of  $1 \times 10^{-6}$  to  $1 \times 10^{-4}$  [USGAO, 1994] values for the population of the study area. A risk value of  $1 \times 10^{-6}$  that is 1 case of cancer out of 1 million people dying from cancer is considered trivial. Comparing the results with the acceptable risk factor, it can be concluded that, all but the risk due to inhalation of radionuclides in ore dusts exceeded the risk factor considered trivial. Also the total fatality cancer risk exceeded  $1 \times 10^{-6}$  making the value in this study as quite significant. However, it should be noted that most direct mode of exposure to the public will be through the ingestion of water and food stuffs grown on the soils and as a result, the risk might be an overestimation of what really persists in the study area.

In the case of hereditary effects, the lifetime risk factors evaluated varied in a range of  $4.2 \times 10^{-10}$  in the ore dusts to  $4.1 \times 10^{-5}$  due to airborne radon with a total value of  $1.0 \times 10^{-4}$ . This means that approximately 1 person out of 10,000 may suffer from some form of hereditary disorders and this can be considered insignificant.

The natural radioactivity in building materials is usually determined from the activity concentrations of  $^{226}\text{Ra}$ ,  $^{232}\text{Th}$  and  $^{40}\text{K}$ . Also because 98.5 % of the radiological hazard of U series is due to Ra and its decay products,  $^{238}\text{U}$  is replaced with concentrations of  $^{226}\text{Ra}$  in hazard assessment. In order to assess whether the soil/rock in the study area could be a source of public radiation exposure if used for building purposes the following hazard assessments were used; radium equivalent ( $\text{Ra}_{\text{eq}}$ ) activity in Bq/kg, external ( $H_{\text{ex}}$ ) and the internal hazard ( $H_{\text{in}}$ ). The radium equivalent activity is related to the external gamma dose from the terrestrial radionuclides and the internal dose due to radon and its decay products of  $^{210}\text{Pb}$  and  $^{210}\text{Po}$ . The maximum value of  $\text{Ra}_{\text{eq}}$  in building materials must be less than 370 Bq/kg for the material to be considered safe for use. The external and internal hazard indices must also be less than unity in order to keep the radiation hazard insignificant. This implies that, the radiation exposure due to the radioactivity from these radionuclides in materials to be used for constructions must be limited to 1.0 mSv/year.

In this study, the results of the  $^{226}\text{Ra}$ ,  $^{232}\text{Th}$  and  $^{40}\text{K}$  activity concentrations, radium equivalent activity in Bq/kg, as well as the absorbed dose rates, annual effective doses, the external and internal hazard indices are presented in Table 4-17. The mean radium equivalent activity in the samples was 61.00 Bq/kg in a range of 18.51-179.37 Bq/kg. The mean external and internal indices were 0.16 and 0.20 respectively. The values of the  $\text{Ra}_{\text{eq}}$ ,  $H_{\text{ex}}$  and  $H_{\text{in}}$  are below the acceptable values. This indicates that soils/rocks from the study area that could be

used for building purposes may not pose any significant radiological radiation hazard and thus are regarded as safe for use as building materials. The mean activity concentration of  $^{226}\text{Ra}$  was  $13.61 \pm 5.39$  Bq/kg in a range of 2.26 Bq/kg from a rock taken at Makulu waste dump (Minesite) to 30.57 Bq/kg from a soil sample in a cocoyam/cassava farm near the Agricultural Hill (Tarkwa) close to Teberebie pit of the mine. The results of the calculated absorbed dose rate in the soil/rock samples varied in a range of 9.05-79.79 nGy/h with a mean value of 27.55 nGy/h. The average absorbed dose rate in this study is lower than the worldwide average value of 60 nGy/h estimated from soil concentrations (UNSCEAR, 2000). The corresponding estimated annual effective dose was 0.17 mSv/year.

A comparison of the mean activity concentrations of  $^{226}\text{Ra}$ ,  $^{232}\text{Th}$  and  $^{40}\text{K}$ , the radium equivalent activities of soil, rock, and tailings from the study area with published data are shown in Table 4-18. The results of the study in some cases are lower than results from other countries and in some cases they compare well. The differences in some results could be attributed to differences in geological formations of the study area as well as differences in geochemical and hydrogeological conditions.

## **5.6 Gross alpha and gross beta measurements**

The activity concentrations of gross- $\alpha$  and gross- $\beta$  in water samples used in the various communities of the study area are shown in Table 4-23. The dominant oxide minerals in the study area include sandstone (quartz), pyrites, silica, haematite, specularite, magnetite and leucoxene with sandstone. Radionuclide concentrations in groundwater depend on the dissolution of minerals from rock aquifers. It has also been established that the water samples studied are acidic and this could facilitate the dissolution of radionuclides and other metals. The activity concentrations of gross- $\alpha$  in the water samples varied in a range of 0.008 Bq/L in Tarkwa

Township to 0.017 Bq/L from minesite (not intended for drinking or domestic purposes) with a mean value of 0.012 Bq/L. For the gross- $\beta$ , the activity concentrations varied in a range of 0.063 Bq/L at New Atuabo to 0.374 Bq/L at Pepesa with a mean value of 0.137 Bq/L. The WHO screening levels for drinking water below which no further action is required are 0.5 Bq/L for gross- $\alpha$  and 1.0 Bq/L for gross- $\beta$  [WHO, 2004]. The guideline values ensure an exposure lower than 0.1 mSv/year assuming a water consumption rate of 2 litre /day. Comparing these results with the WHO guideline values shows that all the values of the gross- $\alpha$  and gross- $\beta$  are lower than the guideline values. This indicates that all the water sources in the study area which are designated for drinking and domestic purposes do not have significant natural radioactivity and do not pose any significant radiological hazard. However for the purpose of gathering base line data of individual radionuclides for the area, radiochemical separation and alpha spectrometry will be carried out.

## **5.7 Geochemical characteristics of the mine**

### **5.7.1 Physical Parameters**

The results of the physical parameters namely; pH, conductivity, temperature and total dissolved solids (TDS) in water sample are presented in Table 4-24. The sources of the water samples include boreholes in the communities, streams and rivers, tap water from homes, treated and raw water from water treatment plants in the Tarkwa Township and Tarkwa Goldmine Ltd, and other surface water sources within the study area.

The pH of the type of water studied varied in the range of 3.55 to 8.95 with an average value of 5.94. Almost all the water sources were acidic with pH values less than 7.0. The WHO recommended pH range for drinking water is 6.50-8.50 [WHO, 2004]. Out of the 29 water samples studied, only 10 samples representing 34 % of the water samples had pH in the WHO

recommended pH range. This implies that 66 % of the water sources had pH values outside the recommended range. The pH of water generally influences the concentration of many metals by altering their availability and toxicity. The most acidic of the water samples with a pH of 3.55 was taken from Pepe pond within the mines. This water is not used for drinking or domestic purposes. The mean concentrations of U, Th and K in the Pepe water sample even with the acidic conditions were low with values of 0.02, 0.03 and 1.2 mg/L respectively. The provisional guideline value of U based only on chemical toxicity in drinking water recommended by the WHO is 0.015 mg/L [WHO, 2004]. The pH and temperature are two important parameters that govern the methylation of elements such as Pb, Hg [Van Loon, 1982]. High temperature and low pH may increase the toxicity of many substances such as trace metals in water. The chemical and biogeochemical processes that result in lowering of pH encourage the dissolution of trace metals as well as radionuclides into the ground water systems in very high concentrations. This could lead to the water becoming hazardous for human consumption. For instance trace metals such as Cd, Hg, Cr, Pb and U are known to be powerful nephrotoxins [Dou et al, 1980]. Exposure to metals such as Fe, Pt, Sb, As, Au and Tl are known to cause renal damage [Maher, 1976].

The electrical conductivity (EC) in the water samples, which is a measure of the ability of an aqueous solutions to carry electric current was determined and it varied in the range of 2.4 – 1208  $\mu\text{S}/\text{cm}$ . The WHO recommended value in drinking water is 700  $\mu\text{S}/\text{cm}$ . A comparison between the results in this study to the recommended value shows that only four of the water sources taken from the minesite were above the recommended value. However these four water sources are not designated for drinking purposes and as a result may not possess a health hazard. The EC is a useful indicator for mineralization in water body and correlates with Total Dissolved Solids (TDS) in water.

The TDS was also determined in all the water samples and results varied in a range of 17.3 to 893.0 mg/L. The WHO recommended value of TDS in drinking water is in the range of 600-1000 mg/L [WHO, 2004]. The results in this study are all below the WHO recommended value.

### 5.7.2 Anions

The results of the anions determined in the water samples are presented in Table 4-24. The mean concentrations of  $\text{Cl}^-$ ,  $\text{NO}_3^-$ ,  $\text{PO}_4^{3-}$  and  $\text{SO}_4^{2-}$  in the water samples were all below the WHO guideline levels in drinking water of 250, 50, 0.3 and 250 mg/L respectively [WHO, 2004]. This implies that, the concentrations of the anions in the water samples are not expected to pose water quality problems in terms of taste and health hazards. For the  $\text{SO}_4^{2-}$ , the concentration in waste water from the plant was 893 mg/L which is higher than the WHO recommended level. For instance, water containing about 250 mg/L of  $\text{Cl}^-$  may have a detectable salty taste if the cation present is sodium. However, even at 1000 mg/L, if the predominant cations are magnesium and calcium; the salty taste will be lost. High chloride content is associated more with waste water than raw water. Water with high chloride content may also have an effect on metallic pipes as well as growing plants.

Nitrates are normally found in trace quantities in surface water but higher values may be associated with some ground water. Excess amount in water may lead to a disease known as Methemoglobinemia in infants (Blue baby syndrome). It is an essential nutrient for many photosynthetic autotrophs and in some cases are also growth limiting nutrients (eutrophication).

Also, phosphate like nitrate is an essential nutrient in fertilizers used for farming and they are used extensively in the treatment of boiler waters. Excessive amount of  $\text{PO}_4^{3-}$  in water may

stimulate the growth of photosynthetic aquatic micro and macro organisms in nuisance quantities resulting in what is known as eutrophication.

The  $\text{SO}_4^{2-}$  is widely distributed in nature and in mine drainage wastes may contribute in large amounts through pyrite oxidation. One of the predominant minerals associated with the gold ore in the study area is pyrites ( $\text{FeS}_2$ ) and as a result more sulphate is expected to be produced due to the oxidation of pyrite.

It can be observed from the anions and physical parameters studied that the levels are within the acceptable limits for each anion and each physical parameter. It should be noted that not all the water sources studied are intended for drinking or domestic purposes. The water sources used for drinking and domestic purposes are the boreholes in the communities as well as the treated water from the Tarkwa Municipality and Tarkwa Goldmine water treatment plants. The anions and the physical parameters levels in these water sources were generally found to be within acceptable limits and of insignificant health hazard.

### **5.7.3 Trace and heavy Metals in water (Cations)**

The mean values of U, Th and K determined by NAA as shown in Table 4-24 were generally low. In general the concentrations of Th were higher than that of U which is unusual due to the relatively low solubility of Th compared to U, and this could be as a result of the water samples not being filtered prior to analysis. The presence of thorium in water samples is generally due to its transport with particulate matter and subsequent deposition. The concentrations of U and Th in water depend on the location of the water. For instance, in mineralised aquifers, values in a range of 0.10-0.46 ppm have been reported by various researchers [Fix, 1956 and Denson et al., 1956]. Values in a range of 0.001-0.013 ppm have been reported in sedimentary rock

drainage systems [Adams, et al., 1959]. The results in this study on underground water samples are within the range of values of similar studies that have been reported in mineralised aquifers.

The results of the other cations studied in the water sources by AAS are also shown in Table 4-24. The metals studied include: Fe, Mn, Cu, Zn, Cr, Pb, Cd, Hg and As. The concentrations of the metals were variable from one location to another. The concentrations of Cr, Hg and Cd in all the water samples studied were below their detection limits.

For Fe, the mean concentrations in all the water samples were below WHO guideline level of 0.3 mg/L which may result in consumers' complaints because it has the ability to decolorise fabrics (aerobic waters) [WHO, 2004]. Water samples taken from a river at Huniso and river Bonsa at Bonsaso about 30 km from the minesite which was taken as a control had higher Fe content. Even though these water sources were not designated as drinking water, there were indications that the inhabitants of the communities used the water for washing, bathing and swimming. Iron in underground water is usually in the ferrous state ( $\text{Fe}^{2+}$ ) since conditions underground are anoxic (reducing conditions). However upon exposure to air or other oxidants, the  $\text{Fe}^{2+}$  becomes oxidized to  $\text{Fe}^{3+}$  (Ferric ion) and may undergo hydrolysis to form insoluble hydrated ferric oxide ( $\text{Fe}_2\text{O}_3$ ). Elevated levels of Fe in water can cause stains in plumbing, laundry, cooking utensils and can impart objectionable taste and colour to food.

For Cu, Zn and As, the mean concentrations were 0.027, 0.042 and 0.004 mg/L and they were below the WHO guideline values of 2.0, 3.0 and 0.01 mg/L respectively [WHO, 2004]. Copper (Cu) occurs in its natural state and also in many minerals such as those containing sulphide compounds (e.g. chalcopyrite) and also with oxides and carbonates. Copper is considered an essential trace element for plants and animals. Some compounds are toxic when ingested and inhaled. It also forms a number of complexes in natural waters with organic and

inorganic ligands. At concentrations above 3 mg/L [WHO, 2004] it has been found to cause nausea and gastrointestinal discomfort. The health based guideline value recommended by WHO is 2 mg/L [WHO, 2004]. Since all the water sources had copper concentrations below the recommended limit of 2 mg/l, it is anticipated that continuous consumption of water from these sources at the current concentration levels would not likely constitute in any significant health risk.

Zinc (Zn) is also an essential growth element for both plants and animals but at elevated levels, it is toxic to some species of aquatic life. The solubility of Zn in natural waters is controlled by adsorption on mineral surfaces, carbonate equilibrium and organic complexes. Zn generally has low toxicity but prolonged consumption of large doses can result in health complications such as fatigue, dizziness, and neutropenia [Hess and Schmidt, 2002]. The Zn concentration in all the water sources were below the recommended limit of 3 mg/L in drinking water and a continuous consumption of water at these concentrations might not pose any significant health risk to members of the public.

The mean concentrations of Pb were variable some water samples had values below detection limit (Abekoase, Brahabebome) whilst others exceeded the WHO guideline levels of 0.01 mg/L [WHO, 2004]. The lead (Pb) concentrations in some of the water sources taken at Abekoase, Brahabebome and New Atuabo were below the detection limit. In others, the concentration varied in a range of 0.04 mg/L at Huniso to 0.168 mg/L at Pepe pond of the minesite. In the other communities and at the minesite the concentrations of Pb were above the recommended levels in drinking water. The highest value was measured in water samples taken from the minesite (Pepe pond and stream near Tebe) and this water body is not designated for drinking. The likely source of contamination of Pb in water bodies in the mine environment

could occur through leaching from welds of pipes and could also occur naturally through the decay of uranium and thorium decay series. Lead is the most common heavy metal and intake of lead occurs through ingestion of food, dirt and inhalation of particulate matter. It is known through sufficient studies in animals to be a possible human carcinogen and particularly lethal to children.

The concentrations of Cr, Cd and Hg in all the water samples were below their detection limits of 0.001, 0.002 and 0.001 mg/L respectively. This also implies that the concentrations of Cr, Cd and Hg were below the WHO recommended values of 0.05, 0.003 and 0.001 mg/L respectively.

The concentrations of arsenic (As) in the water samples were fairly uniform with values in a range of 0.002 to 0.008 mg/L and a mean value of 0.004 mg/L. The WHO recommended limit is 0.01 mg/L [WHO, 2004] and it can be observed that the concentrations of As in all the water sources were below the recommended limit in drinking water. The low values of As in the drinking water suggests that the levels might not pose significant health hazard in the water bodies studied. The very low concentration of arsenic in the water, inspite of the high levels of pyrite ( $\text{FeS}_2$ ) and arsenopyrite ( $\text{FeAsS}$ ) in the gold ore in the study area indicates the possibility of co-precipitation of As with complexes in the creeks before possible infiltration into the aquifer [Smedley et al, 1995]. Low level long-term exposure to As through drinking water could result in increased risk of bladder, kidney, liver and lung tumours as well as skin cancers [WHO, 1993]. It is anticipated that since the concentrations of As in the water samples are below the recommended levels, continuous consumption of these water sources might not lead to any health risk.

Manganese (Mn) is considered an essential trace element for plants and animals since it has low toxicity. The aqueous chemistry of Mn is similar to that of Fe. It can cause stains in plumbing, laundry and cooking utensils if levels are high. The health base guideline value recommended by WHO is 0.4 mg/L [WHO, 2004]. The concentrations of Mn in the water sources studied were variable with values varying from 0.005 to 1.397 mg/L with majority below the WHO recommended level of 0.4 mg/L. Two of the water sources (0.518 mg/L) (borehole water at Huniso) and (1.397) (underground water at Pepe pond) recorded values above the health based recommended value of 0.4 mg/L. At these concentrations, there is likely to be problems with appearance, taste or odour of the borehole water when used as drinking water. The low pH of this water source (Pepe pond) might have accounted for the high concentration of Mn in the water.

Mining areas are generally known to be associated with water quality problems that may result in serious health implications. In such areas, the rocks are often carbonate-deficient resulting in poorly buffered water [Smedley et al, 1995]. Also, in gold and base metal mining areas, sulphides oxidation as a result of chemical and biogeochemical processes may give rise to the production of low pH in ground water and this facilitates the dissolution of trace metals into the ground water systems in high concentrations. The Pepe pond ground water was found to have high concentrations of some metals and the reason could be due to the low pH created by chemical and geochemical processes which result in dissolution of metals. Also it was unclear why toxic trace metals such as Cr, Hg and Cd could not be determined in this water even with the low pH values (acidic). Also it should be noted that in the water sources studied where the concentration of a metal exceeded the WHO recommended limit, the water sources were not designated for drinking or domestic purposes and as a result the risk might be insignificant. Also

the concentrations of the metals and anions and the physical parameters were generally low and as a result not expected to cause any health hazards or cause water quality problems. The results the concentration of the metals in this study, adds to scientific knowledge and any further studies in this area.

#### **5.7.4 Trace and major metals in soil and rock samples.**

The soil and rock samples from the study area were also analysed by NAA in order to quantify the concentration levels of metals. These heavy metals are of environmental and health concern. An earlier study by Kuma and Young in 2001 had established that the soil types in Tarkwa are mostly silty-sand with minor patches of laterite [Kuma and Young, 2001]. Usually in an unaffected environment, the concentration of most metals is usually very low and mostly determined by mineralogy and weathering. However, human activities such as mining, smelting could lead to the release of metals from bedrocks. The concentration of metals in soils as well as the pH of the soil has a controlling factor in their migration and availability in water bodies and their uptake by plants in farmlands. Excess heavy metal accumulation in soils is toxic to humans and other animals.

The results of the mean concentrations of metals of interests U, Th and K measured in soil and rock samples as well as metals such Mn, Si, V, Al, La, As, Cr, Sr, Sc, Fe, Co, Ti, Mg, Ca, Na are shown in Table 4-25. The mean elemental concentrations of U and Th varied in a range of 0.2-1.8  $\mu\text{g/g}$  and 0.9-2.6  $\mu\text{g/g}$ . All the mean concentration values were below the world average values of 2.8 and 7.4  $\mu\text{g/g}$  respectively in soil [UNSCEAR, 2000]. These results indicates that the mean concentrations of the radioactive elements U and Th obtained from the formations studied are by a factor of two to fourteen times lower than the worldwide levels reported. In general, the original uranium, thorium and potassium concentrations in rocks may

vary due to alteration or metamorphic processes [Verdoya et al., 2001]. The most abundant of the three radioelements K is of less concern because K is an essential element for growth. The mean concentration of K varied in a range of 7037  $\mu\text{g/g}$  to 71360  $\mu\text{g/g}$  in soil. For uranium (U), the natural concentration in the earth crust and normal soils are 2.3 ppm and 1.8 ppm respectively. Besides the radiological hazard of uranium, it is also a chemical hazard like arsenic, and has the tendency to cause damage to kidneys and other organs in the body if the levels are significant. High concentrations may be fatal. Uranium forms both soluble and insoluble compounds. The chemical toxicity of uranium thus depends on the oxidation state it forms soluble compounds. The soluble compounds become easily absorbed into the blood stream and a fraction may further become absorbed by bones and the rest goes to the kidneys where they may be excreted through urine. The insoluble compounds on the other hand when swallowed only a small fraction is absorbed into the blood stream from the gut whilst a greater proportion is excreted together with undigested food. The insoluble compounds when inhaled also remain in the lungs for a long time and absorbed slowly into the blood stream and become an internal hazard to the lungs and other organs.

The mean concentrations of the other metals in various materials studied were variable. For instance, the mean concentrations of Si were in a range of 1345  $\mu\text{g/g}$  in soil to 5329  $\mu\text{g/g}$  in rock which is an indication of silica ( $\text{SiO}_2$ ) saturated rock type of the area. Studies have shown that, the content of U and Th generally increase with silicon dioxide ( $\text{SiO}_2$ ) during differentiation, fractional crystallisation, partial melting, etc in the final stages of magmatic procedures (Rollinson, 1993). The results in this study did not reflect this trend where the concentrations of U and Th tend to be high with  $\text{SiO}_2$ .

The results of the major metals such as Fe, Mg, Ca, Na and K were quite high in the soil and rock samples indicating that these essential metals are not strongly leached even though the study area is known for very high rainfall patterns and the slightly acidic conditions. This also means that agricultural activities could still flourish in the study area. The concentrations of the rest of the trace metals in the soil and rock samples were very low and in some cases they were below detection limit. This could be as a result of leaching of these metals due to the high rainfall of the area and the acidic conditions of the area as result of the oxidation of high sulphides and pyrites.

By comparison, the concentrations of the trace metals were far lower than the major metals measured in the soil/rock samples. The reasons for the low levels of trace metals as compared to the major metals could be due to the clayey nature of the soil in the study area as well as the heavy rains resulting in low pH of the area, which could facilitate the leaching of the trace metals. Also soils with large surface areas such as clay minerals have large capacity for adsorption of major cations such as  $\text{Ca}^{2+}$ ,  $\text{Cu}^{2+}$  etc and on the other hand low adsorption for trace metals such as arsenic. This is because ions have different tendencies to form complexes with different substances. For instance, many cations can form complexes with hydroxyl ( $\text{OH}^-$ ) or carboxyl group ( $\text{COOH}$ ) and as a result many metals become easily adsorbed to surfaces of these groups [Asklund and Eldvall, 2005]. The concentrations of the nutrient metals are very high means that the soil type is an intermediate between the forest oxysols (highly leached soils) and the forest ochrosol which are normally less leached and contained all of their nutrients suitable for plant growth.

Figure 4-15 is a comparison of the percentage weighted values of pH, temperature, conductivity, total dissolved solids, and concentrations of uranium, thorium and potassium in

water samples. In general studies have shown that, U, Th and K are generally similar in geochemical behaviour with U and Th. They belong to the actinides series and both exist in the tetravalent state under reducing conditions [Adams et al., 1959]. As can be seen in Figure 4-15, the three elements behave in the same manner under same environmental conditions of temperature, pH, conductivity and total dissolved solids. Figure 4-15 also shows a good relationship between TDS and electrical conductivity and between temperature and pH of the water samples studied.

The Th/U ratio which gives an indication of the relative depletion or enrichment of radioelements was also calculated for the different types of soil and rock samples. The Th/U ratio for normal continental crust varies from 3.8- 4.2 [Plant and Saunders, 1996] with a typical value of 3.0. The results of the ratios, Th/U, K/Th and K/U are shown in Figures 4-16 a, b and c respectively. The calculated Th/U ratios are also shown in Table 4-25 with values varying in a range of 1.1 in soil in Tarkwa to 5.3 in rock sample in a mine pit with a mean value of 2.5. The best fitting relations between Th/U, K/Th and K/U are linear with correlation coefficients of 0.511, 0.555 and 0.008 respectively. The value obtained for this study is closed to the theoretical value. This means that, there seems to be no significant fractionation (enrichment or depletion) during weathering or involvement in metasomatic activity of the radioelement uranium and thorium. Figures 4-17 to 4-20 show comparison of the normalised values of the physical parameters; pH, temperature, conductivity and total dissolved solid each with U, Th and K. As in the case of Figure 4-15, U, Th and K showed the same behaviour with each of the physical parameters. This shows that U, Th and K behave in the same manner under the same conditions of pH, temperature, conductivity and total dissolved solids in water samples in the environment. Since U and Th behave similarly under reducing conditions (+4 oxidation state), it implies the U

and Th exist in the reduced state in the water samples studied. However this can be confirmed if speciation studies are carried out in the study area. This is necessary because whilst the radiological toxicity of  $U^{4+}$  and  $U^{6+}$  might be the same, in terms of their chemical toxicity,  $U^{6+}$  is higher than  $U^{4+}$  mainly due to the higher solubility of the former than the latter.

# KNUST



## CHAPTER SIX

### 6.0 CONCLUSIONS AND RECOMMENDATIONS

#### 6.1 Radiation exposure from NORM and impact on the public

The aim of this research work was to assess the risks to members of the public in the study area from exposure to natural sources of radiation as a result of the mining and mineral processing activities of Tarkwa Goldmine. The four (4) exposure pathways considered for the study were; direct external gamma ray exposure from natural radioactivity concentrations in soil/rocks, internal exposure from drinking water containing natural radioactivity, ingestion of food (cassava), inhalation of radon gas and inhalation of dust containing  $^{238}\text{U}$  and  $^{232}\text{Th}$ . The communities covered during this work include Tarkwa Township, Abekoase, Brahabebom, Huniso, New Atuabo, Pepesa, Samahu and Tebe.

The study was motivated by the fact that the area is known as heavy minerals mining area with operations dating back to the 19<sup>th</sup> Century. It is noted that the geology of the area is similar to the Witwatersrand area of South Africa where gold bearing conglomerates contain uranium in commercial quantities and therefore there is a possibility that the gold ores of the study area could have significant quantities of uranium. Prior to this study, no investigations have been conducted to obtain data on the activity concentration levels of the natural radionuclides  $^{238}\text{U}$ ,  $^{232}\text{Th}$  and  $^{40}\text{K}$  in the area. Consequently, the radiation doses and risks associated with these radionuclides have never been investigated. High levels of these elements could pose chemical and/or radiological hazards.

In this study, data on the activity concentrations of  $^{238}\text{U}$ ,  $^{232}\text{Th}$  and  $^{40}\text{K}$  in different types of samples as well as radiation doses and risks have been established. The activity concentrations of  $^{238}\text{U}$ ,  $^{232}\text{Th}$  and  $^{40}\text{K}$  in different media for all the potential pathways through

which members of the public could be exposed were quantified using direct gamma spectroscopic analysis and neutron activation analysis (NAA).

The mean activity concentrations of  $^{238}\text{U}$ ,  $^{232}\text{Th}$  and  $^{40}\text{K}$  in the soil/rock samples were estimated to be 15.2, 26.9, 157 Bq/kg respectively. For the water samples, the mean activity concentrations of  $^{238}\text{U}$ ,  $^{232}\text{Th}$  and  $^{40}\text{K}$  were 0.54, 0.41, 7.76 Bq/L respectively. The mean activity concentrations of  $^{238}\text{U}$  and  $^{232}\text{Th}$  in dust samples were 4.90 and 2.75  $\mu\text{Bq}/\text{m}^3$  respectively. For the food samples the mean activity concentrations of  $^{238}\text{U}$ ,  $^{232}\text{Th}$  and  $^{40}\text{K}$  (fresh weight) were 0.18, 0.14 and 45.00 Bq/kg respectively. The results in this study compared well with other studies carried out in other countries and with the worldwide average activity concentrations (UNSCEAR, 2000).

The ICRP philosophy of radiological protection aims at preventing deterministic effects and also reducing the occurrence of stochastic effects of cancer and hereditary diseases to acceptable levels. This is achieved by a system of protection that requires justification of practice to ensure it produces a net benefit, optimisation of protection to keep exposures as low as reasonably achievable (ALARA) and the protection of individuals by imposing either dose limits or controls on the risks from potential exposures. As a result, the potential exposure of the population in the study area was assessed by estimating the annual effective doses in various media and the total annual effective dose was determined from the sum of all the mean annual effective doses from all the exposure pathways considered for purposes of comparison with recommended dose limits.

The total annual effective dose for all the exposure pathways was 0.74 mSv. Even though the airborne radon contributed more significantly at 39.2 % to the total annual effective dose, the activity concentrations measured are far below the ICRP recommended level of 1000

Bqm<sup>-3</sup> for which remedial action is needed. However, it is recommended that the mining company establishes a periodic monitoring programme especially for the control of airborne radon. The total annual effective dose is also lower than the 1 mSv per year dose limit recommended by the ICRP for public radiation exposure control. The results indicate insignificant levels of the natural radionuclides, implying that the mining activities do not pose any significant radiological hazard to the communities in this area.

The radiological hazards to the population in the study area were assessed based on the calculation of radium equivalent activity ( $Ra_{eq}$ ), hazard indices (external and internal) as well as the radon emanation coefficient for the soil/rock samples. The  $Ra_{eq}$  was found to be less than the recommended maximum value of 370 Bq/kg, and the external and internal hazard indices had values less than unity. It can be concluded that soil/rock materials that may be used for construction of buildings may not pose any significant radiological hazards.

Radon emanation fraction (EF) is a very important radiological hazard index that is used to evaluate the amount of <sup>222</sup>Rn emanation fraction released from materials containing naturally occurring radionuclides. The assessment of EF was based on the decay of <sup>222</sup>Rn from the parent radionuclide <sup>226</sup>Ra in the soil/rock samples. The results show that EF in the samples is independent of the <sup>226</sup>Ra content in the samples and in a range of 0.506 to 0.795. Typical emanation coefficients for rocks and soils are in a range of 0.05 to 0.7 [Nazaroff et al., 1988]. The results in this study are comparable to typical emanation coefficient in rocks and soils. It also shows that the emanation coefficient of radon from the soil matrix could be significant even though the activity concentrations of <sup>226</sup>Ra are low.

The risks to members of the public, from exposure to naturally occurring radioactive materials (NORM) as a result of the mining and mineral processing activities of Tarkwa

Goldmine was evaluated using the ICRP risk assessment methodology for fatal cancer risk and hereditary effects. The lifetime fatality cancer risks from the exposure pathways considered varied from  $1.2 \times 10^{-6}$  in ore dusts to  $1.1 \times 10^{-3}$  in airborne radon gas. The total lifetime cancer and hereditary effects were estimated to be  $2.8 \times 10^{-3}$  and  $1.0 \times 10^{-4}$  respectively. This means that in terms of the lifetime fatality cancer risk approximately 3 out of 1000 may suffer from some form of cancer fatality and for the lifetime hereditary effect approximately 1 out of 10,000 may suffer some hereditary effect. The negligible cancer fatality risk value recommended by USEPA is in the range of  $1 \times 10^{-6}$  to  $1 \times 10^{-4}$  (i.e. 1 person out of 1 million or 10,000 suffering from some form of cancer fatality). The results of the lifetime cancer risks estimated in this study exceeded the range of acceptable risk for the exposure pathways. Also, the total lifetime risk estimated was above the acceptable range recommended by the USEPA, however the public may not necessarily be exposed to some of these sources.

The activity concentrations of gross- $\alpha$  and gross- $\beta$  in the water samples were all below the WHO recommended guideline values. However, it was observed that where the concentration of K is high in the water samples the gross- $\beta$  activity concentration tends to be higher due to contribution of beta radiation from  $^{40}\text{K}$ . The results obtained in this study show that the background radiation levels are within the natural limits and compared well with similar studies for other countries. The data from this study can be used as baseline for future investigations.

The results of the estimated doses of the other sources of exposure compare quite well with earlier studies on radioactivity in other mines in Ghana and elsewhere [Darko et al., 2010; UNSCEAR, 2000]. This study considers that the ingestion of water and food (cassava) could be the most significant mode of exposure in the study area. On the basis of the results from this

study, consumption of food and water do not pose any significant source of radiation hazard to the population. The results from this study could help in the development of reference levels for natural radioactivity for the study area and Ghana as a whole. However, even though the Tarkwa Goldmine has similar geological formation as the Witwatersrand area of South Africa, where the gold ores contain uranium in commercial quantities, the results in this study showed that the gold ore of the Tarkwa Goldmine does not contain uranium in significant quantities.

The results from this study will serve as reference data for any future studies and also add up to data required to help develop guidelines for the regulation of NORM in Ghana for radiation protection workers and the public. The results which have also been published in peer reviewed journals for the reading public will help create awareness on NORM to individuals, policy makers and academia.

## RECOMMENDATIONS

The following areas are recommended for further research in future:

- Determination of gross alpha and gross beta activity concentration in drinking water sources in the study area using a gross alpha and beta counter.
- Determination of  $^{238}\text{U}$ ,  $^{232}\text{Th}$ ,  $^{226}\text{Ra}$ ,  $^{210}\text{Po}$  and  $^{210}\text{Pb}$  in drinking water from the study area using radiochemical separation and alpha spectrometry.
- Assessment of the  $^{226}\text{Ra}$  and  $^{222}\text{Rn}$  emanation coefficient for Te-NORM scales in pipes of the gold treatment plants in Ghana.
- Determination of activity concentrations of  $^{238}\text{U}$ ,  $^{232}\text{Th}$  and  $^{40}\text{K}$  by gamma spectrometry as well as gross alpha and gross beta activity concentrations in a variety of food products in the study area (e.g. cassava, cabbage, cocoyam, plantain etc).

## 6.2 Geochemical Characteristics of the study area

The geochemistry of the mines was also assessed in addition to the radiological study of the area. The assessment included the determination of the physical parameters as well as the chemical constituents such as trace metals and anions in the water sources. The physical parameters measured in the water sources were pH, temperature, conductivity and total dissolved solids (TDS). The conductivity and TDS were all within the acceptable limits recommended by the WHO in drinking water [WHO, 2004]. In the case of the pH of the water samples, the recommended range in drinking water is 6.5-8.5, but in this study some of the water samples had pH values falling outside the acceptable range. About 90 % of the water samples studied had slightly acidic conditions. The most acidic of the water samples with a pH of 3.55 was water taken from Pepe pond at the Pepe pit. This water sample is not water designated for domestic or consumption purposes and also had restricted access to the public. It was also found that some of the water from the boreholes had pH outside the acceptable range in drinking water. For the electrical conductivity, only four of the water samples had values exceeding the WHO recommended levels in drinking water. However, these water samples were not designated for domestic use or for drinking purposes and as such the results are of insignificant health hazard to the public since there was restricted access to these water bodies by the mining company.

The mean concentration of uranium in the water samples was 0.020 mg/l in a range of 0.010-0.040 mg/l. The mean concentration of thorium was 0.029 mg/l in a range of 0.010-0.060 mg/l. For K the concentrations varied in a range of 0.02 to 3.84 mg/l with a mean value of 1.19 mg/l. The results in this study are comparable to similar studies that have been carried out elsewhere in mineralised aquifer waters. In the case of the other metals, the results of the

concentrations were variable with some metals having concentrations below detection limits and others with concentrations below the WHO guideline values.

For the anions studied, the concentrations in all the water samples were within the WHO guideline values. The following anions:  $\text{Cl}^-$ ,  $\text{NO}_3^-$ ,  $\text{PO}_4^{3-}$  and  $\text{SO}_4^{2-}$  had values below the WHO recommended levels for drinking water. The only exception was  $\text{SO}_4^{2-}$  where some of the samples had values that exceeded the recommended value. These are however surface water bodies within the mine's operational area with restricted access to members of the public and therefore could not be used for any purpose.

A comparison of the behaviour of U, Th and K with physical parameters such as pH, temperature, conductivity, total dissolved solids also showed that all the three radioelements exhibited the same trend of behaviour under the same environmental physical conditions with U and Th showing a stronger relationship under the same environmental conditions.

In the soil and rock samples, the concentrations of U, Th and K were in a range of 0.2-1.8  $\mu\text{g/g}$ , 0.52-2.6  $\mu\text{g/g}$  and 7037-71360  $\mu\text{g/g}$  respectively. These results also compare well with results of normal continental crust rocks and the world average values [UNSCEAR, 2000]. The mean Th/U ratio of all the samples was 2.5 and this also compared well with normal continental crust rock value of 3. This means that the radioelements in soil/rocks did not undergo any enrichment or depletion during weathering of the rocks in the study area.

For the other heavy metals namely; Fe, Mn, Cu, Zn, Cr, Pb, Cd, Hg and As their concentrations were variable from one location to another. Heavy metals may be released into the environment from the following areas; smelting and refining industries, scrap metals, plastic and rubber industries, various consumer products and burning of waste containing these metals. These metals upon release in air may travel long distances and become deposited onto soil,

vegetation and water depending on the density. However, these environmental pollutants are not biodegradable and persist in the environment for many years and humans may become exposed to them through inhalation, ingestion or by dermal contact. The concentrations of the following heavy metals Cr, Cd, and Hg were found to be below their detection limits. The concentrations of Cu, Zn and As were also found to be below the WHO guideline values in drinking water. In the case of Fe, Mn and Pb, there was variability in their concentration in the water samples. In some cases, their concentrations were below the detection limit and the WHO guideline values, and in few cases the concentrations were above the WHO guideline values. Water samples, in which Fe concentrations were above the guideline value, were not meant for drinking purposes. For Pb, the concentrations in the water sources from Samahu, Asuman, Huniso and Pepesa had values exceeding the WHO recommended values. Also, the water sample that was taken from river Bonsa at Bonsaso as a control had the concentration of Fe and Pb exceeding the recommended levels in drinking water whilst the rest of the metals were below their detection limits or below the guideline values.

For the concentrations of metals determined in the soil/rock samples, it was found that all the concentrations of trace metals such as As, V and Co were below the recommended levels. However, the concentrations of the major metals such as Mg, K, Ca and Na in all the soil/rock samples were quite high indicating these metals were less leached as compared to the trace metals which were affected by heavy rainfall and acidic conditions in the area.

In general the results from the study area did not show heavy loading of the physical and chemical constituents in the water sources investigated as usually anticipated for a mining area. These results further complement or corroborate earlier studies in the determination of physical

and chemical characteristics of the study area for decision making [Kortatsi, 2004; Asklund and Eldvall, 2005].

## RECOMMENDATIONS

The following areas are recommended for future research:

- Chemical speciation studies on the geochemistry of U and Th in the study area.
- Assessment of the levels of elemental U and Th, and other major and trace metals in a variety of food items in the study area and the mode of translocation from soil to plants.



## REFERENCES

- Ackers, J. G., Den Boer, J. F., De Jong, P. and Wolschrijn, R. A. (1985). Radioactivity and exhalation rates of building materials in the Netherlands. *Sci. Tot. Environ.* Vol. 45.
- Adams, J. A. S, Osmond, J. K. and Rogers, J. W., (1959). *The Geochemistry of thorium and uranium*, Elsevier.
- Afifi, E. M., Khalifa, S. M., Aly, H. F. (2004). Assessment of the  $^{226}\text{Ra}$  content and the  $^{222}\text{Rn}$  emanation fraction of Te-NORM wastes at certain sites of petroleum and gas production in Egypt, *J. Radioanal. Nucl. Chem*, Vol. 260.
- Alam, M. N., Miah, M, M, H., Chowdhury, M. I., Kamal, M., Ghose, S., Islam, M, N., Mustafa, M. N., and Miah, M. S. R. (1999). Radiation dose estimation from radioactivity analysis of lime and cement used in Bangladesh, *J. Environ. Radioact.* Vol. 42.
- American Public Health Association, (1998). *Standard Methods for the Examination of water and wastewater*, 20<sup>th</sup> Edition, Washington DC.
- Amonoo-Neizer, E. H. and Amekor, E. M. K. (1993). Determination of total arsenic in environmental samples from Kumasi and Obuasi, Ghana, *Environ. Health Perspect.*, Vol. 101
- Andersen, C. E. (1992). Entry of soil gas and radon into houses. *Riso-R-623 (EN)*.
- Andreo, B., Carrasco, F. (1999). Application of geochemistry and radioactivity in the hydrogeological investigation of carbonate aquifers (Sierras Blanca and Mijas, southern Spain), *Appl. Geochem.* Vol.14.
- Aryee, B.N.A. (2001). Ghana's mining sector: its contribution to the national economy, *Resource Policy Statement*, Vol. 27.
- Aryee ,B., Aboagye ,Y. (2008). *Mining and Sustainable Development in Ghana*, Minerals Commission, Ghana
- Asante, K. A., Agusa, T., Subramanian, A., Ansa-Asare, O. D., Biney, C. A., and Tanabe, S. (2007). Contamination status of arsenic and other trace metals in drinking water and residents from Tarkwa, a historic mining township in Ghana, *Chemosphere*, Vol. 66.
- Asante, K. A. and Ntow, W. J. (2009). Status of environmental contamination in Ghana, the perspective of a research scientist: *Interdisciplinary studies on Environmental Chemistry-Environmental Research in Asia*, Eds. Y., Obayashi, T., Isobe, A., Subramanian, S., Suzuki and S., Tanabe.
- Asklund, R. and Eldvall, B. (2005). Contamination of water resources in Tarkwa mining area of Ghana, MSc thesis, lund University, Sweden.

ASTM. (1983). Standard Method for sampling surface soils for radionuclides, American Society for Testing Materials, Report No. C (PA: ASTM).

ASTM. (1986). Recommended practice for investigation and sampling soil and rock for engineering purposes, In: Annal Book of ASTM Standards; (04/08), American Society for Testing Materials, Report No. D, 420 (PA: ASTM).

Avotri, T. S. M, Amegbey, N. A, Sandow, M. A. and Forson, S. A. K. (2002). The Health Impact of cyanide spillage at Goldfields Ghana Ltd, Tarkwa, Ghana, Funded by Goldfields Ghana Ltd., (Unpublished data).

Baird, C., (1999), Environmental Chemistry, W. H. Freeman and Company, New York.

Barsky, G., Swainson, S. J. and Hedley, N. (1962). Dissolution of Gold and Silver in cyanide solutions, Trans. Am. Inst. Min. Metal. Eng., Vol. 122.

Beretka, J. and Mathew, P. J. (1985). Natural radioactivity of Australian Building materials, industrial wastes and by-products, Health Phys. Vol. 48.

Bernhard, G. (2005). Speciation of uranium in environmental relevant compartments, Landbautorschung VÖlkenrode, Vol. 55.

Bliss, J. D. (1978). Radioactivity in selected mineral extraction industries, A literature Review, Technical Note ORP/LV-79-1 Washington, DC: Environmental protection Agency.

Bozkurt, A., Yorulmaz, N., and Kam, E. (2007). Environmental Radioactivity Measurements in Harran Plain of Sanliurfa, Turkey.

Cember, H. (1996). Introduction to Health Physics, 3rd Edition, McGraw-Hill, New York

Clever, H. L. (ed). (1979). Solubility Data Series, Krypton, Xenon and Radon-Gas Solubilities, Volume 2, Pergamon Press.

Colle, R., Rubin, R. J., Knab, L. I., and Hutchinson, J. M. R. (1981). Radon transport through and exhalation from building materials: a review and assessment, NBS Technical Note No. 1139, Washington DC; US Department of Commerce, National Bureau of Standards.

E.C. (1996). Council Directive 96/29/EUROTOM/ of 13 May 1996 Laying Down the Basic Safety Standards for the Protection of the Health of Workers and the General Public against the Dangers Arising from Ionizing Radiation, Official Journal of EC, Commission of the European Communities Series L, No. 159.

Cooper, M. B., Ralph, B. J., Wilks, M. J. (1981). Natural radioactivity in bottled mineral water, Australian Radiation laboratory, ARL-TR-036.

Dahlgaard, H. (1996). Polonium-210 in mussels and fish from the Baltic-North sea estuary, *Journal of Environmental Radioactivity*, Vol. 32.

Darko, E. O. (2004). Radiation Risk from NORMS in Mining and Mineral Processing at the Obuasi Goldmines: Modelling, Dose Intercomparison and Regulatory Control, PhD Thesis, University of Ghana, Ghana.

Darko, E. O., Tetteh, G. K. and Akaho, E. H. K. (2005). Occupational radiation exposure to norms in a gold mine, *Journal of Radiation Protection Dosimetry*, Vol. 114.

Darko, E. O and Faanu, A. (2007). Baseline radioactivity measurements in the vicinity of a Gold Treatment Plant, *Journal of Applied Science and Technology*, Vol. 10, Ghana.

Darko, E.O., Faanu, A., Razak, A., Emi-Reynolds, G., Yeboah, J., Oppon, O. C. and Akaho, E. H. K. (2010). Public exposure hazards associated with natural radioactivity in open-pit mining in Ghana, *Rad. Prot, Dosim.* Vol. 138.

Department of Water Affairs & Forestry. (2002). Radioactivity Dose Calculation and Evaluation Guidelines, Institute for Water Quality Studies, (DWAf), Doc. Ref. PSI/IWQS01 Rev 0, South Africa.

Denson, N., Zeller, H. and Stephens, J. (1956). Water sampling as a guide in the search for uranium deposits and its use in evaluating widespread volcanic units as potential source beds for uranium, U. S. Geol. Survey Prof. Paper 300.

DOE. (2003). Hanford Geophysical Logging Project: Data Analysis Manual, GJO-HGLP 1.6.3 Revision 0, United States Department of Energy USA.

Dou J., Klassen C. D. and Amdur M. O. (1980). Casaret and Dou's Toxicology, 2<sup>nd</sup> Edition, Macmillan publishing, New York.

Egidi, P., and Hull, C. (1999). NORM and TE-NORM: Procedures, users and regulations, 32<sup>rd</sup> Midyear Tropical Meeting of the Health Physics Society, Albuquerque, NM, USA, Jun. 24-27.

El Afifi, E. M., Hilal, M. A., Khalifa, S. M. and Aly, H. F. (2006). Evaluation of U, Th, K and emanated radon in some NORM and TENORM samples. *Radiat. Meas.*, Vol. 41.

Fix, P. F. (1956). Hydrogeological exploration for uranium, U. S. Geol. Survey Prof. Paper 300.

Galbraith, J. H. and Saunders, D. F. (1983). Rock classification by characteristics of aerial gamma-ray measurements, *J. Geochem. Explor.* Vol. 18.

Ghana Standards Board. (2005). Water Quality-Requirements for drinking water, GS 175 PT.1:2005.

Goldfields Ghana Ltd. (2007). Securing the future: mineral resource and ore reserve statement, Tarkwa Goldmine Ltd, Tarkwa, Ghana.

Goldfields Ghana Ltd. (2008a). Delivering value to our stakeholders and caring for the environment, Tarkwa.

Goldfields Ghana Ltd. (2008b). Mining and Exploration Assets, Tarkwa Goldmine, Tarkwa Ghana.

Hess R. and Schmidt B. (2002). Zinc supplement overdose can lead to toxic effects, *J. Paediatr. Haematol./Oncol.* Vol. 24.

Higgy, R. H., El-Tahawy, M. S., Abdel-Fattah, A. T., and Al-Akahawy, U. A. (2000). Radionuclide content of building materials and associated gamma dose rates in Egyptian dwellings, *J. Environ. Radioact.* Vol. 50.

Hilson, G. (2002). Harvesting Mineral riches: 1000 years of gold mining in Ghana, *Resource Policy*, Vol. 28.

HPS. (1996). Radiation Risk in Perspective: Position statement of the Health Physics Society.  
IAEA. (1989). Measurement of Radionuclides in Food and Environment: A Guidebook, IAEA-Technical Reports Series No. 295, Austria.

IAEA. (1996). International Basic Safety Standards for Protection against Ionising Radiation and for the safety of radiation sources, Safety Series No. 115, IAEA, Vienna.

IAEA. (2003). Extent of Environmental Contamination by Naturally Occurring Radioactive Material (NORM), IAEA Technical Report Series No. 419, Vienna-Austria.

IAEA. (2004). Soil sampling for environmental contaminants, IAEA-TECDOC-1415, Austria.

IAEA. (2005). Naturally Occuring Radioactive Materials (IV), proceedings of an international conference held in Szczyrk, IAEA-TECDOC-1472, Poland.

ICRP. (1977). Radiation Protection in Uranium and other mines, Vol. 1, No. 1, Pergamon Press, Oxford.

ICRP. (1991). 1990 recommendations of the International Commission on Radiological Protection, ICRP Publication 60, Pergamon Press, Oxford.

ICRP. (1993). Protection against Radon-222 at home and work, ICRP Publication 65, Pergamon Press, Oxford.

ICRP. (2007). 2006 recommendations of the International Commission on Radiological Protection, ICRP Publication 103, Pergamon Press, Oxford.

IFC. (2003). Socio-Economic Baseline and Impact Assessment Report, Community Development Plan, Iduapriem and Teberebie Goldmines, GAGL, International Finance Corporation Ghana.

Karpeta, W. P. (2000). A Review of the Geology, Mining and Exploration of Tarkwa Mine Area.

Kesse, G. O. (1985). The mineral Rock Resources in Ghana, A. A. Balkenia Publishers, Netherlands.

Knoll, G. F. (1989) Radiation Detection and Measurement, 2nd ed., John Wiley & Sons, New York.

Kortatsi, B. K. (2004). Hydrochemistry of groundwater in the mining area of Tarkwa-Prestea, Ghana, PhD thesis, University of Ghana, Legon-Accra, Ghana.

Kuma, J. S and Younger, P. L. (2001). Pedological characteristics related to groundwater occurrence in the Tarkwa area, Ghana, Journal of African Earth Sciences, vol. 33(2).

Kumah, J. S. (2007). Hydrogeological Studies on the Tarkwa Gold Mining District, Ghana, Bulletin of Engineering Geology and the Environment, (Bull Eng Geol Env), Vol. 66.

Kumar, V., Ramachandran, T. V. and Prasad, R. (1999). Natural radioactivity of Indian Building materials and by products. Appl. Radiat. Isot. Vol. 51.

Landsberger, S. (1994). Delayed Instrumental Neutron Activation Analysis, p. 121-139 in: Chemical Analysis by Nuclear Methods, Chapter 6, (Alfassi, Z. B., ed.), John Wiley & Sons.

Maher J. F.(1976). Toxicology nephropathy, In the Kidney, (B. M. Brenner and F. C. Rector Jr, ed.), W. B. Saunders, Philadelphia.

Malanca, A., Pessina, V. and Dallara, G. (1993). Radionuclide content of building materials and gamma-ray dose rates in dwellings of Rio-Grande Do-Norte Brazil. Radiat. Prot. Dosim., Vol. 48.

Mason, B., Moore, C. B. (1982). Principles of Geochemistry, fourth ed. Wiley, New York.

McDonald P., Baxter M. S. and Scott E. M. (1996). Technological enhancement of natural radionuclides in the marine environment, Journal of Environmental Radioactivity, Vol. 32.

NAS. (1990). Health Effects of exposure to low levels of ionizing radiation, BEIR V, National Academy of Sciences, National Research Council, Academy Press, Washington DC.

NAS. (2006). Health risks from exposure to low levels of ionizing radiation, BEIR VII, National Academy of Sciences National Research Council, Academy Press, Washington DC.

NAS. (1988). Health risks of radon and other internally deposited alpha emitters, BEIR IV, National Academy of Sciences, National Research Council, Academy Press, Washington DC.

NRC. (1999). Evaluation of Guidelines for exposures to Technologically Enhanced Naturally Occurring Radioactive Materials, National Research Council , Washington, DC.

Nazaroff, W. W., Moed, B. A., and Sextro, R. G. (1988). Soil as source of indoor radon: generation, migration and entry, p. 57-112 in: Radon and its decay products in Indoor Air (Nazaroff, W. W and Nero, A. V. Jr., eds.), John Wiley & Sons, New York.

Nielson, K. K., Rogers, V. C. and Rogers V. (1994). The RAETRAD model of radon generation and transport from soils into slab-on-grade houses, Health Phys. Vol. 67.

O'Brien, R. S. and Cooper, M. B. (1998). Technologically Enhanced Naturally Occurring Radioactive Material (NORM): Pathway Analysis and Radiological Impact, Appl. Radiat. Isot, Vol. 49.

OECD/NEA. (1979). Exposure to radiation from natural radioactivity in building materials, Report by NEA Group of Experts, Nuclear Energy Agency (Paris: OECD).

Ofori, A. (2008). Corporate Social Responsibility of Mining Companies in Ghana, MA Thesis, Clark University, USA.

Plant, J. A., Saunders, A. D. (1996). The radioactive earth, Radiat. Prot. Dosim. Vol. 68 (1/2).

Rollinson, H. R. (1993). Using geochemical data: evaluation, presentation, interpretation, Longman.

Rogers, V. C. and Nielson, K. K. (1991). Multiple radon generation and transport in porous materials, Health Phys., Vol. 60.

Sato, J., and Endo, M. (2001). Activity ratios of uranium isotopes in Volcanic Rocks from Izu-Mariana Island-Arc Volcanoes, Journal of Nuclear and Nuclear and Radiochemical Sciences, Vol. 2, Japan.

Smedley P. L., Ednunds W. M., West J. M., Gardner S. J. and Pelig-BA K. B. (1995). Vulnerability shallow Groundwater Quality due to Natural Geochemical Environment, Health Problems related to Groundwater in the Obuasi and Bolgatanga areas, Ghana, Report prepared for ODA under the ODA/BGS Technology Development and Research programme, Project 92/5.

Sood, D. D., Manohar, S. B. and Reddy, A. V. R. (1981). Experiments in Radiochemistry, India Association of Nuclear Chemists and Allied Scientists (IANCAS).

Sorantin, P. and Steger, F., (1984). Natural radioactivity of building materials in Austria. Radiat. Prot. Dosim., vol. 7.

Suzuki, A., Iida, T., Moriizumi, J. and Sakuma, Y. (2000). The effects of different types of concrete on population doses. Radiat. Prot. Dosim., Vol. 90.

Tanner, A. B. (1980). Radon migration in the ground: A supplementary review, In: Gesell, T. F. and Lowder, W. M, Natural radiation environment III, Vol. 1, US Department of Energy Report CONF-780422.

Tay C. K, Asmah. R. and Biney C. A. (2010). Trace metal levels in water and sediments from Sakumono II and Muni lagoons, Ghana, West African J.Appl. Ecology, Vol. 16.

Tzortzis, M. and Tsertos, H. (2004). Determination of thorium, uranium and potassium elemental concentrations in surface soils in Cyprus, J. Environ. Radioact. Vol. 77.

USEPA. (1993). Diffuse NORM Waste Characterization and Preliminary Risk Assessment, Prepared by S. Cohen and Associates, Inc., and Rogers & Associates Engineering Corp. for the US Environmental Protection Agency, Office of Radiation and Indoor Air.

USEPA. (2006). 2006 Edition of the Drinking Water Standards and Health Advisories, EPA 822-R-06-013, Washington DC.

USDA. (2000). Heavy metal soil contamination, United States Department of Agriculture: Natural Resources Conservation Service, USA.

USGAO, 1994. United States General Accounting Office, Nuclear Health and Safety: Consensus on Acceptable Radiation Risk to the Public is lacking. United States General Accounting Office, GAO/RCED-94-190, Washington D.C.

UNSCEAR. (1982). Sources and Biological effects, 1982 report to the General Assembly, with Annexes, United Nations Sales Publication E. 82. IX.8. United nations, New York.

UNSCEAR. (1988). 1988 Report to the General Assembly with Scientific Annexes, United Nations Sales Publication E.88.IX.7, United Nations, New York.

UNSCEAR. (1993). Exposures from Natural Sources of Radiation, 1993 Report to General Assembly, Annex A, New York.

UNSCEAR. (2000). Exposures from Natural Sources, 2000 Report to General Assembly, Annex B, New York.

UNSCEAR. (1996). Sources and Effects of Ionising Radiation , 1996 Report to the General Assembly, with Scientific Annex, United Nations, New York.

Van der Steen J and Van Weers A.W. (1996), Radiation Protection in NORM industries, NRG, Radiation and Environment, Netherlands.

Van Loon J. C. (1982). Chemical Analysis of Inorganic Constituents of Water, CRC Press.

Valkovic, V. (2000). Radioactivity in the environment, Elsevier, The Netherlands.

Verdoya, M., Chiozzi, P. and Pasquale, V. (2001). Heat-producing radionuclides in metamorphic rocks of the Brianconnais-Piedmont Zone (Maritime Alps), *Eclogae Geol. Helv.* Vol. 94.

Washington, J. W. and Rose, A. W. (1992). Temporal variability of radon concentration in the interstitial gas of soils in Pennsylvania, *J. Geophys. Res.*, Vol. 97B.

Water Environment Federation. (1995). Standard Methods for the examination of water and waste water, American Water Works Association, 19<sup>th</sup> Edition.

White, G. J. and Rood, A. S. (2001). Radon emanation from NORM –contaminated pipe scale and soil at petroleum industry sites, *J. Environ. Radioact.*, Vol. 54.

White, W. M. (2007). *Geochemistry*, John Hopkins University Press, USA.

WHO. (1993). Guidelines drinking-water quality, 2<sup>nd</sup> Ed. Recommendations, Vol. 1. World Health Organization, Geneva.

WHO. (2004). Guidelines drinking-water quality, 3<sup>rd</sup> Ed. Recommendations, Vol. 1. World Health Organization, Geneva.

Xinwei, L. (2005). Radioactive analysis of cement and its products collected from Shaanxi, China. *Health Phys.*, Vol. 88.

Xinwei, L., Lingquig, W., Xiaodan, J., Leipeng, Y. and Gelian, D. (2006). Specific activity and hazards of Archeozoic-Cambrian rock samples collected from the Weibei area of Xhaanxi, China, *Rad. Prot. Dosim.*, Vol. 118.

## APPENDICES

### Appendix 1

#### **CALIBRATION**

The quality and reliability of any analytical measurements depends on how well the measuring device is calibrated with standard materials. The high purity germanium detector used for the study was calibrated with respect to energy and efficiency calibration as well as the resolution of the detector. Standard radionuclides in two different geometries were used to calibrate the detector. Radionuclides homogenously distributed in solid water matrix in a one (1) litre Marinelli beaker geometry with density approximately  $1 \text{ g/cm}^3$  and mean atomic number approaching that of water. The standard source was used to calibrate the system for the soil, water and food samples. In the case of the dust samples collected on filter a different geometry made of standard radionuclides uniformly distributed on a plastic foil matrix was used. Efficiency calibration is geometry dependent and necessary for the quantification of  $^{238}\text{U}$ ,  $^{232}\text{Th}$  and  $^{40}\text{K}$  radionuclides in particular geometry. The soil/rock, water and food samples were measured in a 1 litre marinelli beaker on a high purity germanium detector (HPGE) whilst the dust samples collected on filters papers were measured by direct gamma spectrometry and also by NAA.

The energy calibration curves of the detector using standard radionuclides in the marinelli beaker and the plastic foil geometries are shown figures 5-1 and 5-3 respectively with same correlation of  $R^2=1$ . The energy calibration curves indicate the correlation between the energy of radionuclide and the corresponding channel number at the centroid of a full energy peak. The plot fitted a linear function which indicates that the detector system is performing well for the two different matrices of standard radionuclides used for the energy calibration.

The efficiency calibration curves for the two different geometries are also shown in figures 5-2 and 5-4 with correlation coefficients of  $R^2=0.989$  and  $R^2=0.969$  respectively for energies between 100 and 2000 keV. The best fit of the curves was obtained by applying power series resulting in equations (1) and (2). The efficiency curve was obtained by discarding some data points of the radionuclides used in the energy calibration in order to obtain the best fit curve.

$$Y = 1.127X^{-0.7057} \quad (1)$$

$$Y = 17.88X^{-0.95} \quad (2)$$

The generally accepted expression for efficiency calibration is given by equation (3) [IAEA, 1989]:

$$\ln \varepsilon = a_1 + a_2 \ln E \quad (3)$$

Where;

$\varepsilon$  is absolute full energy event efficiency,

$a_1$  and  $a_2$  are the fit parameters,

$E$  is the energy (keV).

By applying natural log of both sides of equations (1) and (2) will result in identical equations as equation 3.

$$\ln \varepsilon = 0.1196 - 0.7057 \ln E$$

The expression is suitable for determining efficiencies of gamma energies between 100 keV and 2000 keV.

The result of resolution of the detector which is a measure of how well the detector can distinguish between two closely lying photopeaks in a spectrum of full energy events is shown in figure 5-1. The resolution of the detector measured at 1332 keV of a  $^{60}\text{Co}$  source was 0.19%. The

typical range of resolution of HPGe detectors is 0.1-0.2 % [Sood et al., 1981]. The measured resolution of the detector used for this study is within the range of the resolution of HPGe detectors which also indicates that the detection system was performing well and suitable for use in this study.

The results of the minimum detectable activities of  $^{238}\text{U}$ ,  $^{232}\text{Th}$  and  $^{40}\text{K}$  which were determined by measuring a 1 L Marinelli beaker filled with distilled water on the detector are shown in table 5-1. The minimum detectable activities of  $^{238}\text{U}$ ,  $^{232}\text{Th}$  and  $^{40}\text{K}$  were estimated to be 0.12, 0.11 and 0.15 Bq/kg respectively. The minimum detectable activities of these radionuclides depends on a number factors including the background radiation in area, adequacy of shielding from environmental background radiation and the inherent activity concentrations of these radionuclides in the sample containers.

#### **Energy calibration results for 1.0 Litre Marinelli beaker Geometry**

Nuclide	Gamma ray energy (keV)	Channel Number
Cadmium-109	85.13	67
Cobalt-57	121.98	96
Caesium-137	662	521
Cobalt-60	1174.07	924
Cobalt-60	1334.17	1050
Yttrium-88	1838.61	1447

#### **Radionuclides used for efficiency calibration**

Energy (keV)	Efficiency
122	0.0383
662	0.0120
1173	0.0072
1332	0.0064
1836	0.0062

The mixed standard source that was used for the energy and efficiency calibrations of the gamma detector has the following specifications as shown in table 4-1.

### Geometry of Reference Source

Source number: NW146

Volume: Approximately 1000 ml

Density: Approximately 1.0 g/m<sup>3</sup>

Reference date: 1<sup>st</sup> February, 2006 at 12:00 GMT.

### Radionuclides in the mixed standard

Nuclide	Gamma ray energy (keV)	Activity Concentration (Bq)	Emission rate (s <sup>-1</sup> )
Americium-241	60	2.97 x 10 <sup>3</sup>	1.06 x 10 <sup>3</sup>
Cadmium-109	88	1.69 x 10 <sup>4</sup>	6.14 x 10 <sup>2</sup>
Cobalt-57	122	8.84 x 10 <sup>2</sup>	7.57 x 10 <sup>2</sup>
Cerium-139	166	9.66 x 10 <sup>2</sup>	7.71 x 10 <sup>2</sup>
Mercury-203	279	2.56 x 10 <sup>3</sup>	2.09 x 10 <sup>3</sup>
Tin-113	392	3.18 x 10 <sup>3</sup>	2.07 x 10 <sup>3</sup>
Strontium-85	514	3.89 x 10 <sup>3</sup>	3.83 x 10 <sup>3</sup>
Caesium-137	662	2.78 x 10 <sup>3</sup>	2.36 x 10 <sup>3</sup>
Yttrium-88	898	6.62 x 10 <sup>3</sup>	6.22 x 10 <sup>3</sup>
Cobalt-60	1173	3.40 x 10 <sup>3</sup>	3.40 x 10 <sup>3</sup>
Cobalt-60	1332	3.40 x 10 <sup>3</sup>	3.40 x 10 <sup>3</sup>
Yttrium-88	1836	6.62 x 10 <sup>3</sup>	6.57 x 10 <sup>3</sup>

## Appendix 2:

### Soil sampling points within the mine and its surrounding communities.

Location code	Location coordinates	Description of sampling location
SS <sub>1</sub> /FS <sub>1</sub>	N 5° 21'22.02" W 2° 01' 31.21"	Soil sample at satellite nursery of the mine
SS <sub>2</sub>	N 5° 21'55.11" W 2° 01' 22.26"	Soil at rehabilitation Plantation of the mines
SS <sub>3</sub>	N 5° 21'13.42" W 2° 01' 23.73"	Waste stockpile use for rehabilitation
SS <sub>4</sub>	N 5° 20'59.40" W 2° 01' 34.22"	Tailings storage dam
SS <sub>5</sub>	N 5° 21'01.28" W 0° 00' 36.34"	North heap leach
SS <sub>6</sub>	N 5° 17'59.76" W 2° 02' 10.07"	Lower Merv waste dump
SS <sub>7</sub>	N 5° 18'02.74" W 2° 02' 04.56"	Upper Merv waste dump
SS <sub>8</sub>	N 5° 17'49.91" W 2° 01' 22.90"	Soil sample at Teberebie pit (cut back)
SS <sub>9</sub>	N 5° 19'44.03" W 2° 00' 11.85"	Soil sample at Pepe open pit
SS <sub>10</sub>	N 5° 19'44.03" W 2° 00' 11.85"	Rock sample from Pepe open pit
SS <sub>11</sub>	N 5° 17' 49.84" W 2° 01' 22.82"	Soil sample from Makulu waste dump
SS <sub>12</sub>	N 5° 17' 49.84" W 2° 01' 22.82"	Rock sample from Makulu waste dump
SS <sub>13</sub>	N 5° 21'29.52" W 2° 02' 54.87"	Soil sample from Kontraverchy open pit
SS <sub>14</sub>	N 5° 21'29.52" W 2° 02' 54.87"	Rock sample from Kontraverchy open pit
SS <sub>15</sub>	N 5° 18'21.23" W 2° 01' 04.28"	Rock sample from Mantrain north
SS <sub>16</sub>	N 5° 19'48.63" W 2° 02' 18.27"	Rock sample from Akontansi Ridge
SS <sub>17</sub>	N 5° 19'15.26" W 2° 01' 44.83"	Rock sample from Akontansi Central
SS <sub>18</sub>	N 5° 18'58.62" W 2° 01' 23.70"	Rock sample from Akontansi under lap
SS <sub>19</sub>	N 5° 19'29.66" W 2° 01' 21.76"	Ore sample from ore stockpile
SS <sub>20</sub>	N 5° 19'22.34" W 1° 58' 36.40"	Soil sample from New Atuabo area
SS <sub>21</sub>	N 5° 18'57.84" W 1° 58' 37.02"	Soil sample from New Atuabo area
SS <sub>22</sub>	N 5° 18'52.03" W 1° 59' 47.23"	Soil sample from Goldfields club house
SS <sub>23</sub>	N 5° 18' 47.44" W 1° 59' 56.72"	Soil sample from Brahabebomi area
SS <sub>24</sub>	N 5° 21'54.82" W 1° 59' 58.46"	Soil sample from Samahu area
SS <sub>25</sub> /FS <sub>5</sub>	N 5° 19'18.99" W 2° 00' 00.87"	Soil sample from Asuman area
SS <sub>26</sub>	N 5° 19'47.45" W 1° 58' 59.53"	Soil sample from Boboobo area
SS <sub>27</sub>	N 5° 22'24.39" W 2° 01' 07.49"	Soil sample in Abekuase area
SS <sub>28</sub>	N 5° 22'59.51" W 2° 03' 55.51"	Soil sample from Huniso area
SS <sub>29</sub> /FS <sub>4</sub>	N 5° 19'56.60" W 2° 00' 11.36"	Soil sample from Pepesa area
SS <sub>30</sub> /FS <sub>6</sub>	-	Soil sample in a farm at Abekuase
SS <sub>31</sub> /FS <sub>3</sub>	N 5° 19'08.02" W 2° 00' 25.21"	Soil sample in a cocoyam/pineapple farm near Samahu
SS <sub>32</sub>	N 5° 17'10.90" W 2° 03' 33.46"	Soil sample from old tailings dam
SS <sub>33</sub>	N 5° 17'38.31" W 2° 02' 34.25"	Soil sample from inactive south heap leach
SS <sub>34</sub>	N 5° 17'59.82" W 2° 02' 59.89"	Soil sample from active south heap leach
SS <sub>35</sub> /FS <sub>2</sub>	N 5° 18'10.83" W 2° 10' 26.59"	Soil sample from cocoyam/cassava from near Agric Hill
SS <sub>36</sub>	N 5° 17'53.71" W 2° 00' 43.66"	Soil sample from a farm Teberebie pit near UMAT lecturers residence
SS <sub>37</sub>	-	Rock sample from the mill area of plant site
SS <sub>38</sub>	-	Rock sample from crusher area of plant site

**Water sampling points within the mine its surrounding communities.**

Location code	Location coordinates	Description of sampling location
WS <sub>1</sub>	N 5 <sup>0</sup> 22'05.18" W 2 <sup>0</sup> 01' 38.76"	River at containment (RCA) area from processing from HL and natural water
WS <sub>2</sub>	N 5 <sup>0</sup> 21' 23.91" W 2 <sup>0</sup> 01' 16.55"	Waste water from barren ponds
WS <sub>3</sub>	N 5 <sup>0</sup> 20'12.23" W 2 <sup>0</sup> 01' 37.04"	Tailing water from the plant (TSF)
WS <sub>4</sub>	N 5 <sup>0</sup> 19'19.68" W 1 <sup>0</sup> 59' 33.12"	Apinto Valley Shaft (AVS), rain and waste water
WS <sub>5</sub>	N 5 <sup>0</sup> 18'51.27" W 2 <sup>0</sup> 10' 36.91"	Mantrain north (rain and underground water)
WS <sub>6</sub>	N 5 <sup>0</sup> 18'51.27" W 2 <sup>0</sup> 10' 36.91"	Mantrain north, underground water
WS <sub>7</sub>	N 5 <sup>0</sup> 18'20.64" W 2 <sup>0</sup> 00' 59.22"	Mantrain south pit, underground water
WS <sub>8</sub>	N 5 <sup>0</sup> 19' 57.84" W 1 <sup>0</sup> 58' 36.40"	Borehole water from New Atuabo area
WS <sub>9</sub>	N 5 <sup>0</sup> 18' 22.34" W 1 <sup>0</sup> 58' 37.02"	Borehole water from New Atuabo area
WS <sub>10</sub>	N 5 <sup>0</sup> 18'52.03" W 1 <sup>0</sup> 59' 47.23"	Tap water at the Goldfields club house
WS <sub>11</sub>	N 5 <sup>0</sup> 19'18.00" W 1 <sup>0</sup> 59' 34.28"	Underground raw water from Goldfields water treatment plant
WS <sub>12</sub>	N 5 <sup>0</sup> 18' 47.44" W 1 <sup>0</sup> 59' 56.72"	Borehole water at Brahabebomi community
WS <sub>13</sub>	N 5 <sup>0</sup> 21'54.82" W 1 <sup>0</sup> 59' 58.46"	Borehole water at Samahu community 1
WS <sub>14</sub>	N 5 <sup>0</sup> 21'54.82" W 1 <sup>0</sup> 59' 58.46"	Borehole water at Samahu community 2
WS <sub>15</sub>	-	Suman river water with source from river Bonsa
WS <sub>16</sub>	N 5 <sup>0</sup> 22'24.02" W 2 <sup>0</sup> 01' 02.16"	Borehole water at Abekuase community
WS <sub>17</sub>	N 5 <sup>0</sup> 22'55.97" W 2 <sup>0</sup> 01' 48.32"	Stream water at Tebe, underground and mine water
WS <sub>18</sub>	N 5 <sup>0</sup> 22'54.70" W 2 <sup>0</sup> 02' 38.55"	Borehole water at Asuman village
WS <sub>19</sub>	N 5 <sup>0</sup> 22'59.51" W 2 <sup>0</sup> 03' 55.51"	River water from River Huni at Huniso
WS <sub>20</sub>	N 5 <sup>0</sup> 22'59.51" W 2 <sup>0</sup> 03' 55.51"	Borehole water from Huniso
WS <sub>21</sub>	N 5 <sup>0</sup> 20'43.49" W 2 <sup>0</sup> 05' 45.46"	Borehole water at Pepesa community
WS <sub>22</sub>	N 5 <sup>0</sup> 22'21.16" W 2 <sup>0</sup> 01' 12.91"	Stream water from Asuman stream
WS <sub>23</sub>	N 5 <sup>0</sup> 17'30.65" W 2 <sup>0</sup> 03' 43.79"	Surface water near old tailing dam and south heap leach
WS <sub>24</sub>	N 5 <sup>0</sup> 17'42.31" W 2 <sup>0</sup> 02' 41.19"	Underground/rain water used at south heap leach
WS <sub>25</sub>	N 5 <sup>0</sup> 18'10.83" W 2 <sup>0</sup> 10' 26.59"	Rain water at Agric Hill residential area
WS <sub>26</sub>	N 5 <sup>0</sup> 17'13.58" W 1 <sup>0</sup> 59' 55.31"	Tap water taken at Hotel de Hilda
WS <sub>27</sub>	N 5 <sup>0</sup> 17'53.71" W 2 <sup>0</sup> 00' 43.66"	Tap water at the UMAT lecturers residence
WS <sub>28</sub>	N 5 <sup>0</sup> 19'44.03" W 2 <sup>0</sup> 00' 11.85"	Underground/rain water at Pepe pond
WS <sub>29</sub>	N 5 <sup>0</sup> 10'47.39" W 2 <sup>0</sup> 02' 35.71"	River water taken from River Bonsa (Control)
WS <sub>30</sub>	N 5 <sup>0</sup> 19'18.00" W 1 <sup>0</sup> 59' 34.28"	Treated water from GF water treatment plant
WS <sub>31</sub>	N 5 <sup>0</sup> 19'50.76" W 1 <sup>0</sup> 58' 58.50"	Borehole water from Boboobo
WS <sub>32</sub>	N 5 <sup>0</sup> 21'22.02" W 2 <sup>0</sup> 01' 31.21"	Stream at satellite nursery

**Dust sampling points within the mine and its surrounding communities.**

Location code	Location coordinates	Description of sampling location
AS <sub>1</sub>	N 5 <sup>0</sup> 19'26.74" W 1 <sup>0</sup> 58' 41.12"	New Atuabo settlement area
AS <sub>2</sub>	N 5 <sup>0</sup> 18'51.68" W 1 <sup>0</sup> 59' 47.41"	Goldfields club house
AS <sub>3</sub>	N 5 <sup>0</sup> 19'50.76" W 1 <sup>0</sup> 58' 58.50"	Boboobo community
AS <sub>4</sub>	N 5 <sup>0</sup> 18'10.83" W 2 <sup>0</sup> 10' 26.59"	At Agric Hill near Ghana Telecom base station
AS <sub>5</sub>	N 5 <sup>0</sup> 17'53.71" W 2 <sup>0</sup> 00' 43.66"	At UMAT lecturers residence near Teberebie pit

KNUST



**Appendix 3:**

**Absorbed dose rates in air and estimated annual effective doses at 1 meter above the ground at the soil sampling points during the first sampling period.**

Location code	Measured dose rate, nGy/h		Calculated effective dose, $\mu$ Sv/year
	Range	Average	
SS <sub>1</sub>	20-80	40	49.1
SS <sub>2</sub>	30-60	30	36.8
SS <sub>3</sub>	20-100	40	49.1
SS <sub>4</sub>	40-100	50	61.3
SS <sub>5</sub>	40-120	50	61.3
SS <sub>6</sub>	70-110	60	73.6
SS <sub>7</sub>	50-100	40	49.1
SS <sub>8</sub>	20-90	50	61.3
SS <sub>9</sub>	40-80	30	36.8
SS <sub>10</sub>	50-90	40	49.1
SS <sub>11</sub>	40-60	30	36.8
SS <sub>12</sub>	60-140	60	73.6
SS <sub>13</sub>	60-110	40	49.1
SS <sub>14</sub>	60-110	40	49.1
SS <sub>15</sub>	70-90	30	36.8
SS <sub>16</sub>	20-90	30	36.8
SS <sub>17</sub>	30-50	20	24.5
SS <sub>18</sub>	30-60	20	24.5
SS <sub>19</sub>	40-40	30	36.8
SS <sub>20</sub>	90-180	70	85.8
SS <sub>21</sub>	30-120	40	49.1
SS <sub>22</sub>	30-50	20	24.5
SS <sub>23</sub>	10-50	40	49.1
SS <sub>24</sub>	20-70	40	49.1
SS <sub>25</sub>	20-60	10	12.3
SS <sub>26</sub>	60-100	50	61.3
SS <sub>27</sub>	50-110	40	49.1
SS <sub>28</sub>	40-60	20	24.5
SS <sub>29</sub>	60-110	30	36.8
SS <sub>30</sub>	70-80	30	36.8
SS <sub>31</sub>	40-90	40	49.1
SS <sub>32</sub>	70-90	30	36.8
SS <sub>33</sub>	50-90	30	36.8
SS <sub>34</sub>	30-60	20	24.5
SS <sub>35</sub>	80-130	50	61.3
SS <sub>36</sub>	90-190	70	85.8
SS <sub>37</sub>	70-150	50	61.3
SS <sub>38</sub>	70-150	50	61.3
<b>Average</b>	<b>20 – 190</b>	<b>38.4</b>	<b>47.1</b>

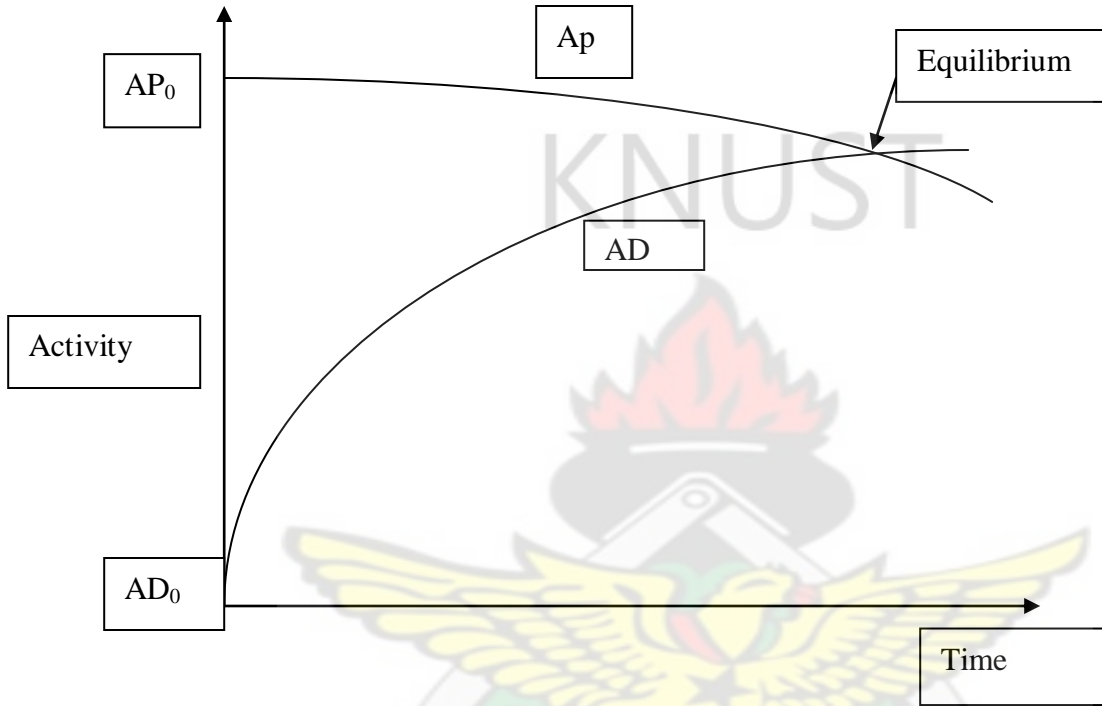
**Absorbed dose rates and estimated annual effective doses at 1 meter above the ground at the water sampling points during the first sampling period.**

Location Code	pH	Measured dose rate, nGy/h		Calculated annual Effective Dose
		Range	Average	μSv/year
WS <sub>1</sub>	6.21	20-70	30	36.8
WS <sub>2</sub>	7.52	10-140	50	61.3
WS <sub>3</sub>	8.95	30-80	30	36.8
WS <sub>4</sub>	7.79	40-200	80	98.1
WS <sub>5</sub>	6.71	40-90	40	49.1
WS <sub>6</sub>	6.51	40-90	40	49.1
WS <sub>7</sub>	6.55	40-90	50	61.3
WS <sub>8</sub>	5.35	70-140	60	73.6
WS <sub>9</sub>	5.55	30-80	30	36.8
WS <sub>10</sub>	6.15	10-210	60	73.6
WS <sub>11</sub>	5.48	70-100	40	49.1
WS <sub>12</sub>	5.18	40-110	60	73.6
WS <sub>13</sub>	5.90	50-70	40	49.1
WS <sub>14</sub>	6.01	50-60	20	24.5
WS <sub>15</sub>	6.92	60-90	30	36.8
WS <sub>16</sub>	5.32	60-90	30	36.8
WS <sub>17</sub>	5.84	20-70	30	36.8
WS <sub>18</sub>	6.38	80-130	60	73.6
WS <sub>19</sub>	6.49	20-40	20	24.5
WS <sub>20</sub>	4.48	20-40	20	24.5
WS <sub>21</sub>	5.26	50-160	70	85.8
WS <sub>22</sub>	6.40	40-110	40	49.1
WS <sub>23</sub>	6.26	40-90	40	49.1
WS <sub>24</sub>	6.69	30-70	10	12.3
WS <sub>25</sub>	5.91	60-110	30	36.8
WS <sub>26</sub>	5.99	20-90	40	49.1
WS <sub>27</sub>	6.85	90-190	70	85.8
WS <sub>28</sub>	3.55	50-140	60	73.6
WS <sub>29</sub>	6.82	50-90	50	61.3
<b>Average</b>	<b>6.17</b>	<b>10 – 210</b>	<b>42.4</b>	<b>52.0</b>

#### **Appendix 4:**

#### **DERIVATION OF THE EXPRESSION FOR ACTIVITY CONCENTRATION**

The derivation of the expression for the calculation of the activity concentrations of  $^{238}\text{U}$ ,  $^{232}\text{Th}$  and  $^{40}\text{K}$  in the soil, water, and dust (air) samples in Bq/kg, Bq/L and Bq/m<sup>3</sup> respectively is shown as follows.



AP is the activity of the parent nuclide at any time t.

AP<sub>0</sub> is the initial activity of the parent nuclide at time zero.

AD<sub>0</sub> is the initial activity of the daughter nuclide at time zero.

AD is the activity of the daughter at any time t.

At secular equilibrium when the activity concentrations of the parents and daughter nuclides are equal, the mathematical expression for the formation of the daughter nuclide from the parent can be expressed as:

$$\frac{dN_D}{dt} = \lambda_p N_{p_0} - \lambda_D N_D \quad (1)$$

but,  $\frac{dN}{dt} = \lambda N$

$$A_P = A_{P_0} e^{-\lambda t} \quad (2)$$

Integrating equation (1),

$$N_D = \frac{\lambda_P N_{P_0}}{\lambda_D - \lambda_P} (e^{-\lambda_P t} - e^{-\lambda_D t}) \quad (3)$$

Multiplying through equation 3 by  $\lambda_D$ ,

$$\lambda_D N_D = \frac{\lambda_D \lambda_P N_{P_0}}{\lambda_D - \lambda_P} (e^{-\lambda_P t} - e^{-\lambda_D t}) \quad (4)$$

$$A_D = \frac{\lambda_D A_P}{\lambda_D - \lambda_P} (e^{-\lambda_P t} - e^{-\lambda_D t})$$

$$A_D = \frac{\lambda_D A_P e^{-\lambda_P t}}{\lambda_D - \lambda_P} \left( 1 - \frac{e^{-\lambda_D t}}{e^{-\lambda_P t}} \right)$$

At secular equilibrium, half-life of the parent nuclide  $\{T_{1/2} (P)\} \gg$  half-life of the daughter nuclide  $\{T_{1/2} (D)\}$ .

Implying  $\lambda_P \ll \lambda_D$

Also it is assumed that  $\lambda_D - \lambda_P$  is approximately equal to  $\lambda_D$

$$A_D = A_P e^{-\lambda_P t} \left( 1 - \frac{e^{-\lambda_D t}}{e^{-\lambda_P t}} \right) \quad (5)$$

Since  $\lambda_D \gg \lambda_P$ , then after a sufficiently long period of time  $e^{-\lambda_D t}$  will be much smaller than  $e^{-\lambda_P t}$  and equation (4) is simplified to be as follows:

$$A_D = A_P e^{-\lambda_P t}$$

$$A_D = \frac{A_P}{e^{\lambda_P t}}$$

This implies the activity of the parent any time t can be written as follows:

$$A_P = A_D e^{\lambda_P t}$$

The above expression can also be written in terms of counts as follows:

$$A_P = \frac{N_D e^{\lambda_P t}}{p.t.\varepsilon}$$

In terms of specific activity concentration the equation is expressed as follows:

$$A_P = \frac{N_D e^{\lambda_P t_d}}{p.T_c.\varepsilon.m} \quad (6)$$

Where;

N is the net counts of the radionuclide in the samples,

$T_d$  is the delay time between sampling and counting,

P is the gamma emission probability (gamma yield),

$\varepsilon$  is the absolute counting efficiency of the detector system,

$T_c$  is the sample counting, and

m is the mass of the sample (kg) or volume (L).

The specific activity concentrations of the samples were calculated from equation (6).

## **Appendix 5**

### **DERIVATION OF UNCERTAINTY ON THE ACTIVITY CONCENTRATIONS**

In this study, the uncertainties associated with the determination of activity a concentration of each radionuclide was estimated from expression used in the calculation of the specific activity concentrations (equation 31).

$$A_{sp} = \frac{N \cdot e^{\lambda \cdot Td}}{\epsilon \cdot Y \cdot M \cdot Tc} \quad (1)$$

Where:

$A_{sp}$  is the specific activity in Bq/kg,

N is the background corrected net peak area,

$\epsilon$  is the absolute detector efficiency,

Y is the gamma yield,

Tc is the counting time of the sample,

$\lambda$  is the decay constant of individual radionuclides,

Td is the time between sampling and time of counting.

Some the uncertainties identified for the quantification of the uncertainty in the determination of the specific activity concentrations include the following:

- Net peak area,
- Detector efficiency,
- Sample mass,
- Counting time.

From equation (1), and taking natural log of both sides gives equation

$$\ln A_{sp} = \ln N + \lambda Td \ln e - \ln \epsilon - \ln Y - \ln M - \ln Tc \quad (2)$$

Differentiating equation (38)

$$\frac{dA_{sp}}{A_{sp}} = \frac{dN}{N} - \frac{d\epsilon}{\epsilon} - \frac{dY}{Y} - \frac{dM}{M} - \frac{dTc}{Tc} \quad (3)$$

Taking square of both sides of equation (3) gives equation (4).

$$\left(\frac{dA_{sp}}{A_{sp}}\right)^2 = \left(\frac{dN}{N}\right)^2 + \left(\frac{d\varepsilon}{\varepsilon}\right)^2 + \left(\frac{dY}{Y}\right)^2 + \left(\frac{dM}{M}\right)^2 + \left(\frac{dTc}{Tc}\right)^2 \quad (4)$$

Taking the square root of both sides of equation (4) gives equation (5).

$$\frac{dA_{sp}}{A_{sp}} = \sqrt{\left(\frac{dN}{N}\right)^2 + \left(\frac{d\varepsilon}{\varepsilon}\right)^2 + \left(\frac{dY}{Y}\right)^2 + \left(\frac{dM}{M}\right)^2 + \left(\frac{dTc}{Tc}\right)^2} \quad (5)$$

Simplifying equation (45) gives equation (6).

$$dA_{sp} = A_{sp} \cdot \sqrt{\left(\frac{dN}{N}\right)^2 + \left(\frac{d\varepsilon}{\varepsilon}\right)^2 + \left(\frac{dY}{Y}\right)^2 + \left(\frac{dM}{M}\right)^2 + \left(\frac{dTc}{Tc}\right)^2} \quad (6)$$

The uncertainties in the counting time and the gamma emission probability are negligible and are ignored in the uncertainty calculation in equation (6).

Thus the overall uncertainty in the determination of the activity concentrations was determined from equation (43).

$$dA_{sp} = A_{sp} \cdot \sqrt{\left(\frac{dN}{N}\right)^2 + \left(\frac{d\varepsilon}{\varepsilon}\right)^2 + \left(\frac{dM}{M}\right)^2} \quad (7)$$

dN is determined from the uncertainty in the integration of the peak area of each full energy event.

dM is the standard uncertainty on the weighing balance used to weigh the samples and the standard uncertainty was quoted to be 0.1 mg.

dε in equation (7) was determined follows.

From equation (1),

$$\varepsilon = \frac{N}{A.Y.Tc} \quad (8)$$

Where: N is the net count of the radionuclide in the standard;

A is the activity of the radionuclide in the standard at the time of counting;

ε is the absolute efficiency of the detector;

Y is the gamma emission probability (gamma yield);

Tc is the counting time.

Take natural log of equation (8).

$$\ln \varepsilon = \ln N - \ln A - \ln Y - \ln Tc \quad (9)$$

Differentiating equation (9).

$$\frac{d\varepsilon}{\varepsilon} = \frac{dN}{N} - \frac{dA}{A} - \frac{dY}{Y} - \frac{dTc}{Tc} \quad (10)$$

Take square of equation (46)

$$\left(\frac{d\varepsilon}{\varepsilon}\right)^2 = \left(\frac{dN}{N}\right)^2 + \left(\frac{dA}{A}\right)^2 + \left(\frac{dY}{Y}\right)^2 + \left(\frac{dTc}{Tc}\right)^2 \quad (11)$$

Since the uncertainties in the counting time and the gamma emission probability are negligible equation (47) reduces to (12):

$$\left(\frac{d\varepsilon}{\varepsilon}\right)^2 = \left(\frac{dN}{N}\right)^2 + \left(\frac{dA}{A}\right)^2 \quad (12)$$

Take square root of both sides

$$d\varepsilon = \varepsilon \cdot \sqrt{\left(\frac{dN}{N}\right)^2 + \left(\frac{dA}{A}\right)^2} \quad (13)$$

Thus the standard uncertainty of the efficiency of the detector was determined from equation (13).

$dN$  is determined from the uncertainty in the integration of the peak area of each full energy event of each radionuclide in the standard.

$dA$  is relative uncertainty of the activity of the calibration standard and this was estimated to be 3.0 %. The reported uncertainty was determined according to the DKD-3 (DEUTSCHER KALIBRIERDIENST, QSA Global GmbH) report is based on the standard uncertainty multiplied by a coverage factor of  $k=2$ , providing a confidence level of 95 % [NIST Technical Note 1297/ "Guide to the expression of uncertainty in measurement" ISO Guide, 1995].

The overall uncertainty determined from equation X6 will be multiplied a coverage factor of  $k=2$  (2 standard deviation) providing a confidence level of 95 %.

## Appendix 6

The activity concentration of the radionuclides in the soil samples.

Sample code	Specific activity/Bq/kg SOIL			Calculated absorbed dose rate, nGy/h	Annual effective dose, mSv/year	
	<sup>238</sup> U	<sup>232</sup> Th	<sup>40</sup> K		Outdoor	Indoor
SS1	20.36±1.74	22.72±1.70	234.95±18.35	32.93	0.04	0.16
SS2	20.67±1.91	20.12±1.02	215.79±17.34	30.70	0.04	0.15
SS3	21.46±1.74	24.32±1.73	63.39±6.26	27.25	0.03	0.13
SS4	5.25±0.79	9.33±0.91	115.16±9.41	12.86	0.02	0.06
SS5	7.93±1.06	19.66±1.53	181.90±14.43	23.12	0.03	0.11
SS6	6.45±1.11	13.31±1.34	297.63±23.07	23.43	0.03	0.11
SS7	6.99±1.28	23.19±1.79	357.71±27.55	53.15	0.04	0.16
SS8	15.00±1.59	10.06±1.27	551.72±41.61	36.01	0.04	0.18
SS9	6.02±0.91	21.11±1.65	327.64±24.98	29.19	0.04	0.14
SS10	5.16±1.13	17.32±1.67	177.89±15.20	20.26	0.03	0.10
SS11	11.87±1.18	7.07±0.85	39.81±4.50	11.41	0.01	0.06
SS12	4.68±0.97	28.99±2.05	328.49±25.16	33.37	0.04	0.16
SS13	11.38±1.30	23.22±1.72	178.51±14.30	26.73	0.03	0.13
SS14	6.86±0.89	8.14±0.90	237.81±18.35	18.00	0.02	0.88
SS15	10.25±1.39	35.55±2.38	231.58±18.18	35.86	0.04	0.18
SS16	4.76±0.87	11.98±1.07	165.73±13.25	16.35	0.02	0.80
SS17	3.51±1.17	20.97±1.96	269.35±21.71	25.52	0.03	0.13
SS18	4.53±0.93	14.98±1.58	351.79±27.43	25.81	0.03	0.13
SS19	7.61±1.11	28.57±2.00	197.75±15.57	29.02	0.04	0.14
SS20	11.98±1.37	26.93±1.94	237.51±18.57	31.70	0.04	0.16
SS21	14.57±1.54	43.42±2.85	151.64±12.36	39.28	0.05	0.19
SS22	24.61±1.97	56.18±3.28	236.36±18.62	55.16	0.07	0.27
SS23	12.62±1.33	18.82±1.51	91.22±8.18	21.00	0.03	0.10
SS24	19.53±1.64	27.29±1.95	185.62±14.92	33.25	0.04	0.16
SS25	9.15±1.03	11.05±1.02	91.20±7.75	14.70	0.02	0.72
SS26	20.04±1.79	31.83±2.24	328.40±25.31	42.18	0.05	0.21
SS27	10.41±1.15	8.08±0.95	59.86±5.82	12.19	0.02	0.60
SS28	6.23±0.76	6.00±0.68	61.19±5.64	9.05	0.01	0.44
SS29	12.24±1.15	10.47±0.99	60.44±5.56	14.50	0.02	0.71
SS30	22.61±1.79	19.41±1.49	191.76±15.67	30.17	0.04	0.15
SS31	16.17±1.49	19.29±1.56	121.03±10.39	24.17	0.03	0.12
SS32	8.48±1.20	20.00±1.60	266.15±20.77	27.10	0.03	0.13
SS33	9.53±1.11	20.36±1.54	194.82±15.74	24.82	0.03	0.12
SS34	9.10±1.11	18.56±1.48	240.69±18.81	25.45	0.03	0.13
SS35	32.83±2.50	93.64±5.25	193.48±15.67	79.79	0.10	0.39
SS36	23.61±1.78	76.02±4.30	224.75±17.47	66.20	0.08	0.33
SS37	12.39±1.43	21.14±1.67	167.59±13.99	25.48	0.03	0.13
SS38	9.48±1.24	17.39±1.48	206.01±16.15	23.47	0.03	0.12
Average	<b>12.27</b>	<b>23.86</b>	<b>206.17</b>	<b>28.68</b>	<b>0.04</b>	<b>0.24</b>

**The activity concentration of the radionuclides in the water samples.**

Sample Code	pH	Specific activity, Bq/l			Annual effective dose, mSv/year
		WATER			
		<sup>238</sup> U	<sup>232</sup> Th	<sup>40</sup> K	
WS1	6.21	0.83 ± 0.02	0.41 ± 0.03	8.67 ± 0.05	0.28
WS2	7.52	0.66 ± 0.05	0.31 ± 0.02	3.44 ± 0.04	0.20
WS3	8.95	0.43 ± 0.03	0.25 ± 0.02	7.86 ± 0.04	0.17
WS4	7.79	1.96 ± 0.03	0.65 ± 0.01	8.12 ± 0.06	0.55
WS5	6.71	0.69 ± 0.03	0.62 ± 0.01	10.09 ± 0.05	0.29
WS6	6.51	1.22 ± 0.03	0.47 ± 0.03	8.06 ± 0.07	0.37
WS7	6.55	0.72 ± 0.04	0.69 ± 0.01	10.72 ± 0.08	0.31
WS8	5.35	0.30 ± 0.04	0.50 ± 0.03	8.76 ± 0.05	0.19
WS9	5.55	0.42 ± 0.03	0.29 ± 0.02	6.98 ± 0.04	0.17
WS10	6.15	0.46 ± 0.03	0.61 ± 0.01	8.44 ± 0.04	0.24
WS11	5.48	0.46 ± 0.03	0.56 ± 0.01	5.13 ± 0.10	0.21
WS12	5.18	0.32 ± 0.03	0.52 ± 0.01	8.86 ± 0.04	0.19
WS13	5.90	0.28 ± 0.05	0.26 ± 0.02	7.87 ± 0.06	0.14
WS14	6.01	0.71 ± 0.03	0.55 ± 0.02	10.93 ± 0.04	0.29
WS15	6.92	0.37 ± 0.04	0.31 ± 0.03	9.93 ± 0.08	0.17
WS16	5.32	0.76 ± 0.03	0.37 ± 0.02	11.14 ± 0.04	0.27
WS17	5.84	0.55 ± 0.03	0.34 ± 0.03	7.46 ± 0.04	0.20
WS18	6.38	0.18 ± 0.04	0.53 ± 0.01	7.04 ± 0.04	0.16
WS19	6.49	0.76 ± 0.03	0.41 ± 0.02	9.29 ± 0.04	0.27
WS20	4.48	0.51 ± 0.06	0.21 ± 0.04	1.65 ± 0.08	0.15
WS21	5.26	0.41 ± 0.03	0.31 ± 0.02	5.93 ± 0.05	0.16
WS22	6.40	0.75 ± 0.02	0.39 ± 0.04	8.69 ± 0.05	0.26
WS23	6.26	0.31 ± 0.04	0.50 ± 0.03	9.95 ± 0.04	0.19
WS24	6.69	0.40 ± 0.03	0.36 ± 0.02	8.37 ± 0.04	0.18
WS25	5.91	0.29 ± 0.05	0.49 ± 0.02	11.99 ± 0.04	0.20
WS26	5.99	0.80 ± 0.03	0.46 ± 0.02	7.97 ± 0.04	0.28
WS27	6.85	0.48 ± 0.03	0.29 ± 0.03	9.66 ± 0.04	0.19
WS28	3.55	0.78 ± 0.03	0.42 ± 0.04	8.13 ± 0.05	0.27
WS29	6.82	0.11 ± 0.09	0.51 ± 0.04	3.11 ± 0.06	0.10
<b>This work Average</b>		<b>0.58±0.36</b>	<b>0.43±0.13</b>	<b>8.08±2.43</b>	<b>0.23±0.09</b>

The specific activity concentrations of radionuclides in dust/air samples using direct gamma ray analysis.

Sample code	Specific activity, $\mu\text{Bq}/\text{m}^3$ DUST/AIR		Absorbed dose rate, $\text{X } 10^{-3} \text{ nGy/h}$	Annual Effective Dose $\mu\text{Sv}/\text{year}$
	$^{238}\text{U}$	$^{232}\text{Th}$		
AS1	3.62	4.29	4.40	4.05
AS2	<0.12	0.65	4.30	0.60
AS3	4.07	3.74	4.20	3.56
AS4	0.82	2.08	1.70	1.93
AS5	11.1	3.00	6.80	3.12
<b>Average</b>	<b>4.90</b>	<b>2.80</b>	<b>4.28</b>	<b>2.70</b>

Legend: AS-Air sample (dust sampling on a filter paper)

Table 5-11: Concentration of U and Th in dust samples using NAA

Sample Code	Dust concentration I				Dust concentration II			
	Uranium Ppm	$^{238}\text{U}$ $\mu\text{Bq/g}$	Thorium ppm	$^{232}\text{Th}$ $\mu\text{Bq/g}$	Uranium ppm	$^{238}\text{U}$ $\mu\text{Bq/g}$	Thorium ppm	$^{232}\text{Th}$ $\mu\text{Bq/g}$
AS1	<0.01	<0.12	0.71±0.12	2.89	<0.01	<0.12	0.65±0.10	2.65
AS2	3.53±0.53	43.60	1.38±0.21	5.62	4.10±0.21	50.60	1.42±0.21	5.78
AS3	2.28±0.31	28.10	1.19±0.18	4.84	2.15±0.32	26.50	1.12±0.17	4.56
AS <sub>4</sub>	0.88±0.13	10.90	<0.01	<0.004	0.92±0.14	11.40	<0.01	<0.004
AS5	0.69±0.10	8.52	2.03±0.31	8.26	0.69±0.10	8.52	1.94±0.29	7.90
<b>Average</b>	<b>1.80±0.27</b>	<b>23.00</b>	<b>1.30±0.21</b>	<b>5.40</b>	<b>2.00±0.19</b>	<b>24.00</b>	<b>1.30±0.19</b>	<b>5.20</b>

I-First batch of dust samples

II- Second batch of dust samples

ppm-  $\mu\text{g}/\text{g}$

The activity concentration of  $^{238}\text{U}$ ,  $^{232}\text{Th}$  and  $^{40}\text{K}$  in fresh food samples by direct gamma ray analysis.

Sample ID	Activity Concentration, (Bq/kg) FOOD (Fresh weight)			Committed annual effective dose, ( $\mu\text{Sv}/\text{year}$ )
	$^{238}\text{U}$	$^{232}\text{Th}$	$^{40}\text{K}$	
FS <sub>1</sub>	0.13±0.04	0.20±0.06	49.96±2.06	61.50
FS <sub>2</sub>	0.24±0.110.	0.32±0.11	85.47±3.37	104.0
FS <sub>3</sub>	0.30±0.16	0.01±0.001	29.34±1.32	33.60
FS <sub>4</sub>	0.07±0.02	0.10±0.06	32.60±1.44	38.80
FS <sub>5</sub>	0.10±0.05	0.08±0.03	38.96±1.66	45.00
FS <sub>6</sub>	0.24±0.09	<0.11	36.62±1.58	40.40
<b>Average</b>	<b>0.18±0.08</b>	<b>0.14±0.05</b>	<b>45.00±1.90</b>	<b>54</b>

Legend: FS- Food sample (cassava root tubers)

The activity concentration of  $^{238}\text{U}$ ,  $^{232}\text{Th}$  and  $^{40}\text{K}$  in dried food samples by direct gamma ray analysis.

Sample ID	Activity Concentration, (Bq/kg) FOOD Dry weight			Committed annual effective dose, ( $\mu\text{Sv}/\text{year}$ )
	$^{238}\text{U}$	$^{232}\text{Th}$	$^{40}\text{K}$	
FS <sub>1</sub>	0.52±0.17	0.88±0.25	229.80±9.46	281
FS <sub>2</sub>	1.13±0.49	1.49±0.50	393.14±15.49	481
FS <sub>3</sub>	1.36±0.72	0.03±0.003	134.96±6.05	154
FS <sub>4</sub>	0.30±0.10	0.47±0.26	149.95±6.63	179
FS <sub>5</sub>	0.47±0.21	0.39±0.16	179.19±7.63	208
FS <sub>6</sub>	1.11±0.41	<0.11	168.43±7.25	188
<b>Average</b>	<b>0.82±0.35</b>	<b>0.65 ± 0.23</b>	<b>209.25±8.75</b>	<b>250</b>

Legend: FS- Food sample (cassava root tubers)

## Appendix 7

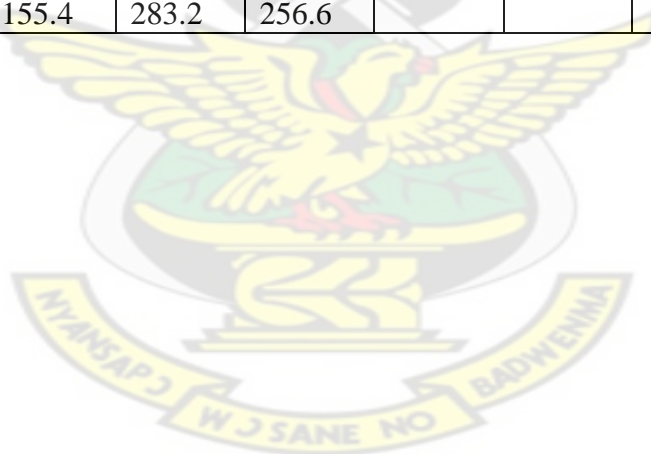
Activity concentration of  $^{226}\text{Ra}$  and emanation coefficient of  $^{222}\text{Rn}$  in different materials.

Sample code	$^{226}\text{Ra}$ Bq/kg	Average Net area (Ao)	Average Net area (N)	EF $\pm$ SD
SS1(GS)	17.18	914	4688	0.540 $\pm$ 0.031
SS2(GS)	22.11	907	5218.5	0.525 $\pm$ 0.032
SS3(M)	30.06	1034	7041.5	0.553 $\pm$ 0.031
SS4(F)	12.50	606.5	3140.5	0.541 $\pm$ 0.028
SS5(M)	9.20	436	2431.5	0.527 $\pm$ 0.031
SS6(GS)	7.07	405	1929	0.482 $\pm$ 0.030
SS7(MS)	7.35	290	1862.5	0.575 $\pm$ 0.039
SS8(M)	8.80	147.5	3170	0.792 $\pm$ 0.039
SS9(GS)	9.27	409	2302.5	0.530 $\pm$ 0.032
SS10(M)	11.13	462	2378	0.536 $\pm$ 0.029
SS11(GS)	9.62	290.5	1776.5	0.531 $\pm$ 0.033
SS12(MS)	10.02	480	3190	0.575 $\pm$ 0.032
SS13(GS)	7.84	507.5	2942.5	0.520 $\pm$ 0.023
SS14(MS)	11.63	396.5	2520	0.560 $\pm$ 0.035
SS15(MS)	8.70	145.5	912	0.551 $\pm$ 0.029
SS16(M)	9.50	464.5	2820.5	0.555 $\pm$ 0.028
SS17(MS)	8.00	365.5	1643	0.464 $\pm$ 0.292
SS18(MS)	12.85	454.5	3189	0.584 $\pm$ 0.031
SS19(MS)	6.50	291.5	1559	0.516 $\pm$ 0.033
SS20(GS)	12.90	728.5	3767	0.491 $\pm$ 0.031
SS21(GS)	9.40	484	2820.5	0.542 $\pm$ 0.029
SS22(GS)	32.41	1376	8766	0.561 $\pm$ 0.028
SS23(GS)	6.20	246.5	1338	0.521 $\pm$ 0.045
SS24(GS)	8.60	985.5	5769	0.540 $\pm$ 0.032
SS25(GS)	24.82	275	5867	0.810 $\pm$ 0.041
SS26(GS)	29.80	1062	6728.5	0.559 $\pm$ 0.032
SS27(GS)	9.34	679	3651	0.529 $\pm$ 0.037
SS28(GS)	14.83	484	3245	0.573 $\pm$ 0.031
SS29(GS)	19.54	868	4917	0.513 $\pm$ 0.302
SS30(GS)	19.60	700	4118	0.554 $\pm$ 0.290
SS31(GS)	21.71	814	4481	0.524 $\pm$ 0.031
SS32(GS)	8.11	471	2123.5	0.471 $\pm$ 0.029
SS33(M)	7.20	325.5	1734.5	0.480 $\pm$ 0.026
SS34(M)	9.33	466.5	2649	0.550 $\pm$ 0.036
SS35(GS)	30.00	1295.5	8122	0.556 $\pm$ 0.033
SS36(GS)	2781	961	7070	0.595 $\pm$ 0.033
SS37(M)	8.62	435.5	2281	0.512 $\pm$ 0.031
SS38(M)	9.80	416	1891.5	0.480 $\pm$ 0.027
SS39(GS)	21.23	892.5	5585	0.552 $\pm$ 0.321
SS40(GS)	19.30	896.5	4664.5	0.510 $\pm$ 0.032

## Appendix 8

### Rainfall data for the study area from 2003 to July 2009

YEAR	JAN	FEB	MAR	APR	MAY	JUN	JUL	AUG	SEP	OCT	NOV	DEC	TOTAL	AVERAGE
2003	55.8	50.2	113.8	185.2	175.7	288.6	15.9	19.3	100.2	225.8	84.1	66.1	<b>1381</b>	<b>115</b>
2004	69.3	30.1	71.1	127.5	141.7	155.8	188.2	48.3	231.3	210.5	142.3	119.5	<b>1536</b>	<b>128</b>
2005	42.8	68.0	101.0	202.5	131.5	280.4	37.5	10.6	38.5	22.1	208.3	86.5	<b>1230</b>	<b>102</b>
2006	64.0	79.5	137.0	195.0	303.5	278.1	128.3	27.5	114	83.1	192	42.3	<b>1644</b>	<b>137</b>
2007	2.1	135.9	64.2	274.6	246.7	283.5	326.1	154.2	222.6	466.8	190.7	149.8	<b>2517</b>	<b>210</b>
2008	17.6	74.8	166.2	212.6	312.8	229.8	220.0	85.0	112	143.8	80.4	89.4	<b>1744</b>	<b>145</b>
2009	2.2	118.4	139.2	88.6	155.4	283.2	256.6						<b>1044</b>	<b>87</b>



## Appendix 9

### Physical and chemical parameters of the mine

#### Statistical summary of water chemistry

Code	pH	T	Cond.	TDS	Cl <sup>-</sup>	NO <sub>3</sub> <sup>-</sup>	PO <sub>4</sub> <sup>3-</sup>	SO <sub>4</sub> <sup>2-</sup>	Fe	Cu	Zn	Cr	Pb	Hg	As	Cd	U	Th	K
		°C	µS/cm																
WS <sub>1</sub>	6.21	26.6	1208	539.0	58.0	4.6	0.02	282.9	0.18	0.012	0.010	<0.001	<0.001	<0.001	0.004	<0.002	0.02	0.04	0.21
WS <sub>2</sub>	7.52	26.1	2.4	893.0	94.0	7.3	0.28	285.9	0.14	0.006	0.003	<0.001	<0.001	<0.001	0.006	<0.002	0.02	0.03	0.40
WS <sub>3</sub>	8.95	25.7	823.0	362.0	36.0	9.9	0.19	51.9	0.42	0.008	0.003	<0.001	<0.001	<0.001	0.003	<0.002	0.01	0.01	0.50
WS <sub>4</sub>	7.79	26.7	597.0	264.0	60.0	0.9	0.01	170.3	0.04	<0.003	<0.001	<0.001	<0.001	<0.001	0.008	<0.002	0.02	0.02	1.30
WS <sub>5</sub>	6.71	26.7	77.1	33.5	4.0	0.9	0.02	10.3	0.08	<0.003	<0.001	<0.001	<0.001	<0.001	0.004	<0.002	0.03	0.03	0.64
WS <sub>6</sub>	6.51	26.5	40.6	17.3	4.0	1.2	0.03	8.0	0.08	<0.003	<0.001	<0.001	<0.001	<0.001	0.006	<0.002	0.04	0.06	0.40
WS <sub>7</sub>	6.55	26.6	234.0	101.1	4.0	1.0	0.05	10.1	<0.001	0.003	0.011	<0.001	<0.001	<0.001	0.008	<0.002	0.02	0.04	2.10
WS <sub>8</sub>	5.35	25.8	443.0	219.0	116	0.9	0.03	6.3	<0.001	<0.003	0.080	<0.001	<0.001	<0.001	0.004	<0.002	0.02	0.05	0.90
WS <sub>9</sub>	5.55	26.6	328.0	144.8	50.0	0.6	0.01	6.6	<0.001	<0.003	0.080	<0.001	<0.001	<0.001	0.003	<0.002	0.03	0.01	0.72
WS <sub>10</sub>	6.15	26.5	390.0	170.5	48.0	1.3	0.01	56.9	0.02	<0.003	0.009	<0.001	<0.001	<0.001	0.005	<0.002	0.01	0.04	0.84
WS <sub>11</sub>	5.48	25.9	1139	498.0	150	0.2	0.02	9.3	0.03	<0.003	0.010	<0.001	<0.001	<0.001	0.003	<0.002	0.02	0.02	2.56
WS <sub>12</sub>	5.18	25.6	277.0	130.1	62.0	1.3	0.01	35.1	0.16	0.005	0.012	<0.001	<0.001	<0.001	0.003	<0.002	0.04	0.04	1.01
WS <sub>13</sub>	5.90	25.9	377.0	165.8	52.0	1.4	0.04	17.4	<0.001	<0.003	0.024	<0.001	0.063	<0.001	0.003	<0.002	0.02	0.03	1.73
WS <sub>14</sub>	6.01	26.5	84.0	37.5	20.0	1.0	0.01	3.3	<0.001	<0.003	0.071	<0.001	0.004	<0.001	0.003	<0.002	0.03	0.05	3.82
WS <sub>15</sub>	6.92	26.2	417.0	181.4	4.0	2.3	0.05	27.1	0.09	0.010	0.002	<0.001	<0.001	<0.001	0.004	<0.002	0.01	0.02	0.92
WS <sub>16</sub>	5.32	27.0	661.0	295.0	58.0	2.3	0.07	76.7	<0.001	<0.003	0.013	<0.001	<0.001	<0.001	0.003	<0.002	0.02	0.04	2.01
WS <sub>17</sub>	5.84	26.8	498.0	224.0	1.6	3.3	<-0.514	131.3	0.43	<0.003	0.011	<0.001	0.106	<0.001	0.004	<0.002	0.01	0.02	1.02
WS <sub>18</sub>	6.38	25.6	95.4	41.8	0.2	2.7	<-0.514	24.0	0.07	<0.003	0.020	<0.001	0.031	<0.001	0.004	<0.002	0.02	0.04	1.40
WS <sub>19</sub>	6.49	27.3	138.3	113.8	0.6	1.6	0.02	28.0	0.42	<0.003	0.008	<0.001	0.045	<0.001	0.006	<0.002	0.01	0.03	0.02
WS <sub>20</sub>	4.48	26.9	440.0	190.7	9.4	3.2	0.03	40.0	<0.001	<0.003	0.128	<0.001	0.030	<0.001	0.007	<0.002	0.02	0.02	2.40
WS <sub>21</sub>	5.26	26.4	541.0	235.0	10.4	1.4	0.01	46.3	0.01	0.086	0.283	<0.001	0.039	<0.001	0.006	<0.002	0.02	0.03	3.84
WS <sub>22</sub>	6.40	27.1	94.6	40.6	0.6	1.9	<-0.514	17.7	0.35	<0.003	0.004	<0.001	0.047	<0.001	0.004	<0.002	0.01	0.02	0.81
WS <sub>23</sub>	6.26	26.1	72.4	31.4	0.3	2.1	<-0.514	11.9	0.09	0.004	0.002	<0.001	<0.001	<0.001	0.006	<0.002	0.02	0.03	1.01
WS <sub>24</sub>	6.69	26.7	161.8	72.1	0.2	1.2	0.05	7.6	0.07	<0.003	0.003	<0.001	<0.001	<0.001	0.006	<0.002	0.03	0.04	0.90
WS <sub>25</sub>	5.91	27.0	453.0	201.0	40.0	1.6	0.02	4.3	0.05	<0.003	0.013	<0.001	<0.001	<0.001	0.005	<0.002	0.02	0.04	0.70
WS <sub>26</sub>	5.99	27.2	362.0	155.3	14.0	2.5	0.01	41.6	<0.001	<0.003	0.016	<0.001	0.080	<0.001	0.004	<0.002	0.01	0.03	0.62
WS <sub>27</sub>	6.85	26.7	466.0	201.0	44.0	1.7	0.01	47.7	0.01	<0.003	0.016	<0.001	<0.001	<0.001	0.004	<0.002	0.01	0.02	0.21
WS <sub>28</sub>	3.55	26.5	112.0	41.6	2.0	2.9	0.01	19.7	0.02	0.011	0.031	<0.001	0.168	<0.001	0.002	<0.002	0.02	0.02	1.02
WS <sub>29</sub>	6.82	26.5	57.2	24.4	2.0	1.9	<-0.514	10.1	0.41	<0.003	0.009	<0.001	0.018	<0.001	0.003	<0.002	0.01	0.01	0.04

### Physical parameters of the water samples

Sample code	pH	Temperature, °C	Conductivity μS/cm	Total dissolved solids, mg/L
WS <sub>1</sub>	6.21	26.6	1208.0	539.0
WS <sub>2</sub>	7.52	26.1	2.4	893.0
WS <sub>3</sub>	8.95	25.7	823.0	362.0
WS <sub>4</sub>	7.79	26.7	597.0	264.0
WS <sub>5</sub>	6.71	26.7	77.1	33.5
WS <sub>6</sub>	6.51	26.5	40.6	17.3
WS <sub>7</sub>	6.55	26.6	234.0	101.1
WS <sub>8</sub>	5.35	25.8	443.0	219.0
WS <sub>9</sub>	5.55	26.6	328	144.8
WS <sub>10</sub>	6.15	26.5	390.0	170.5
WS <sub>11</sub>	5.48	25.9	1139.0	498.0
WS <sub>12</sub>	5.18	25.6	277.0	130.1
WS <sub>13</sub>	5.90	25.9	377.0	165.8
WS <sub>14</sub>	6.01	26.5	84.0	37.5
WS <sub>15</sub>	6.92	26.2	417.0	181.4
WS <sub>16</sub>	5.32	27.0	661.0	295.0
WS <sub>17</sub>	5.84	26.8	498.0	224.0
WS <sub>18</sub>	6.38	25.6	95.4	41.8
WS <sub>19</sub>	6.49	27.3	138.3	113.8
WS <sub>20</sub>	4.48	26.9	440.0	190.7
WS <sub>21</sub>	5.26	26.4	541.0	235.0
WS <sub>22</sub>	6.40	27.1	94.6	40.6
WS <sub>23</sub>	6.26	26.1	72.4	31.4
WS <sub>24</sub>	6.69	26.7	161.8	72.1
WS <sub>25</sub>	5.91	27.0	453.0	201.0
WS <sub>26</sub>	5.99	27.2	362.0	155.3
WS <sub>27</sub>	6.85	26.7	466.0	201.0
WS <sub>28</sub>	3.55	26.5	112.0	41.6
WS <sub>29</sub>	6.82	26.5	57.2	24.4
WS <sub>30</sub>	7.16	27.1	858.0	373.0
WS <sub>31</sub>	6.98	25.5	194.5	87.6

**Concentration of anions in water sources.**

Sample Code	Concentration, mg/L			
	CL <sup>-</sup>	NO <sub>3</sub> <sup>-</sup>	PO <sub>4</sub> <sup>3-</sup>	SO <sub>4</sub> <sup>2-</sup>
WS <sub>1</sub>	57.98	4.64	0.017	282.86
WS <sub>2</sub>	93.97	7.26	0.281	285.86
WS <sub>3</sub>	35.99	9.93	0.185	51.86
WS <sub>4</sub>	59.98	0.94	0.014	170.29
WS <sub>5</sub>	3.99	0.89	0.021	10.29
WS <sub>6</sub>	3.99	1.17	0.026	8.00
WS <sub>7</sub>	3.99	1.04	0.045	10.14
WS <sub>8</sub>	115.96	0.89	0.027	6.29
WS <sub>9</sub>	49.98	0.64	0.009	6.57
WS <sub>10</sub>	47.98	1.25	0.010	56.86
WS <sub>11</sub>	149.95	0.23	0.017	9.29
WS <sub>12</sub>	61.98	1.34	0.003	35.14
WS <sub>13</sub>	51.98	1.42	0.039	17.43
WS <sub>14</sub>	19.99	0.98	0.014	3.29
WS <sub>15</sub>	3.99	2.28	0.050	27.14
WS <sub>16</sub>	57.98	2.25	0.065	76.71
WS <sub>17</sub>	1.60	3.34	<-0.514	131.29
WS <sub>18</sub>	0.20	2.67	<-0.514	24.00
WS <sub>19</sub>	0.60	1.64	0.021	28.00
WS <sub>20</sub>	9.40	3.15	0.034	40.00
WS <sub>21</sub>	10.40	1.40	0.005	46.29
WS <sub>22</sub>	0.60	1.89	<-0.514	17.71
WS <sub>23</sub>	0.30	2.08	<-0.514	11.86
WS <sub>24</sub>	0.20	1.21	0.046	7.57
WS <sub>25</sub>	40.00	1.57	0.024	4.29
WS <sub>26</sub>	14.00	2.49	0.003	41.57
WS <sub>27</sub>	43.98	1.68	0.012	47.71
WS <sub>28</sub>	2.00	2.93	0.005	19.71
WS <sub>29</sub>	2.00	1.94	<-0.514	10.14
WS <sub>30</sub>	117.97	1.23	0.036	41.00
WS <sub>31</sub>	25.99	1.59	<-0.514	8.14

### Concentration of metals in water sources

Sample Code	Concentration, mg/L								
	Fe	Mn	Cu	Zn	Cr	Pb	Cd	Hg	As
WS <sub>1</sub>	0.180	<0.002	0.012	0.010	<0.001	<0.001	<0.002	<0.001	0.004
WS <sub>2</sub>	0.143	<0.002	0.006	0.003	<0.001	<0.001	<0.002	<0.001	0.006
WS <sub>3</sub>	0.419	0.028	0.008	0.003	<0.001	<0.001	<0.002	<0.001	0.003
WS <sub>4</sub>	0.038	<0.002	<0.003	<0.001	<0.001	<0.001	<0.002	<0.001	0.008
WS <sub>5</sub>	0.081	<0.002	<0.003	<0.001	<0.001	<0.001	<0.002	<0.001	0.004
WS <sub>6</sub>	0.083	<0.002	<0.003	<0.001	<0.001	<0.001	<0.002	<0.001	0.006
WS <sub>7</sub>	<0.001	0.253	0.003	0.011	<0.001	<0.001	<0.002	<0.001	0.008
WS <sub>8</sub>	<0.001	<0.002	<0.003	0.080	<0.001	<0.001	<0.002	<0.001	0.004
WS <sub>9</sub>	<0.001	<0.002	<0.003	0.080	<0.001	<0.001	<0.002	<0.001	0.003
WS <sub>10</sub>	0.019	<0.002	<0.003	0.009	<0.001	<0.001	<0.002	<0.001	0.005
WS <sub>11</sub>	0.028	<0.002	<0.003	0.010	<0.001	<0.001	<0.002	<0.001	0.003
WS <sub>12</sub>	0.156	<0.002	0.005	0.012	<0.001	<0.001	<0.002	<0.001	0.003
WS <sub>13</sub>	<0.001	0.234	<0.003	0.024	<0.001	0.063	<0.002	<0.001	0.003
WS <sub>14</sub>	<0.001	0.033	<0.003	0.071	<0.001	0.004	<0.002	<0.001	0.003
WS <sub>15</sub>	0.093	<0.002	0.010	0.002	<0.001	<0.001	<0.002	<0.001	0.004
WS <sub>16</sub>	<0.001	0.052	<0.003	0.013	<0.001	<0.001	<0.002	<0.001	0.003
WS <sub>17</sub>	0.427	0.387	<0.003	0.011	<0.001	0.106	<0.002	<0.001	0.004
WS <sub>18</sub>	0.069	0.007	<0.003	0.020	<0.001	0.031	<0.002	<0.001	0.004
WS <sub>19</sub>	0.418	0.006	<0.003	0.008	<0.001	0.045	<0.002	<0.001	0.006
WS <sub>20</sub>	<0.001	0.518	<0.003	0.128	<0.001	0.030	<0.002	<0.001	0.007
WS <sub>21</sub>	0.009	0.074	0.086	0.283	<0.001	0.039	<0.002	<0.001	0.006
WS <sub>22</sub>	0.352	0.017	<0.003	0.004	<0.001	0.047	<0.002	<0.001	0.004
WS <sub>23</sub>	0.088	0.004	0.004	0.002	<0.001	<0.001	<0.002	<0.001	0.006
WS <sub>24</sub>	0.073	<0.002	<0.003	0.003	<0.001	<0.001	<0.002	<0.001	0.006
WS <sub>25</sub>	0.052	0.007	<0.003	0.013	<0.001	<0.001	<0.002	<0.001	0.005
WS <sub>26</sub>	<0.001	0.061	<0.003	0.016	<0.001	0.080	<0.002	<0.001	0.004
WS <sub>27</sub>	0.006	0.004	<0.003	0.016	<0.001	<0.001	<0.002	<0.001	0.004
WS <sub>28</sub>	0.022	1.397	0.011	0.031	<0.001	0.168	<0.002	<0.001	0.002
WS <sub>29</sub>	0.408	0.010	<0.003	0.009	<0.001	0.018	<0.002	<0.001	0.003
WS <sub>30</sub>	0.201	0.005	0.009	0.008	<0.001	<0.001	<0.002	<0.001	0.004
WS <sub>31</sub>	0.211	<0.002	0.006	0.003	<0.001	<0.001	<0.002	<0.001	0.005
WS <sub>32</sub>	0.076	0.077	<0.003	0.016	<0.001	0.003	<0.002	<0.001	<0.002
<b>Detection Limit</b>	<b>0.006</b>	<b>0.002</b>	<b>0.003</b>	<b>0.001</b>	<b>0.001</b>	<b>0.001</b>	<b>0.002</b>	<b>0.001</b>	<b>0.002</b>

**Trace metals in soil, rock and tailings in the study area**

<b>Location</b>	<b>No. of samples</b>	<b>Mn mg/kg</b>	<b>Si mg/kg</b>	<b>V mg/kg</b>	<b>Al mg/kg</b>	<b>Co mg/kg</b>	<b>Ti mg/kg</b>
Mine soil	6	<0.0001	<1.000	<0.001	<0.01	<0.001	<0.100
Mine rock	6	176±29	5086±322	11.8±0.4	1236±84	5.8±1.0	<0.100
North heap leach	6	<0.0001	<1.000	<0.001	<0.01	<0.001	370±31
South heap leach	3	193±28	4198±209	1.8±0.6	7722±310	6.5±1.0	<0.100
Mine tailings	6	<0.0001	<1.000	<0.001	<0.01	<0.001	<0.100
Mine waste (rock)	12	<0.0001	<1.000	<0.001	<0.01	<0.001	<0.100
Mine pit (Teberebie)	3	<0.0001	<1.000	<0.001	<0.01	3.5±0.1	<0.100
Mine pit (Pepe)	6	<0.0001	<1.000	<0.001	<0.01	9±1.5	2159±135
Mine pit (kontraverchy)	6	426±28	1347±425	32±6	1843±299	<0.001	3579±160
Mine pit (Akontansi)	9	1309±21	2640±239	459±19	2169±423	<0.001	1492±130
Ore stockpile	3	29±12	<1.000	<0.001	2585±138	<0.001	4274±140
Plant site	6	3400±111	5329±143	241±17	9532±370	7.4±0.2	<0.100
New Atuabo (Tarkwa)	6	<0.0001	<1.000	<0.001	<0.01	<0.001	5122±174
Club house area	3	67±20	1081±179	194±16	5766±490	<0.001	<0.100
Brahabebomi (Tarkwa)	3	33±11	<1.000	6.9±0.4	9762±290	<0.001	926±552
Samahu community	9	459±32	1552±318	11.9±0.2	4.6±0.02	<0.001	<0.100
Boboobo community	3	<0.0001	<1.000	<0.001	<0.01	<0.001	<0.100
Abekoase community	6	39±10	7062±363	1.7±0.8	2.4±0.03	<0.001	<0.100
Huniso community	3	<0.0001	<1.000	<0.001	<0.01	<0.001	730±518
Pepesa community	3	357±25	1391±517	11.7±0.2	<0.01	<0.001	1278±592
Agric Hill/UMAT area	6	69±15	2602±503	143±5	9.4±0.04	2.4±0.1	<0.100
Detection limit		0.0001	1.000	0.001	0.01	0.001	0.100

La mg/kg	As mg/kg	Cr mg/kg	Sr mg/kg	Sc mg/kg	Fe mg/kg	U mg/kg	Th mg/kg
23±5	<0.00001	<0.01	<0.100	<0.001	<0.100	<0.0001	<0.001
57±9	3.5±0.3	150±55	<0.100	2.5±0.35	2316±773	2.61±0.39	1.80±0.90
62±10	<0.00001	<0.01	274±79	3.7±0.4	5534±198	<0.0001	<0.001
17.6±2.2	3.9±0.04	<0.01	<0.100	4.5±0.35	2920±813	1.80±0.60	2.60±0.70
62±10	<0.00001	<0.01	<0.100	<0.001	<0.100	<0.0001	<0.001
123.5±14.5	<0.00001	<0.01	<0.100	<0.001	<0.100	<0.0001	<0.001
<0.0001	<0.00001	480±27	274±91	5.6±0.55	1220±887	<0.0001	<0.001
72±9	<0.00001	<0.01	<0.100	3.9±0.3	7624±142	<0.0001	<0.001
21.3±3.64	<0.00001	124±39	2.4±0.25	1.7±0.02	4692±886	0.19±0.06	0.85±0.31
113.5±13	<0.00001	<0.01	116±36	4.6±0.35	7307±105	0.43±0.12	2.09±1.10
150±18	<0.00001	<0.01	<0.100	<0.001	<0.100	<0.0001	<0.001
35±4	<0.00001	170±34	<0.100	4.5±0.15	2330±863	0.52±0.17	1.28±0.43
21.7±3.3	5.1±0.2	<0.01	<0.100	<0.001	<0.100	<0.0001	<0.001
32±4	19.3±0.9	<0.01	193±53	13.5±0.55	3075±173	0.94±0.72	1.10±0.60
19.65±3.05	<0.00001	<0.01	<0.100	<0.001	<0.100	1.82±0.40	1.22±0.40
6.6±2.0	15.2±1.1	<0.01	<0.100	<0.001	<0.100	1.90±0.93	1.41±0.74
<0.0001	<0.00001	<0.01	<0.100	<0.001	<0.100	<0.0001	<0.001
2.1±0.01	6.9±0.7	<0.01	<0.100	<0.001	<0.100	0.84±0.31	1.70±0.80
<0.0001	6.2±0.3	<0.01	<0.100	<0.001	<0.100	<0.0001	<0.001
7.5±0.1	7.6±1.0	<0.01	<0.100	<0.001	<0.100	1.22±0.82	1.42±0.68
17.1±1.7	16.3±0.8	360±18	194±48	4.8±0.33	1210±612	1.41±0.52	2.43±1.01
0.0001	0.00001	0.01	0.100	0.001	0.100	0.0001	0.001

**Major metals in soil, rock and tailings in the study area**

<b>Location</b>	<b>Mg mg/kg</b>	<b>Ca mg/kg</b>	<b>Na Mg/kg</b>	<b>K Mg/kg</b>
Mine soil	<0.100	<1.00	9452±74	61896±2264
Mine rock	8300±600	<1.00	11900±74	52648±216
North heap leach	<0.100	<1.00	11559.5±52	36904±2064
South heap leach	2272±158	<1.00	1241.5±12	2207±214
Mine tailings	<0.100	<1.00	11559.5±52	36904±2064
Mine waste (rock)	<0.100	<1.00	21163±74	111960±3520
Mine pit (Teberebie)	<0.100	<1.00	7673.5±34.5	15703±581
Mine pit (Pepe)	<0.100	<1.00	14355.5±74	5044±212
Mine pit (kontraverchy)	<0.100	<1.00	2445.5±18	7037±363
Mine pit (Akontansi)	2354±565	7143±142	19904±74	71360±3256
Ore stockpile	5457±342	<1.00	16515±74	64520±2840
Plant site	5820±375	1429±571	5170.5±29.5	14190±616
New Atuabo (Tarkwa)	<0.100	<1.00	3478±22	5602±349
Club house area	<0.100	<1.00	5052±26	10846±495
Brahabebomi (Tarkwa)	<0.100	<1.00	3711.5±22.5	11654±1216
Samahu community	<0.100	<1.00	3425.5±422	1594±198
Boboobo community	<0.100	<1.00	10559±44.5	25987±960
Abekoase community	2809±173	<1.00	277±6	1897±162
Huniso community	<0.100	<1.00	2371.5±17.5	3332±271
Pepesa community	<0.100	754±452	893±7.5	2443±251
Agric Hill/UMAT area	<0.100	<1.00	1020±12	2468±202
Detection limit	0.100	1.00	0.001	0.01

## **Appendix 10**

### **a. PREPARATION OF REAGENTS**

#### **1.0 PREPARATION OF 30 % NaCl SOLUTION**

30.0 g of NaCl was accurately weighed and dissolved in 100.0 ml of distilled water.

#### **2.0 PREPARATION OF BRUCINE REAGENT**

- Weigh accurately 1.0 g of brucine sulphate hydrate
- Weigh accurately also 1.0 g of sulphanilic acid
- Dissolve the two substances in 70 ml of distilled water
- Transfer the solution into a dark bottle and store at 5 °C

#### **3.0 PREPARATION OF ASCORBIC ACID**

- Accurately weigh 1.760 g of solid ascorbic acid ( $C_8H_8O_6$ )
- Dissolve in distilled water and transfer the resultant solution into a 100.0 ml volumetric flask
- Top to the mark and shake well to mix.

#### **4.0 PREPARATION OF MOLYBDATE ANTIMONYL REAGENT**

- Weigh 1.875 g of solid Ammonium molybdate
- Weigh 0.0225 g of solid potassium antimonyl tartrate
- Combine both solids and dissolve in distilled water
- Transfer the mixture into a 250 ml volumetric flask
- Add 22.0 ml of Concentrated  $H_2SO_4$  and top it up to the mark with distilled water and shake well to mix.

#### **5.0 PREPARATION OF ACID SALT**

- Weigh 60.0 g of solid NaCl
- Dissolve in distilled water
- Add 5.0 ml of Concentrated HCl
- Transfer resultant solution into a 250.0 ml volumetric flask
- Top up to the mark and shake well to mix.

#### **6.0 PREPARATION OF GLYCEROL (1:1)**

Equal volumes of glycerol and distilled water are mixed together in a ratio of 1:1 and shaken well to mix. E. g. 50 ml of glycerol and 50 ml of distilled water were mixed together.

#### **7.0 PREPARATION OF 0.0141 M $AgNO_3$ TITRANT**

Accurately weigh 2.395 g (AR. 99.9 %) of solid  $AgNO_3$  and dissolve in little distilled water. Transfer the resultant solution to a 1 L volumetric flask. Top to the mark and shake well to mix.

## 8.0 PREPARATION OF 0.27 M K<sub>2</sub>CrO<sub>4</sub> INDICATOR SOLUTIONS

- Dissolve 50 g of AR grade K<sub>2</sub>CrO<sub>4</sub> in a little distilled water
- Add the 0.0141 M AgNO<sub>3</sub> titrant until a definite red precipitate is form
- Allow to stand for 12 hours or overnight
- Filter (or decant) in a 1 L volumetric flask,) an dilute to the mark with distilled water

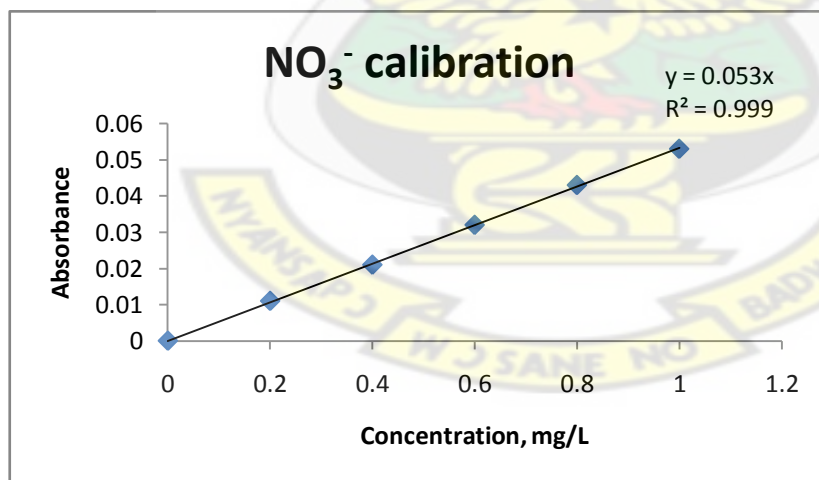
## b. PREPARATION OF CALIBRATION STANDARDS AND CALIBRATION CURVES OF ANIONS

### 1.0 PREPARATION OF NITRATE STANDARDS (100 ppm)

- Accurately weigh 0.7218 g of KNO<sub>3</sub> dried at 105 °C for 24 hours
- Dissolve in distilled water and transfer the solution into 1 L volumetric flask
- Shake well and add 2.0 ml of chloroform ( as preservative)
- Top up to the mark and shake to mix well.

The UV spectrophotometer calibration standards of 0.2 ppm, 0.4 ppm, 0.6 ppm, 0.8 ppm and 1.0 ppm from the stock solution with 1.0 ppm taken from 100 ppm as follows:

- For the 0.0 ppm (blank): 5.0 ml of distilled water
- For the 0.2 ppm: 1.0 ml of stock (1.0 ppm) + 4.0 ml of distilled water
- For the 0.4 ppm: 2.0 ml of stock (1.0 ppm) + 3.0 ml of distilled water
- For the 0.6 ppm: 3.0 ml of stock (1.0 ppm) + 2.0 ml of distilled water
- For the 0.8 ppm: 4.0 ml of stock (1.0 ppm) + 1.0 ml of distilled water
- For the 1.0 ppm: 5.0 ml of stock (1.0 ppm) + 0.0 ml of distilled water



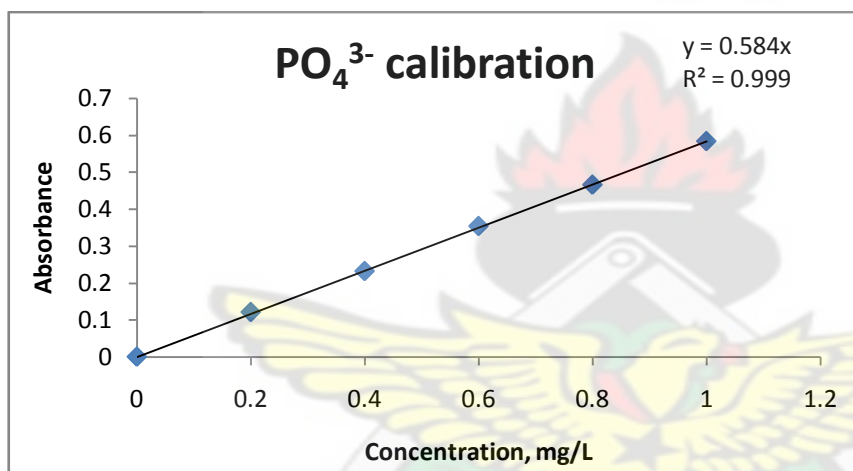
### 2.0 PREPARATION OF PHOSPHATE STANDARD (100 ppm)

- Weigh accurately 219.5 mg (0.2195 g) of anhydrous potassium dehydrate phosphate (KH<sub>2</sub>PO<sub>4</sub>)

- Dissolve in distilled water and transfer into a 1000 ml volumetric flask and top up to the mark with distilled water.

Calibration standards of 0.2 ppm, 0.4 ppm, 0.6 ppm, 0.8 ppm and 1.0 ppm were prepared from a stock of 1.0 ppm taken from 100.0 ppm as follows.

- 0.0 ppm (blank): 10 ml of distilled water
- For the 0.2 ppm: 2.0 ml of stock (1.0 ppm) + 8.0 ml of distilled water
- For the 0.4 ppm: 4.0 ml of stock (1.0 ppm) + 6.0 ml of distilled water
- For the 0.6 ppm: 6.0 ml of stock (1.0 ppm) + 4.0 ml of distilled water
- For the 0.8 ppm: 8.0 ml of stock (1.0 ppm) + 2.0 ml of distilled water
- For the 1.0 ppm: 10.0 ml of stock (1.0 ppm) + 0.0 ml of distilled water

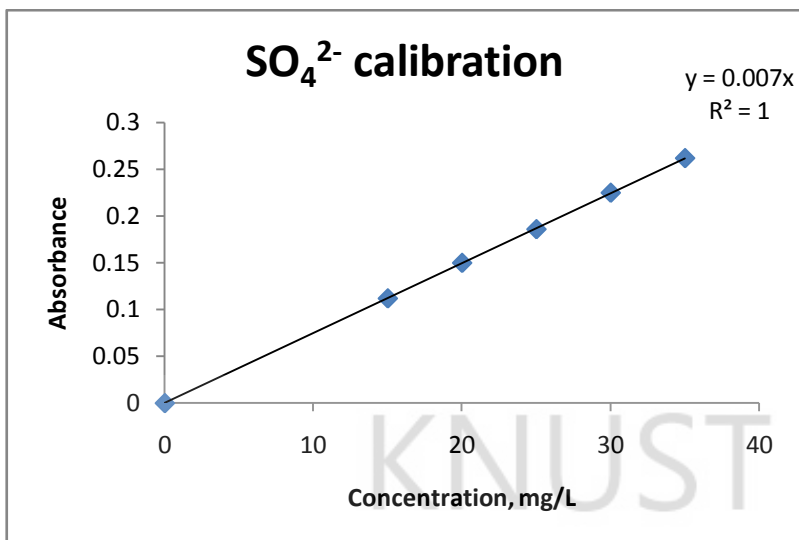


### 3.0 PREPARATION OF SULPHATE STANDARD (100 ppm)

- Weigh accurately 0.1479 g of anhydrous Na<sub>2</sub>SO<sub>4</sub>
- Dissolve in distilled water and transfer into a 1000 ml volumetric flask and top up to the mark with distilled water.

Calibration standards of 15.0 ppm, 20.0 ppm, 25.0 ppm, 30.0 ppm and 35.0 ppm were prepared directly from 100.0 ppm stock solution as follows.

- For the 15.0 ppm: 1.5 ml of stock (100.0 ppm) + 8.5 ml of distilled water
- For the 20.0 ppm: 2.0 ml of stock (100.0 ppm) + 8.0 ml of distilled water
- For the 25.0 ppm: 2.5 ml of stock (100.0 ppm) + 7.5 ml of distilled water
- For the 30.0 ppm: 3.0 ml of stock (100.0 ppm) + 7.0 ml of distilled water
- For the 35.0 ppm: 3.5 ml of stock (100.0 ppm) + 6.5 ml of distilled water



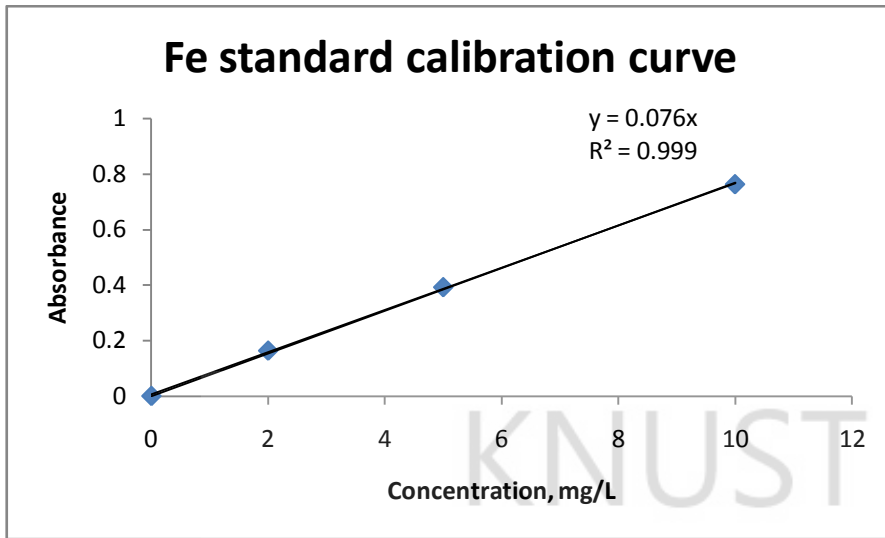
### **PREPARATION OF CALIBRATION STANDARDS AND CALIBRATION CURVES OF CATIONS**

Calibration standards of the cations investigated in this study were manufactured by Technolab AB of Sweden with the brand name Spectrascan in concentrations of 1000 mg/l. In the preparations of the standards of the metals, the stock solution was diluted to the required concentration range for each metal and their corresponding absorbances measured with the AAS.

#### **Iron (Fe)**

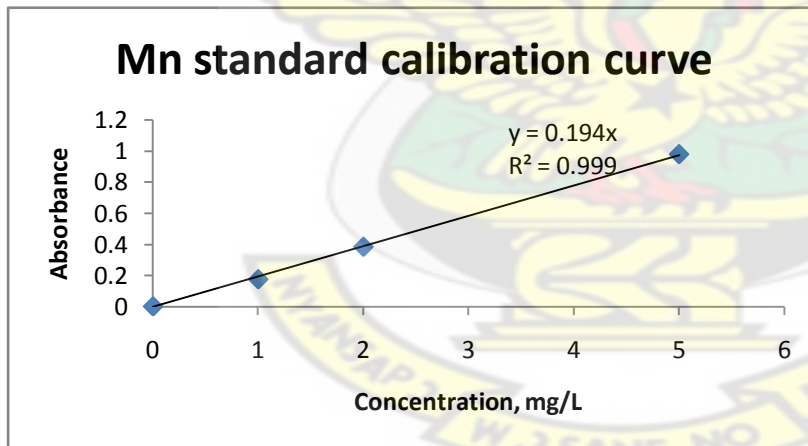
Standards for the determination of Fe were prepared to a maximum concentration of 10 mg/l as follows:

Standard Concentration mg/L	Mean Absorbances
0.000	0.0000
2.000	0.1632
5.000	0.3919
10.000	0.7628



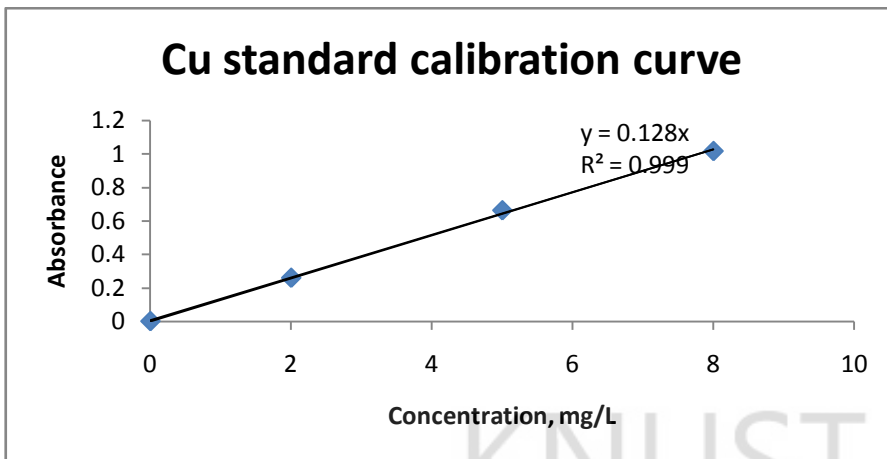
#### Manganese (Mn)

Standard Concentration mg/L	Mean Absorbances
0.000	0.0000
1.000	0.1743
2.000	0.3830
5.000	0.9787



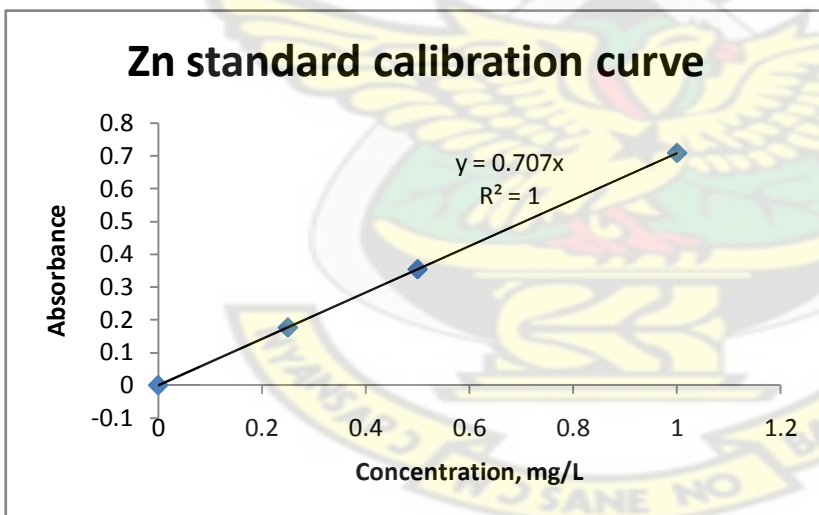
#### Copper (Cu)

Standard Concentration mg/L	Mean Absorbances
0.000	0.0000
2.000	0.2590
5.000	0.6618
8.000	1.0155



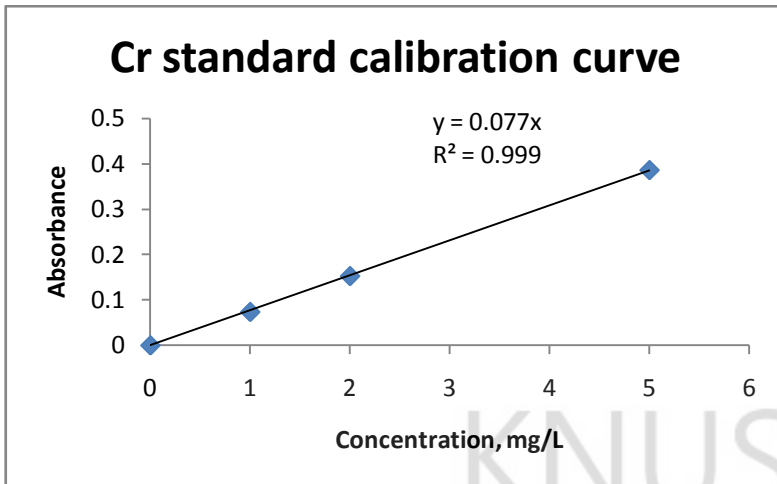
### Zinc (Zn)

Standard Concentration mg/L	Mean Absorbances
0.000	0.0000
0.250	0.1759
0.500	0.3534
1.000	0.7077



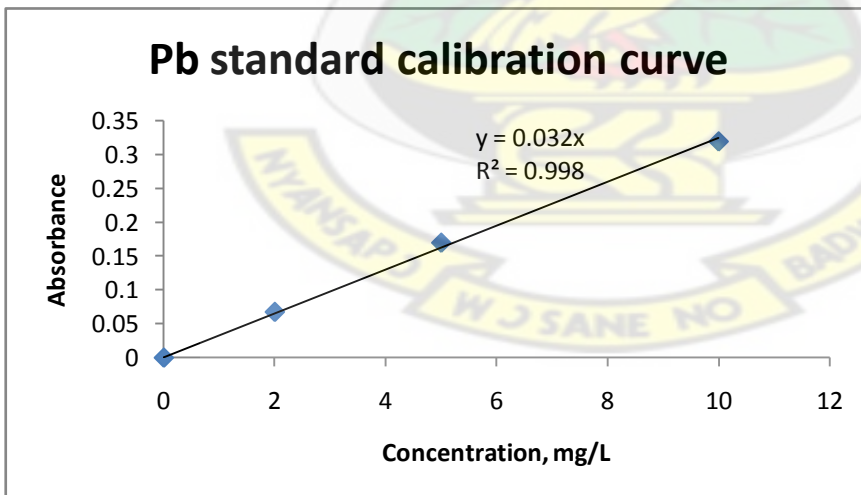
### Chromium (Cr)

Standard Concentration mg/L	Mean Absorbances
0.000	0.0000
1.000	0.0737
2.000	0.1528
5.000	0.3865



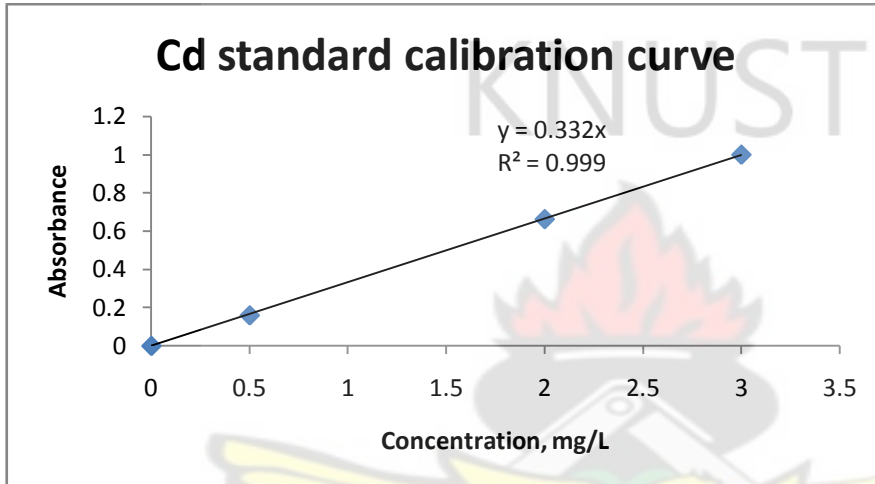
(Pb)

Standard Concentration mg/L	Mean Absorbances
0.000	0.0000
2.000	0.0676
5.000	0.1698
10.000	0.3194



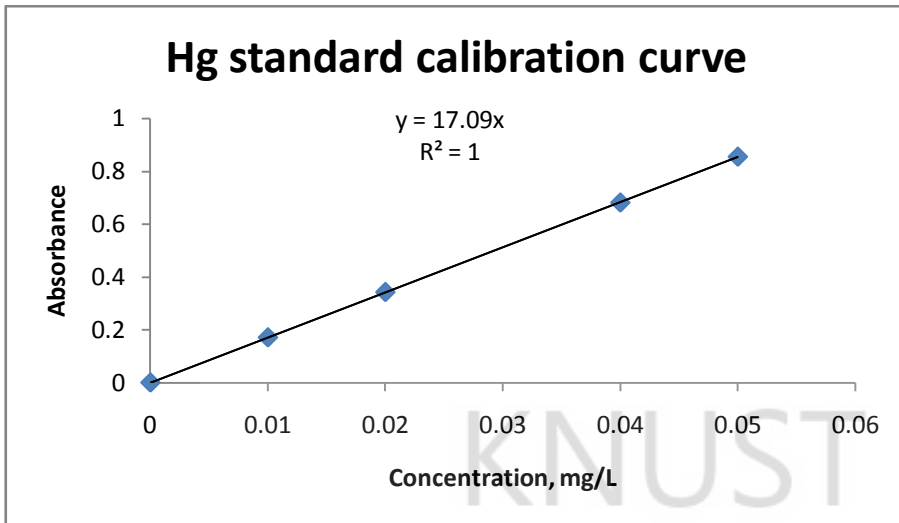
### Cadmium (Cd)

Standard Concentration mg/L	Mean Absorbances
0.000	0.0000
0.500	0.1599
2.000	0.6637
3.000	1.0011



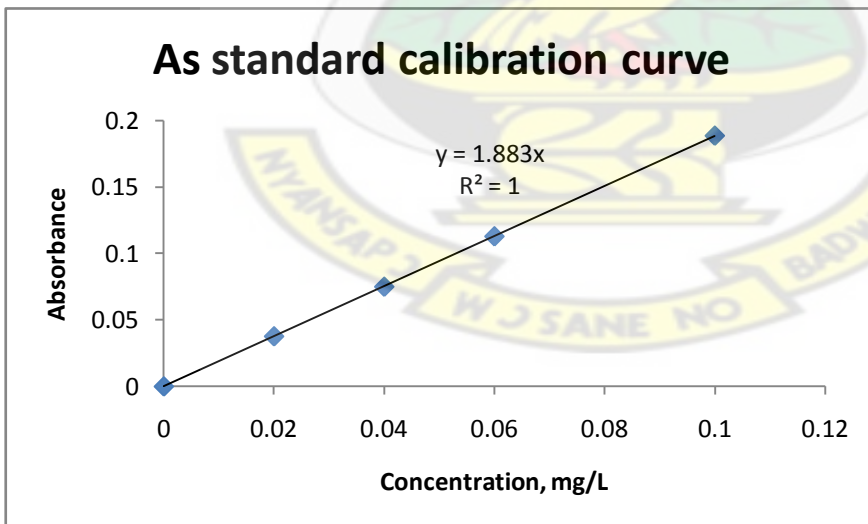
### Mercury (Hg)

Standard Concentration mg/L	Mean Absorbances
0.000	0.0000
0.010	0.1712
0.020	0.3430
0.040	0.6822
0.050	0.8559



Arsenic (As)

Standard Concentration mg/L	Mean Absorbances
0.000	0.0000
0.020	0.0377
0.040	0.0750
0.060	0.1129
0.100	0.1886



**Appendix 11**

**Statistical analysis using SPSS**

Comparison Uranium-238 activity concentrations

T-TEST PAIRS=U-238I WITH U-238II (PAIRED)

/CRITERIA=CI(.9500)

/MISSING=ANALYSIS.

**T-Test**

**Paired Samples Statistics**

	Mean	N	Std. Deviation	Std. Error Mean
Pair 1 First batch	12.2716	38	6.95109	1.12762
Second batch	11.7126	38	7.58066	1.22974

**Paired Samples Correlations**

	N	Correlation	Sig.
Pair 1 First batch & Second batch	38	.779	.000

**Paired Samples Test**

	Paired Differences					t	df	Sig. (2-tailed)
	Mean	Std. Deviation	Std. Error Mean	95% Confidence Interval of the Difference				
				Lower	Upper			
Pair 1 First batch - Second batch	-.55895	4.86246	.78880	-1.03930	2.15720	.709	37	.483

**Thorium-232**

T-TEST PAIRS=Th-232I WITH Th-232II (PAIRED)

/CRITERIA=CI (.9500)

/MISSING=ANALYSIS.

### Paired Samples Statistics

	Mean	N	Std. Deviation	Std. Error Mean
Pair 1 First batch	23.8550	38	17.80030	2.88759
Second batch	21.8818	38	18.12861	2.94085

### Paired Samples Test

	Paired Differences					t	df	Sig. (2-tailed)
	Mean	Std. Deviation	Std. Error Mean	95% Confidence Interval of the Difference				
				Lower	Upper			
Pair 1 First batch - Second batch	-1.97316	9.03181	1.46515	-.99553	4.94184	1.347	37	.186

### Potassium-40

**T-TEST PAIRS=K40I WITH K40II (PAIRED)**

**/CRITERIA=CI (.9500)**

**/MISSING=ANALYSIS.**

### Paired Samples Statistics

	Mean	N	Std. Deviation	Std. Error Mean
Pair 1 First batch	2.0617E2	38	103.07620	16.72117
second batch	1.8615E2	38	95.84787	15.54858

### Paired Samples Correlations

	N	Correlation	Sig.
Pair 1 First batch & second batch	38	.620	.000

**Paired Samples Test**

	Paired Differences					t	df	Sig. (2-tailed)
	Mean	Std. Deviation	Std. Error Mean	95% Confidence Interval of the Difference				
				Lower	Upper			
Pair 1 First batch - second batch	2.00139 E1	86.92014	14.10031	-8.55599	48.58389	1.419	37	.164

**Absorbed dose rates**

**T-TEST PAIRS=SOILDOSEI WITH SOILDOSEII (PAIRED)**

**/CRITERIA=CI (.9500)**

**/MISSING=ANALYSIS.**

**Paired Samples Statistics**

	Mean	N	Std. Deviation	Std. Error Mean
Pair 1 SOILDOSE I	29.2271	38	14.65972	2.37812
SOILDOSE II	26.3900	38	14.85084	2.40912

**Paired Samples Correlations**

	N	Correlation	Sig.
Pair 1 SOILDOSEI & SOILDOSEII	38	.771	.000

**Paired Samples Test**

	Paired Differences					t	df	Sig. (2-tailed)
	Mean	Std. Deviation	Std. Error Mean	95% Confidence Interval of the Difference				
				Lower	Upper			

				Lower	Upper				
Pair 1	SOILDOSEI - SOILDOSEII	2.83711	9.99690	1.62171	-.44879	6.12300	1.749	37	.089

**Annual effective doses**

**T-TEST PAIRS=Effddose1 WITH Effdose11 (PAIRED)**

**/CRITERIA=CI (.9500)**

**/MISSING=ANALYSIS.**

**Paired Samples Statistics**

	Mean	N	Std. Deviation	Std. Error
Pair 1 Effddose1	.1761	38	.08723	.01415
Effdose11	.1626	38	.09108	.01478

**Paired Samples Correlations**

	N	Correlation	Sig.
Pair 1 Effddose1 & Effdose11	38	.800	.000

**Paired Samples Test**

	Paired Differences					t	df	Sig. (2-tailed)
	Mean	Std. Deviation	Std. Error	95% Confidence Interval of the Difference				
				Lower	Upper			
Pair 1 Effddose1 - Effdose11	.01342	.05649	.00916	-.00515	.03199	1.465	37	.151

**Pearson correlation for U-238, Th-232 and K-40**

**CORRELATIONS**

**/VARIABLES=U238 Th232 K40**

**/PRINT=TWOTAIL NOSIG**

/MISSING=PAIRWISE.

### Correlations

		First batch	First batch	First batch
First batch	Pearson Correlation	1	.676**	-.073
	Sig. (2-tailed)		.000	.664
	N	38	38	38
First batch	Pearson Correlation	.676**	1	.112
	Sig. (2-tailed)	.000		.504
	N	38	38	38
First batch	Pearson Correlation	-.073	.112	1
	Sig. (2-tailed)	.664	.504	
	N	38	38	38

\*\* . Correlation is significant at the 0.01 level (2-tailed).

### ANOVA

concentration	Sum of Squares	df	Mean Square	F	Sig.
Between Groups	25.532	2	12.766	39.448	.000
Within Groups	27.183	84	.324		
Total	52.715	86			

### Post Hoc Tests

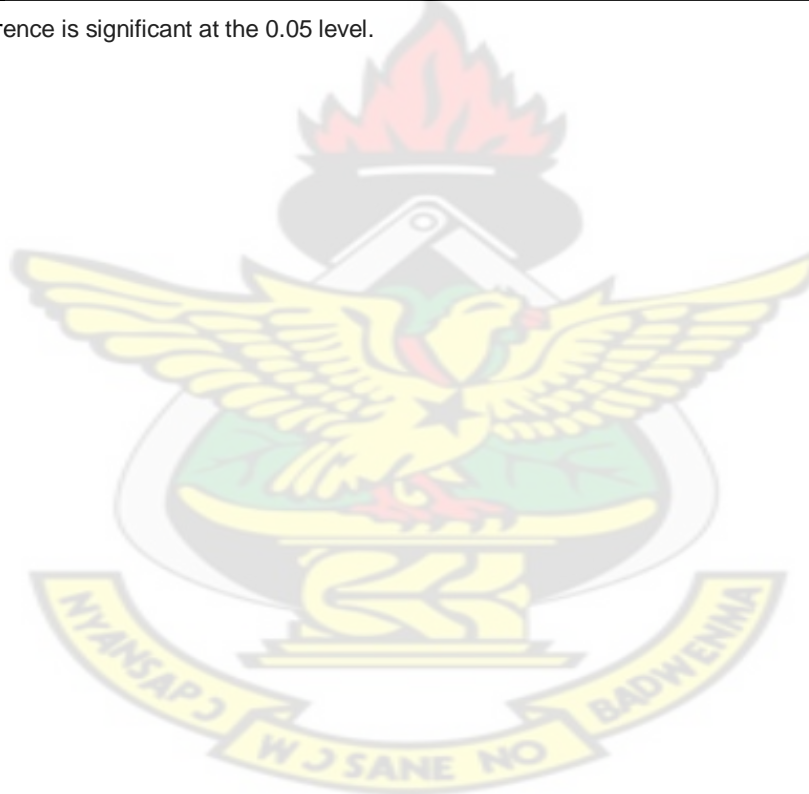
#### Multiple Comparisons

Dependent Variable:concentration

	(I) Nuclide	(J) Nuclide	Mean Difference (I-J)	Std. Error	Sig.	95% Confidence Interval	
						Lower Bound	Upper Bound
Tukey HSD	Uranium	Thorium	-.01069	.14939	.997	-.3671	.3458
		Potassium	-1.15448 <sup>*</sup>	.14939	.000	-1.5109	-.7980

	Thorium	Uranium	.01069	.14939	.997	-.3458	.3671
		Potassium	-1.14379*	.14939	.000	-1.5002	-.7873
	Potassium	Uranium	1.15448*	.14939	.000	.7980	1.5109
		Thorium	1.14379*	.14939	.000	.7873	1.5002
LSD	Uranium	Thorium	-.01069	.14939	.943	-.3078	.2864
		Potassium	-1.15448*	.14939	.000	-1.4516	-.8574
	Thorium	Uranium	.01069	.14939	.943	-.2864	.3078
		Potassium	-1.14379*	.14939	.000	-1.4409	-.8467
	Potassium	Uranium	1.15448*	.14939	.000	.8574	1.4516
		Thorium	1.14379*	.14939	.000	.8467	1.4409

\*. The mean difference is significant at the 0.05 level.



## APPENDIX 12

### List of Publications

1. **Augustine Faanu**, James H. Ephraim and Emmanuel O. Darko, (2010), Assessment of public exposure to naturally occurring radioactive materials from mining and mineral processing activities of Tarkwa Goldmine in Ghana, Environ Monit Assess. DOI 10.1007/s10661-010-1769-9.
2. **A. Faanu**, J. H. Ephraim, E. O. Darko, D. O. Kpeglo, H. Lawluvi and O.Adukpo. Determination of the concentrations of Physicochemical Parameters in Water and Soil from a Gold Mining Area in Ghana, Res. J. Environ. Earth Sci., Vol. 3 (2) (2011).
3. **A. Faanu**, E. O. Darko and J. H. Ephraim' Determination of natural radioactivity and hazard in soil and rock samples in a mining area in Ghana (**In press**: West African Journal of Applied Ecology (WAJAE-IN PRESS)).

